Quantifying the impact of the physical environment during processing

and storage of biopharmaceuticals

Roumteen Tavakoli-Keshe

Department of Biochemical Engineering

University College London

Abstract

As more complex biotherapeutics are produced, the numbers of antibodies exhibiting aggregation phenomenon has increased greatly. It is therefore of growing importance to understand the products and origin of these phenomena and to be able to select candidates that show the greatest stability. The purpose of this work was to assess different methods for determining protein stability and the aspects of stability they measure, analysing the different aggregate species produced to offer a platform solution when dealing with different aggregate phenomenon during process development.

The effect of reversible self association (RSA) on the purification of a product was evaluated and shown to only critically effect the operation of viral filtration steps in a typical bioprocess through blockage of filter pores. A custom made, rotating disc, interfacial shear device was evaluated along with thermal, spectroscopic and molecular modelling methods for their ability to determine the relative stabilities of antibodies to aggregation. A capillary interfacial shear device with 10 fold reduced volume was designed and tested, showing comparability of monomer loss in the capillary with the coefficient of monomer decay in the disc device. This surface related damage was further studied by comparison to thermal methods with a range of known modifications to IgG structures, using modelling techniques to indicate aspects of protein structure key to loss of stability. The interfacial shear device provides an orthogonal measurement related to modification of exposed protein residues whereas thermal techniques trend with intramolecular stability.

It was also concluded that for full characterisation of an aggregate profile SE-HPLC, Nanosight and Microflow Imaging should be used to enable capture of the entire size range of aggregate species from 10nm to 100µm. The work highlights the future prominence of molecular modelling techniques as part of a fully integrated aggregate mitigating solution to determine aggregation hot spots.

Declaration

I Roumteen Tavakoli-Keshe confirm that the work presented in this document is my own. Where information has been derived from other sources, I confirm that this has been indicated in the document.

Signature…………………………………………………….. Date………………

Acknowledgements

Table of Contents

Table of Figures

List of Tables

List of Equations

List of symbols and abbreviations

Symbols and units

[A]	Concentration of component A (mg/mL)
Å	Angstrom
B_{22}	Osmotic second viral coefficient
c	Protein concentration (mg/mL)
C(t)	Protein monomer concentration (mg/mL) at time t
C0	Protein monomer concentration (mg/mL) at time zero
g	Grams
gDa	Gigadaltons
h	Hours
kCal	Kilocalories
kDa	Kilodaltons
kg	Kilograms
k(T)	Reaction rate coefficient (mol L^{-1} s^{-1})
L	Litres
m'	Reaction order for component
m	Metres
M	Molar concentration (mol L^{-1})
mAU	Milli-absorbance units
mg	Milligrams
mL	Millilitres
mm	Millimetres
mM	Millimolar
Mol	Mole
nm	Nanometres
mW	Milliwatts

pI	Isoelectric point
PSI	Pounds per square inch
R	Gas constant ($J K^{-1} mol^{-1}$)
RFU	Relative fluorescence units
s	Seconds
t	Time (seconds)
T	Absolute temperature (°K)
T_m	Protein melting temperature (°C)
µg	Micrograms
µL	Microlitres
µm	Micro meters
π	Osmotic pressure (atmospheres)

Abbreviations

2D	2 dimensional
3D	3 dimensional
ADCC	Antibody-dependent cell-mediated cytotoxicity
AFFF	Asymmetric field flow fractionation
AUC	Analytical ultracentrifugation
CCD	Charge-coupled device
CD	Circular dichroism
CDC	Complement dependent cytotoxicity
CIP	Clean in place
DBC	Dynamic binding capacity
DLS	Dynamic light scattering
DoE	Design of experiment
DSC	Differential scanning calorimetry
DSP	Downstream processing

EDMA	Electrospray differential mobility analysis
EDTA	Ethylenediaminetetraacetic acid
FcRn	Neonatal Fc receptor
FTIR	Fourier transform infra-red spectroscopy
GLP	Good lab practice
GMP	Good manufacturing practice
HETP	Height of equivalent theoretical plate (m)
HPLC	High performance liquid chromatography
IgG	Immunoglobulin G
mAb	Monoclonal Antibody
MALDI	Matrix assisted laser desorption ionisation
MALS	Multi angled light scattering
MFI	Micro flow imaging
Mins	Minutes
NTA	Nanoparticle tracking analysis
PBS	Phospho-buffered saline
PDB	Protein database
PDC	Protein decay coefficient
PES	Polyethersulfone
QA	Quality assurance
RPM	Revolutions per minute
RPS	Revolutions per second
RSA	Reversible self association
SAP	Spatial aggregation propensity
S.D.	Standard deviation
SDS-PAGE	Sodium dodecyl sulphate polyacrylamide gel electrophoresis
SEC	Size exclusion chromatography
SIC	Self interaction chromatography

SINS	Self interaction nanoparticle spectroscopy
SLS	Static light scattering
THT	"Threonine - Histidine - Threonine" amino acid sequence
UF/DF	Ultrafiltration/Diafiltration
UV	Ultraviolet
V/V	Concentration of substance by volume (%)
W/V	Weight of substance by volume (%)
WT	Wild type

1 Introduction

1.1.1 Project aims

The aim of this project is to better understand antibody stability in relation to aggregation phenomenon and to find a way to mitigate the problem in industrial bioprocesses. In achieving this goal the best methods and techniques to quantify antibody presence as well as determine antibody stability will be discerned.

Antibodies aggregate in many different ways to form species with many properties, but regulations only dictate that the levels of aggregates above a certain size have to be kept below certain thresholds. The regulatory reason for removal of aggregates centres on the health risks associated with the injection of aggregated proteins into patients, including the eliciting of immunological responses and the ability to mechanically block capillaries, causing reduced microcirculation in postischemic patients.

From an industrial standpoint, it is important to focus on the issue to gain a more full understanding of what affects antibody stability and how to measure this most efficiently. Some aggregates can lower the efficacy of drug products and can limit the drug storage time once produced. More efficient screening of potential drug molecules for stability during manufacturing, shipping and storage can decrease time to market and increase the time a drug is sold under patent as well as potentially allowing smaller doses and less unused drugs wastage.

1.1.2 Objectives

The overall goal of the project is to be able to understand the products and origin of these phenomena and to select candidates that show the greatest stability. In this project we aim to assess different methods for determining protein stability and the aspects of stability they measure, analysing the different aggregate species

produced to offer a platform solution when dealing with different aggregation phenomena during process development. This is broken down into a series of sub-objectives designed to build towards the final goal.

1 Complete characterisation of the custom UCL disc interfacial shear device

This is required to determine the optimal conditions for collecting the most reliable results with the interfacial disc device and will involve characterising individual un-optimised parameters of operation. Milestones include:

- Determining cooling jacket operating conditions

- Determining the wavelength of light used in SE-HPLC analysis

- Determining the optimal disc speed

- Determining the optimal antibody concentration

2 Develop a higher throughput method of gaining comparable results to the disc shear device

This would be required to increase throughput when determining antibody sample stability with respect to interfacial interactions. This will allow for more samples to be screened earlier in process development, giving more information prior to lead antibody selection. This will involve the design of a fundamentally different device and testing different parameters of operation. Milestones include:

- Determining the mode of operation of the device

- Determining the conditions in the device

- Determining the operating conditions of the device

- Comparing the device results to the disc interfacial shear device

3 Finding an appropriate way to analyse aggregates formed through processing

This is required to fully characterise the aggregation profiles formed from antibodies so the mechanisms of aggregation can be assessed. This will involve determining current best practice from the literature and breaking the size range into

manageable chunks since no one method can cover the entire range required. Milestones include:

- Using the literature to determine the overall size range

- Using the literature to determine the individual size ranges required

- Determining the difference in aggregates formed through thermal and interfacial degradation

- Determining the best device for each size range

4 Determine the effect of RSA on bioprocessing of a target molecule

This is required to understand the effects of this newly observed phenomenon on processing and to determine the disc shear devices' reaction to it. It will also show the consequences of this issue on the downstream processing of a drug. This will involve finding an appropriate antibody and determining the conditions needed to produce RSA. It will then require the running of the individual purification steps to determine the effect of the phenomenon. Milestones include:

- Determining the effect of conditions on RSA expression using DoE

- Determining the effect of RSA presence on accelerated stability and disc shear device results

- Determining the effect of RSA on the capacity of protein-A chromatography

- Determining the effect of RSA on viral filtration

- Evaluating molecular models of RSA prone antibodies

5 Comparison of disc interfacial shear device with thermal methods as tools for determining antibody stability and the use of molecular modelling to explain differences

This is required to put the disc interfacial device into context with the other techniques for determining antibody stability. It is designed to allow for a conclusion to be drawn on the mechanism of aggregate formation at the solid/liquid interface. This will be done by comparing the results for five modified antibodies tested with

the disc shear device, differential scanning calorimetry and accelerated stability techniques. Molecular models would then be used to determine the cause of the difference in stability. Milestones include:

- Determining the PDC of the antibodies with the disc shear device

- Determine the stability of the antibodies using DSC

- Determine the stability of the antibodies using accelerated stability

- Comparison of the stability prediction technique results

- Evaluating molecular models of different antibodies

1.1.3 Description of thesis

The literature review has been structured to explain the background of each concept from the ground up, for instance, beginning with the biochemistry basics then leading to the reasons to remove aggregation. The review then moves on to an increasing order of complex detection methods before going into depth about the general factors that effect aggregation, the factors that occur in different unit operations, aggregation mechanisms and finally to look at cutting edge molecular modelling techniques to determine antibody stability.

The experimental section covers a definition of the standard methods to be used in the studies including conditions for use of a custom interfacial shear device before beginning by looking at the techniques available for analysing the aggregates formed. It then aims to find a higher throughput method for determining the interfacial shear stability before looking at a phenomenon known as Reversible Self Association (RSA) to determine its impact on bioprocessing. The work concludes by comparing the interfacial stability measurement with other techniques for determining protein stability. It proposes a mechanism for aggregation occurring at the solid/liquid surface drawing on both experimental results and a molecular model based understanding for the loss in stability of the antibodies tested.

2 Literature review

2.1 *Antibodies*

2.1.1 Immunoglobulin G
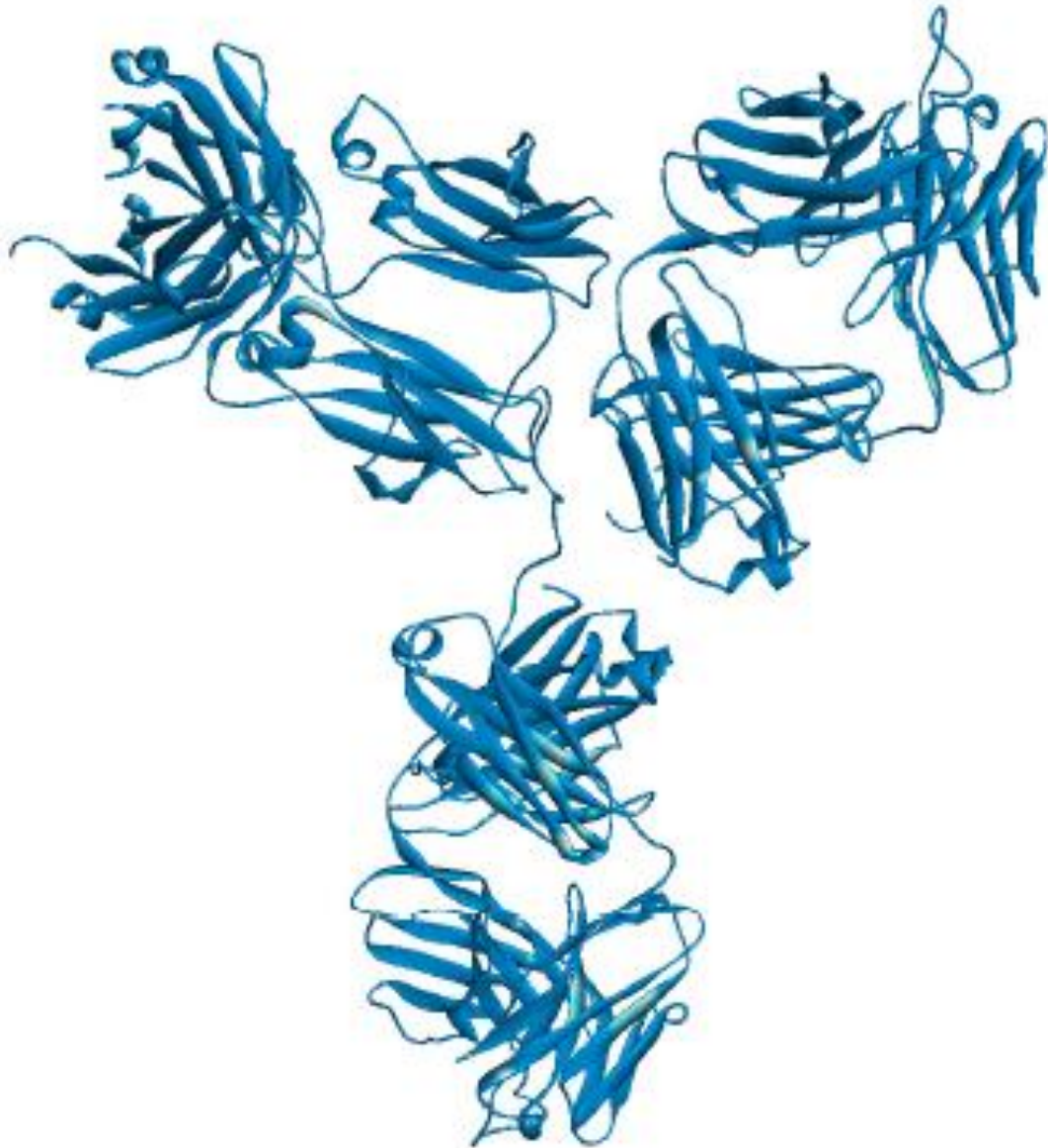
Figure 2-1: 3D model representation of an IgG1 antibody. Protein sequence downloaded from PDB file 1HZH and modelled using Discovery studios.

This study will primarily look at IgG1 and IgG4 antibodies and their homogeneous and heterogeneous interactions within bioprocessing. These are globular plasma glycoproteins with a mass of around 146 kDa (Wang and Ghosh, 2009) consisting of

two light and two heavy peptide chains folding to form two beta sheets, creating a sandwich shape held together by conserved cysteines and other charged amino acids.

The two identical γ heavy chains contain around 450 amino acids and consist of a constant and a variable domain. The light chains contain around 215 amino acids and again consist of a constant and a variable domain. These variable domains are the origin of protein specificity based both on their stereo-chemical and ionic characteristics (Janeway, 2001).

The heavy chains contain a linker region held together by sulphide bonding, which is flexible. This allows the dimeric heads to form the characteristic Y shape which will remain dynamic in solution allowing the arms to conserve more hydrophobic regions on the Fc region (Dangl et al., 1988). The correct glycosylation is essential for the IgG to bind to its receptors (Male, 2006).

2.1.2 The bispecificity of IgG4

IgG subtype 4 behaves differently from normal IgG1 antibodies. They were found to be unable to precipitate purified antibodies (van der Zee et al., 1986) since they are unable to cross-link two antigens due to monovalent behaviour (Aalberse et al., 1983). Additionally, it was found that IgG4 half molecules were present in SDS-PAGE analyses of normal molecules (Colcher et al., 1989, King et al., 1992) but under non-denaturing conditions these half-molecules were not detected (Schuurman et al., 2001). Finally, with the use of size exclusion chromatography, a large number of IgG4 molecules were found to be bi-specific, due to the presence of two different antigen binding sites. This led to them being less effective at inducing inflammatory responses and in fact made them able to inhibit the inflammatory effects of other antibodies (Schuurman et al., 1999).

It has been posited that the Bispecificity is a result of a single Amino Acid change relative to IgG1, which is the change of a proline to a serine in the core of the hinge

of IgG1 (Aalberse and Schuurman, 2002). This allows the molecule to disassociate from this hinge and give two identical monomeric halves, each containing one light chain and one heavy chain. The bi-specificity is observed when two different IgG4 monomeric halves reform together to give a whole bi-clonal antibody.

2.1.3 The IgG hinge

Considerable work has gone into defining the role of the hinge on the effector functions of an antibody. For IgG this hinge can generally be divided into upper, middle and lower regions. The middle hinge stretches from the first to the last of the cysteines that form disulphide bridges and is believed to be rigid due to inter-heavy-chain disulphide bridging and subsequent formation of polyproline helices (Lu et al., 2007). It is considered that the hinge region acts as a spacer effecting segmental flexibility and allows the Fab arms to move in relation to the Fc (Dangl et al., 1988). Further work shows that changes in the amino acid sequences could affect the rigidity of the hinge, which in turn affected the effector function of the antibody (Dall'Acqua et al., 2006a). Studies show that IgG4 has less flexibility in the hinge region than IgG1 and that this correlates with a reduction in stability between the two subgroups (Heads et al., 2012, Kilar et al., 1985). This correlates with a perceived greater stokes radius of the IgG4 subtype.

2.1.4 Protein aggregation

Protein aggregation is a major concern in the production of recombinant protein therapeutics in bioprocessing (Jimenez et al., 2007). In simple terms, it is when many protein monomers adhere to each other through a variety of different types of bonds to form a larger multimer. There is no real end to an aggregation process with many different routes to get to an aggregated state. Very little is known about the specific reactions that drive the process.

Changes in conditions that alter the proteins chemical and physical stability can result in precipitate or aggregate formation (Pease et al., 2008). Precipitation can be used advantageously in certain bioprocesses such as the precipitation of IgG from bovine serum albumin (Venkiteshwaran et al., 2008), but for the majority of purposes aggregates are a negative phenomenon.

Protein aggregates can form from protein-protein interactions alone or from nucleation on foreign micro and nanoparticles that have been shed into the system. The levels of these aggregates can be changed by many factors relevant to the commercial production of proteins.

Stresses, such as shear, directly disrupt the shape of native protein molecules, causing hydrophobic portions of the proteins to then become exposed to the aqueous environment. Interaction of hydrophobic portions allows binding to other similarly affected proteins (Bekard and Dunstan, 2009) and significant amounts of aggregates can form over the typical timeframes relevant to modern pharmaceuticals and under the stress conditions they are exposed to.

It has been well established that these protein aggregates in therapeutic protein products can enhance immunogenicity, leading to the need to remove the aggregates from the product (Carpenter et al., 2009).

To be able to study aggregation, it is necessary to be able to define the type of aggregate that will be discovered. It has already been mentioned that there are different routes to arrive at an aggregate, but due to the lack of classification criteria available it is hard to create discrete classifications of aggregates. Previous work (Philo, 2006) has suggested the use of multiple categories to classify protein interactions, which are further defined:

Reversibility

This is a measure of whether the aggregate, once formed, will revert back to active monomers. There should be a distinction between aggregates that perform this

process of their own accord over time, and those that have to be re-suspended with the aid of an operator or technician. In general, only the smaller species are reversible. Reversible Self Association (RSA) is a further phenomenon that relies on weak intermolecular interactions and will be described in full later.

Size

Definition of size would need the use of several ranges. A sensible division (Mahler et al., 2009) would be:

Small multimers, such as 2 to 10 monomer units

Small sub-visible, soluble particles, up to 1µm in size

Large sub-visible, insoluble particles, up to 25µm in size

Large visible, insoluble particle

Type of Bond

This is a measure of the strength of the forces used to hold the proteins together in the aggregate. Weak bonding could be through forces such as Van der Waals interactions, hydrogen bonding, hydrophobic and electrostatic interactions (Mahler et al., 2009). Stronger covalent interactions can be the result of disulphide bond linkages or non-disulphide cross-linking pathways (Andya et al., 2003).

Protein Conformation

The conformation of the aggregated protein subunits can form a measure of the amount of change in protein native structure that was required to cause the aggregation.

It has to be noted that in some cases, insoluble aggregates can be related to the precipitation of host cell protein impurities, and not the product itself (Shukla et al., 2007a).

2.2   Reasons for prevention and removal of aggregation

With the expanding production of bio-therapeutics, removal of protein aggregates, either by stopping their formation or by physical or chemical removal, is of ever-greater importance to the bioprocess industry. Since 2007, antibodies have been the highest selling category of biologics, with a market value of around $50 billion which is estimated to rise to just under $70 billion in 2015 (Visiongain, 2008). In a recent review of pharmaceutically relevant monoclonal antibodies and Fc fusion proteins, around half of them were found to possess aggregation issues following protein-A purification (Shukla et al., 2007a). If it is possible to stop or reverse 10% of the aggregates formed and removed throughout the process, this will be greatly financially beneficial.

A highly important factor is the loss of bioactivity of the formulation (Sluzky et al., 1991, Pease et al., 2008), which will effect the dose required by a patient. This again affects the profitability of the process, as a higher level of protein in each dose will mean less overall doses per batch.

Of greatest importance is that aggregates can elicit an immunological response in patients (Joubert et al., 2012, Chennamsetty et al., 2009a) that could involve neutralisation of antibodies, cross reactive neutralisation of endogenous protein counterparts or anaphylaxis. This is the reason for the strict guidelines on their removal.

There are currently very few published studies to comprehensively try and investigate the range of parameters that influence the level of immunogenicity of aggregates. It has however been reported (Carpenter et al., 2009) that large protein assemblies with repetitive arrays of antigens in which there is still a majority of natively conformed protein molecules are the most potent at inducing immune responses. In the same report, it was found that the adsorption of antigenic proteins

to nano or micro particles of different materials have the ability of greatly increasing the immunogenicity of the protein.

It is likely that patients' status and the treatment protocols the drug is used in have a critical effect on determining the propensity of the drug to produce an immune response.

Additionally, it has been reported that sufficiently large insoluble aggregates have the ability to mechanically block capillaries, causing reduced microcirculation in postischemic patients (Lehr et al., 2002).

2.3   Analytical methods

Due to the wide usage of proteins in therapies, there is a great need to be able to monitor and characterise protein solutions both in the research phase and during bioprocessing. At research phase, there is a great amount of testing to help characterise the protein and the solutions produced in the potential processes. At production level this monitoring occurs both at various points during production to ensure compliance to validated standards and in storage conditions to monitor solution degradation.

For protein aggregation in bioprocessing, current guidelines state that aggregation should be measured using the light obscuration method as described in the European pharmacopoeia methods 2.9.19 (PE, 2008) and the US pharmacopoeia (USP) <788> (USP, 2008). The guidelines state that particulates greater than 10μm in size should be controlled at or below 6000 particles per container, while particulates greater than 25μm are to be controlled at less than 600 particles per container (Carpenter et al., 2009).

The method uses the opalescent properties of the colloidal protein solutions to give a measure of the turbidity of the solution. The solution is either compared with a reference suspension under defined light conditions to determine the turbidity or an

optical density measurement is taken at around a 350nm wavelength, which could give comparable results to turbidity, but is dependent on the specified method (Mahler et al., 2009).

For research purposes, there are a great many more techniques for measurement employed, and there is no universal method for characterising protein aggregates. This is partially due to the fact that there is no technique that universally covers the entire size range of protein aggregates that can range from nanometre to millimetre sizes. The size ranges of some common techniques are given in table 2-1.

As well as differences in the size ranges measured, the techniques available can give different sizes for comparable samples due to differences in what inherent property of the protein is measured by the technique. One such example being the measurement of the hydrodynamic diameter in light scattering that gives an unrepresentatively large size for fibrilar aggregates.

Table 2-1: Table of functional parameters of detection techniques

Method	Range of operation	V	time	Shape estimation
Static light scattering	1nm to 5µm	50 µL	online	yes
Dynamic light scattering	1nm to 5µm	50 µL	online	no
Refractive index	All	50 µL	online	no
Light obscuration	2µm to 300µm	500 µL	online	no
Electron microscope	1nm to 70µm	10 µL	1 day	yes
Field Flow Fractionation	1nm to 100µm	10µL	2 mins	no
AUC	1nm to 1µm	150µL	1 week	yes
EDMA	2nm to 250nm	1 mL	1 day	no
SDS-PAGE	<1nm to 400nm	200µL	12 hours	no
SE-HPLC	<1nm to 500nm	10µL	1 hour	no
MFI	3µm to 100µm	0.5 - 300µL	200µL/min	yes
Nanosight	25nm to 2µm	0.3 - 0.5mL	10 mins	no
Circular Dichroism	200nm	0.8 mL	1 hour	yes

2.3.1 Detecting aggregates
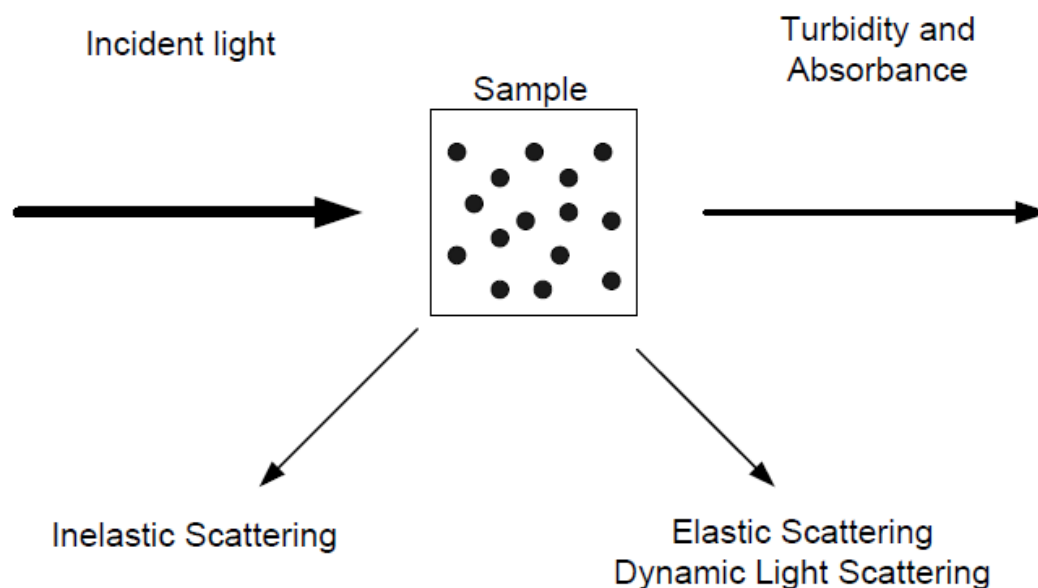
Figure 2-2: **Diagram of angle of measurement used by various light techniques.**

There are many different techniques that could be used to determine the size of proteins and their larger aggregates. The previous section highlighted a few of the most popular and useful methods available. The information given showed that there is a lot of variety in the range of operation of the methods, the sample volumes needed and the times taken to perform the tests. To find the best way of identifying potential aggregate species, all these factors must be taken into account and a compromise between range, time, volume and reliability of results must be made.

The time taken for measurement may be greater than the lifetime of a reversible aggregate, or the measurement techniques themselves may destroy or create further aggregates, posing further challenges for analysis (Philo, 2006).

Factors involved in the analysis that can perturb the distribution of aggregated species include dilution, change of solvent conditions, adsorption to surfaces, physical filtration or disruption, concentration on surfaces and shear (Philo, 2006).

Figure 2-2 shows the different paths that scattered light can follow, with various techniques able to take readings and determine various attributes of the sample.

2.3.1.1 Static light scattering

Static light scattering is a technique from physical chemistry in which a monochromatic light source and multiple detectors are used to measure the intensity of the scattered light to give a value for the average molecular weight of the macromolecule in solution. By measuring the intensity at many angles it is possible to calculate the root mean squared radius of the species.

The sample to be tested should be optically clear and can be quite concentrated meaning little preparation could be necessary to give real time data. The ability to detect in real time can allow the viewing of the kinetics of protein aggregation.

To calibrate the machine, the laser intensity and quantum efficiency of the detector and the full scattering volume and solid angle of each of the detectors is determined by using a known scatterer such as toluene. The calibration will also include normalisation of each detector to the 90° angle detector to take into account the slightly different quantum efficiencies, gains and scattering volumes using an isotropic scatterer.

The results from a static light scattering experiment are input into equations, such as the Zimm equation, to calculate the average molecular weights of the species (Chu, 1991). Furthermore, characterisation of the excess Rayleigh ratio (R) against the composition of a multi-component aggregate may determine the stoichiometry and equilibrium binding affinity of the system as well as binding and dissociation kinetics (Some, 2012).

2.3.1.2 Dynamic light scattering

Dynamic light scattering is another physical chemistry technique where the scattered light intensity measured is proportional to the protein concentration and the hydrodynamic radius of small particles in suspension (Rosenberg et al., 2009).

The theory of the technique is that the light scattering from the particles will give a time-dependant fluctuation that is due to the Brownian motion of the molecules in solution changing the distance from the laser source. This light will additionally undergo both constructive and destructive interference from the surrounding particles. This fluctuation will contain information about the timescale of the particle movement.

The intensity trace can be used to generate a second order autocorrelation curve to elucidate the dynamic information of the particle movement (Chu, 1991). The mAb monomer is generally the first peak at 10nm mean hydrodynamic diameter, with aggregates typically having diameters larger than 100nm (Rosenberg et al., 2009).

A feature of dynamic light scattering is that large particles are very highly sensitively detected, due to an exponential increase in light intensity with hydrodynamic radius (Ahrer et al., 2003). This means that the technique can be very effective for detecting precursors to larger visible particles and tracking sources of stress or damage (Philo, 2006).

2.3.1.3 Refractive index

The refractive index is a fundamental physical property of a substance and can be used to identify particular substances in solution. It is measured with either a refractometer or interferometer in the optical domain. The refractometer measures the ability of the substance to bend light that passes through the solution. It is intimately related to the extinction coefficient and can be computed with ease together with the extinction coefficient to give the complex refractive index.

2.3.1.4 Light obscuration

As previously mentioned, current guidelines state that aggregation should be measured using the light obscuration technique. The method is described in the

European pharmacopoeia methods 2.9.19 (PE, 2008) and the US pharmacopoeia (USP) <788> (USP, 2008).

The opalescent properties of the colloidal protein solution are used to give a measure of the solution's turbidity. The method looks at the reduction of light intensity due to reflection adsorption and scattering as a particle crosses an incident laser beam. This optical measurement is normally taken at around the 350nm wavelength. The decrease in light intensity is proportional to the particle size, so if the particle is spherical a particle size distribution may be given.

2.3.1.5 Fluorescent dyes

Fluorescence has long been used to detect biological molecules and cells (Petushkov et al., 1996, De Foresta et al., 1996). It has not classically been used to detect aggregation in protein solution but recently dyes that begin to fluoresce when aggregates are present have begun to appear on the market including Proteo-stat®, Nile red and Thioflavin T (Hawe et al., 2008, Filipe et al., 2009). The fluorescence intensity of these dyes can be correlated to the concentration of aggregate present in the sample.

2.3.2 Particle sizing of aggregates

Techniques to determine the molecules in solution are often unable to give a reliable result without separating out the components of the solution before testing. Many techniques have been developed for the purpose of separating protein aggregates and most can be used with the multiple online detectors in series 'behind' the technique.

2.3.2.1 Asymmetric field flow fractionation

Asymmetric field flow fractionation (AFFF) is a powerful analytical technique where a sample pulse is made to flow into a perpendicular stream which possess an

asymmetrical flow pattern that separates the pulse's constituents based on their molar mass and size. The principle is shown in figure 2-3. Using the technique it is possible to calculate the diffusion coefficient and the hydrodynamic size from the retention time. It is also possible to use the information to elucidate the structure and conformation of the particle.

The flow pattern is produced due to two factors. Firstly, the retardation effect of the walls of the second stream and the filter on the wall opposite the incoming pulse. Secondly, by the shape of the second pipe itself. There is no pre-treatment of the sample required and material can be separated over a large range with high resolution.

Sample injection

Variable
Flowrates

Filter
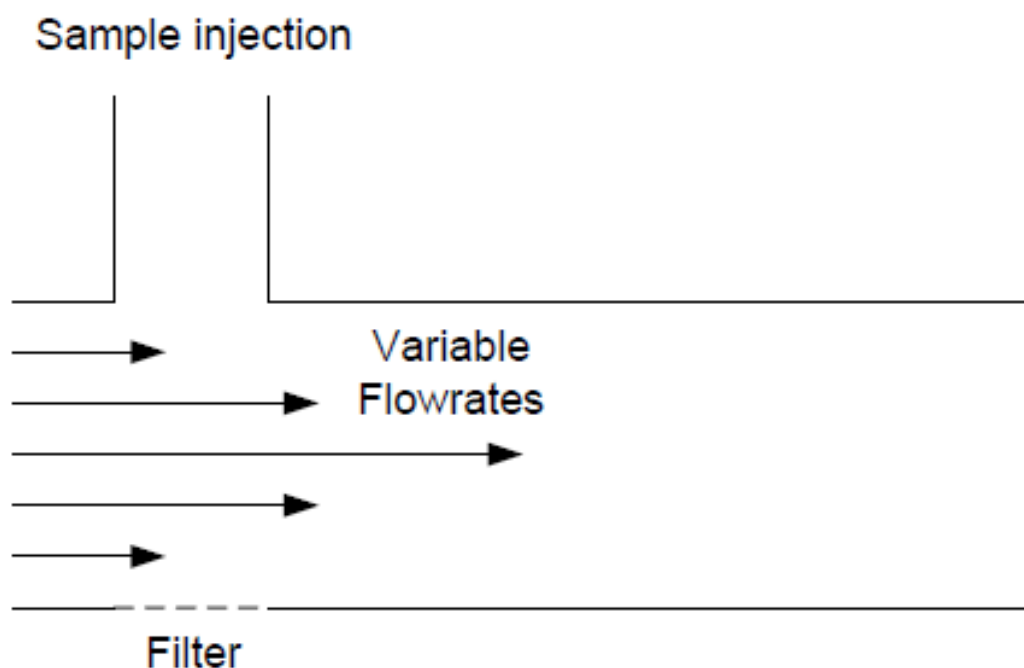
Figure 2-3:   Diagram of AFFF fluid velocities and sample injection point.

The traditional difficulty with AFFF is that the technique is too versatile and so there is no simple way of choosing a sub-technique or the experimental variables, which include the field type, instrument configuration, channel structure, operating mode and experimental conditions. Accordingly, a good understanding of the mechanism

of operation and a high level of experience is needed to apply the principles to a new process.

There are two main sub-techniques which would be applicable to antibodies and their aggregates. For the monomers and smaller aggregates, there would be a normal mode of operation where the smaller particles would elute first. For particles larger than 1µm, steric mode would be used and the larger particles would elute first. Around the 1 µm size, a mixed mode separation may also need to be used.

For antibody separation, aqueous solutions such as PBS buffer would typically be used, with a pH and ionic strength to match the sample solution. Samples would be loaded in the solution at concentrations from 0.01-10mg/ml to give sample sizes of 10µL. Ceramic frits would be used at the inlet and outlets of the system with possible detectors including UV, DLS or fluorescence to determine protein size. Samples with well known diffusion coefficients or hydrodynamic diameters can be used as standards to calibrate the system before use.

2.3.2.2 Analytical ultracentrifugation
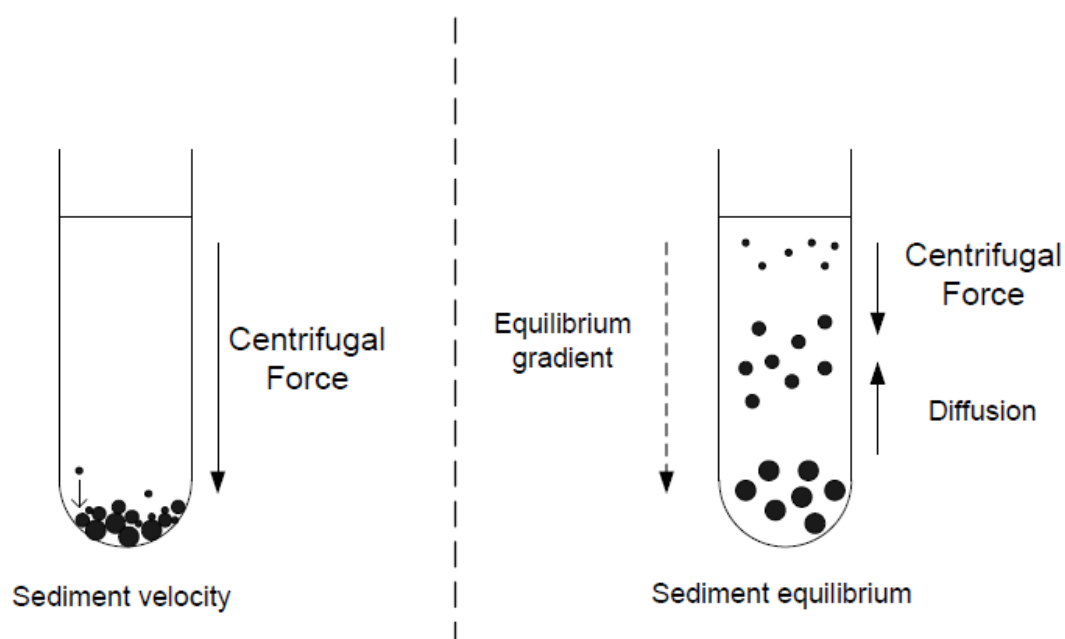
Figure 2-4: Diagram of modes of action for sediment velocity and sediment equilibrium modes of AUC.

Analytical ultracentrifugation (AUC) is a very powerful technique that involves the use of gravitational effects to determine mass (Liu et al., 2006). The process has a lengthy run time, requires highly specialised operators and is expensive, but its use is becoming increasingly more widespread as a technique. Reasons for the increased employment of this technique include the possibility of little sample preparation, not having to compare results to any standards and the size range achievable, which is from 1 kDa to over 1 gDa.

The concept of operation is that of a centrifuge with an optical system synchronised to the rotation of the sample. Samples need to have optical densities between 0.1-1.5 to allow the optical system to detect the aggregates. The peptide backbones can be characterised by analysis at the 230nm wavelength.

A concentration dependent analysis of the behaviour of the molecule of interest gives an information rich dataset which is effective for characterising the solution properties of the proteins. For this reason it is common to use at least three different concentrations of sample with the widest range.

There are two main modes of operation with this equipment shown in figure 2-4:

Sedimentation Velocity

High centrifugal forces are used and the sedimentation process times are recorded.

Sedimentation velocity can be used to analyse interacting systems and data can be collected over a large range of loading concentrations and molar ratios in a wide range around the K_d.

Sedimentation Equilibrium

Low centrifugal forces are used and the diffusion balances the sediment in an equilibrium gradient.

Sedimentation Equilibrium can be performed when there is no change in the concentration distribution of any of the components of the solution. The time taken to attain results is proportional to the square of the height of the solution column. For a molecule of around 200kDa in 100 to 180μL of sample will take between one and two days to perform. The information content of the concentration profile significantly increases with larger column heights.

A lot of analysis is only possible with highly specific software, by fitting sedimentation equilibrium data with specific models to determine the binding constants

The method can distinguish between kinetic dissociation rate constants in the range of 10^{-2} to 10^{-5} s^{-1} and affinities in the range of 104 to 108 M^{-1}. The quantities required to perform the tests are only between 100 to 400μg of solution.

The principle behind the method is that each particle is affected by three forces to varying degrees. These forces are gravitational, buoyancy and frictional and the balance of these forces will define the behaviour of each species. The definitions of these forces are given in equation 2-1. It is important to note that the density effects of glycosylation, bound detergents and preferential hydration could all be relevant factors in the molecule characterisation (Aziz et al., 2005).

Equation 2-1:   Equations for sedimentation equilibrium mode of AUC.

$$
\begin{aligned}
\text{Gravitational:} \quad & F_{sed} = m\,\omega^2\,r \\
\text{Buoyancy:} \quad & F_b = m\,u\,\rho\,\omega^2 \\
\text{Frictional:} \quad & F_f = s\,(kT/D)\,\omega^2 \\
& s = V/\omega^2
\end{aligned}
$$

ω — Rotor angular velocity
u — Effective protein partial-specific volume
k — Boltzmann constant
D — Diffusion constant
T — Absolute temperature
V — Absolute migration volume

2.3.2.3 Electrospray differential mobility analysis

Electrospray differential mobility analysis (EDMA) is a technique that involves the electrospraying of aqueous protein solutions to give an aerosolized mass where various species are separated according to their electrophoretic mobility using a differential mobility analyser (Pease et al., 2008). Conceptually, it is similar to electrospray mass spectrometry, with the important difference that its operation at atmospheric pressure means that proteins are separated according to their charge to aerodynamic size ratio.

The Electrosprayed ions pass through a chamber to standardise the charge on each droplet to +1, 0 or -1 (Bacher et al., 2001) allowing the effective diameter of the particles to be directly determined. Using this method, it is possible to detect aggregates from 3 to 250nm with single monomer resolution, thus allowing the characterisation of the initial forms of aggregation. Additionally, it is possible to distinguish between the IgG's heavy and light chains after denaturing and cleavage of the disulphide bridges (Pease et al., 2008).

2.3.2.4 SDS-PAGE

Sodium dodecyl sulphate polyacrylamide gel electrophoresis is a widespread technique used in biology to separate out proteins based on a function of their molecular weight known as the electrophoretic mobility.

The method involves mixing the protein solution to be analysed with SDS and heating to 60°C to denature secondary and non disulfide linkage structures then applying a negative charge to each protein, proportional to its mass as demonstrated in figure 2-5.
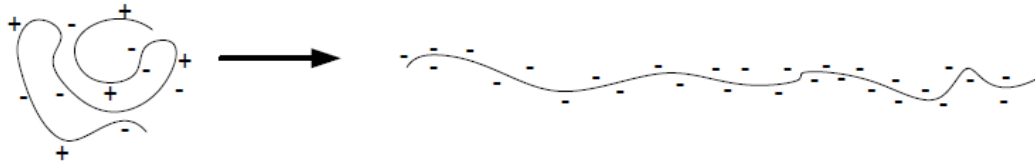
Figure 2-5:   **Mechanism of protein unravelling caused by SDS.**

Different anode and cathode buffers are prepared covering the positive and negative electrode respectively before the denatured sample proteins are applied to the cathode end of the gel with a pipette. Attaching a power source to the electrodes will then begin separation of the protein bands by causing the negative charges to migrate towards the anode. The proteins will move differentially through the porous gel matrix, shown in figure 2-6, based on their size, with smaller proteins able to move faster through the gel.

The rate of protein movement through the gel is also determined by the voltage applied through the gel, with a higher voltage producing a faster movement, but this comes at the cost of protein resolution. The voltage is removed after a set amount of time, usually a few hours, and the proteins will have been separated roughly according to their size.
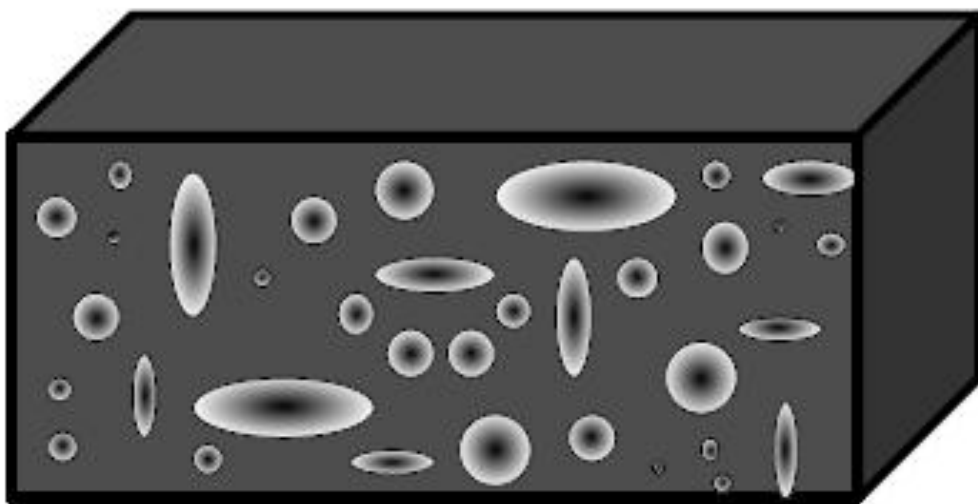
Figure 2-6:   **Two dimensional representation of the pores available for substrate infiltration in a standard polyacrylamide gel.**

To view the results, the gels are stained, usually with Coomassie Brilliant Blue R-250. This shows the separated proteins as distinguishable bands along the gel. Molecular markers of known molecular weight are often run in a separate lane in the gel to calibrate it and determine the unknown proteins weights (Dunn, 1993).

2.3.2.5 Size exclusion chromatography

The mechanism of separation is dominated by a sieving effect of a complex 3D network of beads which hinder the diffusion of the feed into the bead interior (UCL, 2010). The beads will hinder the components of the solute to varying degrees dependent on the size of the components. The smaller the molecule, the more complex the route it will take through the chromatography column and therefore the longer it will take to exit. Conversely, the larger the molecule, the more it will be excluded from the pores and so the faster it will flow through the column. This is visually represented in figure 2-7.
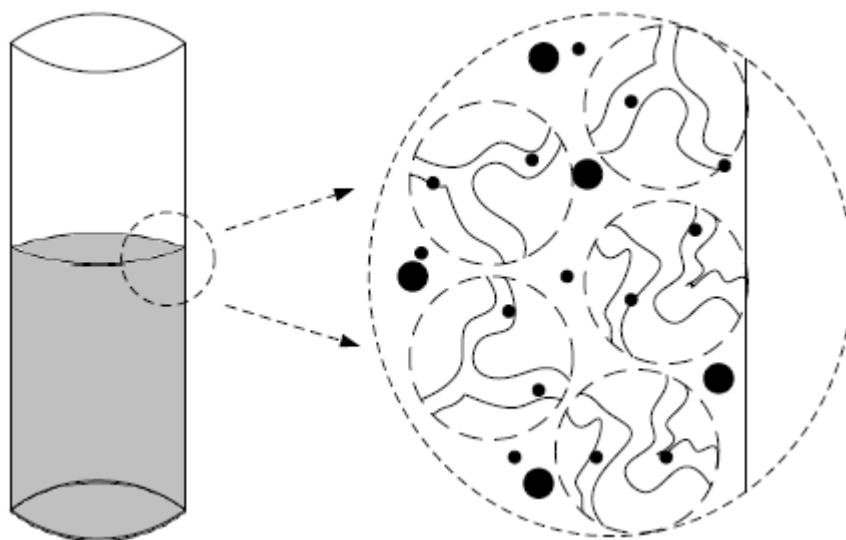
Figure 2-7:   **Representation of differential paths available to different sized particles in SEC.**

A longer column gives a higher resolution and so a greater separation of the aggregates in the feed. The pore size distribution and number of pores of the matrix also affects the resolution of the column.

HPLC (High performance Liquid Chromatography) is a specific type of analytical chromatography that uses smaller beads and pores to increase the resolution of the column. This requires a high pressure pump to push the liquid phase through the column and so increases the pressure of the system. To reduce the compression of the beads inside the column, very small diameters are used to increase the wall support on the column matrix.

Insoluble aggregates may be excluded, resolved or modified by the column (Rosenberg et al., 2009) and some can have a disproportionate hold time in the column because of interactions with the column matrix. This can give false results for sizing of aggregates and so chromatography on its own is not advised for determining the species.

Previous work has been done to characterise eluate from SE-HPLC columns and it was determined that a protein complex containing carbohydrates required a method involving on-line light-scattering, absorbance and refractive index indicators to calculate the Molecular weight and determine the stoichiometry of the molecule (Wen, 2008).

The method uses a circular argument to find the best fit target molecule within multiple assumed stoichiometries that would fit in with the results. To work out the molecular weight and stoichiometry of a complex requires the polypeptide extinction coefficient but the protein extinction coefficients are usually the only values known. The protein extinction coefficients can be used to work out the coefficient for the complex that is then used to work out the molecular weight of the complex (Wen, 2008).

2.3.2.6 Micro flow imaging

Micro flow imaging (MFI) is an imaging technology that has recently been applied to detecting and measuring sub-visible and visible particulate matter in protein containing solutions (Sharma et al., 2007). The technique captures digital images of

particles suspended in a feed as it flows by a digital camera, allowing different sub-populations within this feed to be counted and archived using different adjustable criteria.

The software can then create a database of particles and the results can be used to create particle distributions and to isolate particle subpopulations.

The strengths of this technique are the impressive ranges of operation. It can detect concentrations ranging from 5 to 800,000 parts per mL, at volumes between 0.5 to 300 µL, operating at a rate of processing 200 µL per minute. MFI also allows the user to check for any non-conforming particles or any precipitations or dissolutions in the sample. The particle size range detectable by MFI is also considerable, ranging from 0.75 µm to 100 µm (Huang et al., 2009).

This means that the method is able to measure particles both in the visible and sub visible size ranges using a limited quantity of material with a reasonable level of throughput.

Unlike light obscuration, MFI is able to give accurate size readings for non spherical protein particles, as well as particles that possess a refractive index similar to their solvent (Huang et al., 2009).

This allows the accurate and reproducible detection and quantification of protein particles to monitor characteristics including shape, size and opacity, which could provide a basis for understanding the nature of particle formation.

To summarise, MFI offers the advantages of manual microscopy with the benefit of higher sensitivity, automation, broad size ranges and low sample requirements.

2.3.2.7 Nano-particle tracking
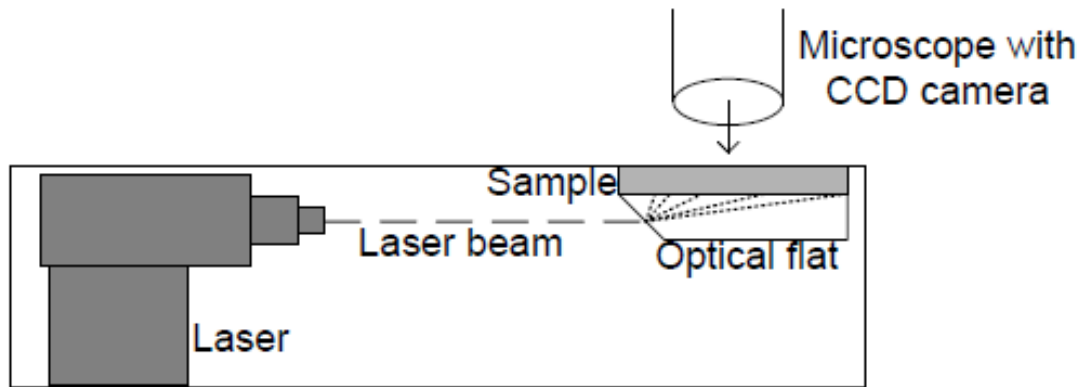
Figure 2-8:   **Diagram of hardware used in Nanosight analysis.**

The Nanosight is a nano particle tracking system developed by Nanosight Ltd to allow the direct visualisation of individual nanoscale particles in suspension to give immediate, independent, quantitative estimations for particle size (hydrodynamic diameter), size distribution and concentration.
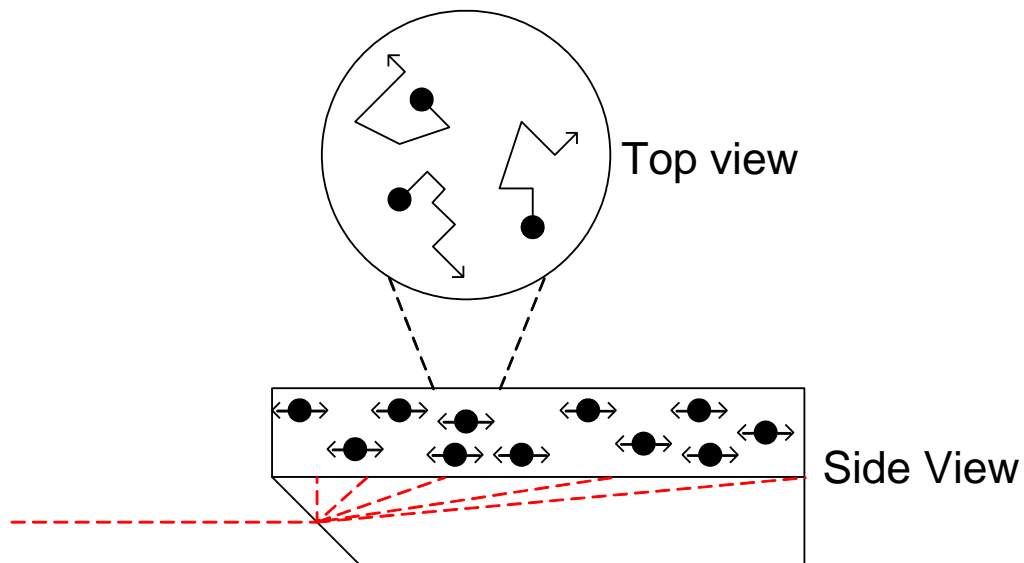
Figure 2-9:   **Mode of action of Nanosight technique.**

The technique uses a finely focused 635nm laser beam and a prism edged optical flat to refract the beam onto a liquid layer above the prism. Compression of the beam gives a low profile intense illumination which is visualised using a 20 times magnification microscope objective and CCD camera operating at 30 frames/second, as shown in figure 2-8. This camera tracks the Brownian motion of

the nanoparticles, separately visualising and tracking each particle and analysing its properties as shown in figure 2-9. This can give quick results for poly-disperse heterogeneous samples with experiments showing that the diameter readings are more accurate than DLS and MALS at multiple concentrations (Nanosight, 2009).

2.3.3 Determining morphology of aggregates

2.3.3.1 Circular dichroism

Circular Dichroism (CD) gives a measure of the difference in absorbance between left and right handed circularly polarised light in the far UV spectrum usually using a xenon source. CD spectrometers can record this difference as a function of the wavelength, temperature and chemical environment, to give absorption bands of chiral molecules. The light is rotated around its propagation direction to give a left or right handed helix, which causes a displacement of charge upon interaction with a molecule. The two oppositely chiral beams will react differently with chiral molecules allowing the difference to be measured

The spectra are useful for characterising the secondary and tertiary structure of the molecule and for determining the structural family to which it belongs. This allows the comparison of proteins from different expression systems or the study of the conformational stability of the protein under different stresses or conditions.

Far UV spectra (<250nm) give the secondary structure protein characteristics and can be used to estimate the fractions of the molecule that are in the different conformations. Near UV spectra (250-300nm) provide information on the tertiary structure of the molecule, although the traces cannot readily be assigned to particular 3D structures.

Issues with use of the system for biological applications involve the use of buffer solutions. Typical buffers such as phosphate, acetate and carbonate differentially absorb the beams making them incompatible unless extremely dilute. The system is

also less specific than comparable crystallography or spectroscopy methods, which can give more information such as atomic resolution data. CD is however a quick, low sample requiring, low data processing method that can be used on experiments involving large numbers of variables (Fasman, 1996).

2.3.3.2 Spectroscopy

Spectroscopy is the use of electromagnetic radiation to measure a quantity as a function of wavelength. The results are usually in the form of a spectrum of the response of the quantity at varying wavelengths and show an average of the entire molecular population.

Nuclear magnetic resonance imaging utilises the fact that an atom will absorb electromagnetic fields and radiate the energy back out at specific frequencies dependent on the strength of the field and the atom. The method analyses the magnetic properties of atomic nuclei, such as hydrogen, to determine different local environments. This can be used to help elucidate the compound's structure.

Absorbance spectroscopy works on the basis that different material will absorb light at different wavelengths to varying degrees and this can be quantified by measuring the transmission.

Simple forms of spectroscopy like near infrared spectroscopy shine monochromatic light through a sample and measure the transmission and then repeat for each different wavelength. This near infrared range can be used for biochemical testing and is often employed for particle sizing.

Similar but complementary information is provided by Raman spectroscopy, which relies on inelastic light scattering to shift the energy levels of laser light. This method can be used to determine changes in the secondary structure or hydrophilic exposure of any side-chains. It is also able to identify reversible and non-reversible changes by determining the presence of more disordered structures common in unfolded proteins (Chen et al., 1974).

A detailed study into using ultraviolet Raman spectroscopy (Lednev et al., 2009) reports that the method is capable of detecting structural intermediates at early stages of fibrillation and determining their sequential order using 2D correctional analysis. The same report states that since the method does not require isotope labelling, it can be used for comparative characterisation of β-sheet structure in fibrils made from fragmented or full proteins and the real time kinetics of formation can be monitored.

Fourier transform spectroscopy is a more developed method to get the same information and involves passing a beam containing multiple frequencies through the sample and measuring how much of the beam is absorbed before changing the composition of the frequencies and repeating. After many repetitions the data is computer analysed to infer the absorption at each wavelength (Hammes, 2005).

Finally, there is mass spectrometry which uses the principles of ionization of chemical compounds to generate charged molecules that can have their mass to charge ratio measured. A promising mass spectroscopy method for biological analysis is matrix assisted laser desorption ionisation (MALDI) imaging. In MALDI analysis the sample is mixed with a matrix and placed on a metal surface. When the UV laser is fired at the matrix it is excited and charge-transfer moves the mix into the gas phase. This gas phase is then accelerated and detected (Bruggeman, 2010).

2.3.4 Assessing aggregation propensity

2.3.4.1 Self interaction chromatography

Self interaction chromatography (SIC) is a relatively unrefined technique to determine the Osmotic second viral coefficient (B_{22}) of antibodies. The antibody of interest is covalently immobilised on chromatographic particles and packed into a column before the same antibody is passed through the column. The retention time reflects the average protein interactions between free and immobilised protein. This

can then be linked to B_{22} by using the potential of mean force and is comparable to the results given by classical techniques (Tessier and Lenhoff, 2003).

In terms of sample volumes, the technique is currently capable of giving results from less than 2.5mg of protein at concentrations of up to 20mg/ml and each run is much faster than SLS.

2.3.4.2 Self-interaction nanoparticle spectroscopy
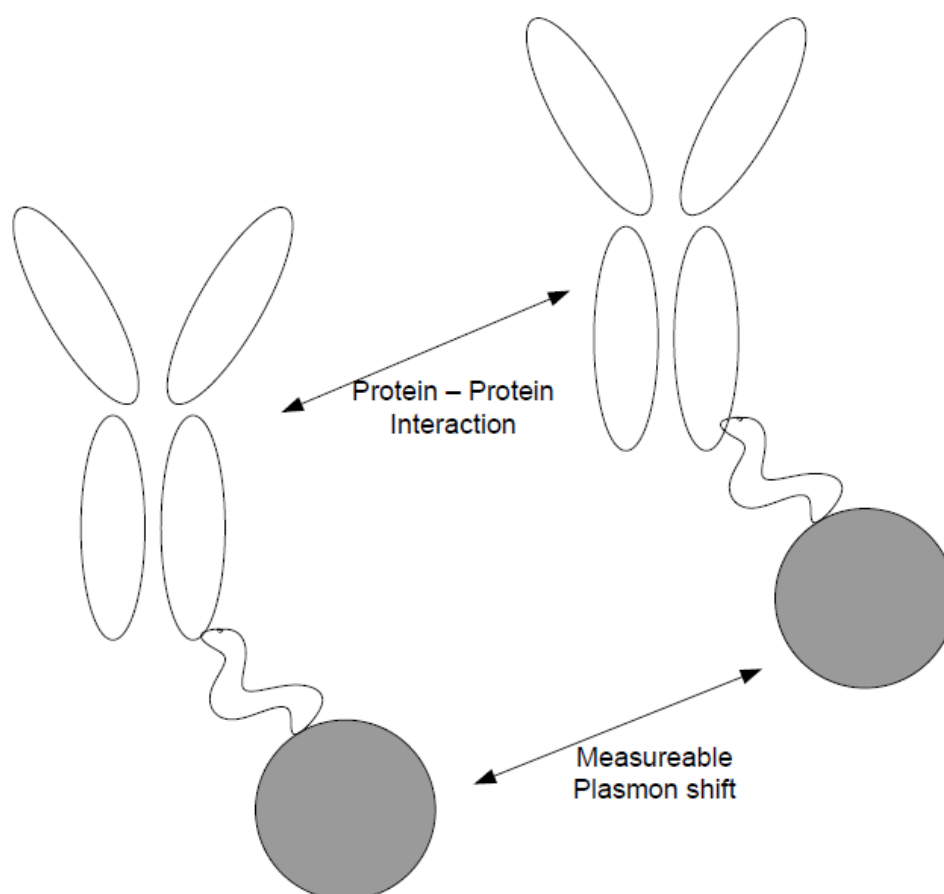
Figure 2-10: **Diagram of SINS mode of action.**

Self-interaction nanoparticle spectroscopy (SINS) is another technique to determine the B_{22} of a protein-protein interaction. The advantage of this method is an ability to characterise protein solutions in a parallel format for high-throughput screening. The method is rather new and suffers from a poor affinity of the proteins to adsorb to the nanoparticle surfaces, which complicates the analysis of the self-association

behaviour. Recent work however has been performed with a highly specific approach to coating the nano-particles with proteins, shown in figure 2-10, using biotin-avidin interactions to generate protein-nanoparticle conjugates that report protein self-interactions through changes in their optical properties (Bengali and Tessier, 2009).

The SINS method is based on the separation-dependent optical properties of gold nanoparticles which are utilized for characterising protein self-association. The surface Plasmon mode shifts to larger wavelengths as the interparticle distance between nanoparticles is decreased. Since B_{22} is based on the preferred separation distances of proteins, the Plasmon mode shift will be inversely correlated with it (Bengali and Tessier, 2009).

Using the method it is possible to perform 96 or 384 measurements in less than a minute using a standard plate reader and each sample requires less than a microgram of protein. However, the method is less quantitative than SLS or SIC. Currently, it is not possible to calculate the value of B_{22} from SINS with those conducting the research positing that the contribution of the particle size to the Plasmon shift needs to be separated from the contribution of the intermolecular protein interactions (Bengali and Tessier, 2009).

2.3.4.3 Interfacial shear device

The interfacial shear device method was developed at UCL where a previous EngD student used a custom made rig to produce a controlled shear environment using a spinning disc inside a 7ml thermally regulated chamber (Biddlecombe et al., 2007, Biddlecombe et al., 2009).

The device gives a measure of the relative stability of a protein by subjecting it to the environment of the spinning disc. It is shown that it is the adsorption of the proteins to the surface of the disc and subsequent removal that causes the proteins

to aggregate. The high shear environment present does not directly cause the aggregation of the proteins, but does contribute to the process by changing their conformation, providing good mixing, and helping to disengage proteins from the disc surface.
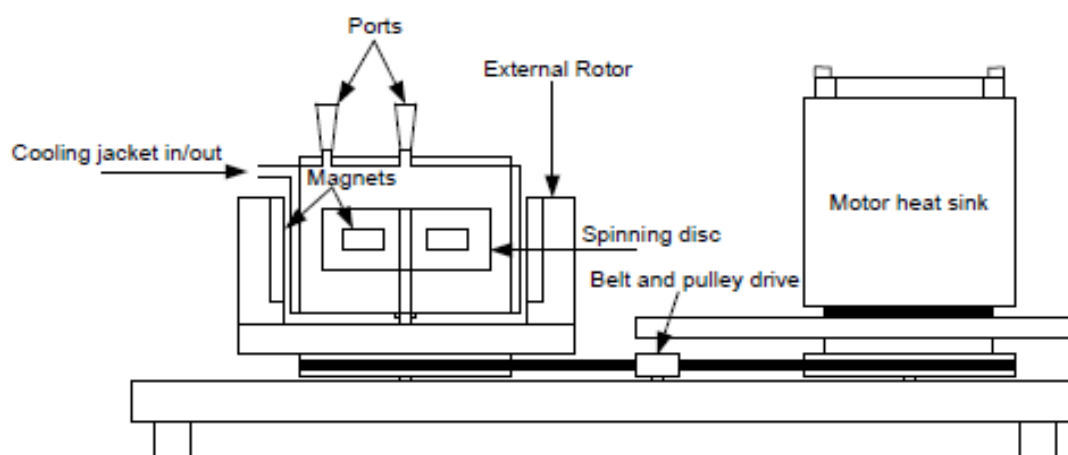
Figure 2-11: **Diagram of previously described shear device used in work by J. Biddlecombe at UCL.**

To get a measureable output, 0.1ml samples are removed from the chamber at 15 minute intervals using positive displacement. These samples are analysed using SE-HPLC to look at the level of monomer determined compared to the level in the sample at time=0. By taking samples for 2 hours, the relative monomer loss can be correlated over the operational period using the formula for an exponential decay curve:

$$C(t) = C_0 e^{-kt}$$

Where *C(t)* is the monomer concentration (mg/ml) at time *t* (h), *C₀* is monomer concentration at time zero and *k* is the protein decay coefficient (PDC) (h⁻¹). The PDC can then be used as a comparator between different antibodies at set conditions to give a measure of relative stability.

2.3.4.4 Computational modelling of aggregation propensity
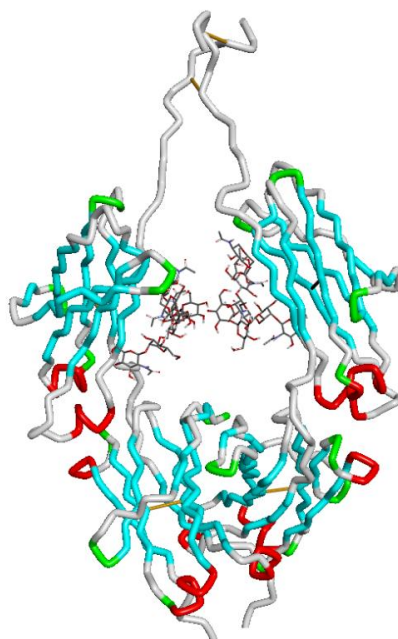
Figure 2-12: **Image of a fucosylated IgG1 Fc region as a molecular model.**

As technology advances, new methods are always being developed to help determine protein stability. With the huge strides forward in computer science, the ability to use computers to determine protein stability has become more sophisticated. What had begun with trying to fold proteins from a known sequence in the correct way (Sali and Blundell, 1993), had been developed to incorporate homology modelling from crystallographic data (Pearlstein et al., 2003) and a series of steps to give a better result for modelling the antibody shape (Combet et al., 2002).

Further advances in the field meant the models were able to look at electrostatic and hydrophobic properties of protein surfaces (Chennamsetty et al., 2009a, Chennamsetty et al., 2009b). These models could now be used to predict the effect of mutations (Oganesyan et al., 2009, Oganesyan et al., 2008, Chennamsetty et al., 2010) and the effect of glycosylation (Kayser et al., 2011) on the stability of the antibody.
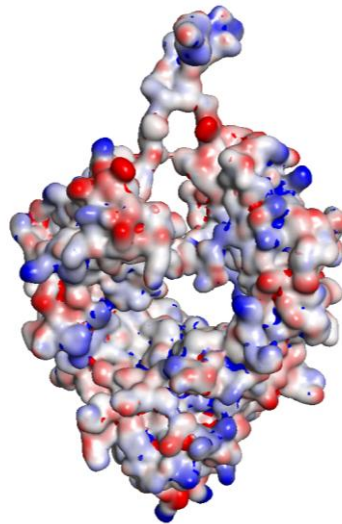
Figure 2-13:   Surface charge distribution on an IgG1 Fc molecular model.

Surface charge distributions have been utilized for some time, which break down the surface charge to positive, negative or neutral, as shown in figure 2-13. However, Spatial Aggregation Propensity (SAP) has become the preferred method for comparing the stabilities of antibodies as it allows various sites of aggregation propensity to be chosen and analysed in isolation (Agrawal et al., 2011) as shown in figure 2-14.
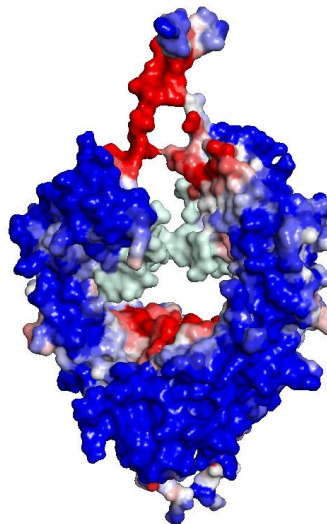
Figure 2-14:   Hydrophobic surface distribution from SAP analysis on an IgG1 Fc molecular model.

2.4 Factors affecting protein aggregation

2.4.1 Aggregation factors

2.4.1.1 Overview

To be able to halt protein aggregation there must be an understanding of the factors causing the aggregation to occur in the first place. Many studies have gone into determining the causes of aggregation of proteins and although there are still no definitive laws which have been set for the process, there are many trends that can be seen in the aggregation of many antibodies.
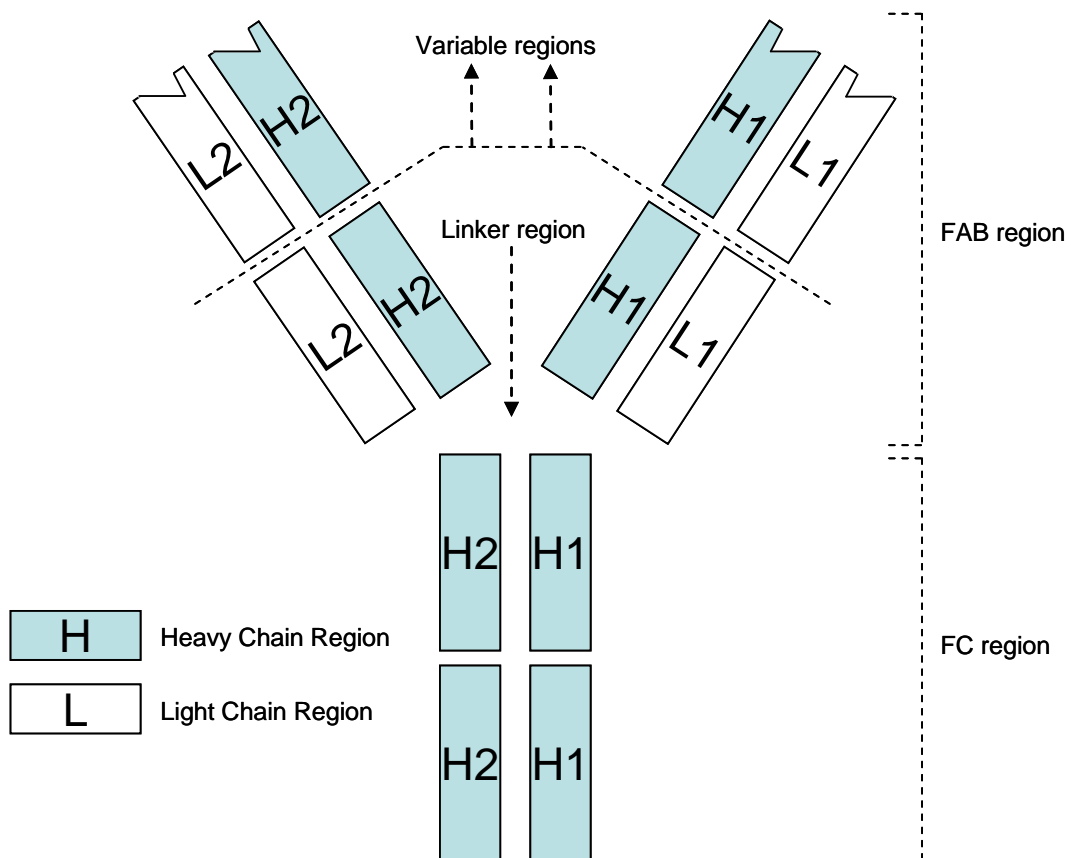
Figure 2-15: **Diagram of monoclonal antibody regions.**

In general, conditions that alter the proteins chemical and physical stability result in denaturation, precipitation, adsorption or aggregation (Pease et al., 2008, Mahler et al., 2005) in bioprocessing.

It has been shown in contrast to model proteins, that antibody stability is not necessarily dependent on protein concentration, buffer concentration, salt concentration or agitation, suggesting the mechanism of aggregation is counter intuitive and unlike other proteins (Perico et al., 2009).

Denatured protein shows a failure of the protein's tertiary and secondary structures and the transition to a denatured state can be direct or can pass through many other intermediary states. Once in this denatured state, aggregation comes into competition with refolding to the native protein structure depending on the level of unfolding it has been exposed to (Mahler et al., 2005). If the protein has been fully unfolded the refolding may result in non reactive molecules when refolded. The aggregation pathway leads first to soluble particles and then to insoluble macroscopic aggregates. However it has been reported that small sized reversible aggregates are more stable and resistant to aggregation than monomers (Sluzky et al., 1991).

Studies have looked into the use of spatial aggregation propensities (SAP) to predict the aggregation prone motifs and regions within monoclonal antibodies (Chennamsetty et al., 2009a). In these studies it was found that IgG1 has more aggregation prone motifs in the Fc fragment compared to the constant region of the Fab fragment. The highest concentration of these motifs was found around the lower hinge region close to the Fc. The motifs found were almost exclusively within the loop and hinge regions connecting the domains and very rarely within the β-sheet regions. Further work confirmed that antibodies within the IgG subclass have similar aggregation prone motifs.

It is accepted that aggregation occurs due to factors effecting protein stability during production, storage, shipping and handling. These factors can include Temperature pH co-solvents, surfactants, stabilizers, hydrophobic interfaces or surfaces (Mahler et al., 2005). Some proteins need to create an intermediate before aggregating,

which gives a lag time in aggregate formation (Sluzky et al., 1991), a phenomenon that will be discussed later.

It has previously been suggested that there is a need to investigate the protein conformations in aggregates (Carpenter et al., 2009) and that molecules absorbed to aggregates had been shown to be able to retain their native conformations.

As previously mentioned, cleavage sites for mAbs are located predominately in the hinge region of the heavy chain. It has been observed that the nature of this site specific fragmentation is driven by molecular kinetics from clipping of the antibody structure leading to a net increase in aggregation at elevated temperatures (Perico et al., 2009) and therefore not by protease contaminants. The same study found that this heterogeneity affected the overall conformation and flexibility of the antibody.

2.4.1.2 Hydrophobic interactions

Hydrophobic interactions are important in the aggregation of proteins. This importance has been proved in experiments where mutations were engineered in proteins to reduce hydrophobic regions, leading to an increase in the stability of the proteins (Chennamsetty et al., 2009b). Aggregate formation can be initiated by the intermolecular interaction of hydrophobic regions of at least two unfolded or partially unfolded denatured protein molecules (Mahler et al., 2005).

The molecular hydration properties near the surface of the protein are determined by the amino acid composition (Gekko and Timasheff, 1981). An increase in the hydrophobic interface with the protein will cause faster aggregation, further facilitated by a simultaneous increase in agitation rate (Sluzky et al., 1991). In certain proteins it has been observed that the molecule is destabilised by adsorption at hydrophobic interfaces creating small intermediate aggregates (Thurow and Geisen, 1984). This adsorption of proteins to hydrophobic surfaces and air water interfaces involves the accumulation of denatured molecules at the surface in question, fostering aggregation processes (Mahler et al., 2005). These intermediate

species of denatured proteins then help facilitate further aggregation (Sluzky et al., 1991).

The introduction of agitation to a system with hydrophobic surfaces dramatically increases the air-water interface and unlike with static storage, continuously refreshes the surface available for reaction (Fesinmeyer et al., 2009).

2.4.1.3 Mechanical stress

Mechanical stress generates a shear in the solution. The solution shear stress magnitude is given by the formula in equation 2-2. From the formula it is possible to see that the composition of the solution has a high effect on the magnitude of the shear stress. The dynamic viscosity of glycerol, for example, is 430 times greater than that of water, giving much higher shear stresses in more organic solutions. In general the maximum shear rate evolved in normal processing is around 20,000 s^{-1} (Bee et al., 2009). This mechanical stress can be generated by pumping, filtration, mixing, fill finishing, shipping or shaking (Mahler et al., 2005).

Equation 2-2: Equation for shear stress magnitude.

$$\tau = \gamma \mu$$

τ = Shear stress magnitude
γ = Shear rate
μ = Dynamic viscosity

It is important to note that shear alone does not appear to cause the formation of large aggregates in mixing, but causes protein unfolding which could lead to aggregation. In experiments done on the response of concentrated mAb's to high shear rates in a stainless steel rheometer (Bee et al., 2009), it was observed that prolonged exposure to shear causes minor reversible aggregation as described on page 28. Previously in the same study, monomeric mAb showed no aggregation after 30-51ms exposures to shears of up to 250,000s^{-1} and after 300s at 20,000s^{-1}

the mAb only gave reversible aggregates in the 40 to 60 unit range. A second sample with an aggregation population of 17% was not significantly altered by the shear rates.

In the same study it was observed that shear has a lower effect than air water interfaces and adsorption to solid surfaces, which could arise from contamination by particulates or pump cavitation stresses. However the shear induced desorption could act together with surface adsorption to give greater levels of aggregation. Finally it was noted that this cavitation-induced protein damage may be exacerbated if solutions are degassed by filtration immediately before pumping. This is because the degassing creates a large liquid-air interface that causes partial denaturation of proteins at the interface.

A further study showed that different types and levels of aggregation were produced if a solution was stirred or if it was shaken (Kiese et al., 2008). It was found that shaking produced lower levels of aggregation than stirring. It is suggested that shear may only cause minor conformational changes to the native structure as demonstrated by 16 hours of shear at a rate of 100,000 s^{-1} (Maa and Hsu, 1996). This can also be reversible as seen with the unfolding of lysosyme, refolding occurred soon after flow was stopped (Ashton et al., 2009).

A major contribution of mechanical agitation to aggregation in a bioprocess is that the protein aggregation rate is dependent upon collisions. The greater the agitation rate, the more evenly distributed the protein molecules are in the solution, meaning a higher chance of collisions and therefore a higher aggregation rate (Kiese et al., 2008). Related to this effect, it was shown that temperature will affect samples differently depending on the agitation regime the protein solution is exposed to (Kiese et al., 2008).

2.4.1.4 Protein concentration

The effect of concentration on protein stability has some cases where it is exceptional. In a study on insulin stability (Sluzky et al., 1991), it was found that stability was enhanced at higher concentrations. Insulin's self-interaction into more stable dimers and trimers was disrupted by dilution.

A review of protein concentration during storage conditions reports that increasing protein concentrations enhance the formation of protein aggregates for many proteins (Mahler et al., 2009). In this study it was found that formation of aggregates occurs by, at minimum, a bimolecular reaction, and so the reaction is concentration dependent.

It has been shown that an increase in protein concentration causes an increase in aggregate size for B-lactoglobulin (Roefs and De Kruif, 1994). This study showed that in general the controlling factor of aggregation is kinetics and that the aggregation rate is proportional to the protein concentration.

2.4.1.5 Surfactants and additives

During unit operations on a manufacturing scale, it is common to add non-ionic surfactants to protein solutions. These amphiphilic molecules tend to position themselves to minimize the exposure of the hydrophobic domain of the molecule and help prevent unwanted adsorption and aggregation at interfaces by limiting the extent of protein adsorption to the surface.

Surfactants behave like other co-solutes by differentially binding to both the native and non-native state of the protein, which will affect the conformational stability of the protein. The most common effect of the preferential binding results in an increase in non-native protein stability (Chi et al., 2003), but the surfactants still inhibit protein interactions at interfaces. For example polysorbate 80 has been used to prevent aggregation of proteins (Jones LaToya et al., 1997).

Surfactants have been shown to act as chemical chaperones, increasing the rates of protein refolding, helping to reduce aggregation (Jones LaToya et al., 1997, Bam et al., 1996). This was shown to be due to a stabilisation of the proteins native state (Timasheff, 1993). It is suggested that the surfactant molecules could interact with the exposed hydrophobic regions of the protein and therefore cover such sites that cause aggregation (Kiese et al., 2008).

2.4.1.6 Temperature

Native protein conformations only have marginal thermodynamic stabilities, with average stabilities only 5-20 Kcal/mol greater in free energy than unfolded proteins (Chi et al., 2003). This free energy comes from many interactions, forces and intrinsic properties, but because of the low conformational stability of the native state, relatively small changes in temperature can destabilise the protein structure and cause denaturation. In addition, this stability in terms of temperature is characterised by a parabolic profile meaning that moving to a too high or too low temperature can cause conformational change.

Incubation of protein solutions at high temperatures leads to physical degradation by promoting chemical reactions including oxidation and deamidation, and by directly affecting the conformation of the polypeptide chain structure on secondary, tertiary and quaternary levels (Fesinmeyer et al., 2009).

This degradation becomes reversible by aggregation of the modified proteins. The stability of proteins against heat is measured by the melting temperature (T_m) (Wang, 1999), which is the temperature at which 50% of the protein molecules are unfolded. This value is between 40°C and 50°C but in general proteins are stored well below this temperature at around 2°C to 8°C (Mahler et al., 2009).

Protein aggregation is usually observed at temperatures well below the melting temperature (Dong et al., 1995), adding evidence to the idea that aggregation does not occur from fully unfolded protein molecules.

It has been shown in lysosyme that brief temperature denaturation under 75°C is reversible, with refolding occurring within 20 seconds of the flow stopping (Ashton et al., 2009).

Temperature has been used to perform accelerated stability studies on protein aggregation using high temperatures such as 40°C to gain stability data in comparably short times. This inherent assumption about the utility of the accelerated data is questioned by many sources (Perico et al., 2009, Mahler et al., 2009).

It was found in a study involving capillary electrophoresis and matrix assisted laser desorption/ionisation (MALDI) mass spectrometry that there was site specific fragmentation of peptide backbones and disulphide bond linkages (Perico et al., 2009). This study found trends at 4°C and 29°C involving pH dependence and concentration dependence on the level of protein "clipping" and aggregation, and showed a reversal in most of the trends at 37°C. This all showed that accelerated data at high temperatures was not indicative of long term stability at temperatures used to store proteins.

2.4.1.7 Salts and ions

Ions have complex effects on the physical stability of proteins by modifying the conformational stability, equilibrium solubility and the rate of formation of aggregates.

The ability of ions to alter protein conformational stability and solubility can be ranked with the use of the Hofmeister series. Chaotropes have a low charge density and are able to increase protein solubility and decrease conformational stability at moderate to high salt concentrations (greater than 0.3M) by pairing with each other

to allow a greater number of water-water interactions. Kosmotropic agents have a high charge density and are able to form more favourable electrostatic interactions with other small ions, so have the opposite effect (Fesinmeyer et al., 2009).

Molar concentrations can be used to promote protein denaturation and crystallisation and to modulate protein-protein interactions. There are two competing theories for these effects. One involves the ions affecting protein solubility and stability through changes in the bulk water structure. The more predominant theory is that the ions interact directly with the protein (Fesinmeyer et al., 2009). At lower concentrations however, charge neutralisation can have a critical effect on the proteins stability and solubility, allowing small concentrations of kosmotrophic ions to solubilise proteins, using charge shielding to reduce the energetic favourability of protein-protein interactions.

Salts bind to proteins by ion interactions with unpaired charged side chains on the protein surface. Binding multivalent ions to the side chains can lead to cross linkage of charged residues on the protein surface which can lead to stabilisation of the native protein state if the ions bind more strongly to it than to the non-native state (Chi et al., 2003).

Salts alter the strength of electrostatic interactions between charged groups both within the protein molecules and between them. So intramolecular charge interactions affect conformational stability, and intermolecular forces effect the equilibrium and rate of aggregate formation (Chi et al., 2003).

Buffering salts can be added to solutions to maintain a desired pH and non-buffering salts can be used to make the solution more isotonic or reduce the viscosity (Fesinmeyer et al., 2009). Whereas some other salts can carry over from chromatography purification steps and potentially effect stability in final dosage.

In a study of the impact of ion strength and density on the effect of agitation and heat on protein aggregation, the propensity for both agitation and heat induced aggregation increases as the charge density of the anion decreases. There was a

dependence of the measured melting temperature on the anion but not on the cation (Fesinmeyer et al., 2009).

It has been noted that the effect of the anionic species follows the ranking of the Hoffmeister series and is much greater than that of the cationic molecules (Arosio et al., 2012). By supercharging these molecules it was found that the maximum charge states of protonated ions formed from native solutions is greater than those obtained from conventional denaturing solutions consisting of water, methanol or acid. The trend of increased charge state runs the opposite direction from the Hoffmeister series (Cassou and Williams, 2014).

Finally, because the pH determines the charge size and location on the proteins, salt binding effects can be strongly pH dependent.

2.4.1.8 pH

Changes in pH have a strong influence on the aggregation rate as the pH determines the electrostatic interactions through charge size and distribution on the protein surface (Chi et al., 2003).

The conformational stabilities of antibodies have been shown to be highly dependent on pH (Perico et al., 2009). As the number of charged groups on the protein is increased by modification of the pH, there is destabilisation of a protein's folded conformation due to increased charge repulsion.

Under acidic conditions protein cleavage may occur, whereas under neutral to alkaline conditions, deamidation and oxidation are favoured (Mahler et al., 2009). So pH induced unfolding gives a lower electrostatic free energy. There is also however the chance of salt bridge formation or ion pairing which could help stabilise the protein.

The overall modification of charge is dependent on the protein primary sequence and the protein structure. It affects protein aggregation differently in different buffer systems with equivalent pHs (Kameoka et al., 2007).

In general it is found that antibodies are most stable against aggregation at pH 4.5-5.5 and that aggregation increases dramatically both outside this range and near neutral pH, or the isoelectric point (pI) (Szenczi et al., 2006). This occurrence at pI is due to protein groups possessing both positive and negative charges giving distributions across the protein surface, leading to dipole formation. In these circumstances, protein-protein interactions could be highly favourable and drive aggregation (Chi et al., 2003).

2.4.1.9 Freeze thawing

Freeze thawing is a stress that therapeutic proteins are commonly exposed to during the life cycle of a product, both to store it and to analyse it. The low temperature causes a change in the pH of the solution due to buffer crystallisation and exposes the protein molecules to ice-liquid interfaces. These forces disturb the protein and cause protein aggregation.

The freezing will also induce localised increases in salt concentration, which will reduce intermolecular repulsion between protein molecules through increased charge shielding, creating more favourable conditions for aggregation (Kueltzo et al., 2008).

Increases in the initial concentration of proteins have often given a reduction in the percentage of protein aggregating in solution. It has been suggested in a study (Kueltzo et al., 2008) that this is due to a reduction in the fraction of protein exposed to the ice liquid interface. This effect can be controlled by the warming and cooling rates used, with a faster cooling rate resulting in larger numbers of smaller ice crystals and therefore more protein damage. A similar effect was observed with the container material and geometry, where adsorption to the container was shown to be a source of product loss by using different containers for storage.

The same report suggested that pH and ionic strength are amongst the most critical factors affecting the magnitude and the nature of the freezing induced stresses.

Using derivative absorbance spectra of the model IgG2 used, five major peaks were identified. By tracking the shifts in these peaks it was possible to gain insight as to the proteins tertiary structure. It was shown that the protein conformation was relatively insensitive to pH changes in range of pH 4-8, but that there was a large shift in the peak position both a pH 2 and at pH 10-12. Analysis of aggregates produced at pH 3, 4 or 5 found them to be irreversible.

2.4.1.10 Osmotic second virial coefficient

The osmotic second virial coefficient (B22) is a thermodynamic measure of protein-protein interactions to the dissociation constant for weak protein interactions. A positive value for B_{22} represents repulsion, while negative represents attraction (Tessier and Lenhoff, 2003).

Equation 2-3: Osmotic virial expansion.

$$\frac{\pi}{c\,R\,T} = 1 + B_{22} \cdot c + \dots$$

π – Osmotic pressure
c – Protein concentration
R – Gas constant
T – Absolute temperature

Techniques to measure B_{22} include measuring the osmotic pressure of protein solutions. However this has problems with experimental complications and low throughput. The most common method is static light scattering (SLS) but this approach has limitations in terms of throughput, protein consumption and the pre-disposition of the method to pick up larger particles, such as aggregates, much more preferentially (Bengali and Tessier, 2009). Other methods include self-interaction chromatography and self-interaction Nanoparticle spectroscopy, which have been previously described in this document.

2.4.2 Factors in bioprocessing

2.4.2.1 Filtration operations

Filtration membranes are used throughout the purification chain in bioprocessing to remove impurities, perform buffer exchange and decrease the volume of feed during downstream processing. This is done in order to decrease the handling and storage costs of the processes and thus allow for smaller unit operations or larger product throughputs.

Ultrafiltration/Diafiltration is typically used in buffer exchange and protein concentration. During UF, proteins face pumping, flow induced shear stress, extensive contact to membrane surfaces and exposure to air-liquid interfaces which produce small aggregations of proteins in a state that is a precursor for larger aggregation (Rosenberg et al., 2009).

Additionally, there are extremely high concentrations in the gel and polarization boundary layer near the membrane (Cromwell et al., 2006) and aggregation at this point is partly responsible for membrane fouling. It was reported that pore blockage in microfiltration is directly related to the concentration of the protein aggregate in the solution (Palacio et al., 2002).
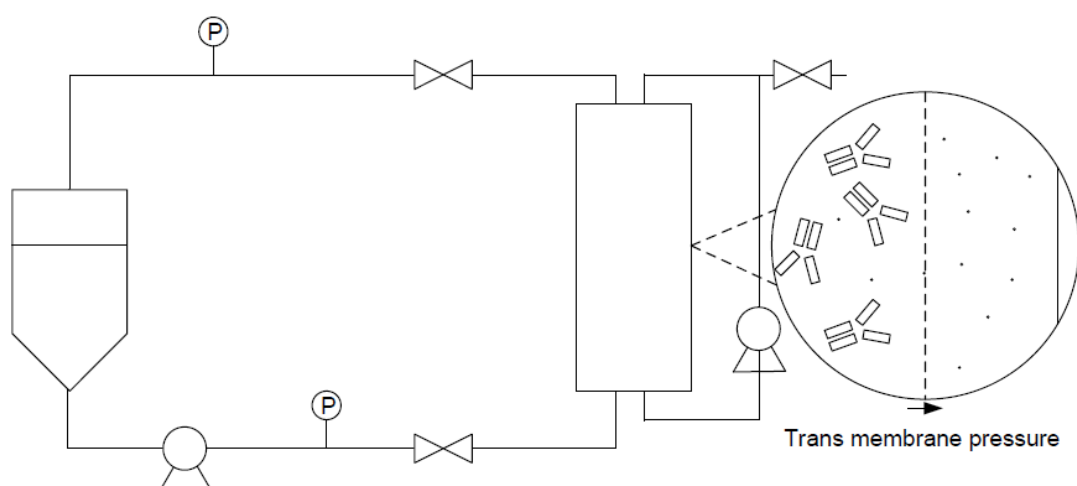
Figure 2-16:   Diagram of mode of action of diafiltration of antibodies.

Adsorption to the membrane itself can be a source of aggregation (Bódalo et al., 2004) and the induction of the aggregates and particles to the membrane increases with shear stress, which has a negative effect on the permeate flux.

In a study of the effects of shear on globular proteins during ultrafiltration (Rosenberg et al., 2009), it was found that constant pressure filtration gives rapid loss in flux and increases in the levels of aggregates. To reduce the generation of aggregates of different sizes, shear induced transport had to be limited. Decreasing the transmembrane pressure during concentration was found to improve the permeate flux, decreasing the process time, avoiding aggregation and causing less accelerated bed degradation due to fouling.

Equation 2-4:   Formula for permeate flux.

$$J = D/\delta \ \ln(Cg/Cb) = k \ \ln(Cg/Cb)$$

J	=	Permeate flux
D	=	Diffusion coefficient
δ	=	Boundary layer thickness
Cg	=	Protein conc. In gel layer
Cb	=	Protein Conc. In bulk
K	=	Mass coefficient

The theory behind this effect is explained in equation 2-4 (Porter, 1972). It is obvious that J can be improved by decreasing δ to get a higher trans-membrane pressure, but this does not take into account for hydrophobic protein interactions in the filter.

During tangential flow filtration, the protein is reported to be exposed to shear rates of between 1000 and 10,000 s^{-1} for a couple of seconds per pass over the membrane (Bee et al., 2009).

Analysis of the residues from membrane operations were analysed (Rosenberg et al., 2009) and it was found that membrane absorbed proteins remained in a state very close to native state, and the separated insoluble aggregates showed a loss in the proportion of their β-sheets.

In addition to the membrane, the protein solution is continually being pumped, with a typical membrane operation involving 50 passes through the system, adding mechanical stress to the proteins which could further encourage aggregation (Cromwell et al., 2006).

2.4.2.2 Chromatography operations
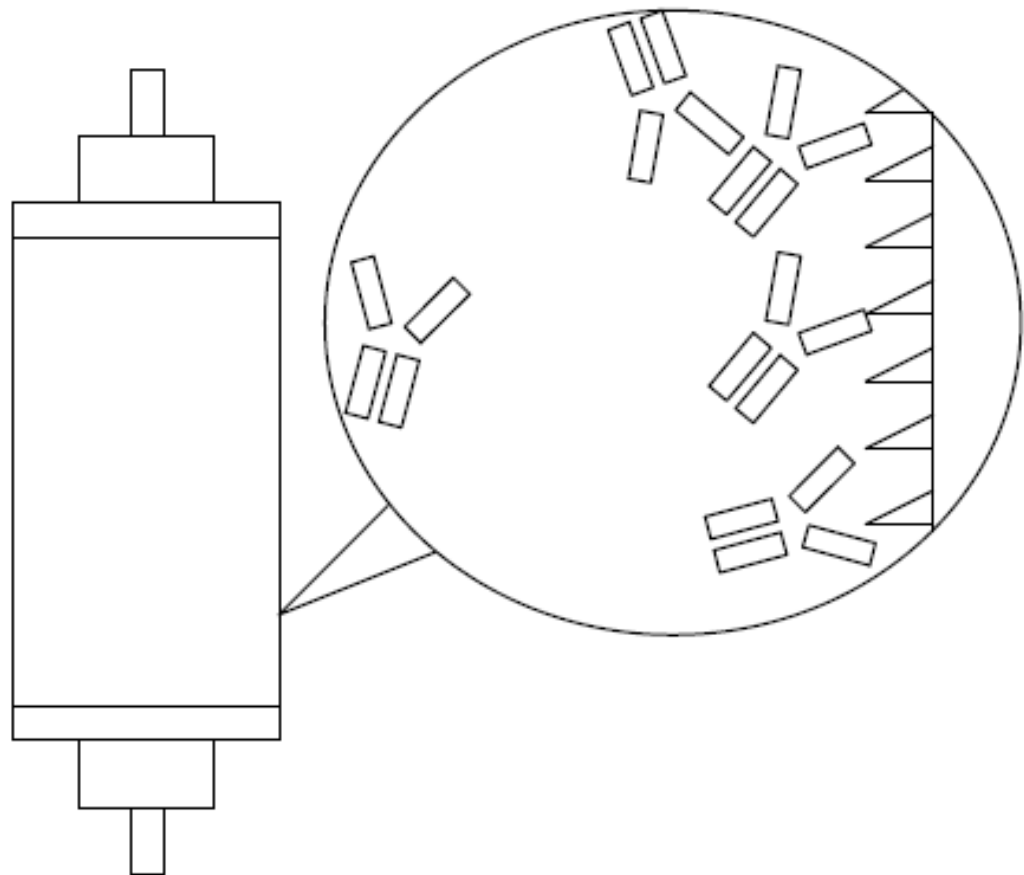
Figure 2-17:   **Diagram of interaction between chromatography column and antibody.**

Chromatography is a technique used in the downstream processing of therapeutics, which can separate substances based on different attributes. For the processing of mAbs Protein-A or G affinity chromatography are powerful purification techniques that can produce up to and sometimes higher than 95% purities due to high affinities for the Fc region of the antibody (Arakawa et al., 2004) of the resin. This high affinity requires relatively strong acidic conditions to denature the proteins to allow them to elute, as experimentally shown in the lack of elution of any antibody at pH 5.8

(Arakawa et al., 2004). Exposure to these conditions can result in the formation of aggregates, for example a 25% aggregated material solution from an elution at pH 3.2 (Cromwell et al., 2006).

The electrostatic interaction with affinity chromatography depends critically on the distance between the charged atoms. A study performed on the effect of the introduction of a histidine at various candidate positions within eight Angstroms of the site of protein G interaction with the Fc (Watanabe et al., 2009) shows the pH sensitivity can be drastically improved, lowering the required pH change for elution.

Another study was performed on the use of Arginine as an eluent (Arakawa et al., 2004) and the results were then compared with those of the more typically used citrate buffer. Arginine does not affect the native protein conformational stability but seems to prevent aggregation during refolding, like a chaperone. SE-HPLC tests on the eluted fractions indicated that the proteins were mostly monomeric.

A possible complication with protein-A has been observed when a histidyl residue in the middle of the protein's protein-A binding faced a complementary histidyl residue on the protein A. At low pH, the residues develop positive charges and cause a destabilisation of the product structure, leading to greater levels of aggregation than with low pH alone (Shukla et al., 2007a).

A further factor in the strength of the ligand-Fc bond is the glycosylation of the antibody, as it was shown that antibodies with higher mannose oligosaccharides, eluted later from a protein-A column and earlier from protein-G (Gaza-Bulseco et al., 2009).

It has been suggested the pH required for elution of the protein from a protein-A column should be increased, thereby reducing the level of protein deformation, by the addition of various substances to the elution buffer. These additives include sodium chloride or hydrophobic competitors (surfactants) such as ethylene glycol (Shukla et al., 2007a).

Another type of chromatography sometimes used for monoclonal antibodies is Hydrophobic Interaction Chromatography, which also interacts with the hinge region of the IgG subclasses. There is variability in the strength of the interaction with different subclasses due to their differing hinge regions allowing separation of subclasses of proteins. More importantly this suggests the resin interacts more strongly with protein complexes the more aggregated they are (Wang and Ghosh, 2009).

Moving on from the columns themselves, the proteins will elute off and be stored in protein rich formulation, with concentrations of up to 40g/L possible. This will again be a potential source of aggregation.

2.4.2.3 Pump filling and vialing operations

Pump filling is used to transfer the product from the final holding and mixing tank into vials for transport before use. There are no filtration or aggregation removal steps after pump filling, so it is important not to produce any unwanted aggregates at this point.

A study performed on the operation (Carpenter et al., 2009) found that during pump filling, IgG formed hundreds of thousands of particles per mL in the 1.5 to 3µm size range, but critically less than 1000 particles in the 8-15µm ranges.

Vial filling is typically performed using a positive displacement pump to inject solution into each of the vials. There are two main locations for possible aggregation to occur in this operation. The first of these is in the pump used to displace the liquid and the second is in the vials themselves.

The type of pump can be the reason for any aggregation. It was shown in a study, that while a rotary piston pump caused aggregation, the same system with a rolling diaphragm pump could be used to stop aggregation (Cromwell et al., 2006). Unfortunately this quick fix cannot always be used, usually due to constraints of the manufacturing site and previously validated processes. A further study (Tyagi et al.,

2009) determined that nano particles shed from the surface of the pump in contact with the solution acted as heterogeneous nuclei for protein aggregation and particle formation.

A study was also taken into the vials used to receive the protein solution (Chi et al., 2005) and it was found that glass nanoparticles left at the bottom of the vials were in some cases responsible for heterogeneous nucleation of the protein.

2.4.2.4 Pumping materials

Pumps are required in large scale bioprocessing to ensure the movement of the feed from one unit operation to the next. Pumps exert forces on the liquid phase due to a changing of internal dimensions from the surrounding pipes and because of high piston or rotary velocities. Most fluid in a pump will experience similar orders of magnitudes of shear rates as in the adjacent pipes (Bee et al., 2009).

Monoclonal antibodies have been found to unfold at shear rates around 10,000 s^{-1} (Jaspe and Hagen, 2006), and the rates evolved in piston and rotary lobe pumps are around 20,000s^{-1}. It has been reported however that using a rolling diaphragm pump instead of a radial piston pump will reduce the level of aggregation (Bee et al., 2009).

There are two possible factors for the difference in aggregation levels. The first is that leaching or fragmentation of metals or polymers could act as particulates to catalyse the aggregate formation (Bee et al., 2009). The second and more prevalent factor is that cavitation occurs in the pumps and valves as the movement creates and destroys microbubbles in the fluid. These bubbles have a large hydrophobic surface area that would cause protein to be drawn to them (Narendranathan and Dunnill, 1982). During certain unit operations there would be multiple passes through pumps and valves, further increasing the level of aggregation.

2.5 Aggregate formation

2.5.1 Introduction to mechanisms

The first possible mechanism of protein aggregation was published in 1954 (Lumry and Eyring, 1954) when Lumry and Eyring described it as a change in protein conformation that led to an altered state of the protein that was then susceptible to aggregation. They described the protein unfolding to form an unstable intermediate state that is in equilibrium with the native protein structure. This then serves as an intermediate leading to an irreversible aggregated state.

Since this definition many, further studies have been performed into the area, but to a great extent, the findings seem to be case dependent, with most protein aggregations dependent on protein concentration, buffer concentration and agitation. Antibody stability is not necessarily dependent on these factors, suggesting the mechanism is counter intuitive and unlike other proteins (Perico et al., 2009). Certain studies have used bioinformatics techniques to try and model the locations on the antibody at which adherence to other proteins is likely. One particular group (Chennamsetty et al., 2009a) showed the strength of their technique of using what they term spatial aggregation propensity (SAP) to predict the aggregation prone motifs and regions on the antibodies. These regions with high SAP were areas of hydrophobicity on the protein surface. Mutation of the primary structure of these areas to make them more hydrophilic resulted in increased stability of the tertiary structure, showing that the hydrophobic interactions are important for aggregation.

Having discussed the causes of aggregation, and the methods available to analyse the resulting species, it is time to look at the different forms of aggregation and the way in which they are produced. Figure 2-18 shows some of the different ways in which we can categorise aggregates.

It would be interesting to show which of these subcategories of aggregates are produced with different mechanisms of aggregation and which lie on the same aggregation pathways.

Many studies have been performed on the effect of aggregation on the proteins within the multimers to determine their secondary structure. It has been reported in some cases (Schule et al., 2007) that a β-sheet structure appears in the secondary structure; however it has not yet been confirmed if this change is always related to aggregation.

In terms of the structures, it is suggested that reversible denaturation occurs due to changes in the tertiary structure whereas irreversible changes are changes in the secondary structure (Lumry and Eyring, 1954).

A study on the effect of temperature on the local conformational perturbation of the antibodies (Perico et al., 2009) suggested that the structure of the antibody became perturbed well below the global thermal unfolding point, and that acidic formulations at elevated temperatures underwent clipping that led to higher order aggregates. The amount of high molecular weight aggregate generated then depends quite strongly on the product concentration (Shukla et al., 2007a).
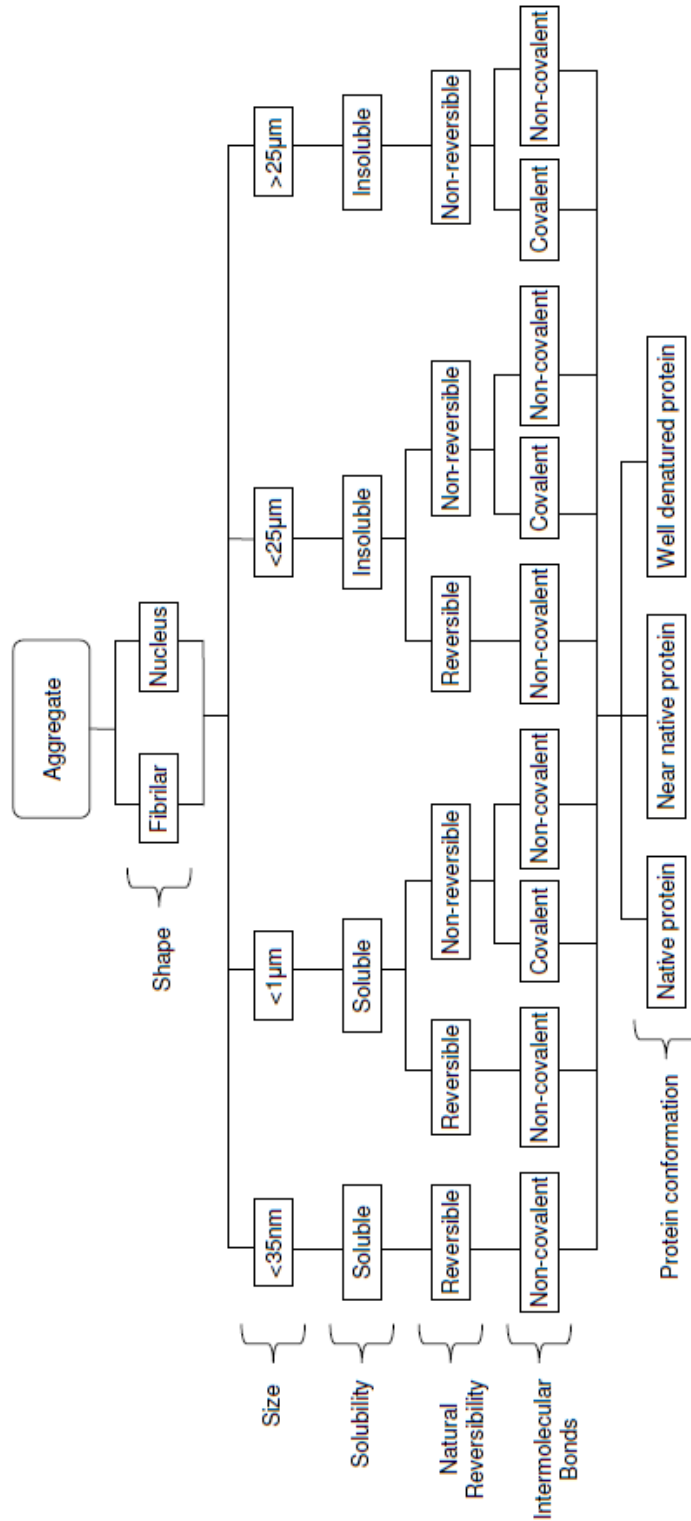
Figure 2-18: Possible protein aggregation pathways based on literature.

2.5.1.1 Aggregation rates

Equation 2-5:   Kinetic rate equation.

$$r = k(T) \, [A]^{n'} [B]^{m'}$$

k(T)= Reaction rate coefficient
[A]=Concentration of component A
[B}=Concentration of component B
n'=Reaction order for A
m'=Reaction order for B

The different possible mechanisms for aggregation produce not only different shapes and sizes, but can take different amounts of time, with various stages sometimes acting as rate limiting steps. Kinetic mechanisms that have been proposed have different rates of reaction and different orders of magnitude, which do not have to be whole numbers. The rate equation is shown in equation 2-5 and shows the relationship between the reaction rate, the rate coefficient and the concentrations and orders of magnitude of the various components. The rate equations for multistep mechanisms cannot usually be derived from any stoichiometry and require experimental determination.

The reaction orders can be determined by the effect the concentration of the component has on the rate of reaction. A zero-order constituent's concentration will have no effect on the rate. A first-order reaction depends only on the concentration of one of the reactants, so any other reactions occurring will be zero-order. Second order reactions can then depend on either one second-order reactant or two first-order reactants. Second order reactants have half lives which progressively double, giving a second-order exponential decay of reactants.

Equilibrium reactions are common in aggregation whether this be for protein conformation or protein-protein interactions leading to temporary intermediate species. In these reactions, a pair of forward and reverse reactions act on a point in the reaction and the reaction rate can be expressed as shown in equation 2-6.

External factors can sometimes affect the equilibrium in the favour of a state that promotes aggregation which can then allow a sequential reaction to begin the production of aggregates.

Equation 2-6:   Rate equation for a reversible reaction.

$$r = k_1 [A]^s [B]^t - k_2 [X]^u [Y]^v$$

r	=	Reaction rate
k_1	=	Forward rate coefficient
k_2	=	Backwards rate coefficient
[C]	=	Concentration of component
x	=	Order of reaction

Real world examples can be found in the literature. One paper (Shukla et al., 2007a) shows that their mAb is highly susceptible to aggregation at low pH and was found to have first order kinetics over a wide range of conditions. This study also found that elution from the protein-A resin increased the rate constant which would be expected with pH degradation alone, suggesting that the protein-A destabilizes the product structure and increases the tendency to aggregate.

Another paper (Perico et al., 2009) shows a reaction which has greater aggregation with increasing pH but with an inversed pH dependence being concentration dependent, suggesting a reaction rate-limited by self association.

2.5.2 Nucleation and fibrillation of aggregates

Many aggregation reactions seem to start when aggregation prone monomers assemble into fibrils and rapidly elongate via a slower nucleation-dependent pathway (Kim et al., 2002). As previously described, the proteins aggregate when structurally perturbed intermediary species react with each other to give larger assemblies of proteins. Some reports refer to this nucleation as the formation of a minimal fibril unit, but they agree that this represents the rate limiting step of the fibril formation, with subsequent growth proceeding rapidly via the incorporation of monomers into the ends of the nucleated fibrils (Sasahara et al., 2008).

The nucleation step is relatively poorly characterised, with few experimental technique available to allow the direct monitoring of the nucleus formation. In a study into the nucleation step on egg lysozyme, it was found that in a parallel process mechanism, the sheet and random coil are produced directly from the native protein. β-sheet was found to develop from the partially unfolded intermediate and the formation of the β-sheet and the partially unfolded intermediate could be partially correlated. When followed step by step, a newly formed β-sheet in solution could be assigned to the fibrillation nucleus. The independence of characteristic times on the protein concentration indicated that the early stages of fibrillation, irreversible partial unfolding and nucleus formation were intramolecular processes (Lednev et al., 2009).

The fibrillar structures that can form are then dependent on a variety of factors, with one report showing that β2-m protein can produce a well organised mature, long fibril at low ionic strength with a lag phase in aggregate production. At higher salt concentrations, rapid formation with no lag phase results in short curved and thin, worm like fibrils. The more mature fibrils were more thermodynamically stable than the worm like fibrils (Sasahara et al., 2008).

One paper states that the assumption that a lag phase in the kinetics always represents nucleation is a fallacy and that the end of the lag phase does not always correspond to the end of nucleation (Ferrone, 1999). This same paper goes on to explain that although initially imagined to be an abrupt transition, nucleation has a curved thermodynamic barrier. The nucleus size is also shown to be dependent on the concentration of monomer.

2.5.3 Reversible self association of proteins

Reversible self association (RSA) is a phenomenon that is slowly becoming more observed as more exotic and hydrophobic monoclonal antibodies are produced. At higher concentrations antibodies come within closer contact of each other and are

more likely to interact (Kanai et al., 2008). In these conditions the antibodies in their native configuration begin to form loose bonding to each other where they begin to form clusters in the solution (Chaudhri, 2012). These clusters have been reported to differ in size from 2 units to many more. One known result of RSA is that the viscosity of solution is increased (Liu et al., 2005), but in general there is little documented about the phenomenon.

3 Materials and methods

3.1 *Antibodies utilised in studies*

3.1.1 Medi/UCL001

One human monoclonal antibody (IgG1) designated Medi/UCL001 was provided by MedImmune (Cambridge, UK) in a state after primary clarification of broth from fermentation. The samples provided were taken from 5 days before the normal harvest time and then for two days after the time. The concentration of antibody at the end of the fermentation was around 2g/L.

Buffers used for elution from Protein-A were sodium based. The buffer used for viral inactivation was Acetic acid and Tris was used for neutralisation.

3.1.2 Medi/UCL002

One human monoclonal antibody (IgG1) designated Medi/UCL002 was provided by MedImmune (Cambridge, UK) in a fully purified state at a concentration of 50mg/ml in PBS. This was diluted to a concentration of 0.5mg/ml before experiments.

3.1.3 Medi/UCL003-008

Six lots of human monoclonal antibody were designated, Medi/UCL003, Medi/UCL004, Medi/UCL005, Medi/UCL006, Medi/UCL007 and Medi/UCL008. For initial experiments purified amounts of these antibodies were supplied by MedImmune in stability buffer for testing. These were tested for purity and then diluted to 1mg/ml prior to filtration and aliquoting.

During the course of the project, more material was needed and so approximately 30L of fermentation broth of each of the antibodies was produced by the sponsor company using their platform process.

The antibodies all had identical variable regions but the Fc region was modified as below. The YTE/TM nomenclature is explained in section 3.2:

Medi/UCL003 & 007   -   IgG4 YTE

Medi/UCL004   -   IgG4

Medi/UCL005   -   IgG1 TM YTE

Medi/UCL006   -   IgG1 YTE

Medi/UCL008   -   IgG1

The material was then purified using the same protocol in each case. Firstly, the antibody was filtered using a 0.45µm pore size membrane prior to purification using Protein-A chromatography. Viral Inactivation was then performed, followed by a Fractogel polishing chromatography step. Purified material was then formulated using UF/DF to a final concentration of 50mg/ml in a stability buffer comprising of a mixture of L-Histidine and Trehalose at a pH of 5.5.

3.1.4 Medi/UCL009

One human monoclonal antibody (IgG1) designated Medi/UCL009 was provided by MedImmune (Cambridge, UK) in a purified state at 50mg/mL in a pH 5.5 L-Histidine and D (+) trehalose stability buffer. The antibody was reformulated using desalting columns into nine different formulations outlined in table 3-1.

Table 3-1:   **Conditions used for formulating Medi/UCL009.**

Sample	pH	Salt Conc. (M)	Ab Conc. (mg mL^{-1})
1	4.4	0.03	5
2	4.4	0.03	15
3	4.4	0.15	5
4	4.4	0.15	15
5	5	0.09	10
6	5.6	0.03	5
7	5.6	0.03	15
8	5.6	0.15	5
9	5.6	0.15	15

3.2   Modifications used in studies

Medi/UCL003-008 were modified using a combination of two triple amino acid substitutions. These mutations were developed as stand alone modifications to change the pharmacokinetic properties of any antibodies they were inserted into.

3.2.1 YTE
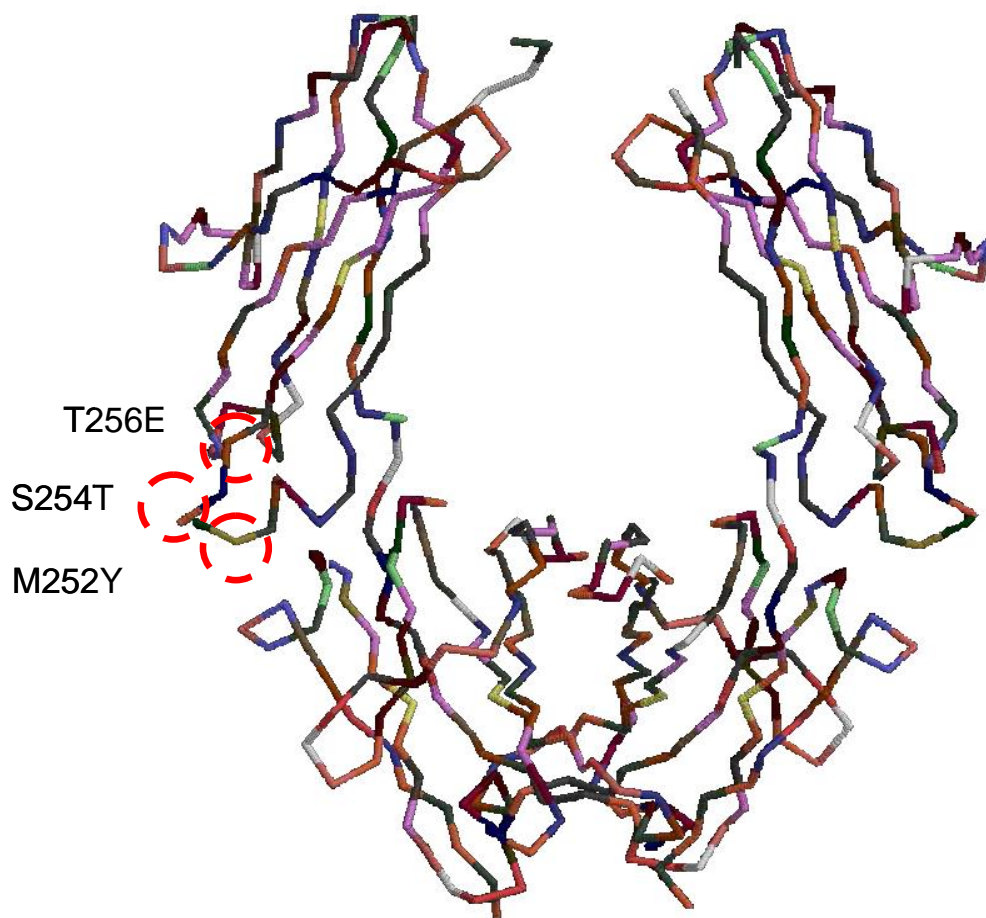
Figure 3-1:   Image of YTE mutation locations on an IgG1 Fc.

The YTE modification (Dall'Acqua et al., 2006a, Dall'Acqua et al., 2006b) comprises of the triple antibody substitution M252Y/S254T/T256E shown in figure 3-1. The modifications increase the IgG binding to the neonatal Fc receptor (FcRn) giving a 10 fold increase in both Human and cynomolgus monkey over the non-modified state. This results in a four-fold increase in the serum half life of the molecule. The modification was also shown to modulate the antibody-dependent cell-mediated

cytotoxicity (ADCC) of a humanised IgG1 directed against the human integrin $\alpha_v\beta_3$ (Dall'Acqua et al., 2006b). Molecular modelling of the modification suggests that this behaviour is accounted for by potential favourable hydrogen bonds and an increase in surface contact between the antibody and the FcRn (Oganesyan et al., 2009).

3.2.2 TM
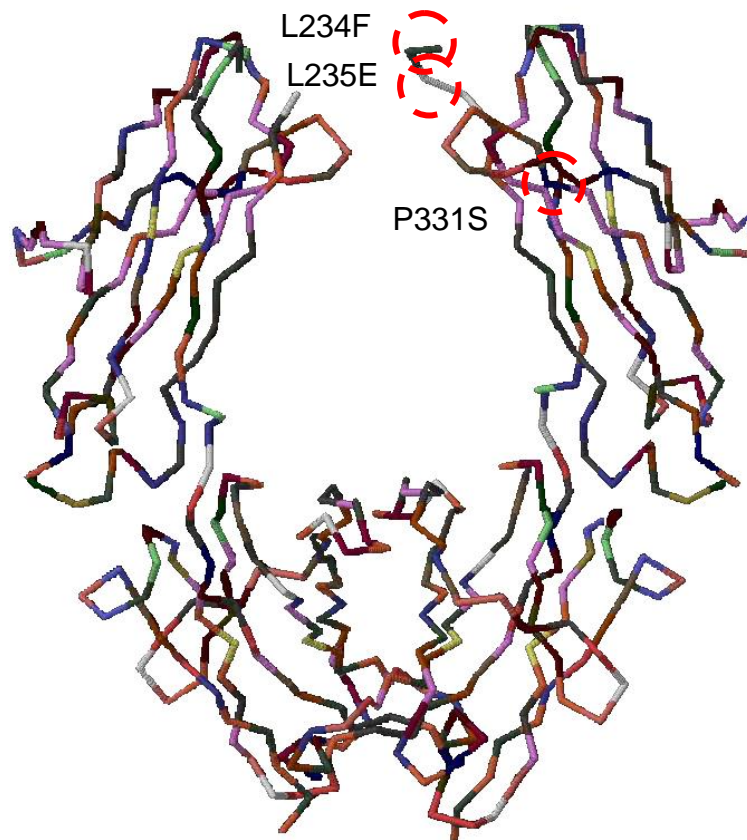
Figure 3-2:   **Image of TM mutation locations on an IgG1 Fc.**

 The TM modification (Oganesyan et al., 2008) comprises of the triple amino acid substitution L234F/L235E/P331S shown in figure 3-2. The modification eliminates various antibody effector functions, which is thought to decrease the IgG-mediated toxicity events. The modification results in a large decrease in the binding activity of the Fc portion of human IgG to human C1q, CD64, CD32A and CD16 which are known to trigger ADCC and complement dependent cytotoxicity (CDC) events.

Work done on modelling of antibodies including the mutation has shown that the broad ranging effects of TM cannot be explained in terms of major structural rearrangements in the vicinity of the modification.

3.3   Primary recovery; filtration

Antibody produced for this study was clarified in one of two ways depending on the volume needed to be processed. Volumes larger than one or two litres were filtered using a sterile, inline, disposable Millipak™ (Millipore, Billerica, MA, USA) filter with 0.45 micron Durapore™ (Millipore, Billerica, MA, USA) PVDF membranes. Feed was pumped through from a storage vessel using a LoadSure peristaltic pump (Watson-Marlow, Falmouth, UK) into a sterilised disposable plastic vessel ready for the next stage in its purification.

Volumes up to and around two litres were filtered using 1L volume Stericups™ (Millipore, Billerica, MA, USA) with 0.45 micron Durapore™ (Millipore, Billerica, MA, USA) PVDF membranes. The filtrate was collected in a sterile container connected to the membrane ready for the next stage in its purification.

3.4   Chromatography techniques

Antibody was purified using chromatographic techniques. This project used Protein A, size exclusion and ion exchange chromatography as methods for protein separation. The exact column used and the stages run were dependent on the type of chromatography and the volume of matrix needed for that step.

In all cases an AKTA purifier (GE Healthcare, Uppsala, Sweden) was used to pump the media through the column. UV, pH and conductivity results were used to monitor the process as different wash steps were put across the column before elution and stripping of bound proteins (MedImmune, Cambridge, UK).
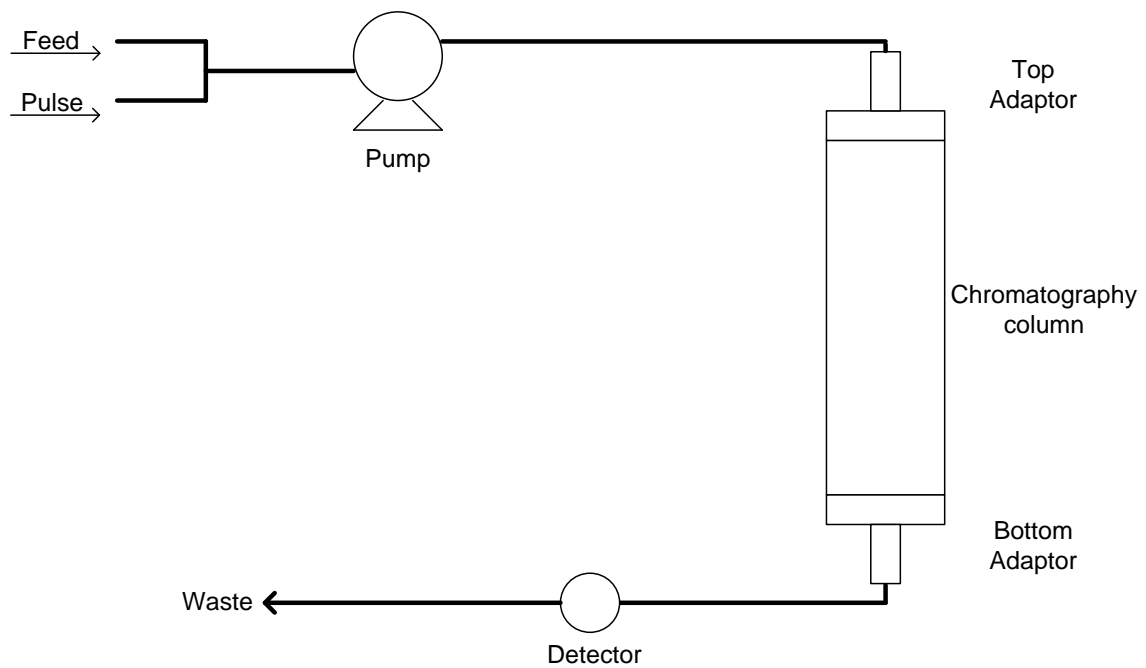
Figure 3-3: Diagram of chromatography rig.

All processes were controlled using Unicorn software (GE Healthcare, Uppsala, Sweden) and the software was used to determine when to collect the antibody in aliquots, using Falcon Bluemax™ conical tubes (BD, NJ, USA), by tracking when the absorbance at 280nm went up at a previously defined rate in the elution stage.

For smaller matrix volumes a HiTrap™ or Tricorn™ column (GE Healthcare, Uppsala, Sweden) was used, but these were upgraded to an XK 16, XK26 or XK50 column (GE Healthcare, Uppsala, Sweden) as the volume of matrix demanded a larger diameter while keeping a fixed bed height of around 20cm for all columns except the HiTrap™.

The method of protein loading depended on the volume of antibody that required purifying. For smaller volumes of up to 50ml, a super loop (GE Healthcare, Uppsala, Sweden) was used. For larger volumes of up to 30L, the feed was loaded directly using one of the buffer lines.

The matrix used depended on the type of separation that was required. For a primary purification step, this project always used MabSelect sure matrix™ (GE

Healthcare, Uppsala, Sweden). If anion exchange was required, Fractogel™ matrix (GE Healthcare, Uppsala, Sweden) was used.

The Protein-A chromatography step was run at a constant linear flowrate of 200cm/h and started with an equilibration step for 10 column volumes using PBS buffer followed by the loading step. Wash step 1 used 5 column volumes of PBS to wash off any unbound material from the matrix. Wash buffers 2 and 3 then incremented towards the conditions used in the elution step. After elution, 5 column volumes of 100mM Acetic acid was used to strip the column before CIP using 2 column volumes of NaOH and a 15 minute hold.

The anion exchange chromatography was performed at a linear flow rate of 200cm/h and started with equilibration of the column for 10 column volumes using a low salt buffer. The antibody was then loaded onto the column and the column was rinsed with another low salt buffer. The salt molarity of buffer was then steadily increased and fractions were collected as various proteins were unbound from the column. High salt buffer containing EDTA was then used to strip the column before CIP using 2 column volumes of NaOH and a 15 minute hold.

3.5   Viral inactivation

A Meterlab® PHM220 lab pH meter (Radiometer Analytical SAS, Villeurbanne Cedex, France) was put in the eluate from Protein-A to view the pH which was slowly reduced using Acetic acid to a low holding pH. After an hour, a sample was taken from the treated eluate before Tris buffer was used to neutralise the pH. A further sample was taken at this point.

3.6   Viral filtration

In the course of the study on reversible aggregation a pressurised viral filtration step was performed. A diagram of the equipment is shown in Figure 3-4.

Feed streams consisted of purified material formulated into a final buffer. The material was loaded into a pressure vessel (Millipore, Darmstadt, Germany) and passed through a series of filters each with a 3.94cm height and 3.10cm diameter with purge valves on the permeate side. A stop valve was placed between each of the filters to allow sequential purging of each filter. The first filter was a Virosolve pre filter (Millipore, Darmstadt, Germany) with a mixed cellulose ester membrane. The second filter was a Virosolve guard filter with a polyethersulfone (PES) membrane. The third filter was a Virosolve Pro filter with 20nm pore size PES membrane.
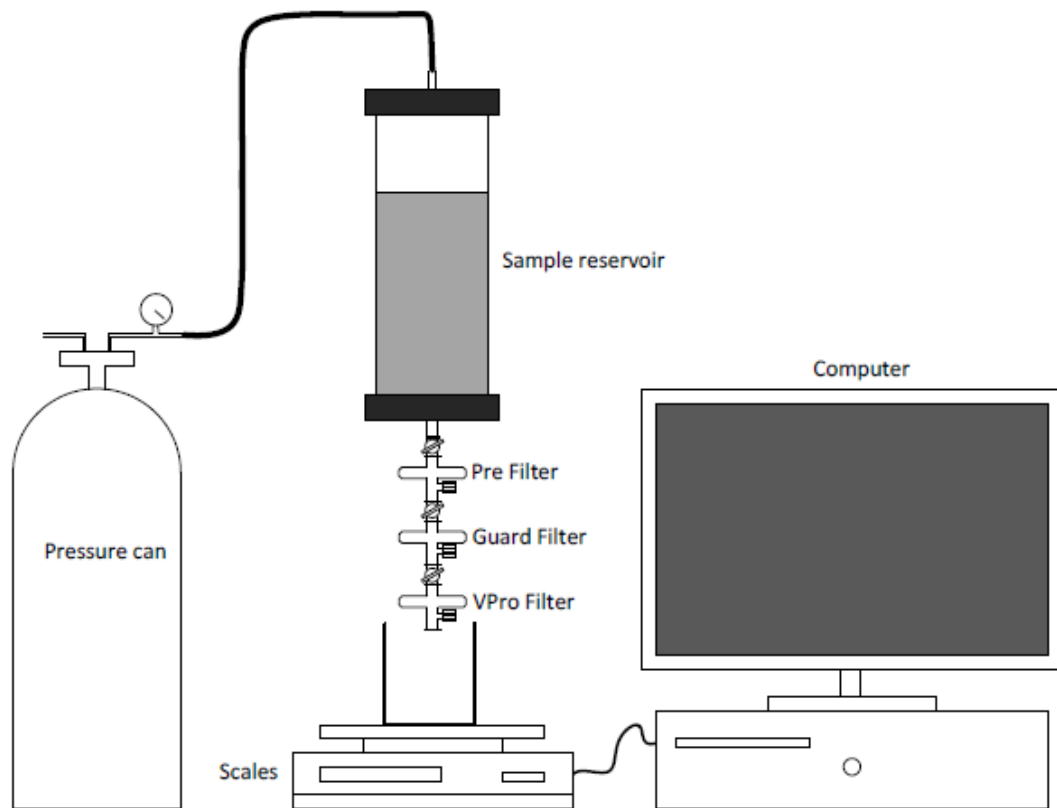
Figure 3-4: **Diagram of viral filtration equipment setup.**

Operation of the device began by filling the sample reservoir with water and sealing the lid before setting the pressure to 30 PSI. The filters were then wetted one at a time from the top by closing the stop valve below the filter and collecting 15ml of liquid through the purge valve. The purge valve for the first filter was then closed and the valve below opened to allow wetting of the second filter which was then purged for 15ml before repeating for the third. After the wetting, the water in the

reservoir was removed and some buffer was placed in the reservoir to equilibrate the filter membranes. The process of sequential purging was then repeated and the buffer replaced by the antibody feed. At this point the scales (Sartorius, Epsom, UK) were tared and a system link to the PC was initiated to record the value on the balance on an Excel (Microsoft, CA, USA) spreadsheet. At this point all the valves were opened and measurement of flux began until either it fell below 100LMH or the sample was finished.

3.7 SE-HPLC analysis of low molecular weight aggregates

For SE-HPLC analysis the System used was an Agilent 1200 series (Agilent technologies, Santa Clara, CA, USA) rig comprising of a solvent pump, degasser, injector and a diode array detector (DAD) UV detector. A 4cm by 6.0mm TOSOH TSK gel SWXL Guardcol (TOSOH Biosciences, Tokyo, Japan) followed by a 30cm by 7.8mm TOSOH Hichrom TSK gel G300SWXL column (TOSOH Biosciences, Tokyo, Japan) were used to analyse results. The running buffer (MedImmune specification, Gaithersburg, USA) was pumped through at 1ml/min to equilibrate the column for half an hour prior to a run. The flowrate and buffer were kept the same and 25µL samples were injected onto the column. The eluate was monitored for absorbance at 280nm wavelength and the peaks were integrated using the Agilent HPLC software.

Prior to analysis all samples were either filtered using Ultrafree® MC 0.5ml Centrifugal filters with Durapore PVDF 0.45µm membranes (Millipore, Billerica, MA, USA) for 1 minute at 13000 rpm in a Micro centaur centrifuge (MSE, London, UK) or span down for 10 minutes at 13000 rpm in a Micro centaur centrifuge in a 1.5ml test tube (eppendorf, Hamburg, Germany), to remove any aggregates larger than the SE-HPLC columns could differentiate. Samples of 1µm volume were then pipetted

into HPLC vials with 0.1ml inserts (Kinesis, Cambridgeshire, England) before being placed in the HPLC machine.

3.8   280nm absorbance of proteins

A Beckman DU 520 UV/VIS-spectrophotometer (Beckman Coulter, Brea, CA, USA) was used to determine the absorbance at 280nm to allow the determination of the concentration of the solutions. The samples taken from various experiments were diluted to approximately 0.5mg/ml prior to analysis with their native buffer, before being placed in the colorimeter to give a reliable absorbance reading in the 0-1AU range. A quick analysis of the amount of absorbance at 280nm gives a value which can be put into the Beer-Lambert law equation for molar absorbance along with the extinction coefficient to give the concentration of the solution.

3.9   Ultrafiltration/diafiltration of samples

The experimental setup for the ultrafiltration/diafiltration (UF/DF) step is shown in figure 3-5. The pilot scale filtrations were performed using a Minim™ rig (Pall, NY, USA) running a Minimate™ capsule membrane filter unit. Circulation of the retentate was achieved with the use of a peristaltic pump on the rig itself. The inlet flow rate was controlled by adjusting the pump rate. The transmembrane pressure was adjusted to 20 bars by adjusting the valves and was kept at this value over the course of the unit operation. The permeate valve was left open during operation of the rig and the permeate mass was measured by collection in a vessel placed on a CPA4202s tabletop scale (Sartorius, IL, USA).

During Ultrafiltration operation of the rig, the reservoir top was left unsealed and volume of liquid in the reservoir was allowed to reduce. During Diafiltration the reservoir was vacuum sealed with a pipe leading to the Diafiltration buffer to replace the buffer that was being lost in the permeate.

Membrane equilibration was performed using the buffer that the sample had been eluted with from the previous step, for samples that were being purified, or by using the buffer the antibody had been formulated in for samples that were being buffer exchanged. Membrane cleaning was performed after each experiment by recirculation of 0.5M NaOH solution for 5 minutes, followed by a 30 min hold. After cleaning, the entire system was rinsed with deionised water.
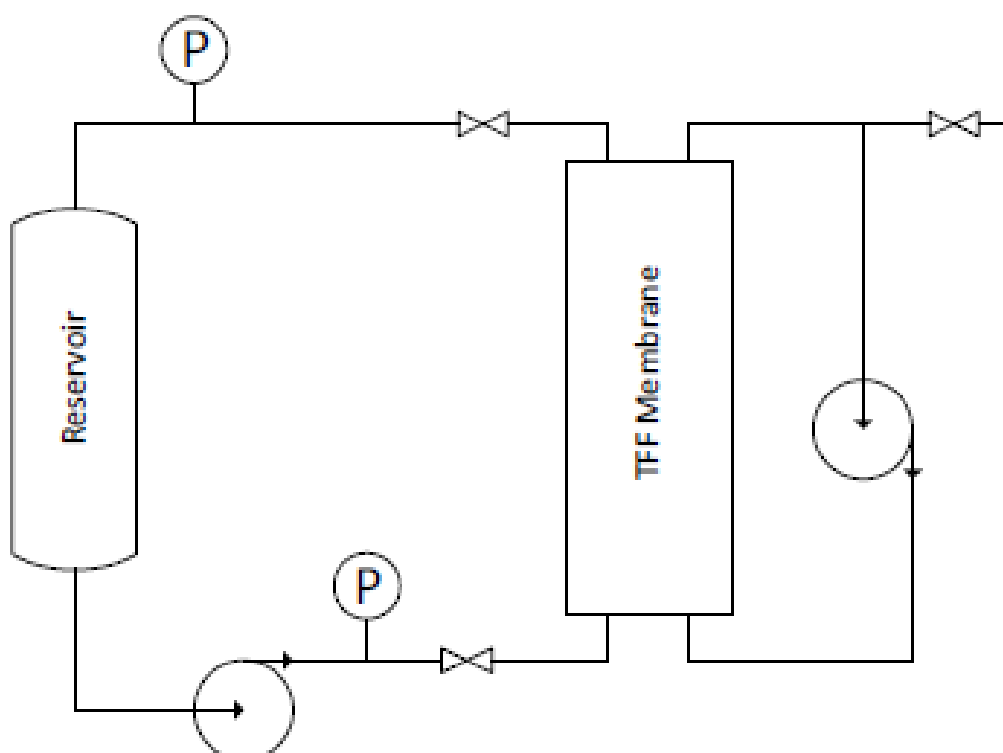
Figure 3-5:   **Diagram of a TFF filtration rig.**

3.10 Desalting columns

Desalting columns were used for buffer exchange when small volumes of many different formulations were required. Disposable PD10 columns (GE Healthcare, Uppsala, Sweden) were equilibrated by running through 5ml of the formulation buffer required until the liquid had finished passing through the column. This was repeated four more times and the column left until there was no more liquid waiting to pass through the matrix. 2.5ml of the sample was then added to the column and

allowed to pass through before placing a receptacle to collect the eluate and a final

3.5ml of the formulation buffer was added to push through the eluate.

3.11   Shear device operation
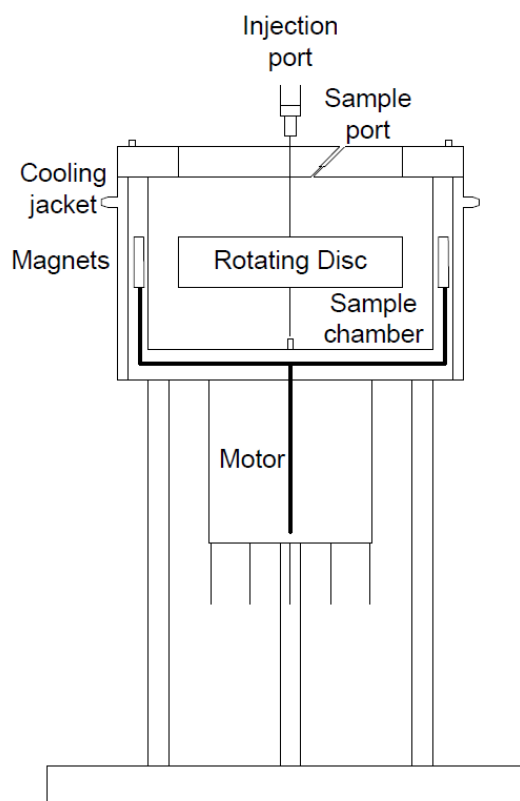
Figure 3-6:   **Diagram of redesigned disc interfacial shear device.**

The shear device used is an upgrade of one previously described in a paper

(Biddlecombe et al., 2007) and uses a magnetically driven ferrous disc in the centre

of a chamber to simulate liquid-solid interface shear damage with the absence of

any liquid-air interfaces. The disc is driven by a magnet in the outer casing, which is

in turn driven by a motor. For the experiments, the disc speeds used were 3000,

6000, 7500, 9000, 12000 and 15000rpm. Each 2 hour experiment had samples

taken every 15 minutes to be analysed by SE-HPLC. Figure 3-6 shows a

diagrammatic representation of the device while figure 3-7 and 3-8 show the device

in various stages of assembly.
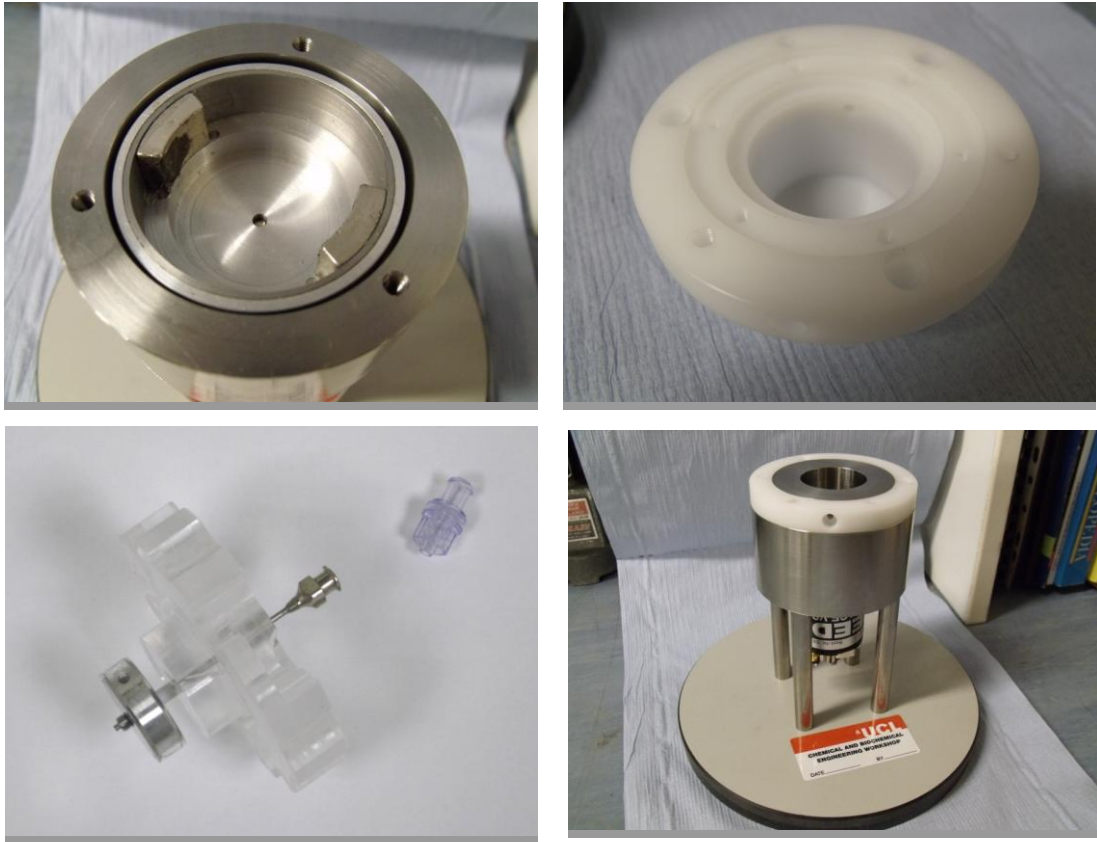
Figure 3-7: Images of the shear device clockwise from the top left; the magnet seat, cooling jacket lid, assembled shear device base, assembled lid with disc attached and one way valve adjacent.

Solution was introduced to the device at the base of the chamber by a one way injection port running down from the top face and time samples were taken via a separate sample port at the top of the chamber. A LoadSure peristaltic pump (Watson-Marlow, Falmouth, UK) was used to pump water from a cooling tank to the cooling jacket around the sample to allow temperature control at high shear rates.

CIP consisted of running the device with Sodium Hydroxide for 10 minutes, emptying the chamber, then running the device with phosphoric acid for 10 minutes before emptying the chamber and equilibrating the device with the formulation buffer of the sample to be analysed.
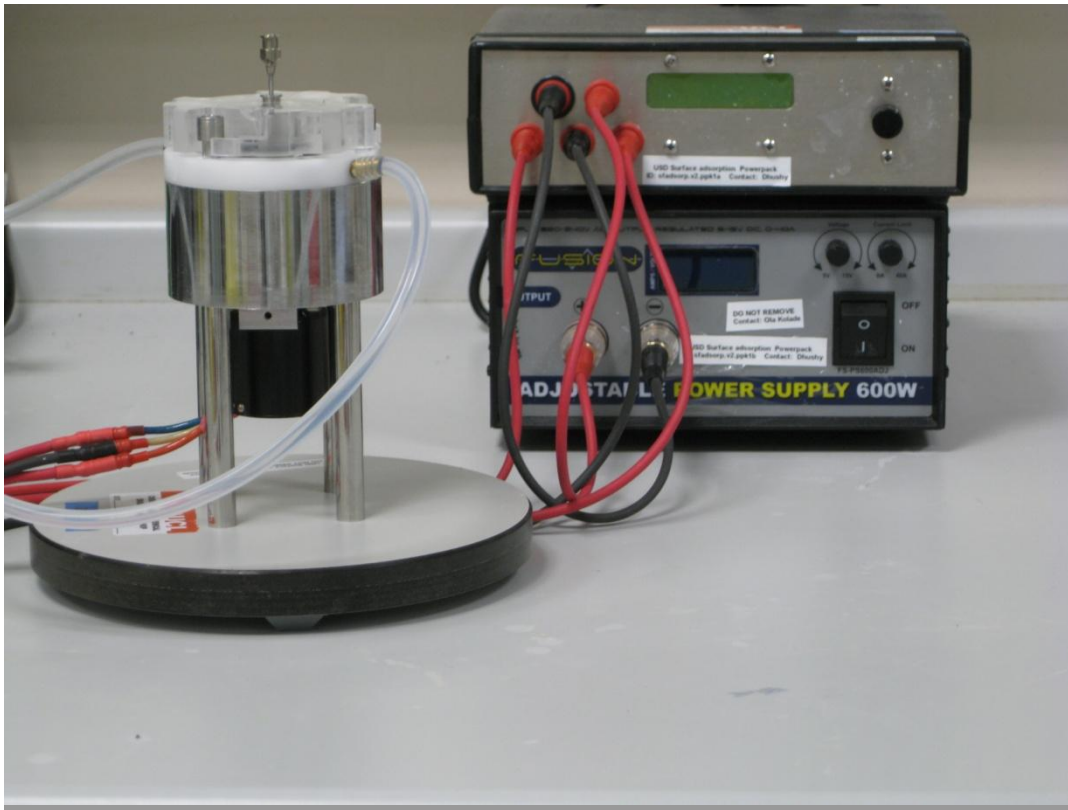
Figure 3-8: Image of the fully assembled device connected to the power pack, with rubber tubing leading to a water bath and pump assembly.

3.12 Nanoparticle tracking analysis

The device used was a Nanosight LM10 (Nanosight ltd, London, England) which shines laser light at particles and tracks them using a microscope connected to Nanoparticle Tracking Analysis (NTA) software (Nanosight ltd, London, England) capable of automatically tracking and sizing nanoparticles on an individual basis. The instrument itself is based on a normal optical microscope with a CCD camera allowing the images to be viewed on a computer.

For the analysis, 3ml of sample were injected into the visualising area before the image was captured for 60 seconds. The resulting video was analysed with the NTA software (Nanosight ltd, London, England), correcting the number of counts per frame to around 100 using the level of sensitivity in picking up particles to give results for particles size and concentration.

3.13 Differential scanning calorimetry

The Differential Scanning Calorimetry (DSC) technique was performed using a Microcal VP-Capillary DSC (GE Healthcare, Bucks, UK). Samples were prepared on a 96-well plate in triplicate suspended in stability buffer at concentrations of 1mg/ml. The change in the heat capacity of the sample was measured in comparison to a sample of buffer alone as samples were heated from 45°C to 95°C at a rate of 60°C/hour in the device. The heat capacity data was normalized and corrected for the baseline to improve the ability to compare peaks.

3.14 Accelerated stability of proteins

Accelerated stability was performed by preparing 5ml aliquots of samples in Falcon Bluemax™ conical tubes (BD, Oxford, UK) and storing these tubes at either 20°C or 40°C for a month. Before storage, the samples were tested using the SE-HPLC method to give an absorbance area value under the monomer peak at 280nm. After one month, the samples were again tested using the SE-HPLC method and the absorbance area value was compared against the original value to give a percentage loss of monomer over the course of the hold.

3.15 Fourier transform infra-red spectroscopy

The Fourier Transform Infra-Red Spectroscopy (FTIR) technique was performed using a Spectrum 100 optica (Perkin-Elmer, MA, USA) with a glass Biocell (Biotools, FL, USA). 15uL of antibody solution was loaded onto the Biocell before analysis from 1000-3000cm^{-1} frequency. Analysis was performed using Grams AI software (Thermo Scientific, PA, USA) with PROTA (Biotools, FL, USA). The protein solution absorbance was determined by removing the background absorbance from the protein spectrum. The Buffer absorbance was then determined by removing the

background absorbance from the buffer spectrum. The buffer spectrum was then subtracted from that of the protein solution to give a spectrum for the protein. This spectrum then had the water vapor spectrum subtracted from it before being processed by the software to give results for the secondary structure.

3.16 Proteo-stat® dyes

The method first involved preparation of the positive and negative controls for monitoring and detection of protein aggregation. Both controls were supplied as 300µg aliquots of lyophilized powder. Each was reconstituted using 500µL of deionised water to generate a 40µM stock solution. These solutions were gently mixed with vortexing and bubbles were avoided for their effect on protein stability.

Proteo-stat® dye (Enzo Life Sciences, NY, USA) was prepared by addition of 10µL of Proteo-stat detection reagent and 20µL of 10x assay buffer into 170µL of deionised water before mixing.

2µL of the prepared Proteo-Stat® detection reagent was dispensed into the bottom of each well of a 96 microwell plate (Life technologies, Paisley, UK). 98µL of the protein of interest was then added to each well in triplicate for each sample at a concentration range of 1µg/ml to 10mg/ml.

The microwell plate was then incubated for 15 minutes in the dark at room temperature before being placed into a fluorescence microwell plate reader using an excitation setting of 550nm and an emission filter of 600nm.

Emission data from buffer samples was then subtracted from the antibody samples using Excel (Microsoft, CA, USA) to give an emission spectrum for each.

3.17 Design of experiment

Jmp software (SAS, NC, USA) was used to perform design of experiment. By inputting the variables to be tested and the number of midpoints into a 3x3 matrix

the software determined the order of experiments to do. Following input of the experimental results, their analysis gave the trends reported.

3.18 Capillary shear device operation

The capillary shear device method was developed during the course of the project and the usage parameters were defined as part of the project. The device consisted of an Aladdin-6 syringe pump (WPI, Herts, UK) with six 316 grade stainless steel 18 gauge capillaries fitted with luer fittings (Coopers Needle Works, Birmingham, UK) connected to each of the 6 syringes in the pump. 0.6ml of sample was loaded into a sample tube (eppendorf, Stevenage, UK) and placed at the end of the device with a capillary resting at the bottom of each one. The device is shown in figure 3-9 with a diagram in figure 3-10.

The capillaries were primed by extracting 0.075ml of sample from the sample tube before regular withdrawing and dispensing of 0.45ml of sample for different periods of time.

When the method had finished, the entire sample was expelled from the capillaries into the sample tubes. The samples were then analysed using the SE-HPLC method previously described.
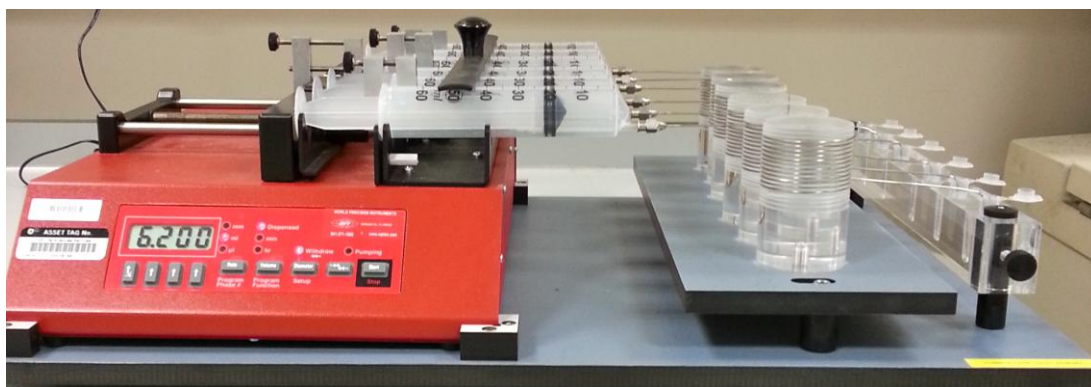
Figure 3-9:   Photograph of capillary syringe device from front view.

Top View
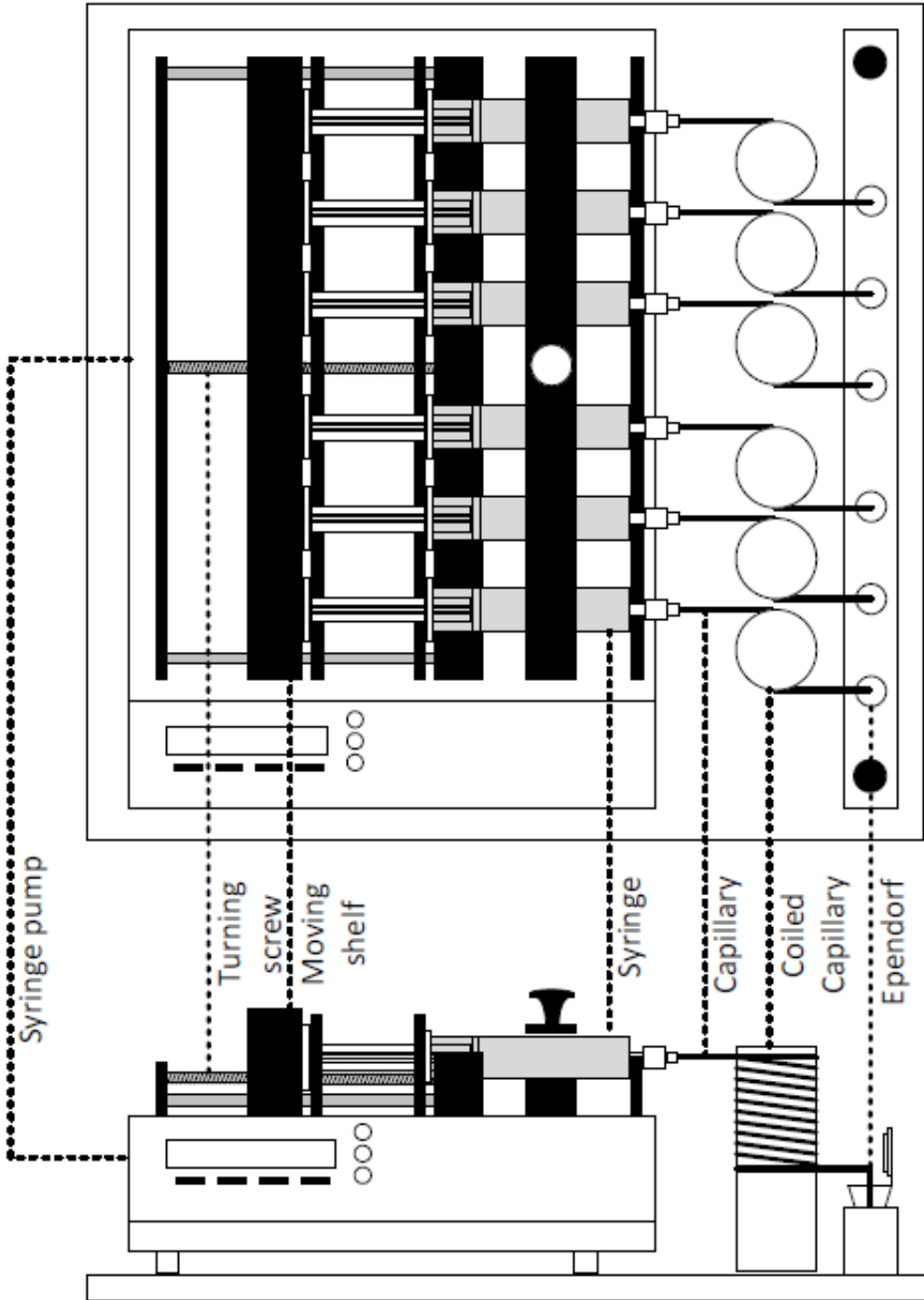
Front View

Figure 3-10: **Diagram of capillary shear device from a top view and a front on view.**

3.19   Creating molecular models

Molecular modelling was performed on the Fc regions of several of the antibodies used in the project. Crystallographic data was either downloaded from the corresponding files on PDB or from data donated by the sponsor company. If the full crystallographic data of the protein Fc regions was not available online, homology models were produced.

The flow chart for producing homology models is outlined in figure 3-11.
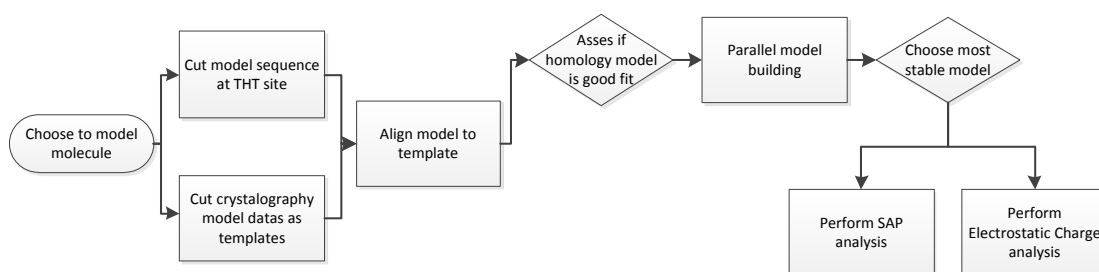
Figure 3-11:   **Flow chart of modelling operation.**

Having chosen the complete models to use in producing parts of the homology model, the sequences were downloaded in FASTA format and cut at the appropriate points in the sequence. Theses were then aligned in Discovery Studio 3.5 (Accelyrys, CA, USA), as shown in figure 3-12, to give a fit for the entire molecule.
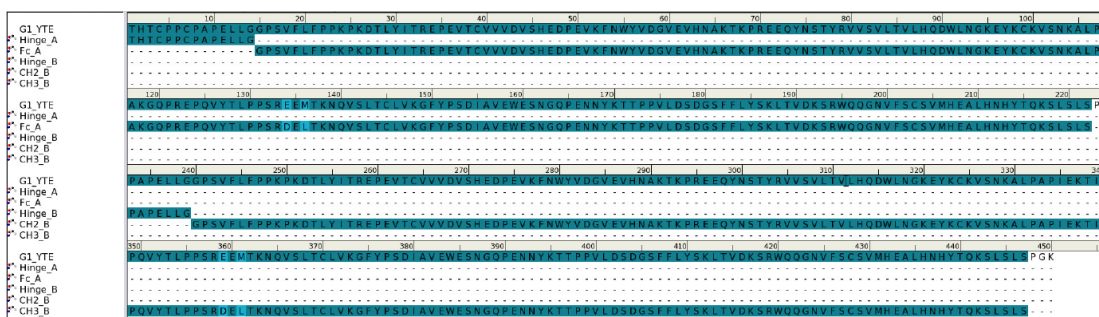
Figure 3-12:   **Screenshot of aligning sequences for molecular models.**

The crystallographic data was then opened in PyMol software (Schrodinger, Munich, Germany) and the models were cut to the same points as the sequence data and aligned with each other, as shown in figure 3-13.
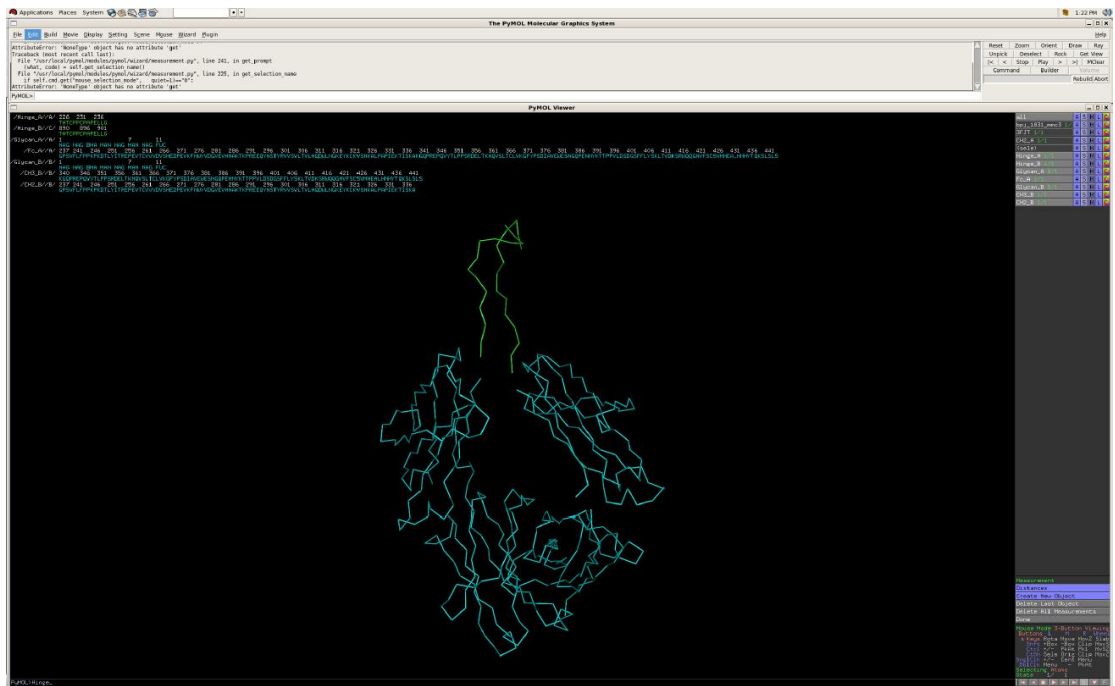
Figure 3-13:   Screenshot of molecule in Pymol.

The software was then used to create 100 different models in parallel, based on folding using a proprietary MedImmune force field. The force field used the data provided in the sequence and the structural data files and a manual input of data on disulfide bridges and Cis-Pro bonding in and between the two halves of the Fc to build differentially folded proteins.

The models created were then ranked using PDF total energy and DOPE scores to give a view of how stable the molecular configurations were. The lowest scores for both these rankings were chosen for this study provided they checked against a ramachandran plot, as in figure 3-14, and the Procheck tool on the software.
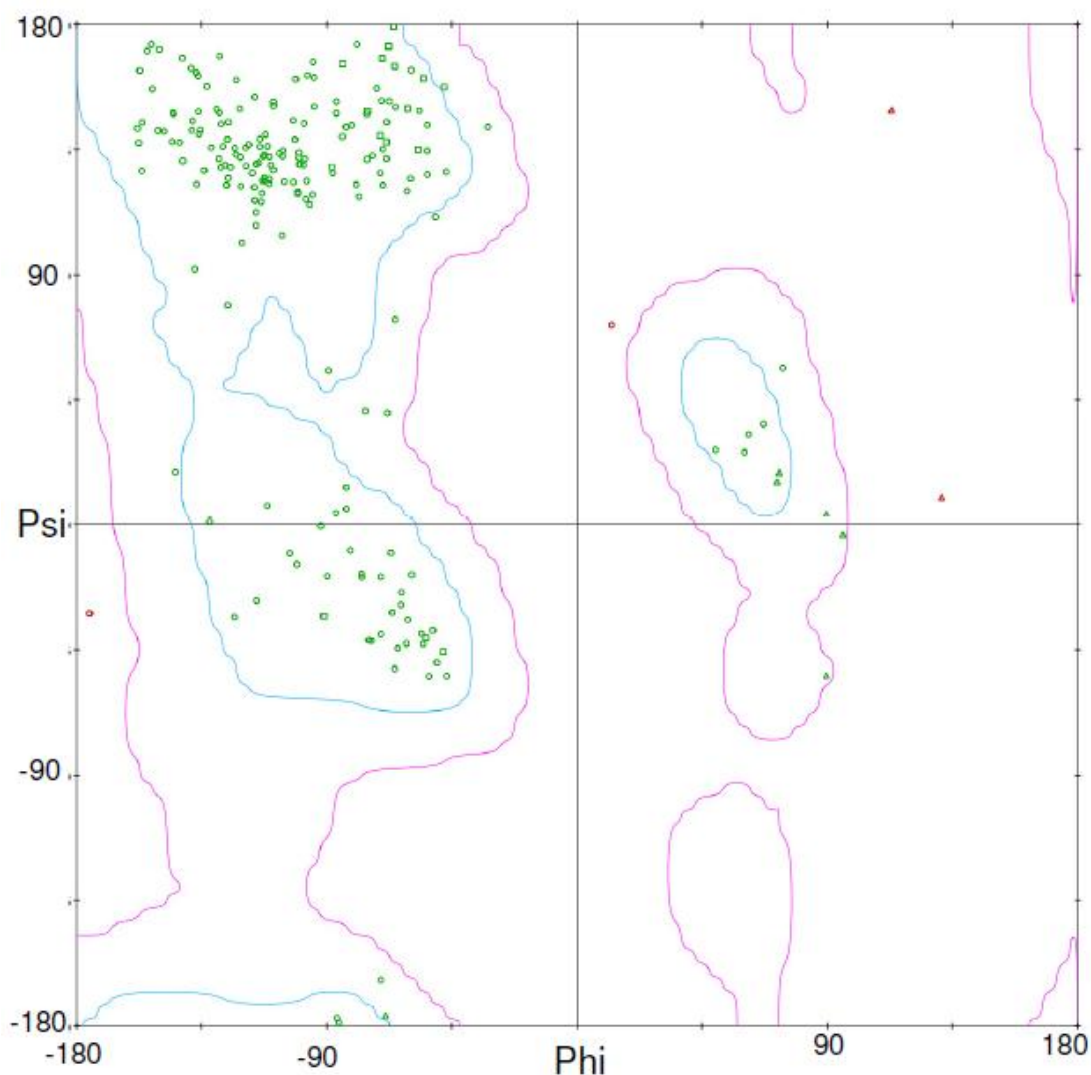
Figure 3-14:   Ramachandran plot of an acceptable molecular model.

3.20   Using molecular models to determine molecular properties

Once the models were ready, Discovery Studio 3.5 (Accelyrys, CA, USA) was used to perform the operations required as part of this study.

First, the software could be used to calculate the developability index of the molecule to give a measure of the molecular stability. Next the SAP was determined by using a 5Å atomic radius to give SAP scores for individual aggregation hot-spots as well as an overall map of SAP on the molecular surface. Finally the electrostatic surface charge was calculated using a fine grid filled by solute.

4 Characterising antibody purification, assays and shear device methods

4.1 Introduction

Before commencing any investigations, it was necessary to define a range of operating procedures. This chapter details the work needed to prepare for the experiments that would follow.

Details such as the effect of the day of fermentor harvest on the level of aggregation were looked into, before defining the entire downstream process to be used.

The reproducibility of the SE-HPLC and absorbance at 280nm methods was checked to give a measure of the error in the results reported using these methods.

Finally aspects of the shear device operation were examined to determine best operating procedures for future experiments.

4.2   Choosing a harvest time for fermentation

The first parameter to be examined was the day of harvesting antibodies grown for use in the project. The sponsor company had its own standard operating procedures for the day of fermentor harvest, so the effect of harvesting 7 different days around this standard was investigated. Samples of IgG1 (Medi/UCL001) were taken each day from a fermentor 5 days before the normal day of harvest until 2 days after. Upon sampling, the concentration of the antibody was determined. This was done by filtering and performing protein-A on the sample before using absorbance at 280nm. By knowing the total mass of protein collected and the original sample volume, the concentration in fermentation could be determined.
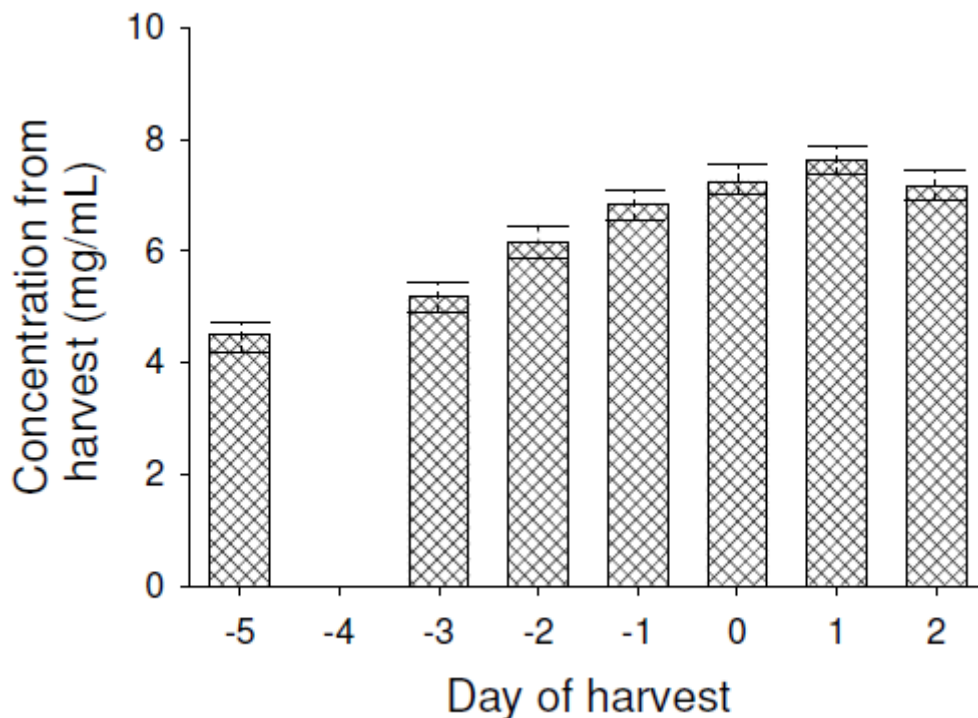
Figure 4-1:   **Graph of antibody concentration over day of harvest of IgG1 (Medi/UCL001) during fed batch production using defined media. Error bars using compounded standard sampling error and error of measurement.**

The results for this, seen in figure 4-1, show a clear trend that the longer the fermentation is run, the higher the antibody concentration in the sample. This trend does seem to peak the day after normal harvest, followed by a drop the day after that. This could be due to antibody loss to large complex aggregates within the fermentor, or from digestion of peptides in the fermentor by enzymes released by cell apoptosis (Mahler et al., 2009).
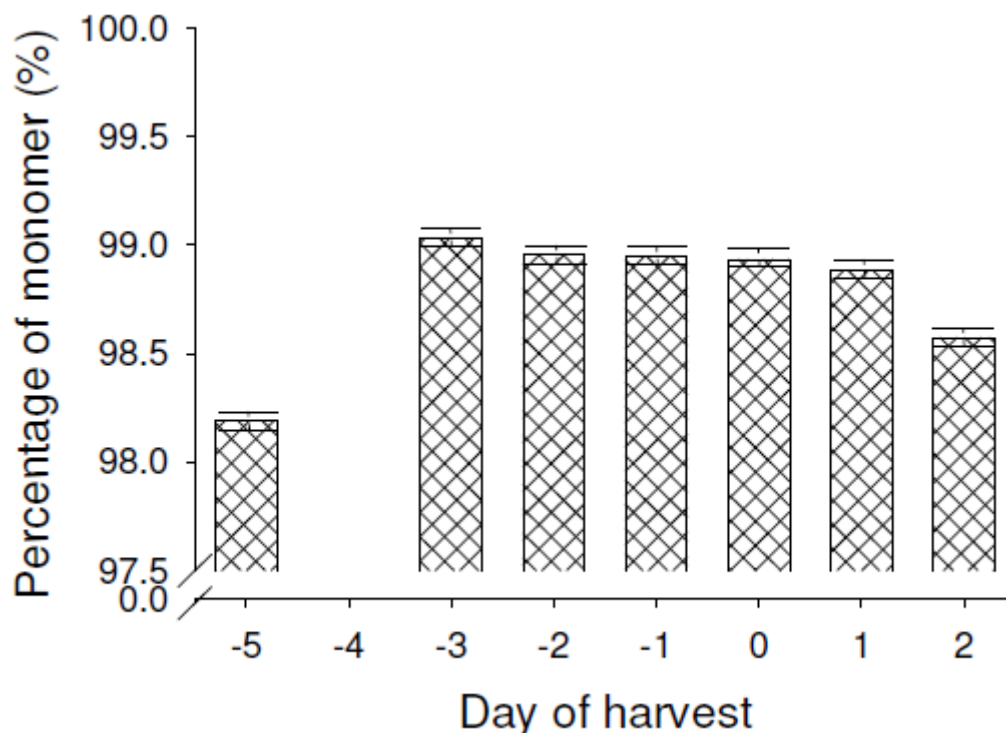
Figure 4-2: **Graph of monomer percentage determined by SE-HPLC over day of harvest for IgG1 (Medi/UCL001) during fed batch production using defined media. Error bars determines from standard error of HPLC method.**

The samples were then checked for the purity of monomer within the antibody that had been clarified using the SE-HPLC method. The percentage of monomer for each day is shown in figure 4-2. There is an obvious exception to the trend on the first measurement, but the antibody concentration is so low at this point that this could be due to a lot of experimental factors. Results from day -3 to day +1 show a consistant level of monomer in the samples. In day +2 however we do see a drop in the monomer percentage as the sample begins to degrade. This would suggest that

either the antibody that is produced later into fermentation is less well folded and so prone to forming smaller aggregates (Jahn and Radford, 2005) or that retention of antibody in fermentation conditions for too long will cause proteins to slowly lose stability (Welfle et al., 1999). For this project, large amounts of relatively stable antibody needed to be produced, so it was decided to keep the fermentation day as the company standard, as a compromise to the two factors.

4.3   Downstream processing operations for antibody purification

Production and purification of large masses of IgG1 and IgG4 antibodies (Medi/UCL003-008) were required for the project, so the fermentation and subsequent purification steps had to be defined. A platform process was defined as shown in figure 4-3 and all antibodies were purified using it.
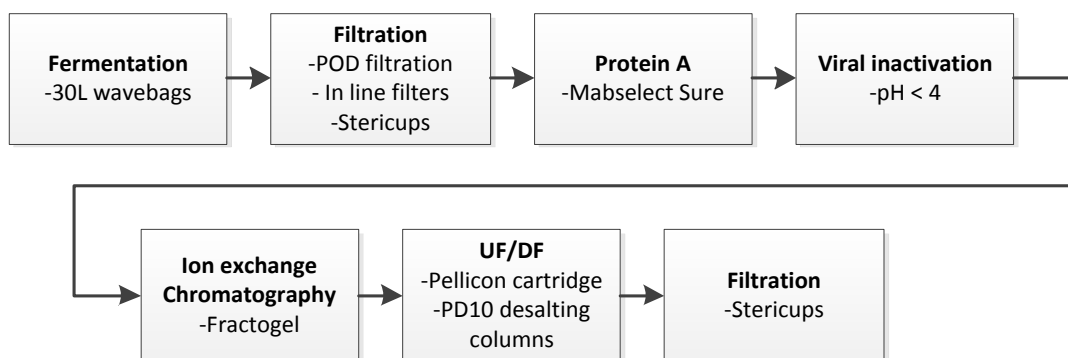
Figure 4-3:   **Flowchart of antibody purification process used in purification of samples for experimental use.**

Due to competitive nature of biopharmaceutical purification and the cost of research into process optimisation, many of the descriptions of these steps here and in the materials and methods section will use generalisations to protect proprietary information. The methods are described in detail in the materials and methods section.

Fermentation was performed by the MedImmune upstream development team in Cambridge, UK. Standard MedImmune procedures were used to grow up to 27L of fermentation media in un-optimised conditions giving concentrations ranging from 0.1 to 3 g/L using disposable wavebag technology and defined media.

Primary recovery was performed with the use of membrane filtration to remove whole cells, particulates, cell debris and organelles from the fermented feed.

Protein-A chromatography was then used to purify the antibody. This step is widely used in the purification of monoclonal antibodies because of its highly specific

binding to the Fc region of the antibodies and the high affinity of the molecule allows

for high dynamic binding capacities to be achieved.
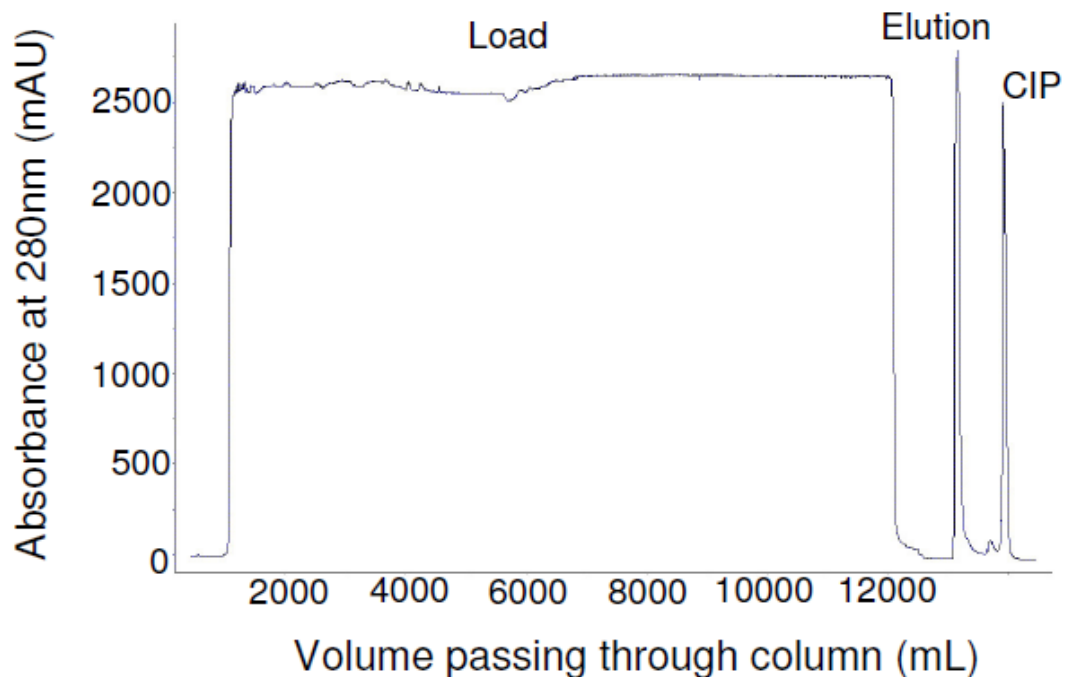
Figure 4-4: Graph of absorbance at 280nm after the column during protein-A operation for purification of IgG1. Column volume of 109ml and a volumetric flow rate of 31ml/min.

Figure 4-4 shows a chromatogram of the protein-A step for one of the purifications.

This particular run has a long loading time due to the low concentration of antibody

in the load and the high affinity of the matrix. It clearly shows the waste coming

through the column during the load stage followed by one large peak corresponding

to the antibody monomer. This is followed by one small impurity peak and then a

sharp, larger impurity peak corresponding to impurities removed in the strip and CIP

steps respectively.

Viral inactivation was then performed by lowering the pH to below 4 to kill off any

virus that had not been purified out from the sample before beginning the anion

exchange chromatography step. In this step, the feed was loaded onto a fractogel

column and as the elution step started, fractions were collected and pooled. During

the course of this operation the majority of fragments, aggregates, antibodies with

different isoelectric points or any other impurities that was still in the solution would

separate out from the monomer. Figure 4-5 is an elution curve from the operation showing a large peak of monomer with a small tail that would not have been collected. There was also a sharp peak after this which corresponds to the strip and CIP stages.
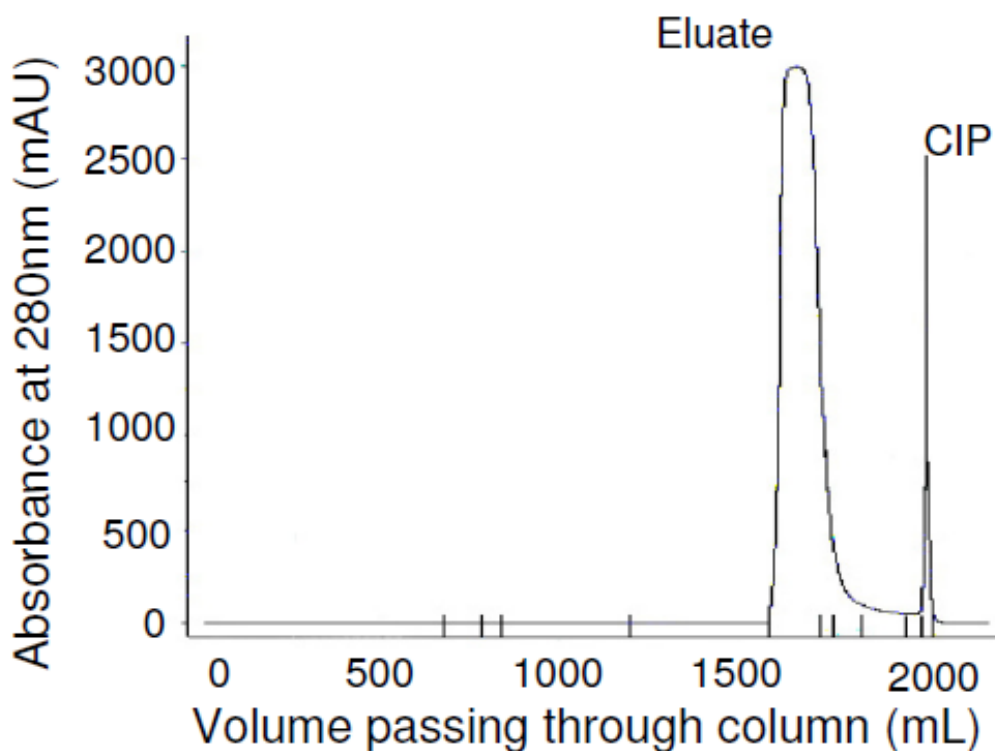
Figure 4-5: Graph of absorbance at 280nm after the column during fractogel operation for purification of IgG1. Column volume of 80ml and a volumetric flow rate of 31ml/min.

The antibody was then diafiltered into the stability buffer and the concentration was altered to the required level using either ultrafiltration or addition of buffer. The formulated protein was then filtered using a Stericup™ filter and aliquots apportioned into storage vials using aseptic technique.

4.4 Characterisation of analytical methods

4.4.1 SE-HPLC for low molecular weight aggregates
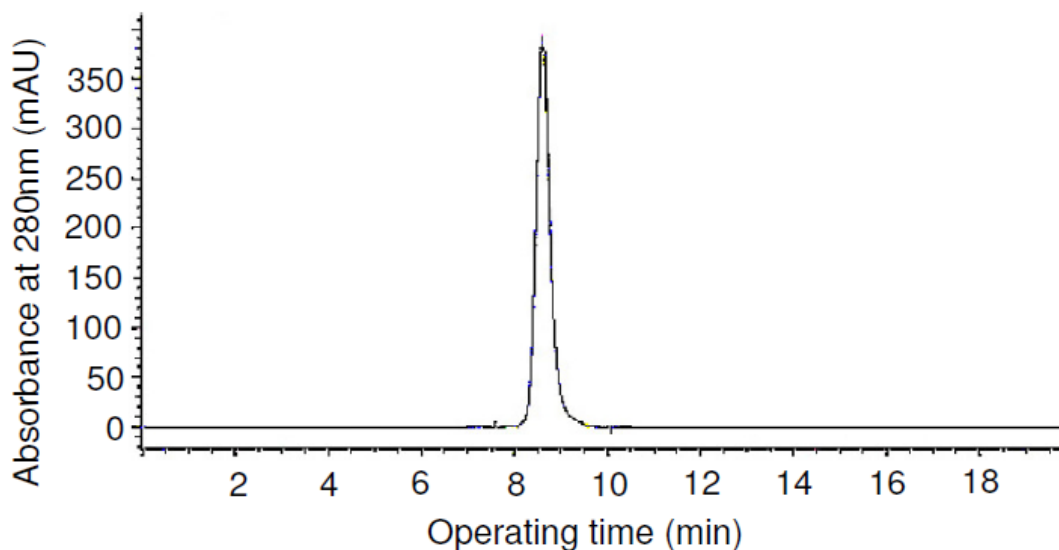
Figure 4-6: SE-HPLC chromatogram of IgG1 (Medi/UCL001) using Tosoh TSK gel SWXL3000 column with MedImmune running buffer running at 1mg/ml.

Figure 4-6 is a SE-HPLC chromatogram taken using the protocol defined in the material and methods section that shows a pure monomer peak. The sharp resolution of the peak and the symmetry show that the method uses a matrix that has a very high plate number and that it is nearly perfectly packed.

Table 4-1: SE-HPLC validation test results for 1mg/ml IgG1 (Medi/UCL008) using Tosoh TSK gel SWXL3000 column with MedImmune running buffer running at 1ml/min.

Vial	1	2	3	4	5	AVG	S.D
A280 Reading (mAU)	8646	8681	8692	8749	8728	8699	40

Many of the experiments in this project rely on the accuracy and reproducibility of the SE-HPLC technique to give a good representation of the differences between samples taken from a system to be able to draw conclusions. To have utmost faith in these results, it is critical that the method itself should be validated. To achieve validation of the method, five samples were taken from a 5mg/ml solution of IgG1

(Medi/UCL008) and run sequentially on the SE-HPLC. The results are shown in table 4-1 and show an average reading for the sample of 8700 mAU with a standard deviation of 40 mAU. This means the error for the device is around 0.46%, allowing the conclusion to be drawn that the technique is very reliable and reproducible.

4.4.2 Absorbance at 280nm for protein concentration

The absorbance at 280nm is used to determine the concentrations of antibody in solution. It is paramount to have an accurate reading for concentration because a false concentration of antibody used in the experiments may have an effect on the mechanisms observed and in turn, could skew the result. To determine the risk of getting an erroneous reading, the reproducibility of the method was tested. It was decided that both a low concentration reading and a high concentration reading would be taken to determine if there was a more reliable concentration to take absorbance readings at.

Table 4-2:   **A280 validation test results for IgG1 (Medi/UCL008) using a Beckman DU 520 UV/VIS-spectrophotometer.**

Attempt	1	2	3	4	5	AVG	S.D
Low value	0.467	0.467	0.466	0.467	0.465	0.466	8.94E-04
High value	0.841	0.839	0.837	0.839	0.841	0.839	1.67E-04

Table 4-2 shows that the low value gave an average of 0.466 and a standard deviation of 8.94 $\times 10^{-4}$ which equated to a 0.2% error. The high value gave an average of 0.839 and a standard deviation of 1.67 $\times 10^{-4}$ which also equated to a 0.2% error. This showed that not only was the method highly reliable, but the concentration of antibody used in the device, if within specifications, did not affect reliability of the concentration reading result.

4.5 Determining optimal conditions for disc shear device operation

Operation of the shear device method was defined by previous work (Biddlecombe et al., 2007) but before continuing with its use, the decision was made to look at a wider range of operating factors to determine the optimum operating conditions.

4.5.1 Optimisation of the cooling jacket temperature

The operation of the shear device exposes the antibody to interfaces and levels of shear that lead to monomer loss through aggregation pathways, but the rate of monomer loss is also affected by the temperature of the solution (Hawe et al., 2009). To negate the effect of increased heat generation from increases in the rotational speed of the spinning disc that are needed to generate higher levels of shear in the solution, the coolant temperature would need to be adjusted.

The relationship between cooling water temperature and shear rate was determined with Alex Berrill (Post-Doc, UCL, UK) by shearing PBS solution in the chamber and fixing the cooling water flow rate. A temperature probe was used to determine the cooling water temperature needed to keep the chamber temperature constant. In this determination, 5 sample points were used at 1, 4, 8, 12 and 15 $x10^3$ rpm.

By plotting the points on a graph as shown on figure 4-7, it was possible to derive Equation 4-1, which could be used to determine the temperature needed for whichever disc speed was chosen.

Equation 4-1: Equation to determine cooling jacket temperature.

Cooling Temp (°C) = $-3x10^{-8}$ Disc speed^2 – $4x10^{-6}$Disc speed +19.59
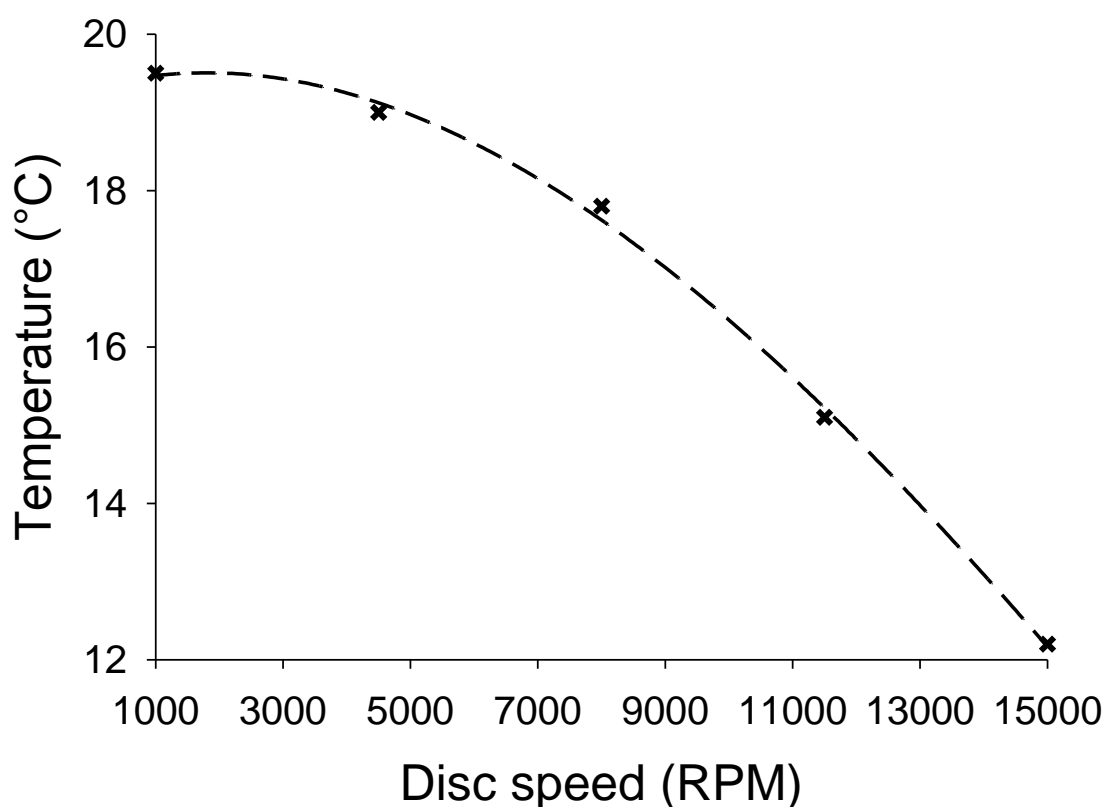
Figure 4-7: **Graph to determine the cooling water tank temperature required for cooling jacket to keep shear device chamber at 20°C at a flowrate of 200ml/min.**

The cooling temperature needed for each of the conditions used in the study were

then calculated and shown in figure 4-3.

Table 4-3: **Table of Shear strain rates and Cooling temperatures.**

Run	RPM	RPS	Shear strain rate (s^{-1})	Cooling temp (°C)
1	3000	50	1.35	19.3
2	6000	100	1.86	18.4
3	7500	125	2.12	18
4	9000	150	2.38	16.9
5	12000	200	2.89	14.9

4.5.2 Choosing an absorbance wavelength for SE-HPLC analysis

Once samples were prepared and put through the SE-HPLC, they were analysed at

two different wavelengths using the DAD detector to determine the level of monomer

loss. Any large aggregates formed would have been removed from the solution

before this reading with the use of a centrifuge or a centrifugal filter. The wavelengths used were 220nm to look at the peptide bonds in the antibodies and 280nm to look at the amino acids with aromatic rings present in the antibodies which would include Tyrosine and Tryptophan.

The results for the loss of signal at 220nm and 280nm for a set of shear device experiments on 1mg/ml IgG1 (Medi/UCL002) are shown in figures 4-8 and 4-9 respectively. These graphs both show unequivocally that there is significant loss of monomer from the solution during the 2 hours of shear. The results taken are adjusted to compensate for the reduction in the concentration of monomer in the chamber due to the process of taking of samples. Each sample volume taken is around 1% of the total chamber volume.
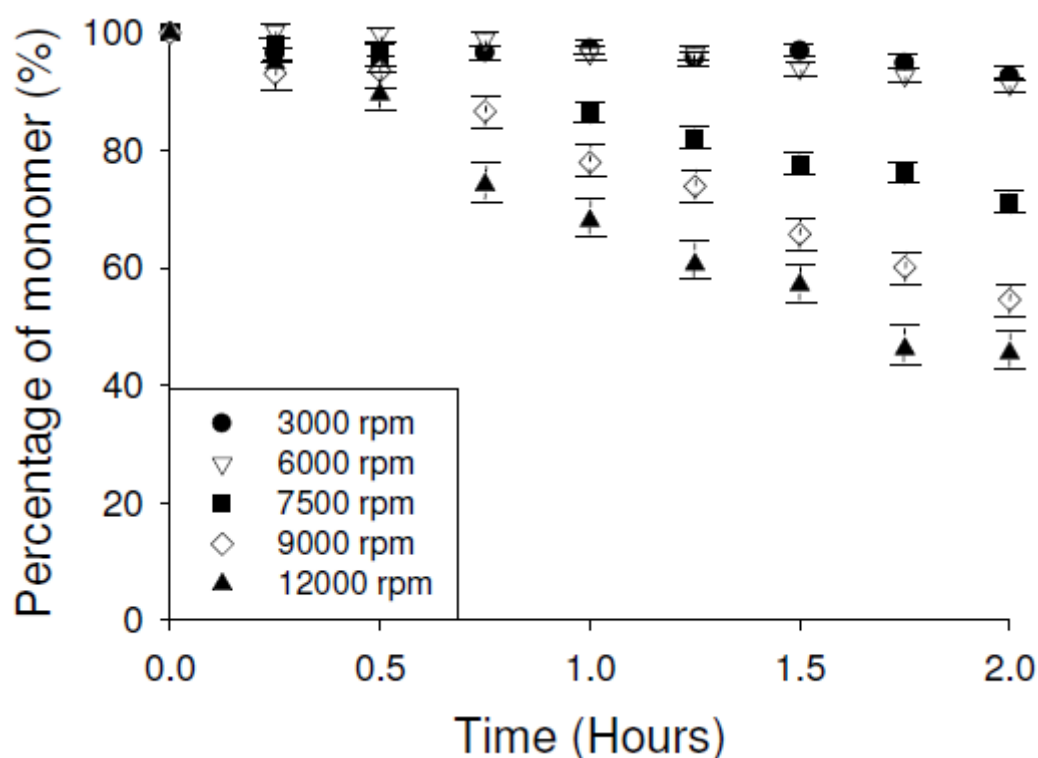
Figure 4-8: Loss of signal at 220nm at 15 minute intervals over 2 hours of shear for various speeds using IgG1 1mg/ml (Medi/UCL002) in PBS buffer. Error bars corresponding to standard error from line of best fit.
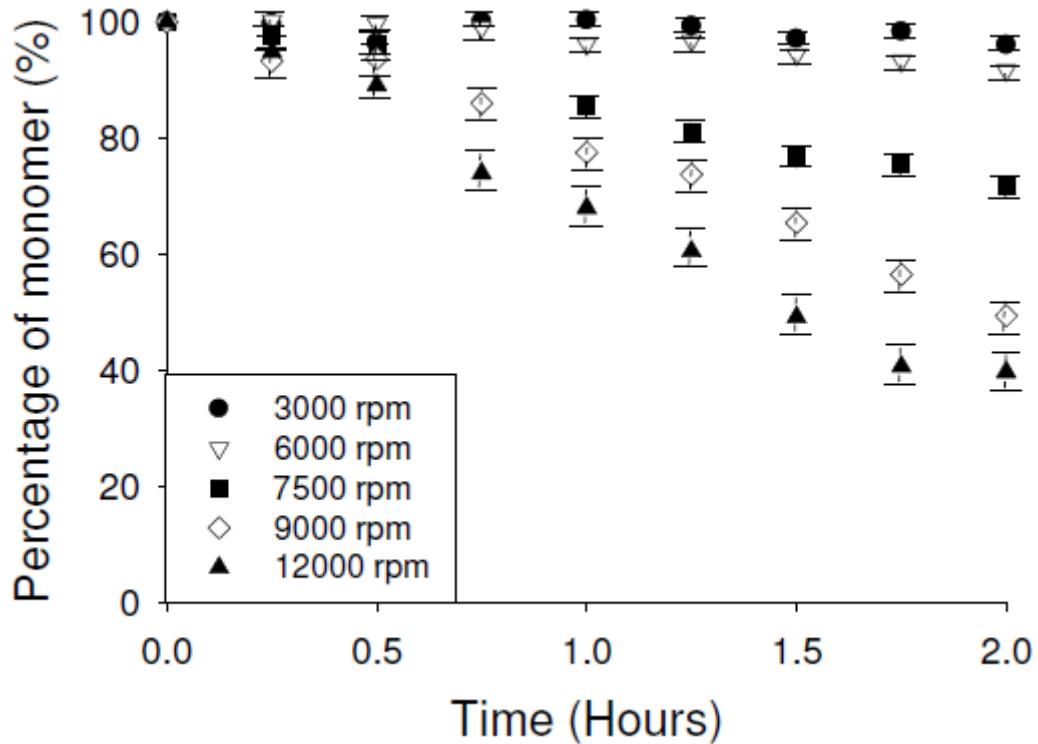
Figure 4-9: Loss of signal at 280nm at 15 minute intervals over 2 hours of shear for various speeds using 1mg/ml IgG1 (Medi/UCL002) in PBS buffer. Error bars corresponding to standard error from line of best fit.

Looking at figures 4-8 and 4-9, we can see there is a definite trend in the level of monomer loss dependent on the shear rate. The higher the shear rate, the higher the rate of monomer loss, and ultimately the less monomer left in solution.

In the 12000rpm experiments at both 220nm and 280nm, it seems like the rate of monomer loss slows down again in what would appear to be a second order kinetic reaction.

The data in figures 4-8 and 4-9 do however show a difference in the overall level of loss which is highlighted in figure 4-10. This is due to the different parameters that the wavelengths measure against, and this difference could hint to the type of effects the shear is having on the monomers. If there is more of a loss at 280nm absorption than at 220nm absorption, then there must be a change in the ability of the protein to absorb the waves at one of the wavelengths. The 280nm reading looks at the aromatic rings within certain amino acids, and as such is less likely to be effected by strains in the peptide backbone caused by exposure to the shear

device chambers environment. Thus it was concluded that using the 280nm reading would give a more reliable result.
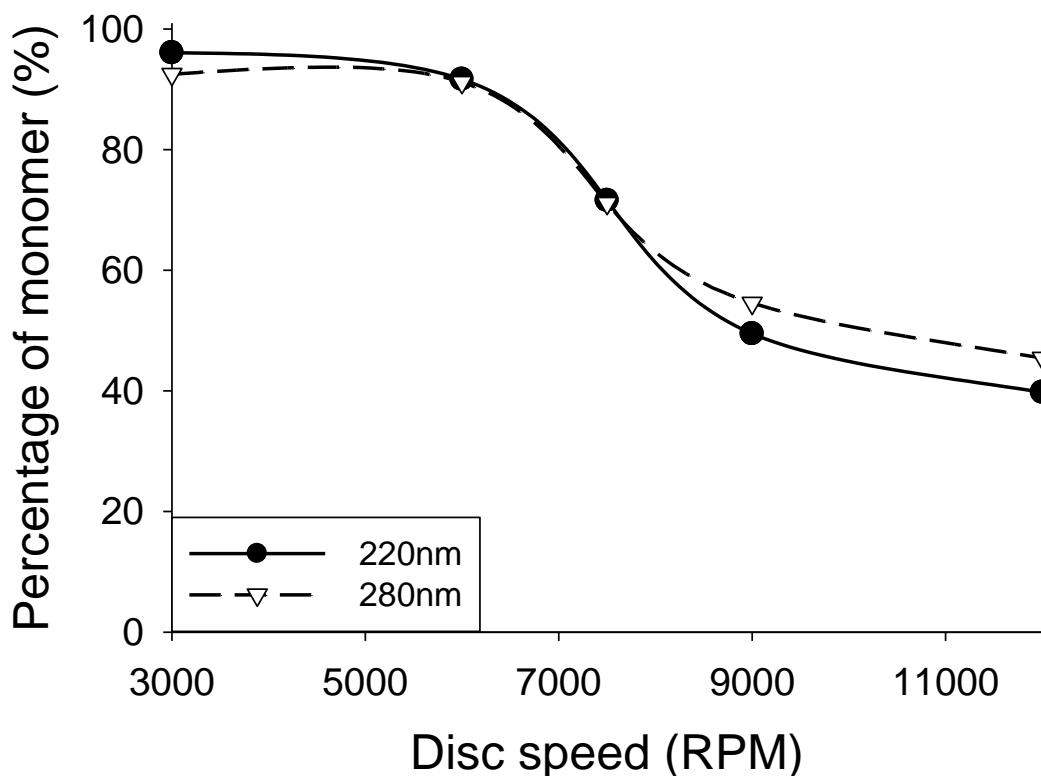
Figure 4-10: Effect of disc speed on monomer loss after 2 hours of shear as determined at 220nm and 280nm for 1mg/ml IgG1 (Medi/UCL002) in PBS buffer.

4.5.3 Choosing a disc speed for the shear device

The rate at which the disc revolves inside the chamber affects the level of monomer loss subsequently measured by SE-HPLC. Being able to set the disc speed allows for choosing the level of degradation that will give optimum level of monomer loss. The parameters that define the optimum level of monomer loss were chosen to be the differentiation of antibodies during the course of a two hour operation and the error in the measurements when fitting the first order exponential decay curve. Having a greater level of differentiation would allow for selection between antibodies with more similar stabilities. The fit with the first order exponential decay curve will determine how accurate and reliable the PDC value determined by the method is.

Figure 4-11 shows the monomer loss profiles of 1mg/ml IgG4 (Medi/UCL003) at increasing disc speeds. It shows a clear trend of decreasing fit with the exponential decay curve as the disc speed increases.
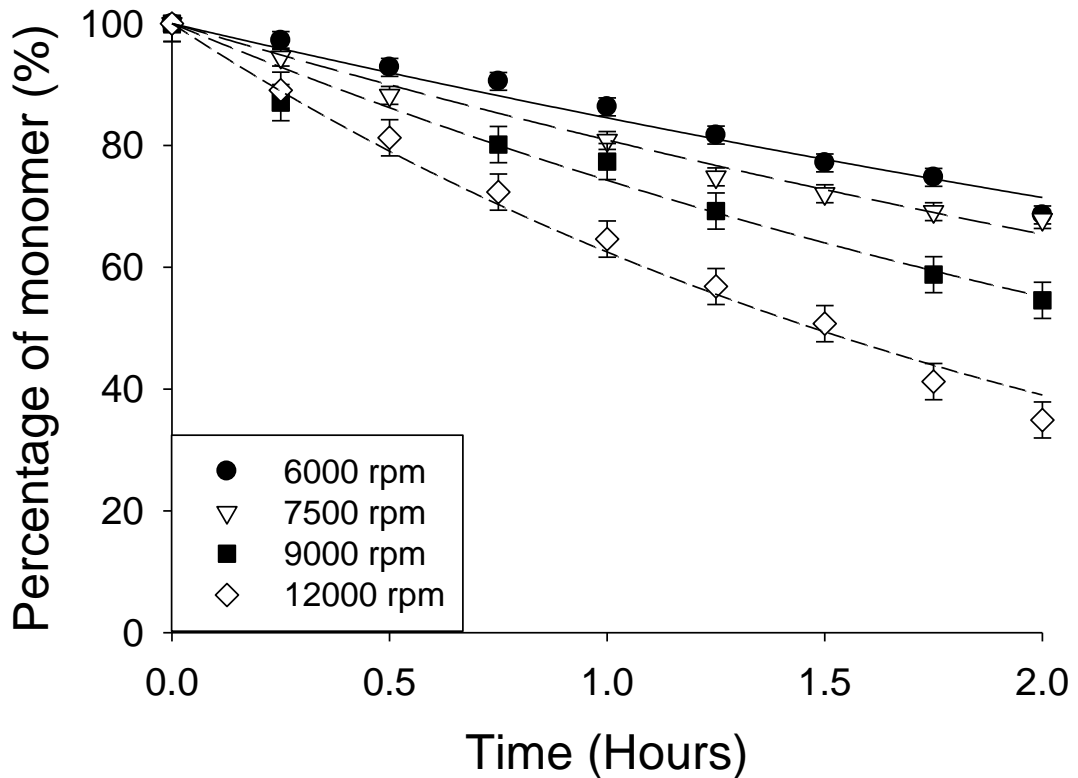
Figure 4-11: **Monomer loss seen at disc speeds of 6000, 7500, 9000 and 12000 rpm for 1mg/ml IgG4 (Medi/UCL003) in L-Histidine and (D+) Trehalose buffer pH5.5.**

Figure 4-12 shows a fitting of the PDC values for 1mg/ml IgG4 (Medi/UCL003-008) in L-Histidine and D (+) trehalose buffer at pH 5.5 for the various disc speeds. By increasing the disc speed there is a clear trend of increasing the differentiation of the molecules.

By comparing the two parameters for deciding the optimum disc speed, there is a compromise that needs to be found between increased differentiation of antibodies and reproducibility of results. As the differentiation of stability would in turn allow for greater margins of error for the individual results, it was decided to assign it higher priority. Moving to a second order decay after a certain amount of monomer loss

was not desired, so this then discounted the highest disc speed. Ultimately it was decided that the optimum disc speed was 9000rpm.
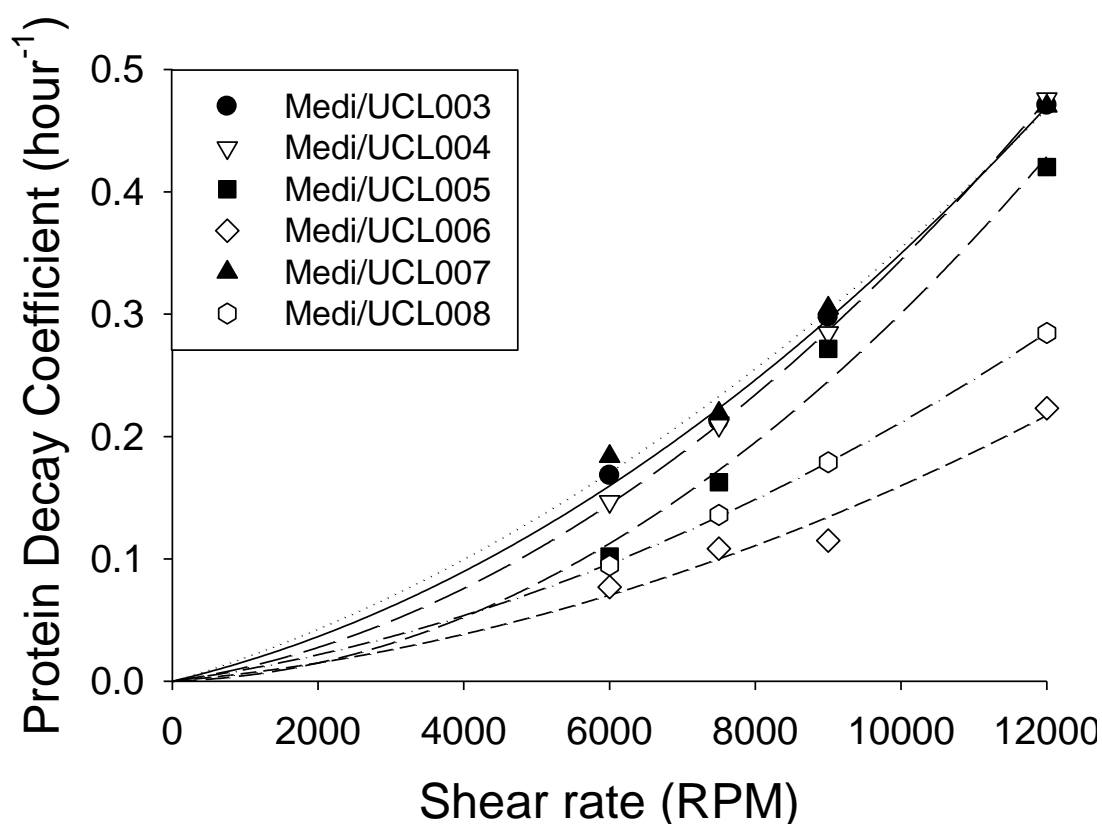
Figure 4-12: **PDC determined for various disc speeds for 1mg/ml IgG1 and IgG4 antibodies (Medi/UCL003-008) in L-Histidine and (D+) Trehalose buffer pH5.5.**

4.5.4 Choosing the sample's antibody concentration

The concentration chosen to perform the tests on would affect various factors associated with operation of the shear device. The first aspect is that having a higher concentration within the device would require the production of a larger amount of antibody. During the early stages of drug development, companies would decide upon their lead molecule using a whole host of methods to determine key product attributes. Producing large amounts of all the different candidates is extremely expensive, so if the company is interested in keeping costs down, then a lower antibody concentration would be advantageous.

The second aspect of concentration is the fit with the exponential decay curve. As with other operational parameters, a worse fit will equate to a less reliable reading.

The third parameter is the differentiation of the antibodies analysed. The larger the differentiation achieved, the better, because it would allow selection of the most stable of similar antibodies.

Due to the constraint of the antibody concentration that can be accurately read by the UV lamp before there is oversaturation of the HPLC sensors, samples taken from the shear device with concentrations over 10mg/ml had to be diluted before being placed on the HPLC. This exposed the results for the 25mg/ml and 50mg/ml samples to another significant source of error from the small volumes of liquids being handled. Any antibody adhering to the outside wall of the transfer pipette or any air in the pipette chamber would have a significant effect on the level of monomer present as determined by SE-HPLC. When looking at the levels of monomer loss occurring between the 15 minute sample times in the device, the cumulative levels of error could possibly give erroneous PDC results.

A further source of error that would become more significant with higher concentrations of antibody is that any solution held in the hold up volume between the chamber and the accessible area of the sample port between 15 minute samples would mix with the later sample and have an effect on the monomer loss viewed.

Figure 4-13 shows the monomer loss results for IgG4 (Medi/UCL004) in an L-Histidine and D (+) trehalose buffer at pH 5.5 at 50, 25 and 5 mg/ml at 9000rpm. The data shows that the trends are a lot noisier with higher concentrations of antibody solution. Therefore, it would appear that lower concentrations of antibody solutions give more reproducible PDC. The trends themselves however do still exist and show that the higher the concentration of the feed, the lower the relative level of monomer loss. The overall mass of monomer lost however, does increase with increased concentration, from 31mg total loss at 5mg/ml to 120mg at 25mg/ml and

128mg at 50mg/ml. This suggests that with higher concentrations there is a limiting factor to the forces involved in the aggregation mechanism of the device.
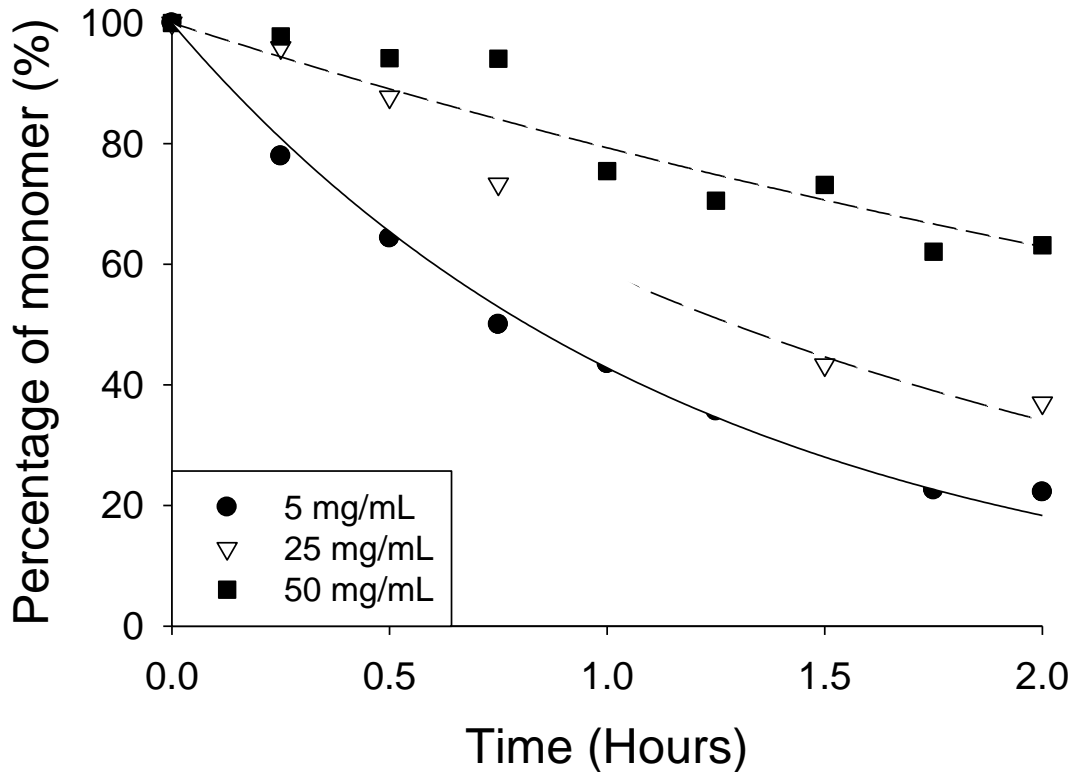
Figure 4-13: **Monomer remaining during processing in disc device at 15 minute time points over 2 hours for IgG4 (Medi/UCL004) at 5, 25 and 50mg/ml in L-Histidine and (D+) Trehalose buffer pH5.5.**

Figure 4-14 shows the PDC's of IgG1 and IgG4 antibodies (Medi/UCL003-008) formulated at 5, 25 and 50mg/ml in L-Histidine and D (+) trehalose buffer at pH 5.5 after 2 hours shear at 9000rpm. The results show that more differentiation of antibody candidates is possible at higher antibody concentrations. This however may be an effect of the higher level of error at the higher antibody concentrations, and therefore unreliable as a metric to determine the optimum antibody concentration.
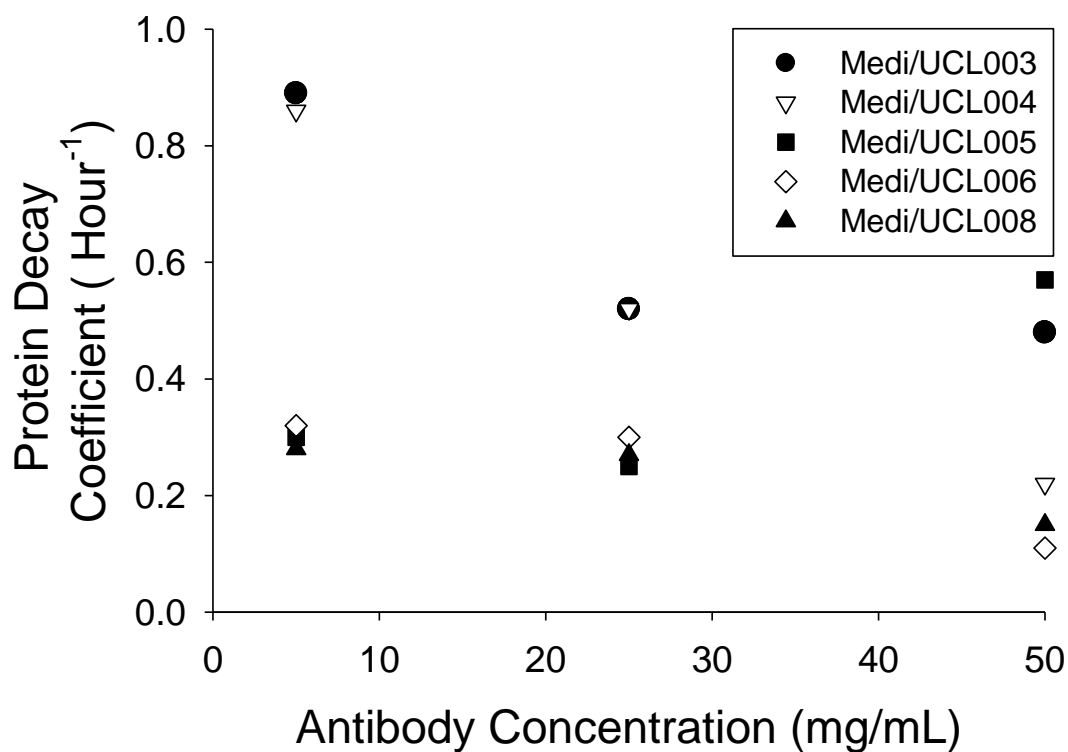
Figure 4-14: **PDC of IgG1 and IgG4 antibodies (Medi/UCL003-008) in L-Histidine and D (+) trehalose buffer at pH 5.5 at different antibody concentrations.**

It was concluded that keeping the concentration of antibody relatively low would be optimal. This gave the most reliable results, and importantly keeps the mass of protein required to a minimum. It is recommended that an antibody concentration of 1mg/ml be used to determine relative stability between different proteins.

4.6   Summary of technique development

The section summarized some of the background work that went into the development of the techniques used in the course of the research. The details for the harvesting and a platform process for the purification of the antibodies to be used in experiments are developed and defined, as is standard practice in industry (Shukla et al., 2007b). The main analytical methods to be used are also characterized and shown to be highly accurate and reproducible. Finally the operating conditions for the interfacial shear disc device are explored and the recommendations for use are given, in addition to what was currently published (Biddlecombe et al., 2007). They include cooling jacket temperatures to be used, the use of 280nm wavelength readings for SE-HPLC, running the disc at 9000rpm and using an antibody concentration of 1mg/ml.

5   Design and operation of the capillary shear device

5.1   Introduction

In the course of the project, the author determined that the shear device method consumed too much material and was not optimised for taking many readings. This led to the development of a device that could produce a comparable measurement using a fraction of the material, in a fraction of the time, in a way that could later be automated to allow scale up of the method. The device was designed and assembled, operating methods were optimised and proof of concept work was conducted using 1mg/ml IgG1 and IgG4 antibodies (Medi/UCL003-008) formulated in a pH5.5 L-Histidine and (D+) Trehelose buffer to determine the validity of the method. It was then used to determine the relative stabilities of Medi/UCL003-008 to be compared with the results from the rotating disc shear device.

5.2   Designing the capillary shear device

The device was developed by trying to understand the reason for the monomer loss observed in the rotating disc shear device. With the disc device, it is believed that the antibody associates with the disc and it is at the surface that modifications occur to the antibody structure which then disassociate from the surface, possibly due to shear and remain in the boundary layer. In the boundary layer they react with other antibodies to create aggregates which can grow before re-entering the bulk solution. The role of the shear in the device is to help disassociate the antibody from the surface and to promote mixing of these highly reactive aggregates out of the boundary layer and into the bulk solution. Increasing the rate of rotation of the disc is hypothesized in practice to increase the effective surface area for association during a set period because the disc surface is "wiped" of antibodies more often.

It was postulated that a similar force could be applied to antibodies along a linear path with the use of a capillary. The low volume and high surface area of a thin capillary would help increase the effective surface area for association of antibody. The disassociation would be provided by shear produced by pumping fluid backwards and forwards through the capillary.

In designing the method, it was important to limit the role of liquid/air interfaces and to try and focus on the solid/liquid interface effects. For this reason it was decided to prime the capillaries with a small amount of the sample prior to any regular processing of the antibody. This would limit the air liquid interface on one side of the sample to the cross sectional area of capillary, and on the other to the cross sectional area of the sample tube. It would also eliminate any potential bubbling or micro cavitation that could introduce more air/liquid interface to the system as the sample was dispensed back into the sample tube.

When dispensing the liquid, the sample was pushed by the air coming from the syringe and displacement was quick. However when extracting the liquid, the syringe would create a vacuum which would then cause the liquid to be drawn up the capillary, which was found to be slightly slower. To stop this affecting the net volume of sample left in the sample tube after each draw-dispense cycle, it was decided to introduce a 2 second pause between each change in direction to allow the liquid to settle at the correct level.

It was noted during initial testing that any difference in the path taken by the capillaries would slightly affect the amount of sample that was extracted by the capillary. Over a two hour operation this would have a significant effect on the effective surface area the antibody was exposed to, so it was concluded that each capillary should be coiled in the same way.

Further testing showed that vertical coils were capable of holding up amounts of liquid that would subsequently be drawn up further into the capillary and eventually into the syringe. It was concluded that to mitigate against any holdup of sample, the capillaries should be coiled in a horizontal plane, making sure that when leaving the syringe there was always a decline in the capillaries vertical path so that sample would always naturally drain into the sample tube.

5.2.1 Determining the methods mode of operation

With the design of the device finalised, the mode of operation was formalised. It was decided that the sample size would be set at 0.6ml. This would allow 0.075ml to be initially drawn as a primer to mitigate bubble formation and then 0.45ml of the sample to be withdrawn and dispensed over the course of the operation. This would leave 0.075ml of sample in the sample tube at the end of the withdrawal, enough to come above the end of the capillary, and therefore stop the formation of any air liquid interface that would introduce bubbles.
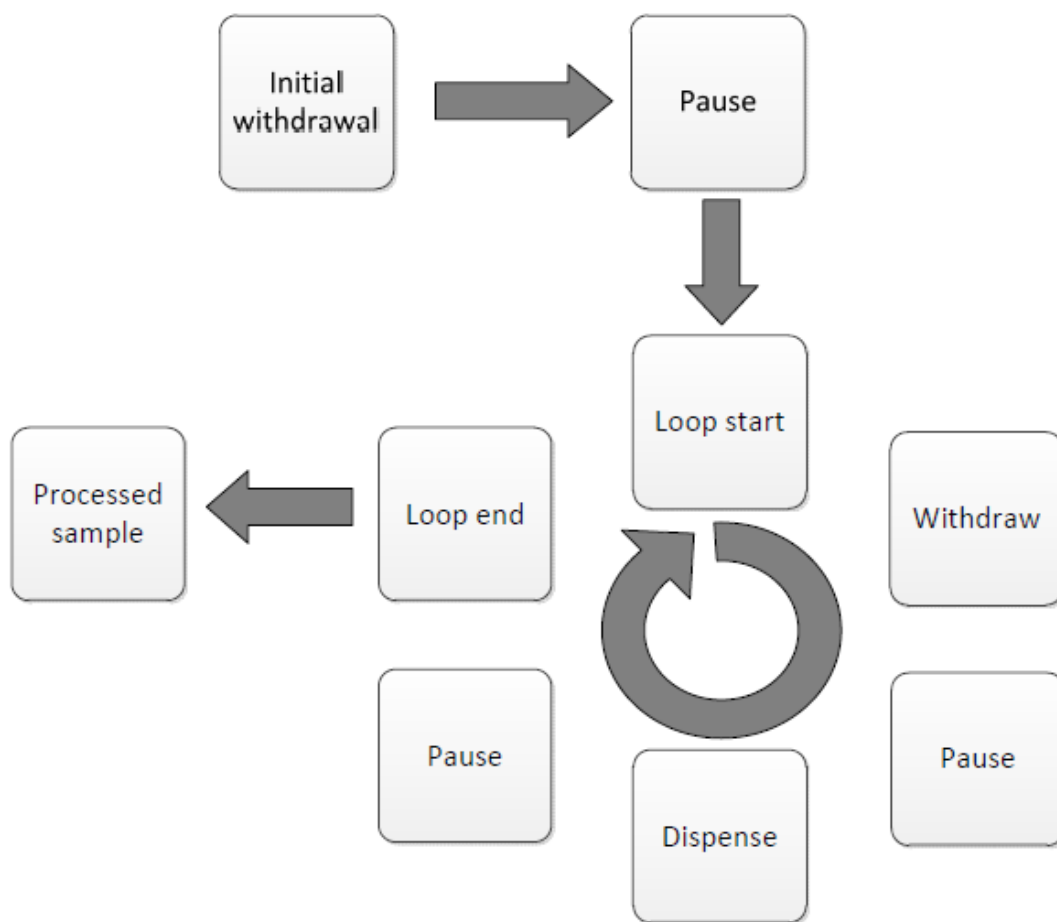
Figure 5-1: **Program steps for capillary shear device operation.**

The flow rate was set as 236ml/h, and the pump was programmed with the steps shown in figure 5-1. This would give the stages for liquid pumping as shown in figure 5-2. The process was then timed using a stopwatch for the required amount of time and the capillaries were manually purged to ensure the entire sample was collected into the sample tube to be analysed for level of monomer loss compared to an unprocessed sample using the SE-HPLC method.
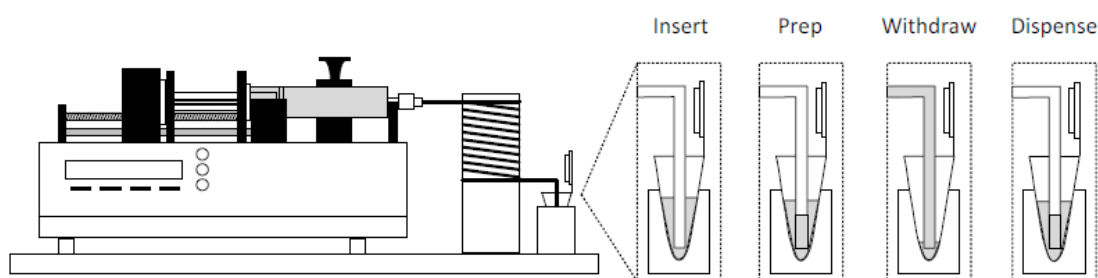
Figure 5-2: **Diagram of capillary shear device mode of action showing the empty, prepped, withdrawn and dispensed positions of the liquid level.**

The CIP for the method was performed by placing sample tubes containing 0.6ml of 0.5M NaOH into the sample area and performing the standard operation of the device. The capillary was then cleared by processing a sample tube containing 1ml of de-ionised water for a further 5 minutes. The length of the NaOH CIP required was determined by testing increasingly long periods of operation and then operating a buffer sample for 20 minutes after the water clearing step. The results for 5 and 10 minutes are shown in figure 5-3, and show that the capillaries are cleaned fully at 10 minutes.
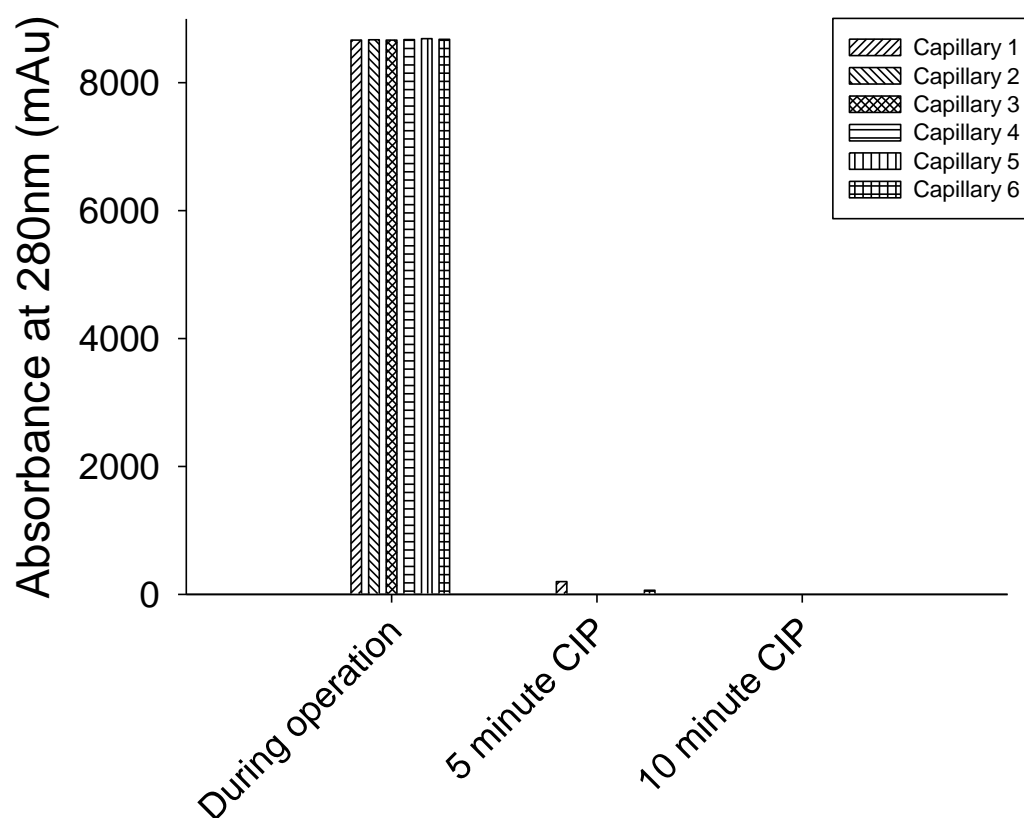
Figure 5-3: **Signal at 280nm determined by SE-HPLC for different lengths of time of NaOH wash during CIP of device.**

5.2.2 Syringe selection to increase method reproducibility

During initial operation of the device it was observed that there was a lot of disparity in the levels of liquid withdrawn from the sample tubes. One of the main causes of

this was determined to be the size of the syringe being utilized. The volumetric flow rate was constrained by the maximum speed at which the syringe pump's turning screw could move the plunger shelf to either push it in or pull it out of the syringe casing. Initially a 50ml syringe was used because the large diameter allowed for a faster volumetric flow rate which meant a higher effective surface area for a given time. Each draw gives a surface area exposure of 300mm^2, the 50ml syringe with an ID of 26.6mm gives a nine times faster displacement of solution than the 2mm syringe with an ID of 8.66mm. This would expose the antibody in solution to nine times more surface area for the time of displacement, giving a higher loss of monomer to aggregate. However, the moving shelf did not seem to always give an even horizontal distance moved for all the syringes. With the 50ml syringe, this was equivalent to a high degree of variability due to the distance needed to push or pull 2ml volume. This error led to a great difference in the measurements calculated from each syringe.
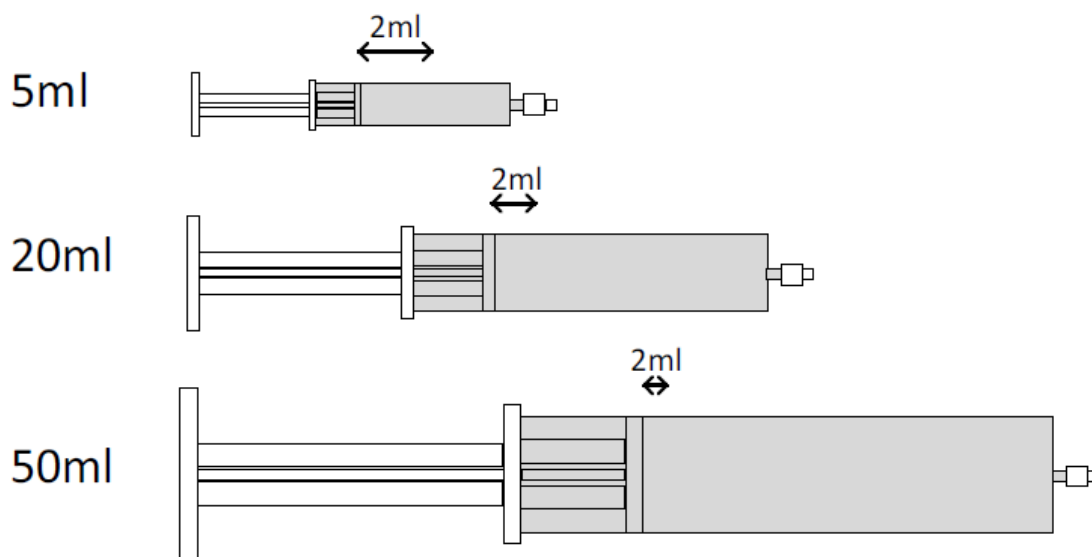
Figure 5-4: Diagram to illustrate how syringe size effects capillary shear device operation and reproducibility (not to scale).

Figure 5-4 gives a not to scale graphical representation of the distances required by different sized syringes to displace 2ml. From this it could be determined that by

using a smaller syringe the effect of this error would be greatly reduced and this was experimentally proven to be so.

The 5ml syringe was used to give the maximum level of reproducibility available to the use of the syringe pump, and the results of the level of reproducibility across all six capillaries in the device are shown in figure 5-5. It was however concluded that should the device be developed further, an alternative to the syringe pump would be required to produce the push and pull of the samples in the capillary.
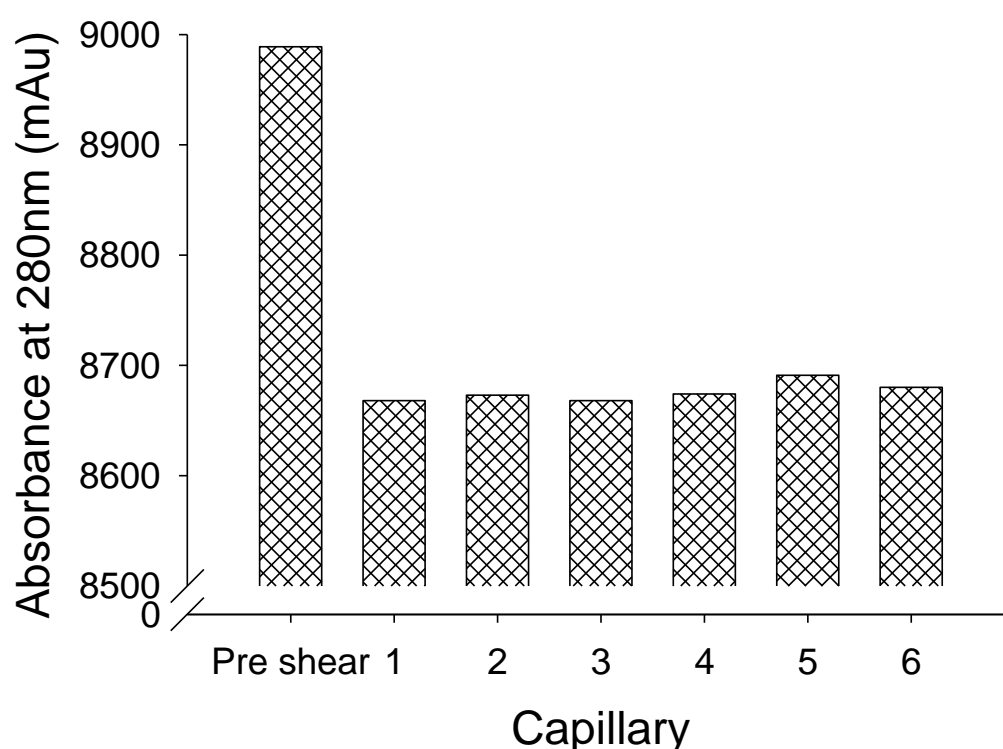
Figure 5-5: **Reproducibility of results as determined by SE-HPLC after 2 hours processing of 5mg/ml IgG1 (Medi/UCL008) in L-Histidine and (D+) Trehalose buffer pH5.5 in the capillary shear device.**

5.3 Calculating the capillary flow regime

The capillaries would be pumped at a volumetric flow rate of 236ml/hr, which would translate to a linear flow rate of 0.119m/s. By using a 5mg/ml sample of IgG1 (Medi/UCL008) in L-histidine and (D+) Trehelose buffer at pH5.6 as an example, the flow regime in the capillary can be determined. By using the measured kinematic viscosity of the solution at $1.02m^2/s$ and assuming a density of 1050 kg/m^3 for the

solution, the dynamic viscosity can be determined for the sample. By using the equation for Reynolds number in a pipe:

Equation 5-1:   Reynolds number in a pipe.

$$Re = \frac{Du\rho}{\mu}$$

Where D is pipe diameter, u is average linear velocity of the fluid, ρ is fluid density and μ is the dynamic viscosity. By putting in the values determined for the 18 gauge capillary and the sample solution into the equation, the Reynolds number returned is 102, which corresponds to laminar flow in the capillary (Doran, 1995).

5.4   The effect of time on antibody monomer loss
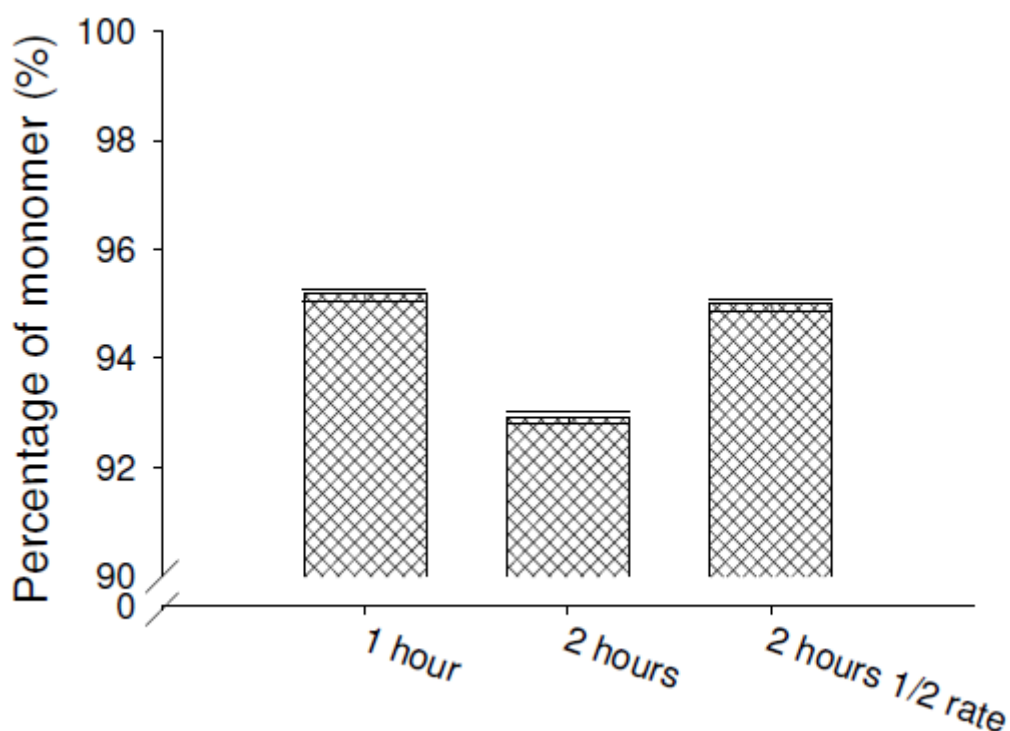
Figure 5-6:   **Effect of flowrate of pumping on the level of monomer lost using 5mg/ml IgG1 (Medi/UCL008) in L-Histidine and (D+) Trehalose buffer pH5.5 in capillary shear device. Error bars for the standard error of the SEC measurement technique and the experimental method.**

To test the theory of effective surface area being the cause of the monomer loss and that monomer loss was not being propagated simply by the time spent in the capillary or the shear evolved, samples were run at the highest flow rate for one

hour and then further samples were run for two hours. As expected, the level of monomer loss increased almost double from around 4.5% to around 7.5%. Samples were then run at half the volumetric flow rate for two hours, effectively exposing the antibody to half the effective surface area as at full speed, or the same effective surface area as running the device at full speed for one hour. During this operation, there would be much lower shear evolved due to the lower fluid velocities at the capillary surface and the sample would be in the capillary for the same amount of time.

Figure 5-6 shows the monomer loss from the three samples and confirms that the half rate samples have the same level of monomer loss as the samples processed for half the time at the full rate, supporting the effective surface area hypothesis.

Since the length of time that the samples would be processed at would affect the effective surface area that the antibody would be exposed to, by having a greater effective surface area, the level of monomer loss would be increased in a sample. This would not only marginalise any sources of outside error, but also help differentiate antibodies with more closely related stabilities.

Figure 5-7 shows the results for IgG1 (Medi/UCL008) samples at 5mg/ml in L-Histidine and (D+) Trehelose buffer at pH5.5 processed for 1, 2, 3, 4, 5 and 6 hours and tested for the level of monomer remaining. These results show that the level of monomer loss follows a near linear path, similar to the path of the shear device during degradation at the same levels of monomer loss. This path seems to intercept the y-axis at 2% monomer loss. This 2% loss could be accounted for by the amount of protein that is adsorbed to the surface (Dee et al., 2003). This would amount to 0.045mg of protein bound to a surface area of 2.63×10^{-3} m^2 at a density of 17.1 g m^{-2}. To determine if this is the case, capillaries of various diameters could be used to determine if the density calculated is similar.

A monomer loss of 7% at 2 hours in Figure 5-7 was significant for the IgG1 (Medi/UCL008) which was one of the more stable antibodies tested in the disc shear

device and the high level of reproducibility of the method would ensure that any differentiation of stability between antibodies was detected. It was concluded that to keep the operating time down, the method would be run for 2 hours.
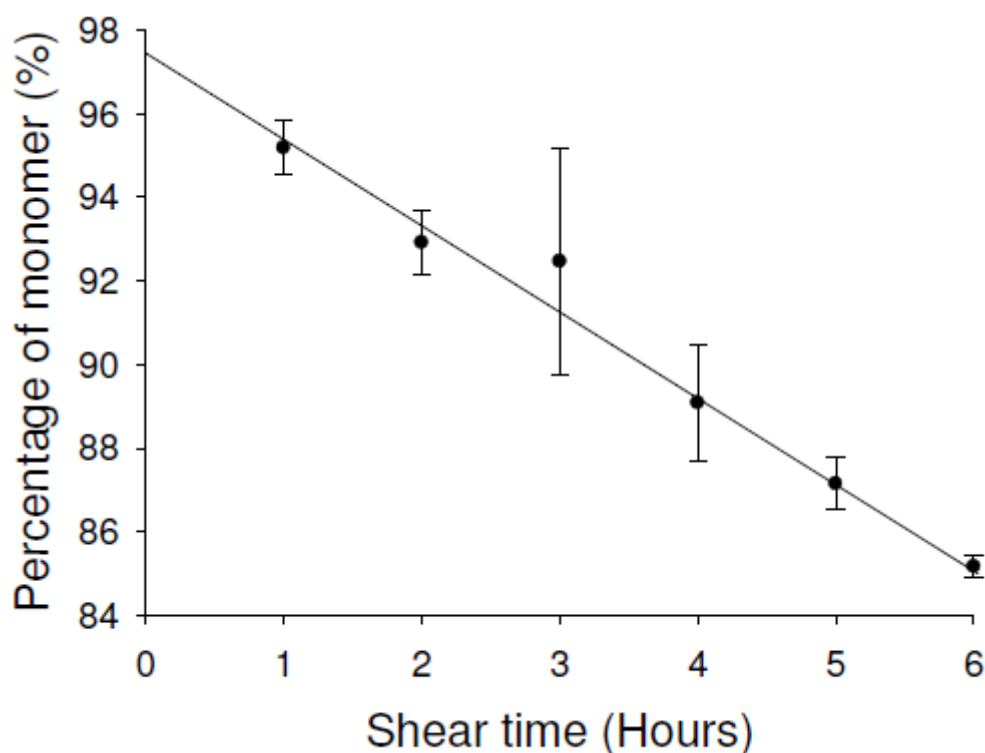
Figure 5-7: **IgG1 (Medi/UCL008) monomer remaining after 1-6 hours of capillary shear device operation. 5mg/ml protein samples suspended in L-histidine and (D+) Trehelose buffer at pH5.5.**

5.5   The effect of concentration on monomer loss in the capillary

When operating the disc shear device, increasing the concentration of the sample appeared to be limited in its effect of increasing monomer degradation rate. It was hypothesized that this was due to limited surface area available on the disc to allow monomer to bind. When using a capillary, the surface area to volume ratio changes from $228m^{-1}$ in the shear device to $4773m^{-1}$ due to the capillaries inner diameter of 0.26mm, an almost 21 fold increase. The capillary device was expected to increase the rate of monomer loss to a much greater extent with increased concentration.
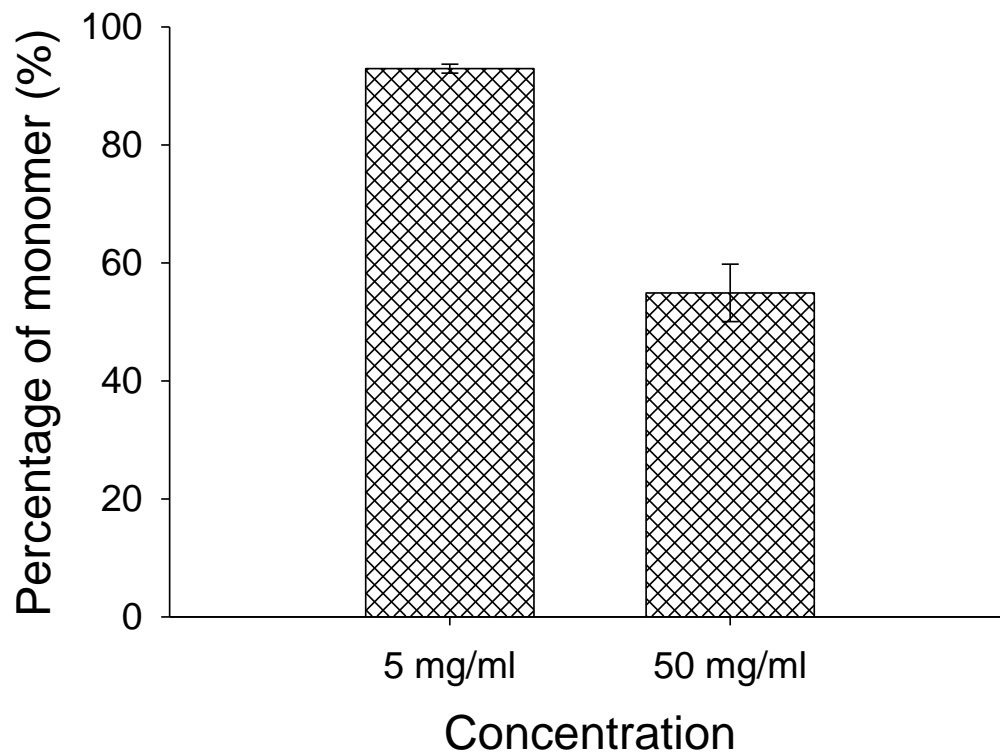
Figure 5-8: Comparison of monomer remaining of IgG1 (Medi/UCL008) at 50 and 5 mg/ml after 2 hours of processing in capillary shear device.

Figure 5-8 shows the monomer percentage remaining for increasing the concentration 10-fold, from 5mg/ml to 50mg/ml during a two hour operation. For the disc device, there is a decrease in the percentage of monomer lost from 45% to 26% (figure 4-14). In real terms however, this equates to a 5.8 times increase in the mass of antibody lost at 50mg/ml, from 1.5mg to 9.1mg. For the capillary device, there is an increase in the percentage of monomer lost when increasing the concentration, going from 7% at 5mg/ml to 45% at 50mg/ml. This equates to a 64 times increase in the mass of antibody lost, going from 0.19mg at 5mg/ml to 12.38mg at 50mg/ml.

When comparing the increase in rate of degradation between the concentrations, the capillary device gave an 11-fold greater effect than the disc device for the 20-fold increase in surface area to volume ratio.

This leads to the hypothesis that the rate limiting factor in the disc device was indeed the surface area available for adsorption of protein as supported by previous

experiments into similar issues (Bee et al., 2010, Brummitt et al., 2011). The protein is hypothesized not to become unstable until it comes into contact with the surface material and enter a non-native state (Roberts, 2007).

The large increase in monomer loss rate from such a low level at 5mg/ml would also indicate a limiting factor in the capillary device. With the disc device, the turbulent flow ensures good mixing and a near constant refreshing of the concentration of monomer at the boundary layer. At 50mg/ml the monomer population spread at any given cross section in the capillary is quite dense so movement of antibody into the boundary layer is not constrained. At 5mg/ml however, the lack of good mixing in the laminar flow of the capillary means the concentration gradient between the boundary layer and bulk fluid is not very high which may be the reason for the low levels of degradation at low concentration (Roberts, 2003). Faster flow rates in the capillary would give better mixing and a thinner boundary layer, so improving the concentration gradient across to the capillary wall as well as removal of antibody from the wall itself (Doran, 1995).

5.6   Comparability of the capillary device with the disc interfacial shear device

The final test of the capillary system was to determine comparability with the disc device in determining the stability of IgG1 and IgG4 antibodies Medi/UCL003-008. By comparing the monomer lost after capillary operation with the PDC determined by disc operation, it was hypothesized that there should be a correlation.

Figure 5-9 shows that as hypothesised there is a correlation between the stability determined by the disc device with the monomer loss determined in the capillary device. There is perfect correlation between the IgG1 antibodies. For the IgG4 candidates, the PDC values are so close that they are within error of each other and it is uncertain if they correlate with the capillary results. To better determine whether

the methods correlate for the IgG4, conditions with greater differentiation in the disc shear device would need to be developed and used. The biggest issue with creating such conditions is that the two molecules seem to be so unstable in the disc device that they seem to be degrading at the maximum rate for each of the conditions used.
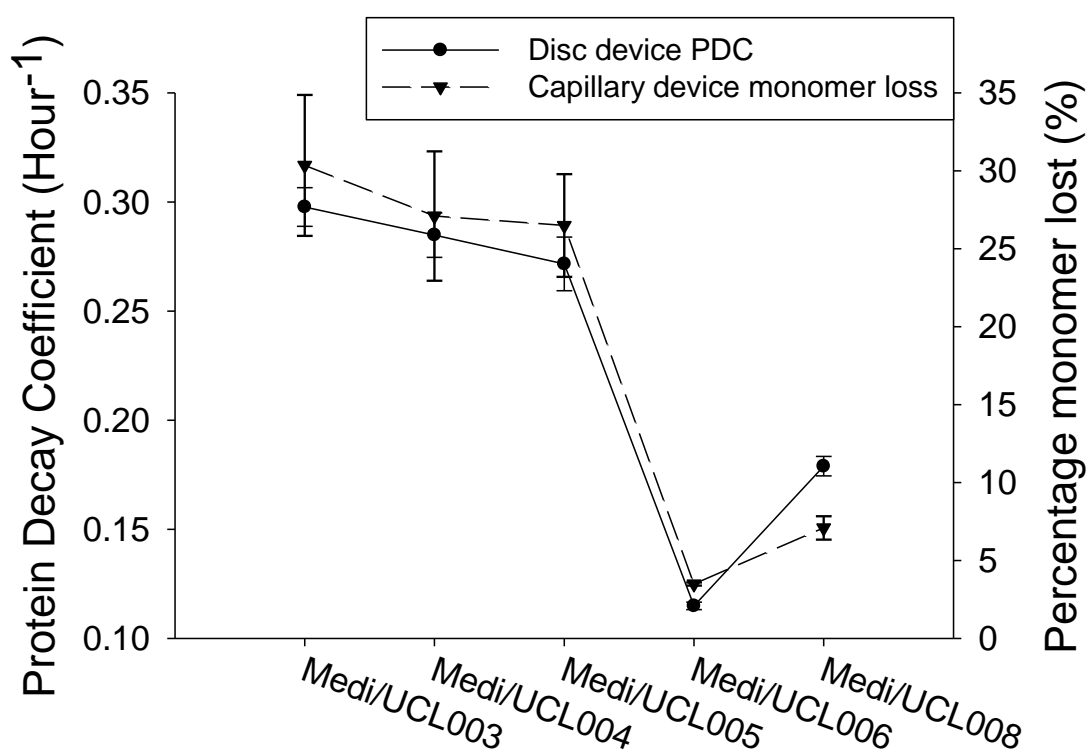
Figure 5-9: Comparison of monomer loss in capillary device with PDC in disc device for various IgG1 and IgG4 candidates (Medi/UCL003-008). Error bars for disc device show Standard Error, error bars for capillary show Standard Deviation. Disc device corresponds to left Y-axis while capillary device corresponds to right Y-Axis.

5.7   Implications of the capillary device on processing time

Table 5-1: Comparison of disc and capillary devices in terms of sample needed and processing time needed.

The ability of the capillaries to enable parallel processing opens the door to using 96 well plates to allow 96 samples to be queued up. Parallel capillaries could process 8 wells simultaneously every 2 hours before CIP, with the samples ready to be placed directly onto a HPLC for SE-HPLC analysis.

		1 sample	8 samples	96 samples	288 samples
Sample (ml)	Disc device	7	56	672	2016
	Capillary device	0.6	4.8	57	172
Time (hours)	Disc device	2.5	20	240	720
	Capillary device	2.25	2.25	27	81
Working days (days)	Disc device	1	3	32	96
	Capillary device	1	1	2	4

The simplicity of the method could allow automation either on an established robotic platform such as a Tecan, or on a custom produced platform that could be designed and assembled in the future. A fully developed technique of this kind, with a 15 minute clean in place protocol would be able to process 96 different samples within 27 hours. Multiple plates could be loaded onto a system before the weekend to allow 192 or 288 samples to be processed in one batch using a total of 57.6mg of protein per plate. Using the current method, a maximum of 3 runs can be completed in a working day so it would take 32 days, or six and a half weeks and 672mg of protein to get the same number of results as one plate. This is an order of magnitude reduction in time and material requirements. Details of benefits are given in table 5-1.

5.8 Conclusions: Is the capillary device capable of giving comparable results to the disc device?

It is concluded that the capillary device gives a monomer loss reading that is dependent on concentration, flow rate, and time of shear. Longer operating times give greater levels of monomer loss. With the flow rate conditions used for the proof of concept device, the concentration has a big influence on the monomer loss observed. It is hypothesized that this is due to a lack of driving force into the boundary layer, due to the laminar flow rates, to bring the monomer into contact with the capillary surface. The results from the concentration experiments and the apparent effect of the increased surface area also points to the adsorption at the solid/liquid interface being a key rate limiting step in the mechanism of protein aggregation. The significant effect of increasing concentration would support the involvement of mass transfer into and out of an intermediate boundary layer.

The results of the method were shown to correlate to the results derived from operation of the disc device and so lead to a recommendation to develop the technique further. Since the maximum volumetric flow rate achievable for the syringe pump is utilized, it is recommended for further studies to use a different method to withdraw and dispense sample. This experiment was completed towards the end of the project, so it was not possible to use device for the rest of the experiments and investigations.

6 Evaluation of aggregate analysis

Having determined the effect of various degradation pathways on the monomer and its subsequent rate of loss to the aggregated form, the logical step is to then look at the aggregates that are formed.

The optimal conditions for running Proteo-stat fluorescent dye experiments were determined before testing both thermal and shear degraded samples with the method to determine its usefulness in tracking aggregation.

The nanoparticle tracking analysis technique run on the Nanosight was then evaluated alongside the dynamic light scattering (DLS) method to determine its suitability for polydisperse solutions before being used to analyse shear degraded samples taken every 20 minutes of operation from the disc shear device.

Finally the data was used to try and explore a mechanism for aggregation during the interfacial shear methods.

6.1   Materials and methods

5mg/ml IgG1 (Medi/UCL008) in a pH 5.5 L-Histidine and (D+) Trehelose buffer was used. The SE-HPLC method was employed to evaluate antibody degraded at 40°C at a low pH for 24 hours compared to antibody degraded by two hours processing in the shear device. Proteo-stat dye running conditions were then determined and used to look at aggregates formed during shear device operation and thermal degradation. Nanosight was then validated and used to determine aggregates for samples taken at 20 minute intervals in the shear device. All protocols are described in detail in the materials and methods chapter.

6.2   Using Proteo-stat for determining aggregate levels

Proteo-stat dye was used to determine the aggregate levels present in degraded samples. The dye is a molecular rotor that rotates like a propeller in the absence of protein aggregates and does not fluoresce, as shown in figure 6-1. Upon binding with aggregates, the rotation is immobilized and the dye fluoresces (Khurana et al., 2005). The dye assay kit was relatively new and no characterisation studies had been performed by the sponsor company so the operating conditions were determined before use. The excitation measurements were read on a plate reader across a spectrum from 580nm to 680nm. The reading at 590nm was around the peak for most antibody readings, so this was the value used for comparison.
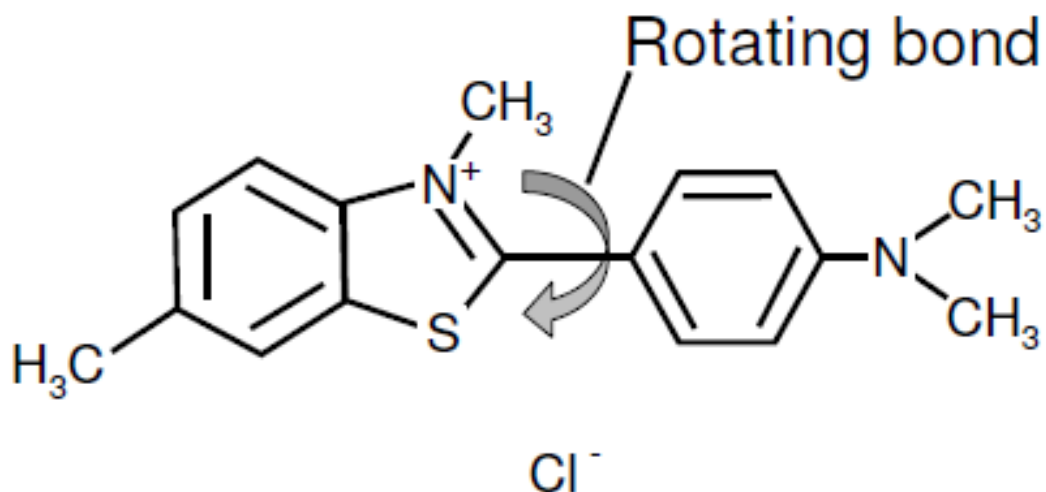
Figure 6-1: Structural diagram of Thioflavin T molecule used as Proteo-stat dye. Structure based on figure from Proteo-stat website.

6.2.1 Determining operating conditions

The first operating condition to be determined was to look at the size of antibody that the method was able to detect. The sample used to test the dyes was IgG1 (Medi/UCL008) in PBS processed in the disc shear device for 1 hour. To determine size detected, unfiltered samples were tested against samples purified with filters of different sizes, and then samples with no aggregate present at all to get a determination of the level of sensitivity of the technique to aggregates at different sizes.

Figure 6-2 shows the results for the filter experiment and shows that using filters of 0.65nm and 0.22nm will decrease the emission from around 3750 RFU to around 1750 RFU. The buffer has an emission around 500 RFU at 590nm on the spectrum. This means that up to 1250 RFU is contributed by the aggregates under the size of 0.65µm or 1150 RFU are smaller than 0.22µm. This leaves 2000 RFU that is contributed by aggregates larger than 0.65µm, representing around 70% of the emission overall. It also suggests that there are significant numbers of aggregates under the size of 0.22µm in the sample. SE-HPLC of the samples showed no low molecular weight aggregates present, so it would appear that the dye has either

been activated by monomer or it has helped to precipitate aggregates that were not previously present and then bound to them to become activated. This would suggest that the optimum method for use of the dyes would not involve the use of filters.
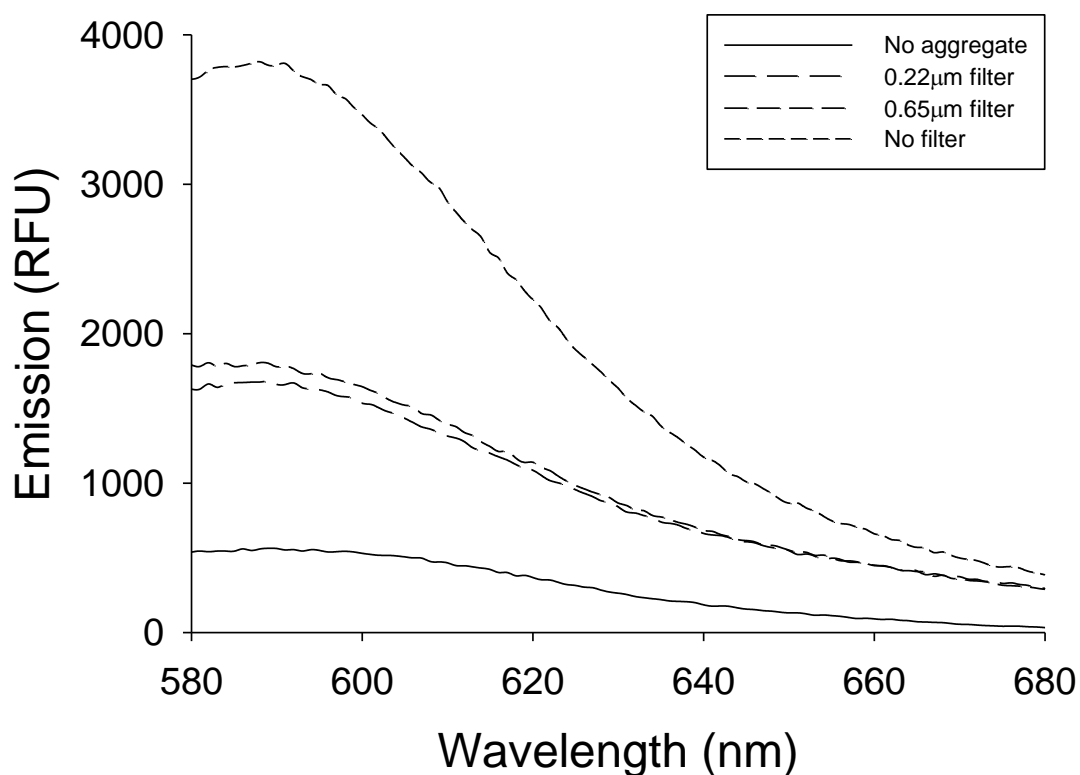
Figure 6-2: **Proteo-stat dye emission values after filtration of aggregated 1mg/ml IgG1 (Medi/UCL008) samples in PBS using 0.22 and 0.65µm pore sized filter compared to no filtration.**

To test the linearity of the emission spectra with regards to the level of aggregate present, an aggregated sample of IgG1 (Medi/UCL008) in PBS produced by 2 hours processing in the disc shear device was used. Samples of the processed antibody were sequentially diluted with monomeric, unprocessed antibody to give samples with progressively less aggregate present.
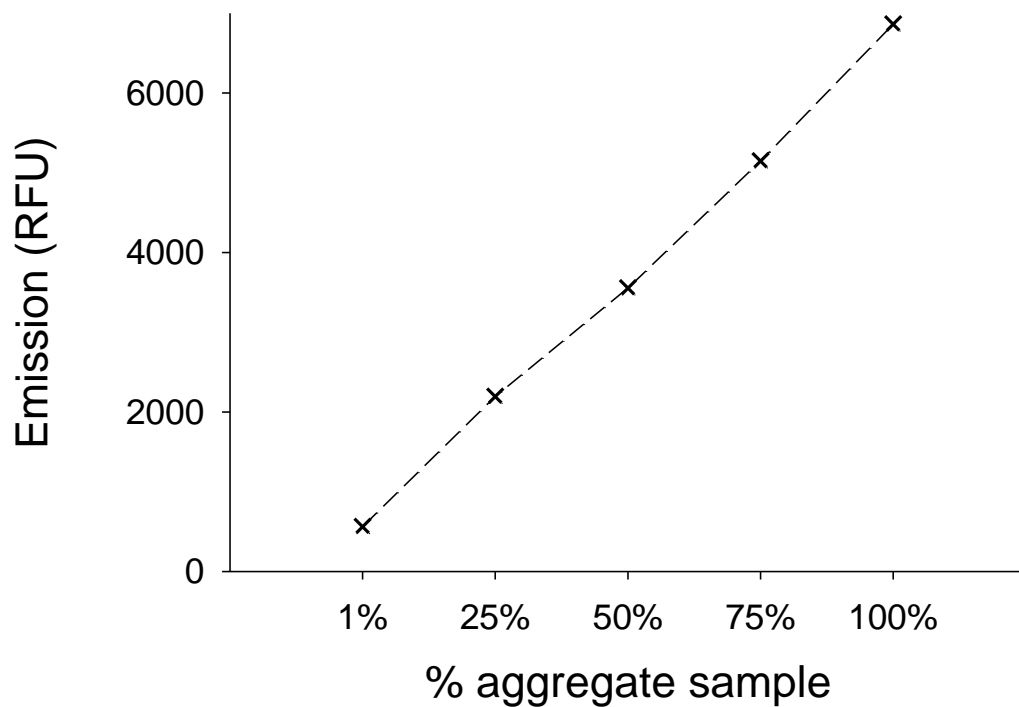
Figure 6-3:   **Proteo-stat dye emission at 590nm for aggregated 5mg/ml IgG1 (Medi/UCL008) in PBS samples diluted to 100, 75, 50, 25 and 1% of original solution with monomeric antibody.**

Figure 6-3 shows the results from the dilution experiment and outlines a near step-wise loss in the level of emission from 100% processed solution down every 25% dilution and at 99% monomer. This supports the manufacturer's claims that the emission of the dye follows a linear path with levels of aggregate.

The final parameter to check with the dye was the reproducibility of the results. To accomplish this, all readings were performed in triplicate and the standard deviation was determined for these readings, figure 6-4 gives the curve for an IgG1 antibody (Medi/UCL008) processed for 2 hours in the shear device and not being diluted. The graph shows that the standard deviation at around the 590nm wavelength is quite high, and would hinder the ability of the technique to be able to differentiate close results of total aggregated antibody.
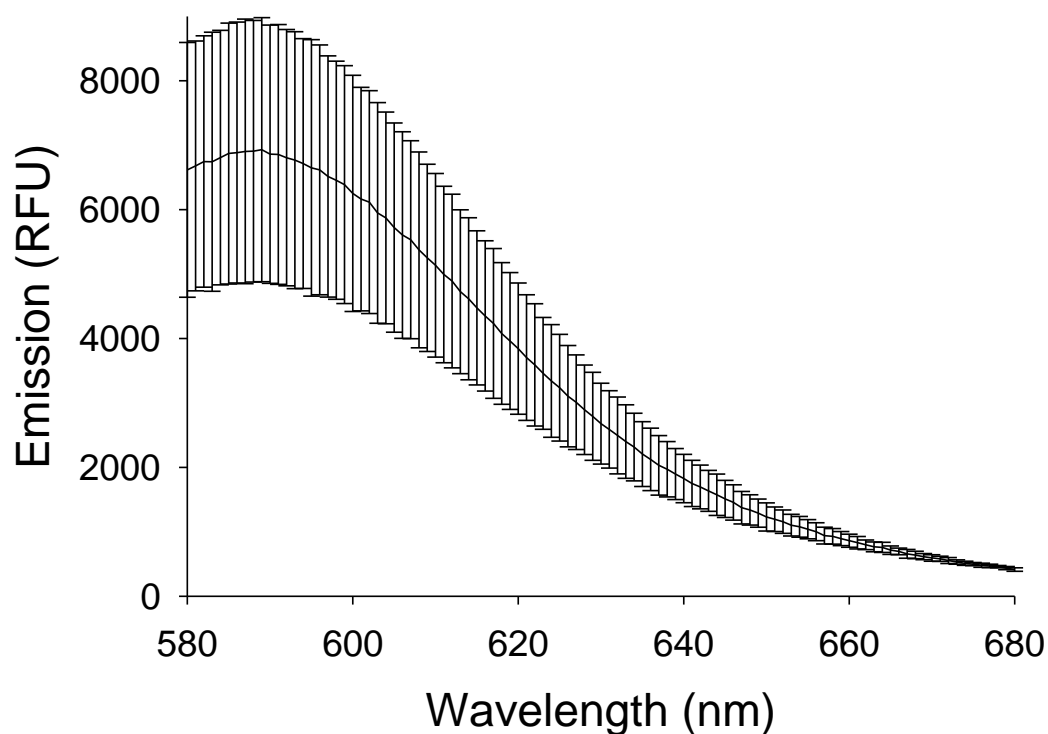
Figure 6-4: Graph of standard deviation of triplicate readings for Proteo-stat results for 5mg/ml IgG1 (Medi/UCL008) in PBS processed for 2 hours at 9000rpm in disc shear device.

6.2.2 Analysis of thermally degraded samples

The method was used to try and determine the level of aggregate present in samples of 5mg/ml IgG1 (Medi/UCL008) that had been denatured for 24 hours at 40°C at a low pH. The aggregate profile for this was determined by SE-HPLC and the chromatogram shown in figure 6-1. SE-HPLC showed the sample to contain a great deal of low molecular weight aggregate and very minimal amounts of monomer loss from that range. Emission spectra from samples prepared in this way all failed to show any increase from the negative controls, leading to the conclusion that the dye is incapable of binding to low molecular weight aggregates in the conditions used. This is in contradiction to the results gained from the use of shear device denatured samples filtered with a 220nm centrifugal filter, which did show significant levels of emission.

6.2.3 Analysis of shear degraded samples

The Proteo-stat dye was used to look at the levels of aggregate present in samples of 5mg/ml IgG1 (Medi/UCL008) taken at 15 minute intervals from the disc shear device during its normal operation. The results of this are shown in figure 6-5 and show that the level of aggregate determined by the technique does increase with the increased operating time. While the amount does increase this is within the large level of error inherent in the technique and the results are very noisy. There is no clear step change in the emission spectra values at 590nm.
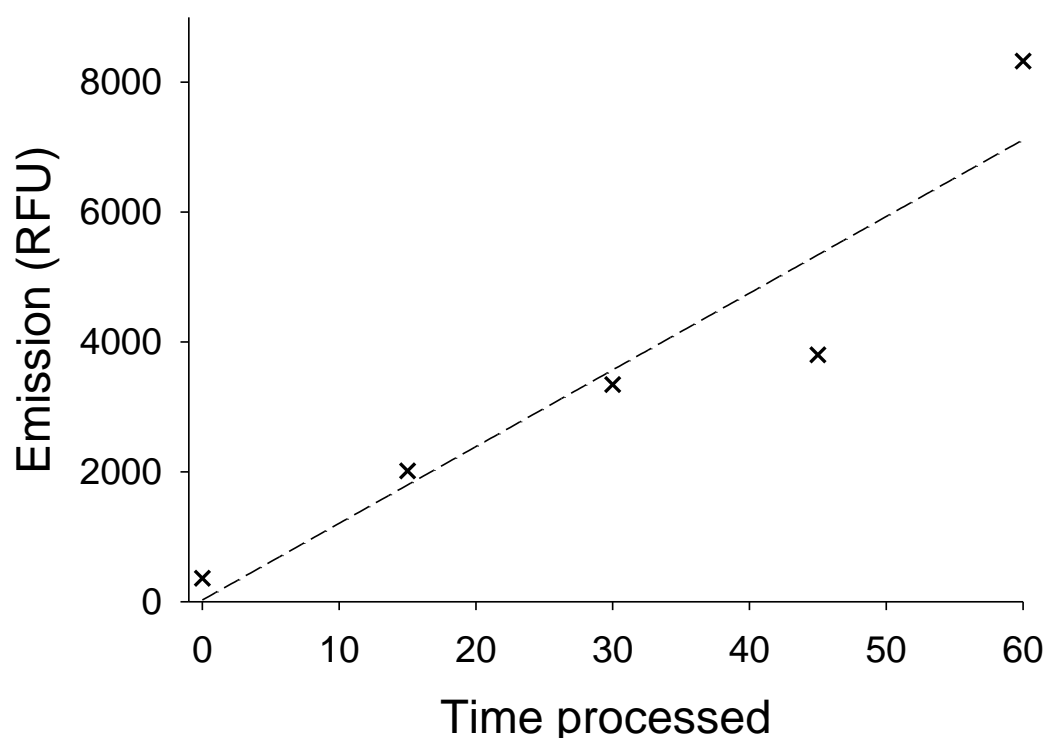
Figure 6-5:   **Proteo-stat emission from samples of 5mg/ml IgG1 (Medi/UCL008) in PBS taken every 15 minutes from the disc shear device operated at 9000rpm.**

6.2.4 Conclusion regarding Proteo-stat dyes

The Proteo-stat method does not seem like an optimal way to measure the levels of aggregate formed. The high standard deviation in the results points to an inability of the method to differentiate between samples. Additionally, the results from the filter

experiments, when coupled with those from the temperature degradation experiments, suggest that either the method cannot detect low molecular weight aggregates in certain conditions or the dye gives false positives for aggregates in certain conditions. For the conditions used, the technique is not recommended for use in determining levels of aggregation present. The molecule is however good at binding to ordered fibrils, so the technique could be used to determine aggregate morphology and tracking fibril growth.

6.3 Nanoparticle tracking analysis

The nanoparticle tracking analysis technique was performed using the Nanosight which was used to determine the level of aggregate present in degraded samples and to give a measure of the level of each size range of particle present in solution. The method individually tracks the refracted light from all the molecules present in a cross section of the sample volume viewed by a microscope and determines the particle size by assuming Brownian motion (Nanosight, 2009).

6.3.1 Analysis of shear degraded samples

The method was tested on a sample of 1mg/ml IgG1 (Medi/UCL008) in pH 5.5 L-Histidine and (D+) Trehelose buffer that had been processed in the disc shear device for 2 hours at 9000 rpm.

Figure 6-6 shows the concentration of the particles at different particle sizes that were detected by the method. Since the method takes each particle as one count irrespective of size, the standard output of the method does not give a good measure for the amount of antibody present in each sample. To account for this, the assumption was made that the particles detected were spherical, and it was decided to report the level of antibody present as the volume of protein present at each particle size using the equation for a sphere, Volume = 4/3 π x Radius^3.
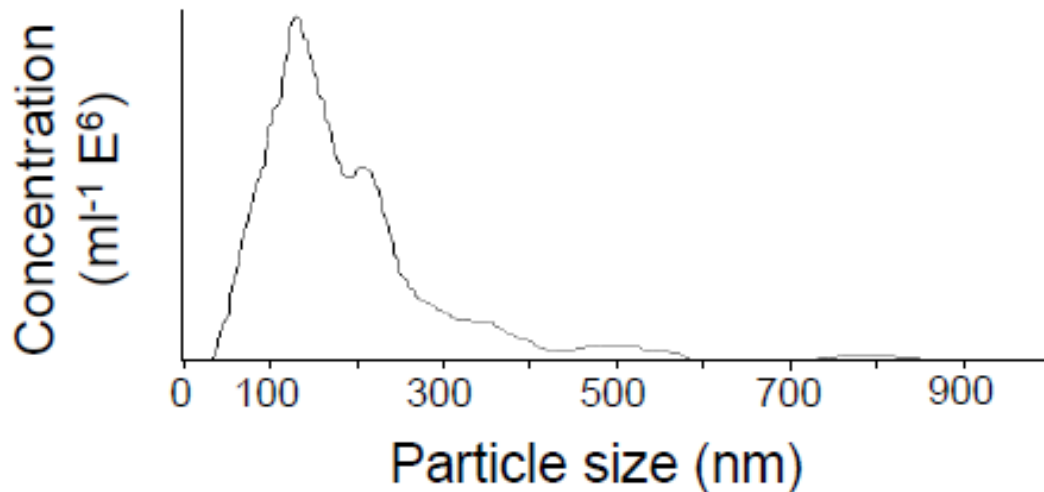
Figure 6-6: **Example of Nanosight result from a polydisperse aggregated sample of IgG1 (Medi/UCL008) in L-Histidine and (D+) Trehelose buffer pH 5.5 processed for 2 hours at 9000rpm in the disc shear device.**

The monomer loss for 5mg/ml IgG1 (Medi/UCL008) in pH 5.5 L-Histidine and (D+) Trehelose solution over 2 hours processing in the disc shear device is shown in figure 6-7 as determined by SE-HPLC. As previously stated, little can be determined about the aggregates produced using this method except that there are no low molecular weight aggregates present. By taking the samples from the shear device and then processing them in real time using the Nanosight, it was possible to get a picture of the different sizes of antibody present at different times in the device chamber, and as such track the growth of aggregates.
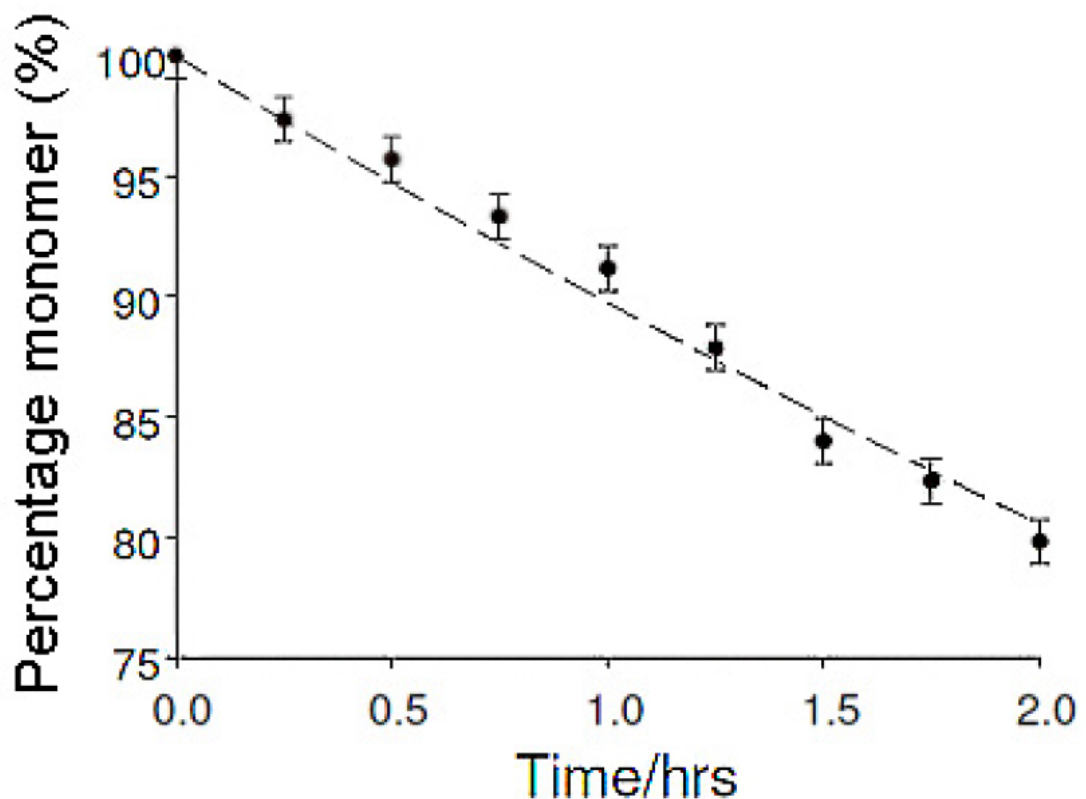
Figure 6-7: **Monomer loss for 5mg/ml IgG1 (Medi/UCL008) in L-Histidine and (D+) Trehelose solution at pH5.5 over 2 hour of shear at 9000rpm in the disc shear device as determined by SE-HPLC.**

Figure 6-8 shows the results from one such run where samples were taken every 20 minutes due to limitations at the time for turning around the Nanosight technique. As previously described, the raw results were adjusted to show the volume of protein present. The results can be broken into two distinct regions, the medium sized aggregates from the lower limit of the device to around 1000nm, and the large aggregates from 1000nm to the upper limit of the device. The large aggregates viewable do not seem to give a trend. This can be explained since any large particles captured will give a very high reading because the volume of protein rises exponentially with size. Thus what appears to be a large reading is in fact a single particle being tracked within the sample space. Due to the capture method and the relatively small volume of sample that is being tested, the appearance of large molecules has a high degree of chance associated with it. This would suggest that the method is not very suitable for determining aggregate levels in the larger ranges at the same time as looking at the smaller ranges.

In the 50nm to 1000nm range however there does seem to be a clear trend with the levels of aggregates in the range. They seem to increase, peak and then decrease.
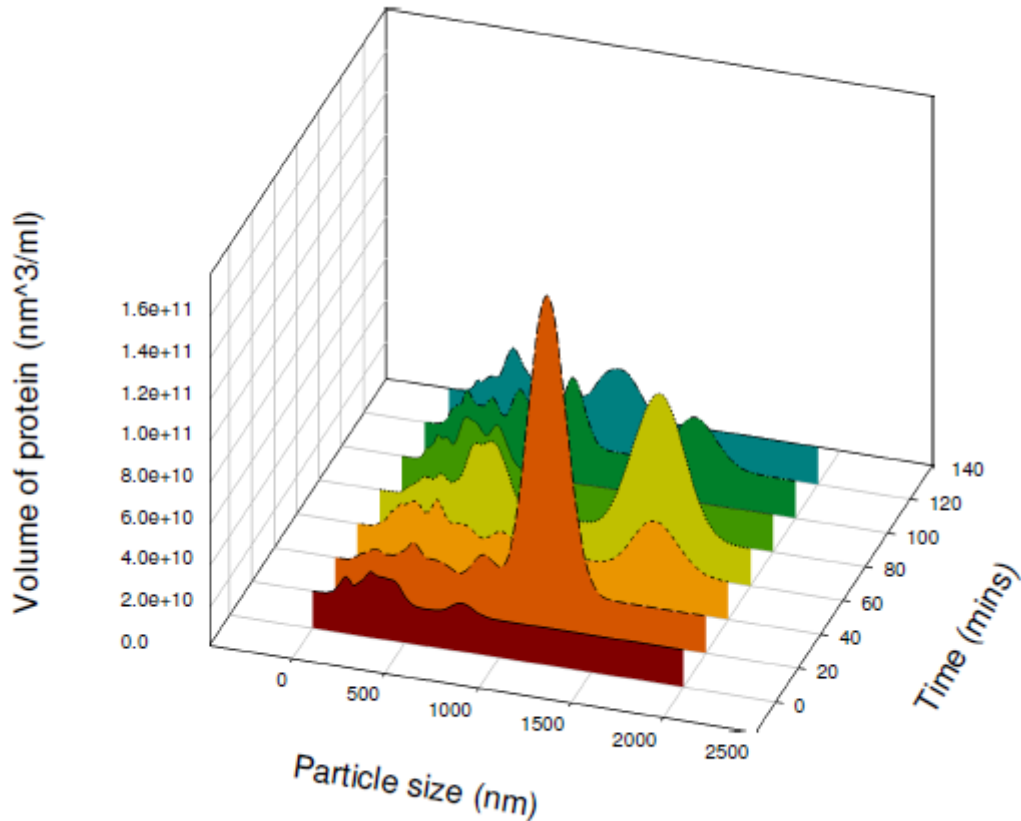
Figure 6-8: Particle size distribution for volume of protein in samples of 5mg/ml IgG1 (Medi/UCL008) in L-Histidine and (D+) Trehelose buffer at pH5.5 taken every 20 minutes over 2 hour of processing at 9000rpm in disc shear device.

6.3.2 Determining aggregate growth patterns in the shear device

It was decided to look further into the aggregate growth pattern, and after refining the Nanosight turnaround technique, a further experiment was performed taking samples of 5mg/ml IgG1 (Medi/UCL008) in pH 5.5 L-Histidine and (D+) Trehelose buffer every 15 minutes from the shear device and analysing them using the Nanosight. This time however, the results would be grouped into four different size ranges that had been seen to have repeated peaks of certain sizes during operation.
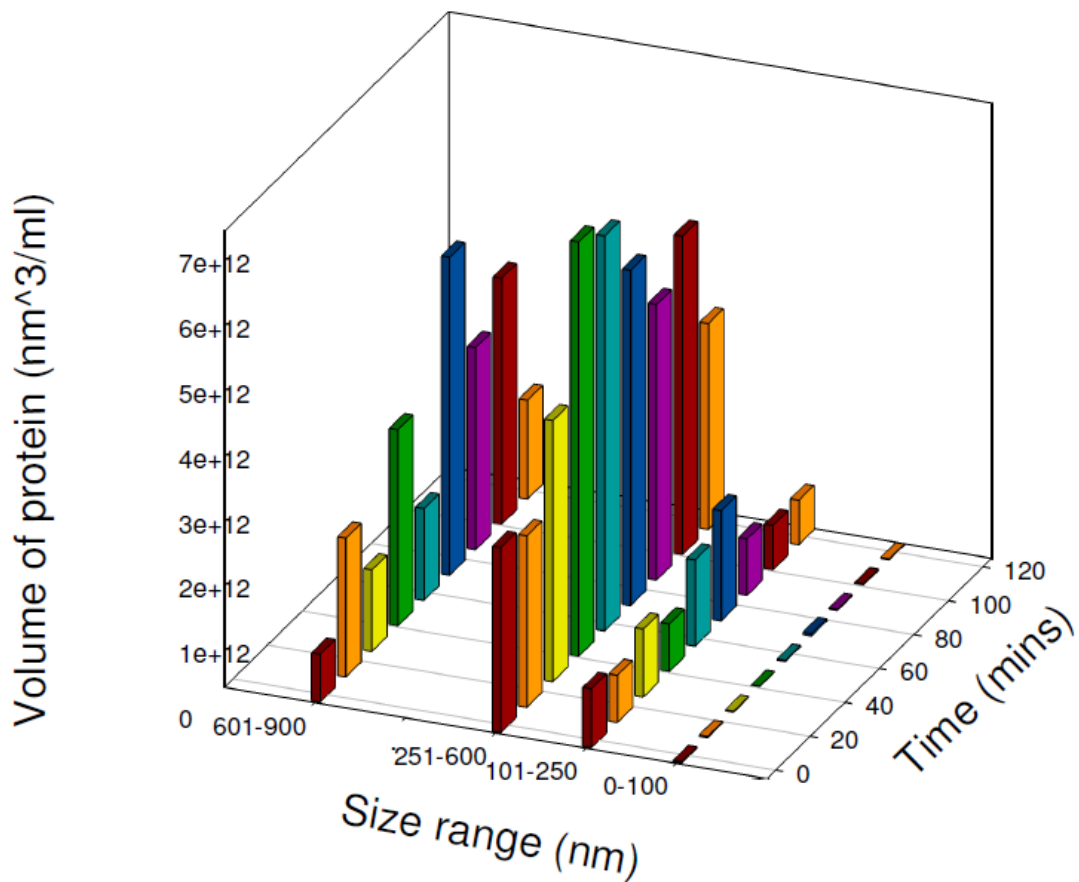
Figure 6-9: Particle size range distribution for volume of protein in samples of 5mg/ml IgG1 (Medi/UCL008) in L-Histidine and (D+) Trehelose solution at pH5.5 taken every 15 minutes over 2 hour of shear at 9000rpm in disc shear device.

Figure 6-9 shows the results for this experiment. The first size range from 0nm to 100nm has a very low volume of protein at all times in the processing. This points to the size range being home to short lived intermediaries in the subsequent growth of larger aggregates. The 101nm to 250nm range seems to stay quite steady with a small peak between 60 and 80 minutes of processing, pointing to this size range again containing mostly short lived intermediaries. The 251nm to 600nm range has the highest volume of protein present and does seem to build up to a maximum somewhere between 40 and 60 minutes of processing before again falling. This suggests that this size range is a key intermediate in the growth of larger aggregates that is longer lived than most. This would corroborate with the work done on defining aggregation as nucleation followed by fibrillation (Holm et al., 2007, Bhak et al., 2009) and seems like a likely candidate for being a relatively stable aggregation

nucleus or settling point during growth. This is further corroborated by the results for the 601nm to 900nm range, which show a lower level of protein volume that peaks around 80 minutes of shear before falling. This shows proof that the aggregates are building up on each other on their route to forming the very large and insoluble aggregates that cause the solution to become cloudy. The results themselves do show a certain amount of noise, so further work should go into finding the best way for averaging out the results.

6.4 Conclusions: How best to characterise process aggregation?

Aggregates produced in the course of processing have a wide range of sizes that require a series of techniques to determine the levels in all the size ranges. The size range is a product of the mechanisms by which aggregates form, with smaller aggregates acting as precursors or nuclei for subsequent larger aggregates (Joubert et al., 2011). By using complementary techniques, it is possible to create a portfolio of techniques that can analyse the aggregates formed in the shortest amount of time, with lowest costs and required level of reliability. For very large particles a whole range of techniques outlined in the literature review are available, with microflow imaging standing out as a particularly reliable, simple and high throughput method that can characterise particles from 2μm to 100μm. For low molecular weight particles, the SE-HPLC method is an industry standard that can give incredibly reliable, high throughput and cheap results on a single column in the size range of 1nm to 50nm, as shown in this work and others (Carpenter et al., 2009). This leaves the middle and large sized aggregate range from 50nm to 2μm. The Proteo-stat dyes tested are unable to give quantitative analysis of the different sizes and the DLS is unable to differentiate the different sizes present, giving a weighted average in favour of larger particles. The work performed on producing size distributions of aggregates every 15 minutes over the operation of the shear device shows that the Nanosight is capable of filling this gap as a low cost, quick and accurate technique. The technique highlighted the growth and decline in the volume of different sizes of aggregates during processing in the disc shear device, showing the pathways for formation of large insoluble aggregates.

7 Characterising reversible self association in a typical biopharmaceutical process

7.1 Introduction

As alternative molecules with higher affinities are developed, the level of hydrophobicity present on the molecular surfaces of lead candidates is increasing. Reversible self association (RSA) is a phenomenon that occurs during processing of highly hydrophobic molecules (Bethea et al., 2012). It was observed that at specific conditions, certain molecules would have a hydrodynamic radius measured by DLS equivalent to dimeric antibody aggregates. However when these molecules were processed using methods such as size exclusion SE-HPLC they would appear to consist of only monomer, as shown in figure 7-1.
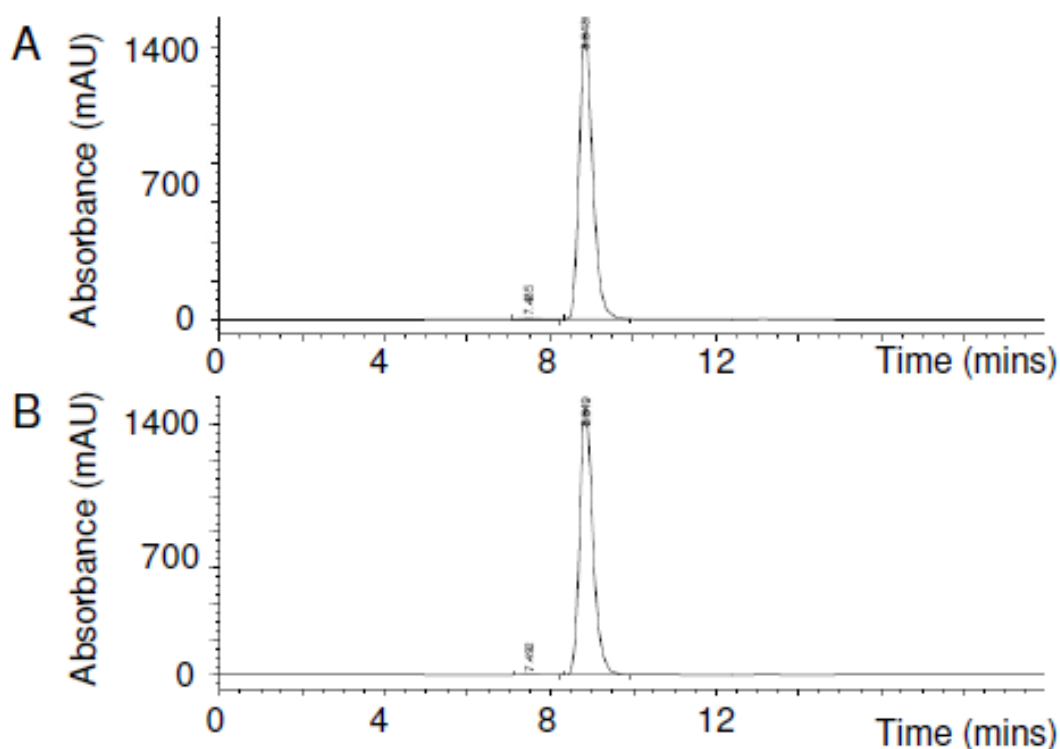
Figure 7-1: SE-HPLC for IgG1 (Medi/UCL009) at 15mg/ml in pH5.6 buffer containing 30mM L-Histidine and A) 0.03M NaCl with a hydrodynamic radius of 18.09nm B) 0.15M NaCl with a hydrodynamic radius of 12.29nm.

It is important to understand the effect of these reversibly self associated molecules on the purification process. Since the molecules only express the RSA characteristics in specific conditions and seem to leave no lasting effect on the molecule, it would be possible to change conditions of the solution to remove the RSA prior to a step if a certain operation was shown to perform adequately sub-optimally with RSA present.

In this chapter, an IgG1 molecule that was seen to exhibit RSA characteristics was investigated. The conditions where the molecule exhibited RSA behaviour were determined to allow for process step characterisation. The steps investigated included pumping, storage, protein A chromatography and viral filtration. Molecular modelling was then performed on the Fc region to determine if there was a cause for the RSA that could be determined from the surface chemistry.

7.2   Materials and methods

IgG1 (Medi/UCL009) was transferred into the different buffer conditions using PD10 desalting columns for initial stages and UF/DF for the later more antibody intensive stages of protein-A and viral filtration. The design of experiment was performed using JMP software to give conditions where the expression of RSA occurred by altering the pH, salt concentration and antibody concentration. These conditions were then carried forward to the rest of the experiment. Shear studies and accelerated stability studies were performed for the four higher pH conditions using the methods described, where the antibodies were held at 20°C. The effect of RSA on loading onto a protein-A column was determined using a Hi-Trap (GE healthcare, Uppsala, Sweden). Finally filterability was performed using the viral filtration method for the four higher pH conditions. Molecular modelling was then performed on the antibody to try and determine the cause of the RSA characteristic.

7.3   Design of experiment for manipulating antibody size

To determine the conditions at which RSA was present for the IgG1 (Medi/UCL009) molecule, a 2^3 factorial design of experiment (DoE) was performed to establish the relationship between the three variable conditions and the size of the antibodies in the resultant solution, as determined by DLS. As part of the reading, viscosity would also be measured. The variables to be considered were chosen to be the concentration of salt (NaCl), antibody concentration and the pH of solution. The pH range was chosen as 4.4 to 5.6 with a midpoint at 5. The salt concentration range was chosen to be 0.03M to 0.15M with a midpoint at 0.09M. The antibody concentration range was chosen to be 5mg/ml to 15mg/ml with a midpoint of 10mg/ml. Three midpoint measurements were taken. As standard, each condition would be measured in triplicate.

Table 7-1: DoE conditions and resultant hydrodynamic diameter readings of IgG1 (Medi/UCL009).

Sample	pH	Salt Conc. (M)	Ab Conc. (mg mL^{-1})	Viscosity (mPa s)	Hydrodynamic diameter (nm)
1	4.4	0.03	5	1.0552	11.56
2	4.4	0.03	15	1.1033	11.63
3	4.4	0.15	5	1.0637	10.95
4	4.4	0.15	15	1.159	11.51
5	5	0.09	10	1.1825	12.66
5	5	0.09	10	1.1825	12.71
5	5	0.09	10	1.1825	12.78
6	5.6	0.03	5	1.0797	12.47
7	5.6	0.03	15	1.2588	18.09
8	5.6	0.15	5	1.0797	10.83
9	5.6	0.15	15	1.2127	12.29

Table 7-1 shows the results seen for the different conditions. The viscosity measurements were taken separately prior to analysis with the DLS. There seems to be a correlation between the viscosity of the solution and the size of the molecules as determined by the DLS method. This could be due to increased Van der Waals interactions between the larger molecules with larger surface areas in solutions (Bethea et al., 2012). The differences in sizes measured suggest that either the different conditions had an effect on the hydrodynamic diameters of the molecules by changing the conformation in solution, or that levels of RSA in solution were modulated by the solution which would move the average reading of the DLS between the monomer and the dimer size (Chu, 1991). Condition 7 was shown to promote RSA formation to a large extent. Figure 7-2 shows the contour plots for the different variables and their effects on the size of the antibody in solution. The plots show the relationships between couples of variables and show that the most sensitive conditional changes in molecular size came from a combination of the NaCl concentration and pH.
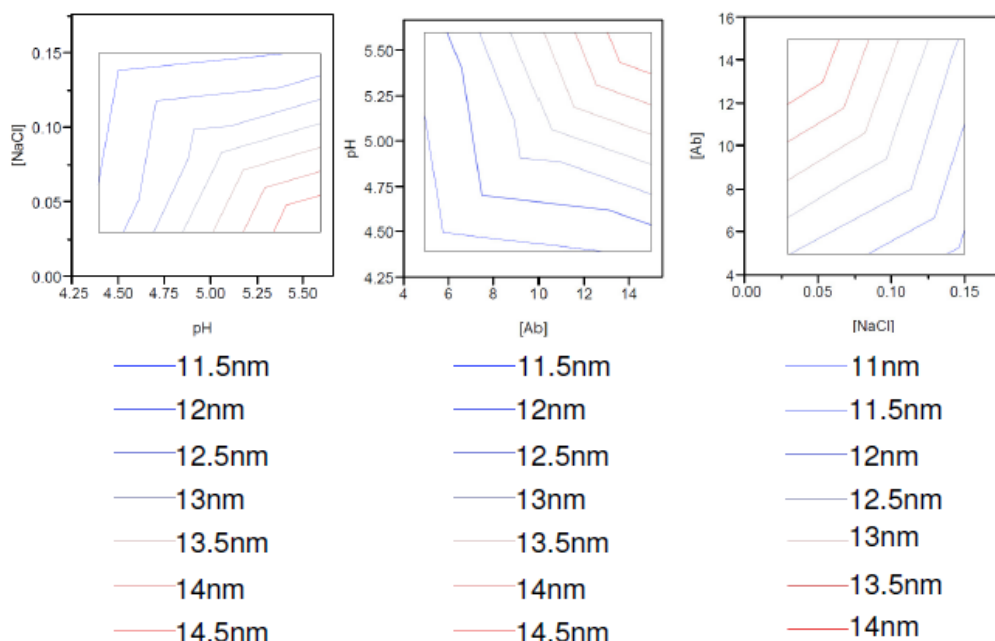
Figure 7-2: DoE Contour plots for IgG1 (Medi/UCL009) varying pH, antibody concentration and salt concentration.

The factors were tested to see which were the most statistically relevant by using the fit least squares function of the DoE software, shown in figure 7-3. Here the results again show the most significant factors are the salt concentration and pH of solution. This also shows that the effect, beyond statistical doubt, is caused by the factors chosen and is not random.

Conditions 6, 7, 8 and 9 were chosen to take forward for further testing in order to remove the need for one of the variables. It was decided to remove pH as a variable to stop the possibility of it affecting the loss of monomer due to degradation at the lower pH.

Term	Estimate	Std Error	t Ratio		Prob>|t|
[NaCl](0.03,0.15)	-1.022083	0.028926	-35.33		<.0001*
pH(4.4,5.6)	1.0029167	0.028926	34.67		<.0001*
[Ab](5,15)	0.9629167	0.028926	33.29		<.0001*
[NaCl]*pH	-0.840417	0.028926	-29.05		<.0001*
pH*[Ab]	0.8079167	0.028926	27.93		<.0001*
[NaCl]*pH*[Ab]	-0.582083	0.028926	-20.12		<.0001*
[NaCl]*[Ab]	-0.45875	0.028926	-15.86		<.0001*
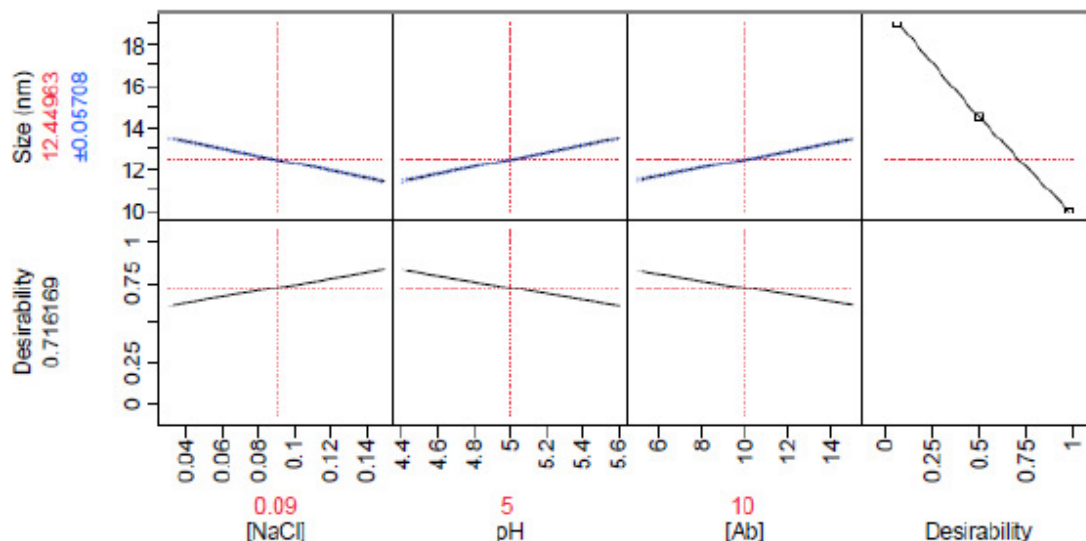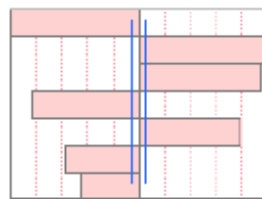
Figure 7-3: DoE fit least squares for IgG1 (Medi/UCL009) from varying pH, antibody concentration and salt concentration.

7.4 The effect of shear and accelerated stability on monomer levels at different conditions

During the course of antibody purification, the sample will come into contact with many solid-liquid interfaces, high levels of shear and will be held in various tanks and vessels for short periods of time. All these factors will promote aggregation (Bee et al., 2010, Tyagi et al., 2009). Conditions 6, 7, 8 and 9 of IgG1 (Medi/UCL009) were processed in the shear device to asses the effect of RSA on antibody stability in shear conditions during processing.

Holding samples for accelerated stability experiments was done in conjunction with the shear study to more fully characterise the conditions the proteins would be exposed to in processing.

Figure 7-4 shows the monomer percentage of samples processed over two hours in the shear device. The monomer loss shows that there is very little difference between the conditions during operation.
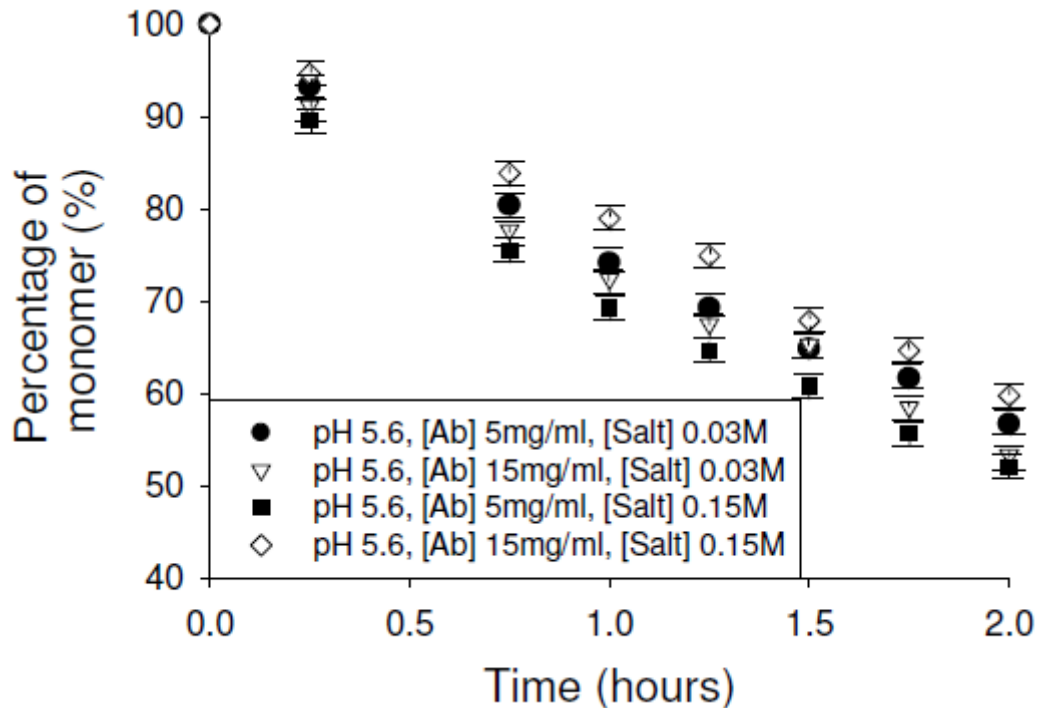
Figure 7-4: Monomer loss of IgG1 (Medi/UCL009) in conditions 6-9 at 15 minute intervals over 2 hours processing in disc interfacial shear device. Error bars for error in the shear device method.

There is however a subtle difference in the results. When increasing antibody concentration from condition 8 to condition 9 there was an increase in the stability of solution, as was shown in previous experiments to determine the effect of increased concentration on shear device results. When increasing the concentration in condition 6 to condition 7 however, there was a decrease in stability. This would suggest that the presence of RSA does have a slight negative effect on the stability of the solution when exposed to shear. The change in salt concentration may also affect the level of monomer loss outside the effect on protein size. Studies have shown the effect of NaCl on solid-liquid interfaces (Chao and Paolo, 2012), causing an increase in the surface tension and residence time of interfacial water molecules. This would effectively increase the viscosity at the interface and so affect the shear rate on the proteins as well as reduce the Reynolds number in the chamber.

There is a concentration difference between samples 6 and 8 at 5 mg/ml and 7 and 9 at 15 mg/ml. To take this into account, figure 7-5 shows the mass of antibody lost in each of the runs assuming a sample volume of 7ml. The data shows that there is a greater amount of antibody lost with the higher concentrations, as is to be expected. Overall it can be concluded that there is such a low difference in stability for the different conditions that it is not a factor that needs to be considered during high shear operations in processing of an antibody.
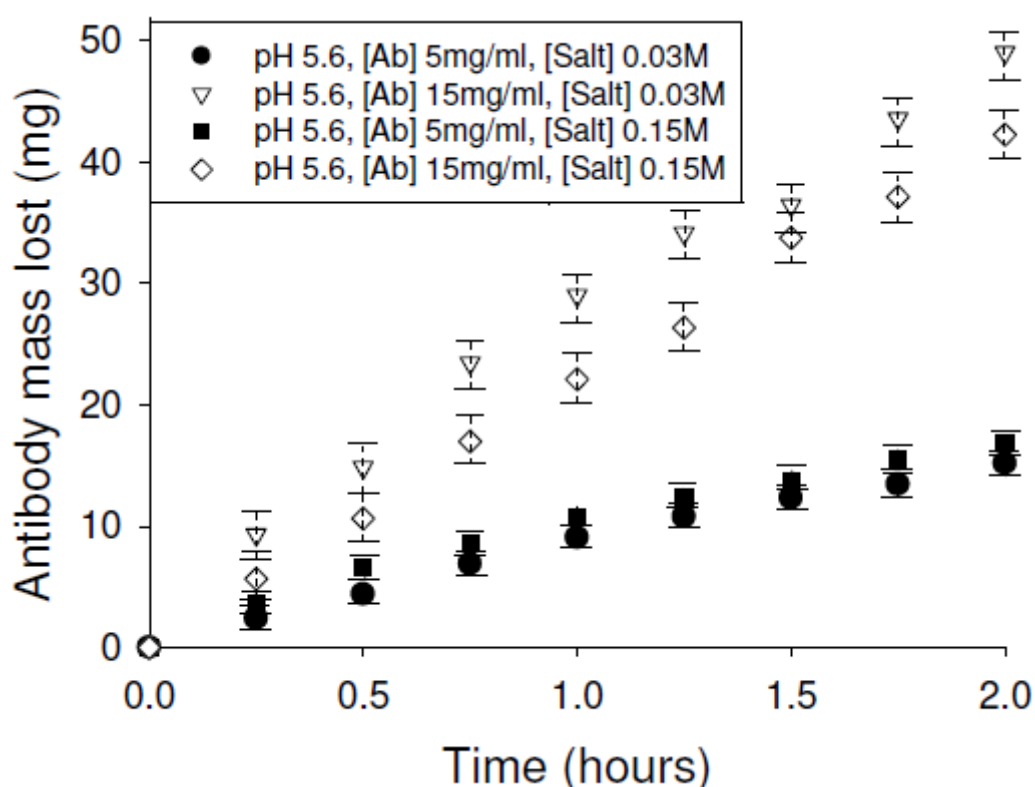
Figure 7-5: **Mass of IgG1 (Medi/UCL009) in conditions 6-9 lost at 15 minute intervals over 2 hours processing in disc interfacial shear device. Error bars for error in the shear device method.**

When looking at the accelerated stability results over the month hold, shown in figure 7-6, the level of monomer loss is quite consistent and low between all the conditions. For the non RSA conditions there seems to be more monomer loss in antibody samples that had been sheared then there was for antibody samples that had not been sheared. This seems to be reversed in the conditions where RSA is present. However, the level of monomer loss is so low over such a long period of

time that again it is not recommended to be a factor to be considered during processing of an antibody.
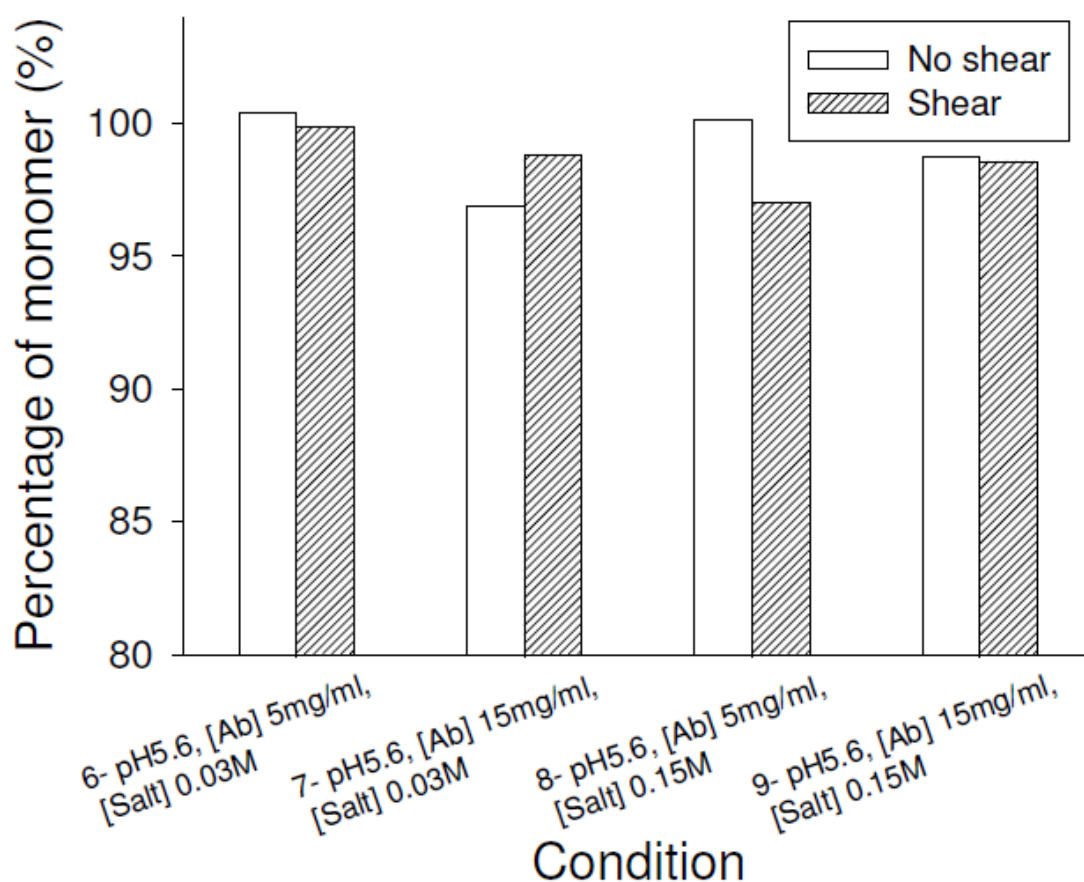
Figure 7-6: **Accelerated stability results of IgG1 (Medi/UCL009) in conditions 6-9 both with and without 2 hours processing in disc interfacial shear device prior to storage.**

7.5 The effect of RSA and size on the DBC of protein-A

The most important unit operations through the purification of a protein therapeutic are the chromatography steps. During these steps it is important to keep the level of antibody loss to a minimum to keep the purification process as profitable as possible. With antibody therapeutics, the Protein-A step is the work horse of the process, able to provide up to 95% purity and retention of the antibody of interest. Medi/UCL009 (IgG1) was formulated in conditions 6 and 7 as well as in PBS buffer.

Medi/UCL008 (IgG1) was also formulated in these three conditions to provide a control for any effect of the buffer.

The dynamic binding capacity (DBC) was used as the comparator to determine the effect of RSA on the step. To determine a benchmark DBC value, Medi/UCL008 and Medi/UCL009 formulated in PBS buffer were run at a linear flow rate of 200cm/hour on a standard Protein-A HiTrap. The HiTrap has a suggested DBC of 40mg of antibody, so 100mg of antibody was loaded onto the column to get full loading of the matrix. The matrix was eluted and the eluate was collected in pre weighed 15ml Falcon Bluemax™ tubes. The strip was also collected to check there was no antibody that kept bound to the matrix due to conformational changes.

The tubes, filled with eluate and strip, were weighed again to allow the determination of the mass of liquid collected. The concentrations of these samples were then determined by analysis of absorbance at 280nm. These two readings allowed the mass of antibody bound to the column to be calculated.

Table 7-2: **Protein-A capacity for Medi/UCL008 (IgG1) and Medi/UCL009 (IgG1) prepared in conditions 6, 7 and at 5mg/ml in PBS.**

Condition	Hydrodynamic diameter (nm)	Mass of Ab bound to column (mg)
Medi/UCL008 - 7- pH5.6, [Ab} 15mg/ml,[Salt] 0.03M	12.31	39.4
Medi/UCL008 - 6- pH5.6, [Ab} 5mg/ml,[Salt] 0.03M	12.28	42.8
Medi/UCL008 - PBS	11.87	46.7
Medi/UCL009 - 7 - pH5.6, [Ab} 15mg/ml,[Salt] 0.03M	18.04	42.6
Medi/UCL009 - 6- pH5.6, [Ab} 5mg/ml,[Salt] 0.03M	12.47	48.0
Medi/UCL009 - PBS	11.54	52.8

Table 7-2 shows the values of the mass of antibody bound to the matrix for the six conditions examined. The results show that the DBC for Medi/UCL009 is inherently better than that of Medi/UCL008. The PBS buffer condition is close to the ideal loading conditions for a protein-A column, so it was used as the base case for both antibodies. The other conditions were prepared as a percentage of the capacity of the PBS condition and plotted on figure 7-7. The results show firstly that the pH 5.6 and 0.03M NaCl condition gives a much less ideal environment for binding to the

protein-A matrix as witnessed by the average drops of around 10% and 18% binding

for conditions 6 and 7. Secondly, it appears that the higher concentration of antibody

gives a lower DBC. This is due to the rate of absorption of antibody into the matrix

beads reaching its limit, so any extra antibody in the higher concentration feed will

be excluded from the beads and pass through the column unbound. For the RSA

condition of Medi/UCL009 there seems to be a greater level of loss of DBC than for

Medi/UCL008, but this is only around 4% extra on a drop of 16% from the PBS

condition, and in real terms the total mass of protein bound is greater. From a

processing point of view, it would appear that RSA is not a major problem to be

worried about during protein-A chromatography.
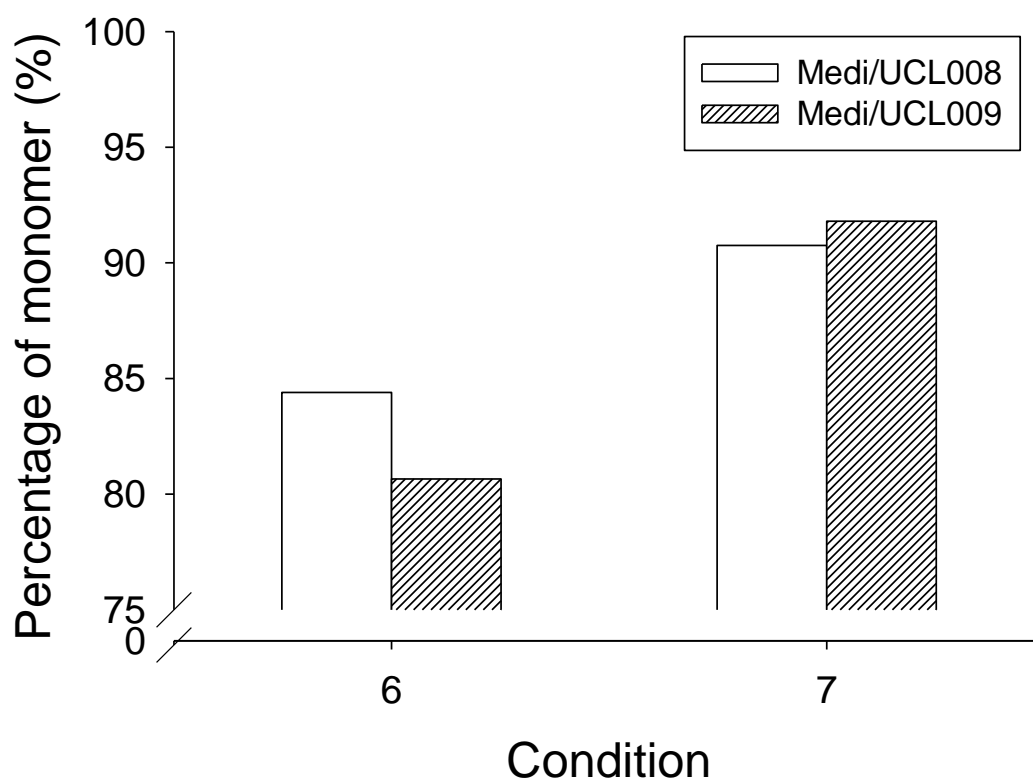
Figure 7-7: **Percentage of DBC of PBS condition on protein-A of Medi/UCL008 (IgG1) and Medi/UCL009 (IgG1) in conditions 6- pH5.6, [Ab} 5mg/ml,[Salt] 0.03M and 7- pH5.6, [Ab} 15mg/ml,[Salt] 0.03M.**

7.6   The effect of RSA and size on viral filtration

The viral filtration step of a process is the final step before filling vials ready for transport (Shukla et al., 2007b). At this point in the process the antibody will be formulated in its final stability buffer. The effect of RSA on the viral filtration step of a process was determined by using conditions 6, 7, 8 and 9 with IgG1 (Medi/UCL009). To test the membrane system each buffer was run through the viral filtration rig for 40 minutes as part of the equilibration process prior to running through the antibody solutions. In each case, there was no drop in the flux after 40 minutes of flow.
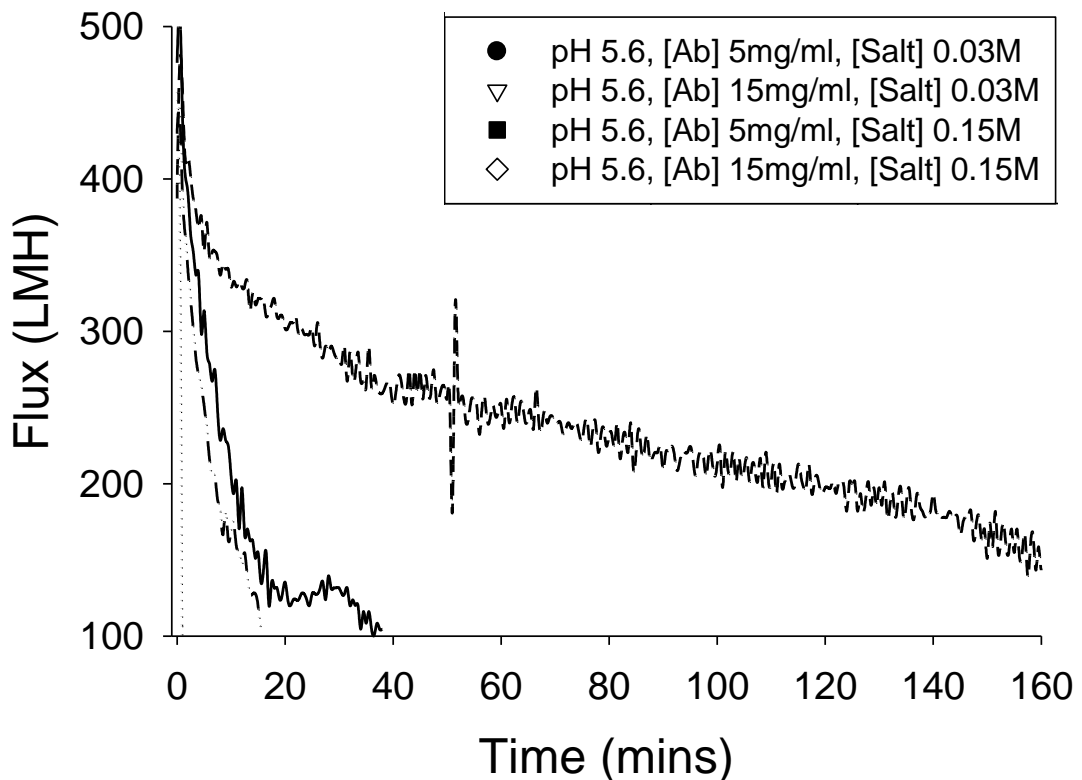
Figure 7-8:   **Flux of IgG1 (Medi/UCL009) in buffer conditions 6-9 through a 20nm pore sized membrane.**

Figure 7-8 shows the flux of antibody feed through the membrane until it reached 100LMH. The results clearly show that condition 8, which ran out of sample before the flux hit below 100LMH, has a much longer membrane life than the other conditions. They also show that with condition 7, the RSA condition blocks the

membrane almost instantly. This suggests that the RSA with a hydrodynamic diameter of 18nm blocks the filter pores which are at an average of 20m. This could be due to mechanical blockage of the pores or due to adhesion of the RSA to the membrane surface which would exclude further material passing through the filter (van Reis and Zydney, 2001). The low operating times of conditions 6 and 9 would suggest that the reason their DLS results show larger antibody hydrodynamic diameter is that there is RSA present in these samples which skews the peak towards a larger hydrodynamic diameter reading.
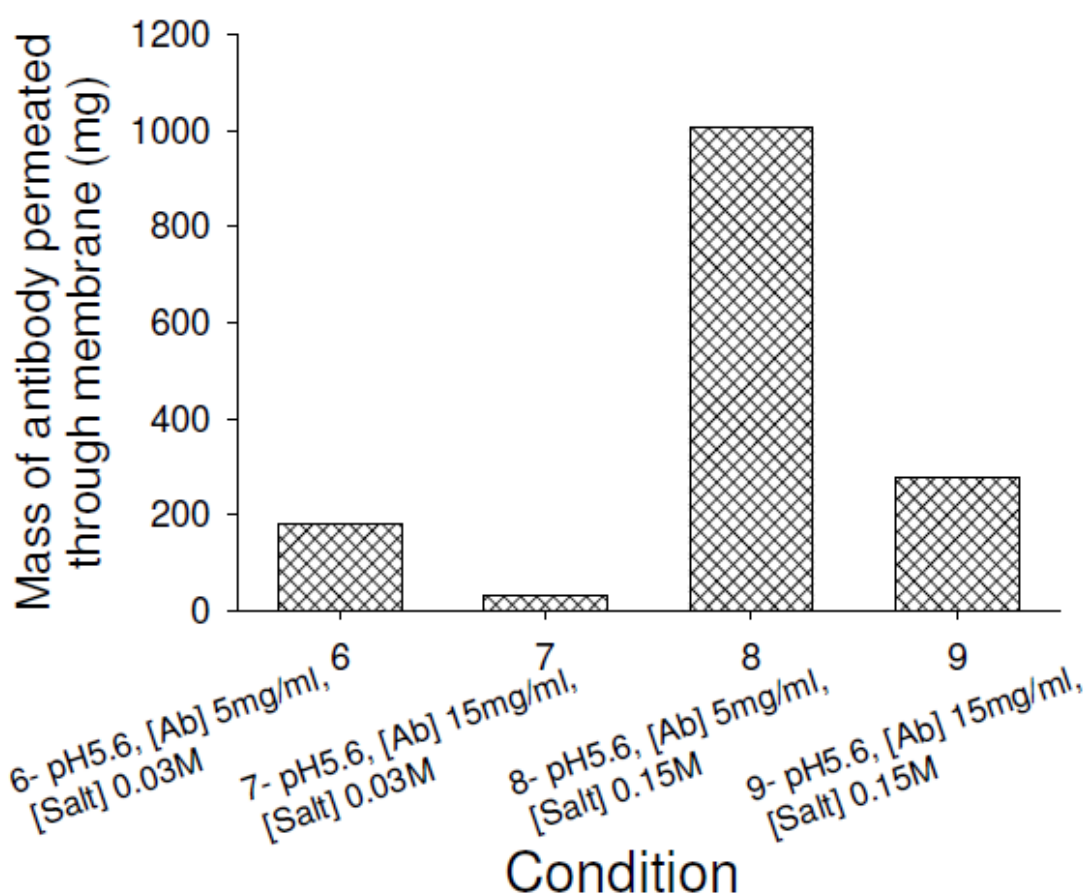
Figure 7-9: **Mass of IgG1 (Medi/UCL009) in conditions 6-9 through 20nm pore sized membrane.**

Figure 7-9 shows the mass of antibody that was passed through the membrane for each condition. It is evident that despite blocking the membrane quicker, condition 9 allows more mass of antibody to permeate the membrane. By plotting the mass of antibody that is filtered through the membrane against the hydrodynamic diameter of

the sample derived from DLS in figure 7-10, it is apparent that there is a correlation. The larger the measure of hydrodynamic diameter, the less mass of antibody permeates the membrane before blockage occurs. If as postulated, the larger hydrodynamic diameter determined by the DLS is due to a skewing of the distribution by the presence of RSA, then the larger hydrodynamic diameter samples would have a larger proportion of RSA present. With the larger proportions of RSA present, the amount of monomer that can pass through the viral filter before the level of RSA required to block the filter comes into contact with it is reduced.
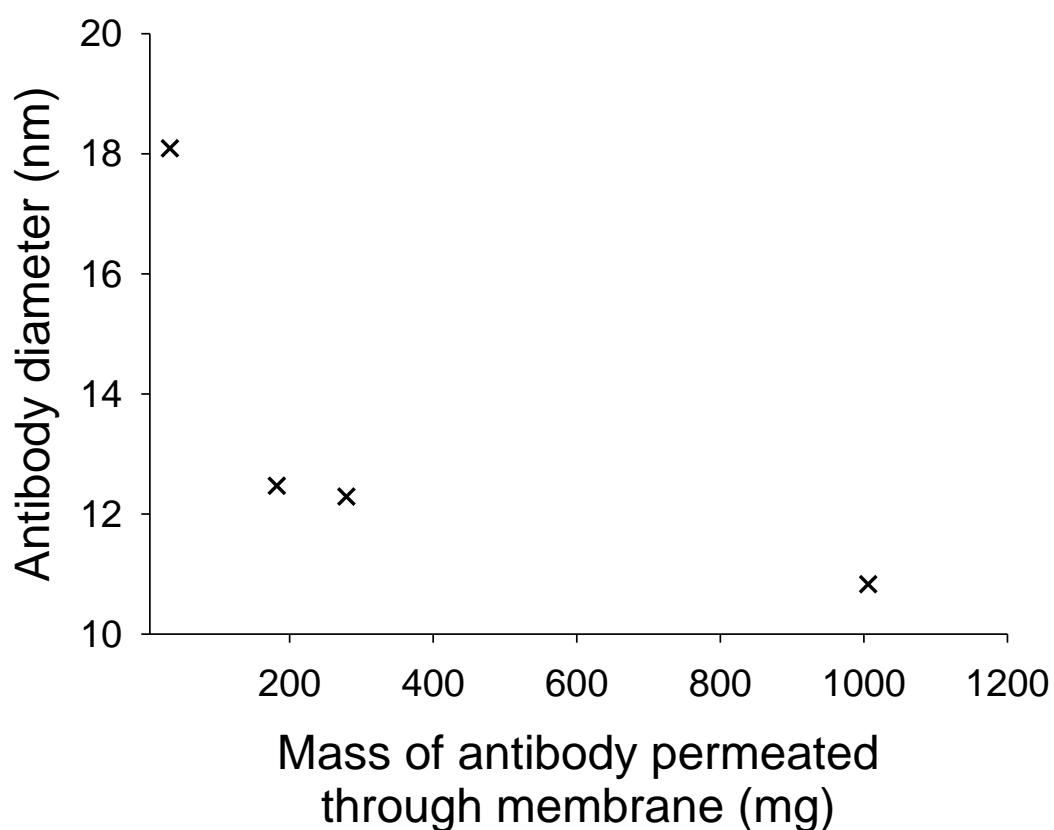
Figure 7-10:   Mass of IgG1 (Medi/UCL009) permeated through membrane against Hydrodynamic diameter.

It is concluded that for viral filtration, RSA is a concern and has to be avoided in the final formulation step. Additionally it is recommended that the effect of RSA should be of concern in any dead end filtration taking place in a process.

7.7   Molecular modelling of Medi/UCL009

To determine the reason for RSA behaviour, molecular modelling was performed on the Fc region of IgG1 molecule Medi/UCL009 and compared to that of Medi/UCL008, an IgG1 with significantly enhanced bioprocessing-related physicochemical properties that has never shown any RSA behaviour.
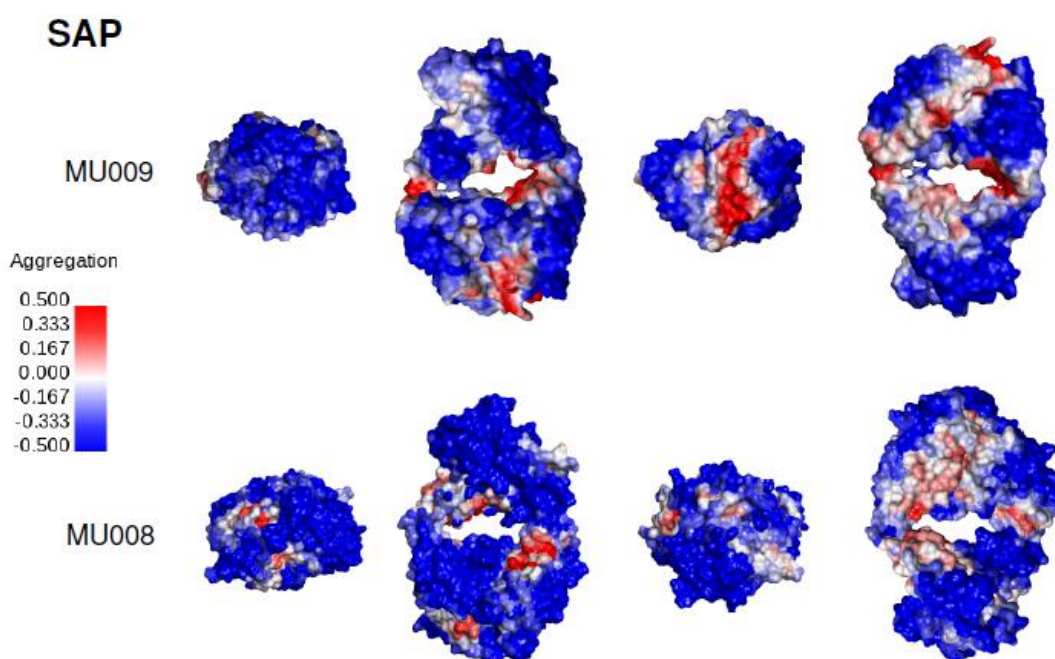
Figure 7-11:   Comparison of SAP of Molecular models of Medi/UCL009 (IgG1) and Medi/UCL008 (IgG1) rotated views from left to right showing hinge end, upwards side, c-terminus, downwards side.

Figure 7-11 shows the molecules created when they were tested using SAP analysis. The molecules are shown in 4 equal stages of 360° rotation along an axis running through both chains of the Fc at the midpoint of the section, starting from the view of the hinge end and then rotating so the hinge end is at the top. Figure 7-12 was then produced using electrostatic potential analysis with a 5Å radius size to give a surface charge map of the molecules. These were again shown in 4 equal stages of 360° rotation along an axis running through both chains of the Fc at the

midpoint of the section, starting from the view of the hinge end and then rotating so the hinge end is at the top.

The surface charge analysis does not show any obvious large areas where there is a lack of charge and similarly, the spread of charge in both molecules is also quite even, although there is a large patch of positive charge on the c-terminus.

Surface Charge

MU009

■ Positive charge
■ Negative charge

MU008
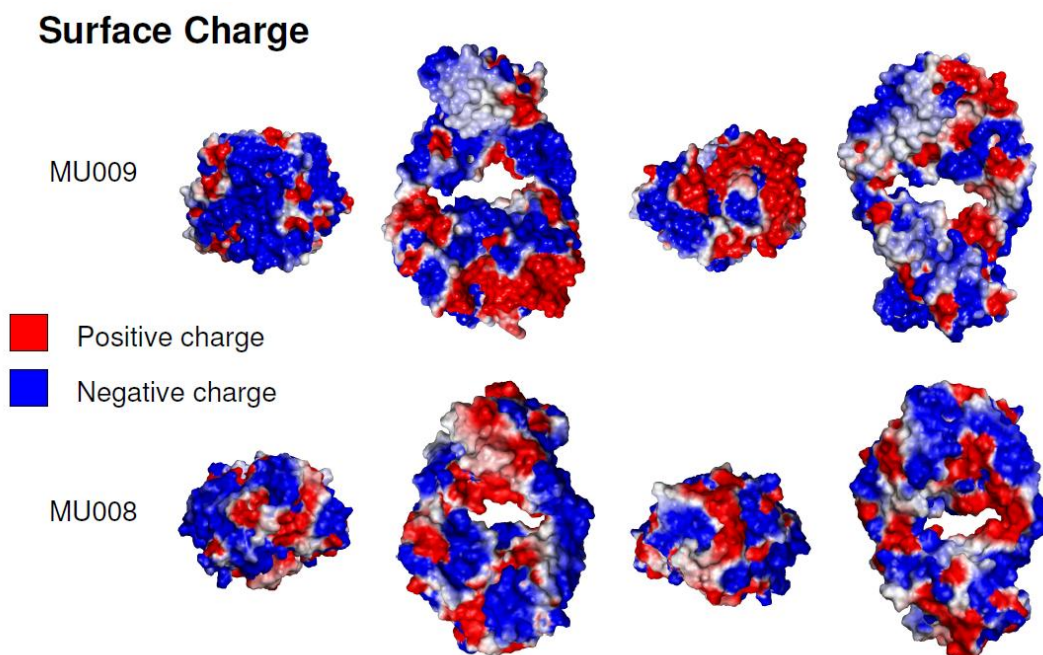
Figure 7-12: **Comparison of Surface charge of Molecular models of Medi/UCL009 (IgG1) and Medi/UCL008 (IgG1) rotated views from left to right showing hinge end, upwards side, c-terminus, downwards side.**

There is however a major difference in figure 7-11 where a large patch on the c-terminus, reaching around to the anterior face of the Fc is predicted to be aggregation-prone by the SAP algorithm (Kayser et al., 2011, Chennamsetty et al., 2010). This region would normally be exposed to the solution, and it is postulated that it would have a tendency to bind reversibly with one other similar unit on the mirrored patch on its c-terminus. The factors that were determined to effect RSA formation help support this. Salt concentration in solution would regulate the level of ionic shielding and higher concentrations of salt, to a certain point, would help shield the patches from each other and keep them separated (Dandliker et al., 1967). By extension, higher concentrations of antibodies would cause the individual antibodies

to be in closer proximity to each other and so have a greater probability of interacting. The effect of pH on the presence of RSA would likely be related to the regulation of the surface charge on the c-terminus, which at certain levels must be able to keep the molecules separated from each other.

7.8   Conclusions: Should RSA be a cause for concern at certain stages of bioprocessing?

It has been concluded in this chapter that RSA is an avoidable problem in the purification of an antibody product if antibodies are not screened for it prior to lead selection. This screening should be performed in conjunction with the use of the disc shear device to make process development easier. If RSA is a characteristic, it does not critically affect primary recovery, pumping and holding operations, UF/DF or protein-A chromatography. RSA was shown however to cause problems when performing viral filtration and potentially any depth filtration, so it is important when designing a process with an RSA exhibiting molecule to formulate the antibody in a condition that does not present RSA prior to the final viral filtration step or in any other filtration steps.

The cause of RSA as exhibited by the IgG1 (Medi/UCL009) has been concluded to be the hydrophobic patch on the c-terminus of the Fc region identified from the high SAP score (Chennamsetty et al., 2010), which could react with similar patches on other Medi/UCL009 molecules to form reversible dimers. The interaction of these patches would be regulated by antibody concentration, salt concentration and pH both experimentally and from the literature (Dandliker et al., 1967).

8 Comparison of monomer loss in thermal and shear techniques and the effect of antibody structure

In this chapter, the effects of controlled antibody modifications TM and YTE on a drug candidate's secondary and tertiary structure and overall charge were evaluated. The relative stabilities of these candidates were then determined and compared with the use of the protein decay coefficient (PDC), using a custom shear device to create surface adsorption in a high shear environment. This technique was then compared with melting temperature (T_m) data from differential scanning calorimetry (DSC) and the results from a 4 week accelerated stability study to determine if the shear method could be used as a complementary or replacement stability indicator for lead antibody screening.

Both Fourier Transform Infra-Red (FTIR) spectroscopy and molecular modeling techniques were used to help determine the effect of the modifications on the secondary and tertiary structures of the antibodies to help explain any trends seen.

8.1 Antibody candidates utilised
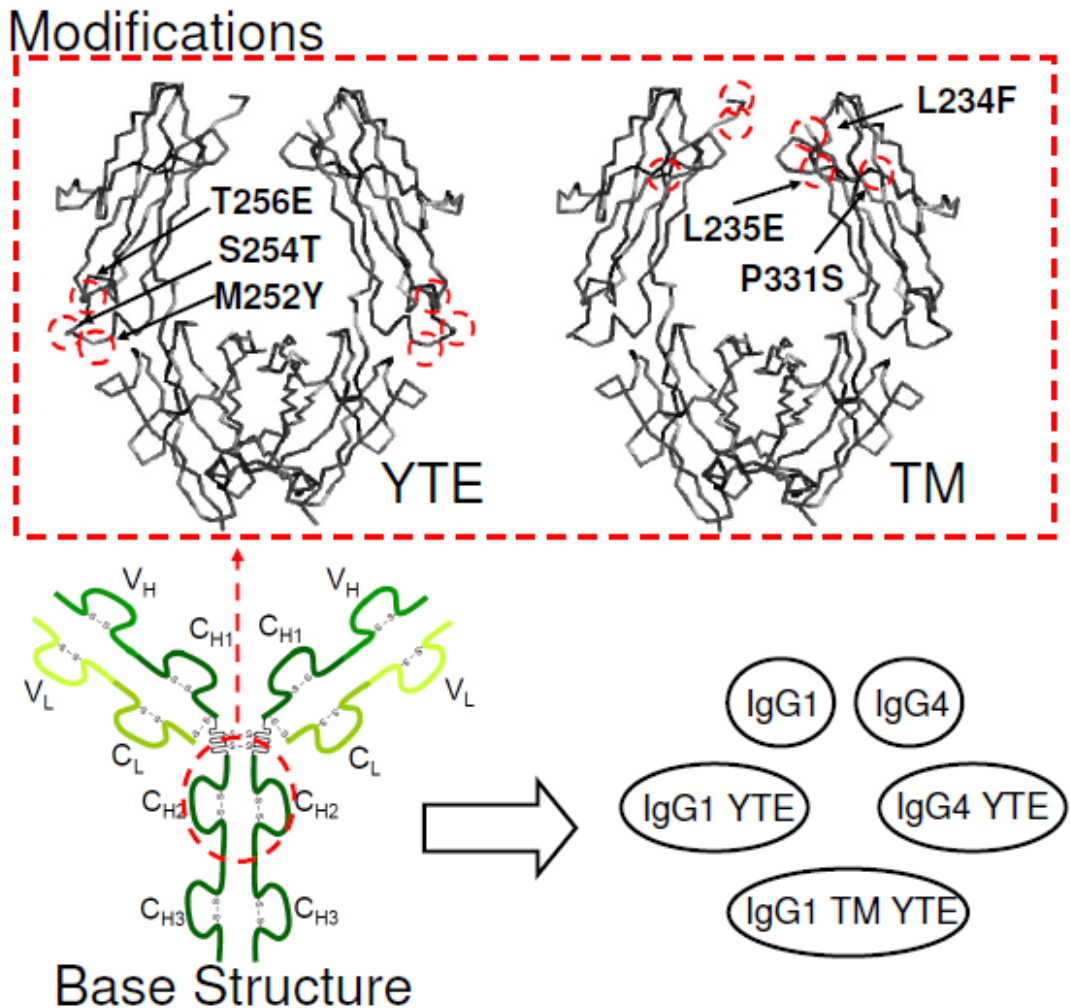
Figure 8-1: Diagram showing the site of each mutation on the structure of the antibody and the resultant antibody formats used for comparison with 3D protein structure taken from PDB, filename 2DQT.

The mutations used to modify the IgG1 and IgG4 base structures and the resultant antibodies are shown in figure 8-1. The YTE modification gives an increase in the serum half life by reducing binding to the Fc neonatal receptor. The TM modification was shown to decrease toxicity by reducing ADCC and CDC. The resultant antibodies were named Medi/UCL003-008 as described in the materials and methods section. However, in this section they will be denoted as their base structure followed by the modification or WT (wild type) for ease of reference.

8.2 Shear device results

The five different antibodies were processed in the shear device at 6000, 7500, 9000 and 12000rpm. Each processed sample was cloudy when removed from the chamber, indicating the presence of aggregate. The insoluble material was removed by centrifugation prior to SE-HPLC. The area under the monomer curve at 15 minute intervals was fitted to an exponential decay curve:

$C(t) = C_0e^{-kt}$

Where $C(t)$ is the monomer concentration (mg/ml) at time t(h), C_0 is monomer concentration at time zero and k is the PDC (h^{-1}). Statistical T-tests performed on the groups of results from each shear rate gave a confidence level of 97.5% that the trend seen was significant.

Table 8-1: **PDC results from shear device for 2 hour processing of 1mg/ml samples of IgG1 and IgG4 molecules (Medi/UCL003-008) in L-Histidine and (D+) Trehalose buffer pH5.5 at different disc speeds.**

Antibody	Protein Decay Coefficient (hour^{-1})			
	6000	7500	9000	12000
IgG1 WT	0.095	0.136	0.179	0.285
IgG1 YTE	0.077	0.108	0.115	0.223
IgG1 TM YTE	0.102	0.163	0.272	0.420
IgG4 WT	0.147	0.209	0.285	0.476
IgG4 YTE 1	0.168	0.212	0.298	0.471
IgG4 YTE 2	0.184	0.219	0.305	0.470

The PDC values for different disk speeds were used to compare monomer losses between each run. These were fitted to a second order regression to highlight clear trends that showed the antibodies to have varying levels of sensitivity to increases in the disk speed shown in table 8-1, caused by their different inherent stabilities in these conditions.

Overall, the IgG1 subtype candidates had a lower monomer loss than the IgG4s at any given disc speed. There was however more variability between mutants in the IgG1 PDC values at each disc speed, with the IgG4 candidates showing similar,

high PDC values possibly indicating their interfacial shear stability is already compromised. This is likely related to the lack of a stable hinge region holding the antibody halves together (Aalberse and Schuurman, 2002).

Two distinct lots of the IgG4 YTE were separately produced and purified to test the reproducibility of the interfacial shear device result. The results showed the error of the PDC derived decreases with disk speed, creating a need to compromise between ensuring reproducibility of data without losing sensitivity of the technique. A disk speed of 9000rpm was chosen to be the optimum level.

The increase in soluble monomer loss with disk speed could be due to an increase in its loss to aggregate nuclei in solution or to an increase in the rate of dissociation of aggregate precursors from the disk surface, resulting in an increased rate of aggregation. The work also supported previous observations that an increase in large aggregates (based on the increased opalescence of the solution) did not serve to increase the rate of monomer loss (Biddlecombe et al., 2007). The relatively steady rate of monomer loss differs from some reported routes of protein aggregation where the level of monomer loss seems to be low for a nucleation phase, followed by rapid fibrillation (Sasahara et al., 2008, Kim et al., 2002), indicating the presence of different mechanisms of aggregation.

8.3   *Differential scanning calorimetry of candidates*

The DSC profiles in figure 8-2 shows that the antibodies have two clearly resolved transitions, each peak in the trace giving a melting temperature value for the unfolding of each protein domain. The first peak (T_m1) representing the unfolding transition of the CH2 domain was well resolved for most of the antibody candidates. The Fab and CH3 were unresolved in the second unfolding transition (T_m2) with a higher enthalpy than in T_m1, possibly indicating stronger interactions between sub

domains in this region(Tischenko et al., 1982). As expected, the modifications in the CH2 change the T_m1 value significantly.
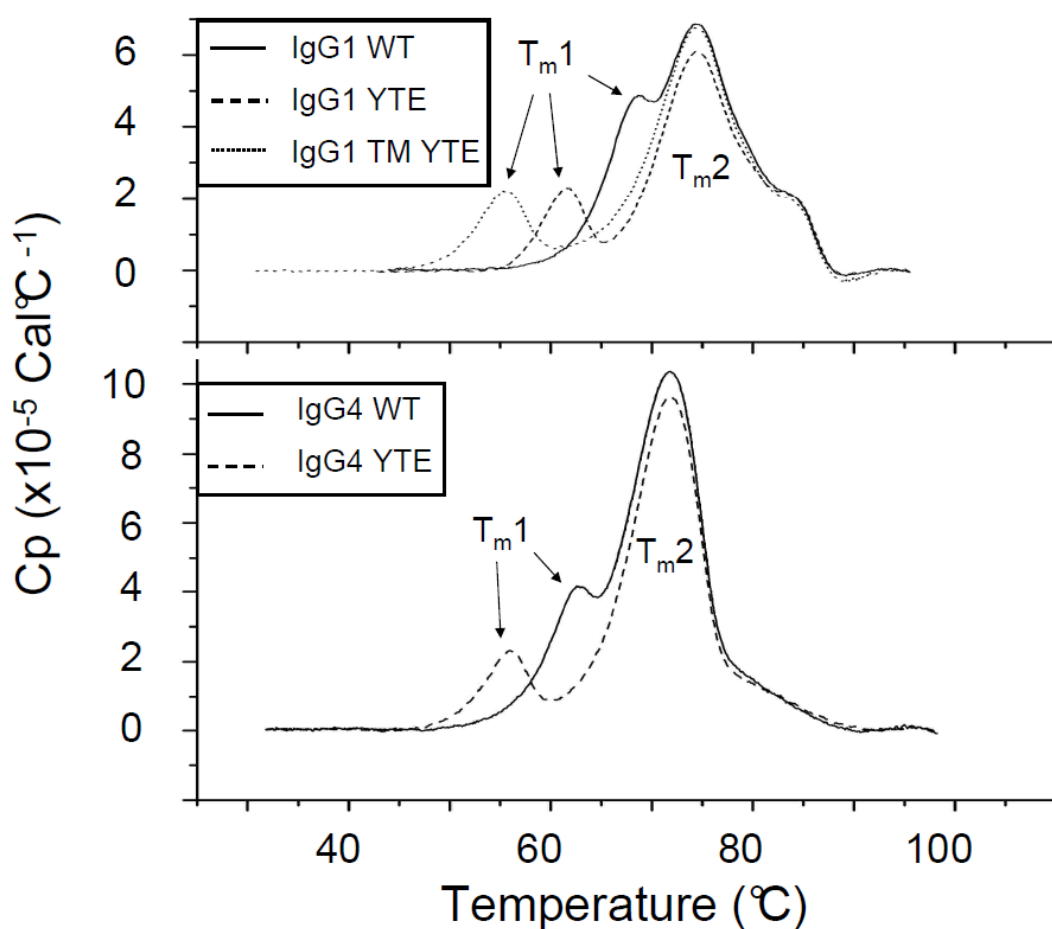
Figure 8-2: **Effect of modifications on thermal stability determined by DSC using 1 mg/ml samples of IgG1 WT, YTE, TM YTE and IgG4 WT and YTE in L-histidine and D (+) trehalose buffer pH5.5.**

The T_m1 values for the antibody variants showed a greater range than the T_m2 values giving different resolutions of the peaks. Some previous work intimates that peak resolution is related to the level of inter-domain interaction in the antibody (Privalov and Potekhin, 1986, Gill et al., 2010), suggesting the closer and less resolved two peaks appear, the more interaction they have with each other during unfolding. Other sources however dispute this and state that the individual domain peaks unfold independently (Vermeer and Norde, 2000) and just happen to overlap due to similar unfolding temperatures. IgG1 WT displayed the least resolution of the subtype, with closely associated peaks with a high T_m1 value. IgG1 YTE and TM

YTE had similar profiles with two distinct individual peaks, but IgG1 TM YTE had a lower T_m1 value. It is interesting to note that IgG4 WT also had a near identical T_m2 value to IgG4 YTE. The T_m1 value for IgG4 WT was much higher than for IgG4 YTE, giving less resolution between the peaks. The emerging shoulder on the right of T_m2 unfolding transition for the IgG1 subtype compared to the trailing edge on the corresponding transition for the IgG4 subtype showed the greater stability in the CH3 region of the IgG1. It is speculated that the greater areas of the peaks could be a result of IgG4's ability to rotate and translate more than the IgG1 due to the IgG4's aforementioned weaker linker hinge in the Fc.

The T_m1 value is predominantly used in industry as an approximation to screen the relative stability of antibodies and determine the optimal temperature to perform accelerated stability testing (Fesinmeyer et al., 2009), although use of this over T_m2 is being increasingly challenged. Comparison of T_m1 values with the PDC comparator obtained from the interfacial shear device monomer loss data would show how related the two stability readings are. Based on the greater enthalpy, the T_m2 value should represent the major unfolding transition of the molecules. It has also been reported that while changes to the protein structure at T_m1 values are reversible, changes that occur at T_m2 values are irreversible (Brummitt et al., 2011). This could mean the T_m2 value is in fact more pertinent to predicting protein aggregation. However, the data showed negligible difference with T_m2 readings for the modifications although the IgG1 and IgG4 populations did fall into two distinct sub-sets. It is logical that the modifications located in the CH2 region would not greatly affect the stability of the Fab transition. The weak linker region in IgG4 molecules could account for the lower stability seen in general for the IgG4 candidates. This region has reduced inter-heavy chain disulphide bridge stability, allowing the molecule to detach into two monomeric halves (Aalberse and Schuurman, 2002). The resistance of the whole molecule to degradation must be

greater than the sum of the two halves. It should be stated that the stability of these molecules is not necessarily related to their efficacy.

8.4 Accelerated stability
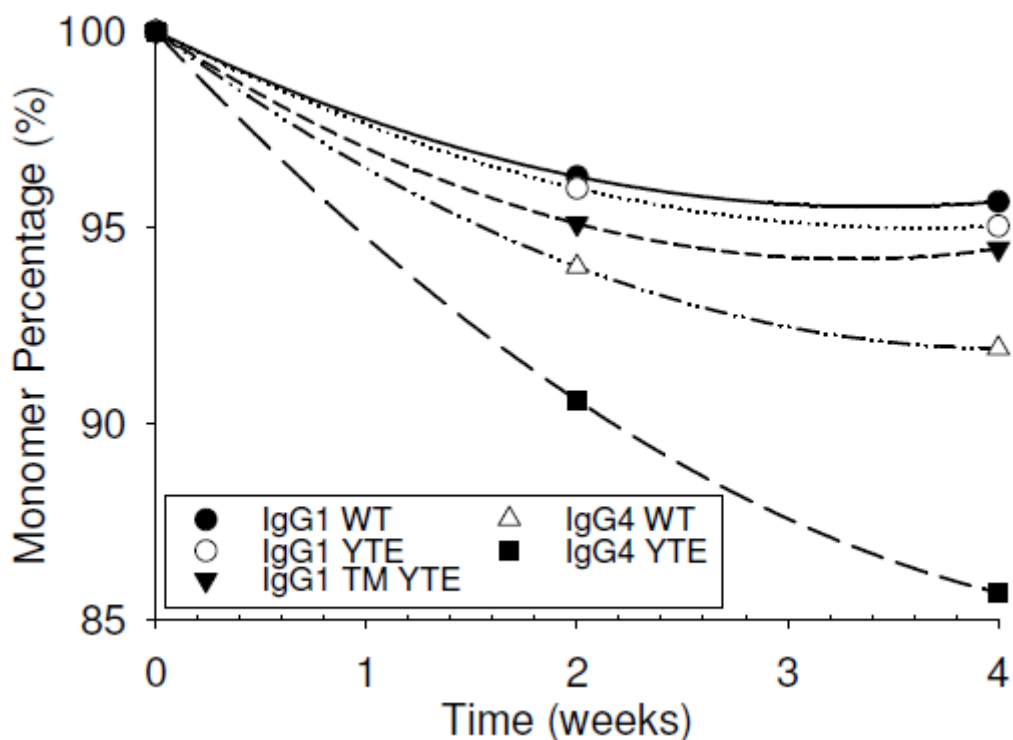
Figure 8-3: Effect of modifications on accelerated stability studies, monomer percentage determined by SE-HPLC at 0, 2 and 4 weeks using 10mg/ml antibody samples in L-histidine and trehalose buffer pH5.5 held at 40°C.

The accelerated stability results did differentiate between the IgG1 and IgG4 candidates as shown in figure 8-3. In line with previous reports (Ishikawa et al., 2010) there were minimal amounts of fragmentation present in the thermally denatured samples, with the vast majority of monomer loss through aggregation mechanisms. Curves for loss were fitted to a second order polynomial curve, showing a clear trend for each antibody. IgG4 candidates showed reduced thermal stability in comparison to IgG1 candidates. Since the trends reported did not converge, the value of the monomer percentage at week four was used for further analysis of the data.

8.5   Comparison of PDC and thermal stability
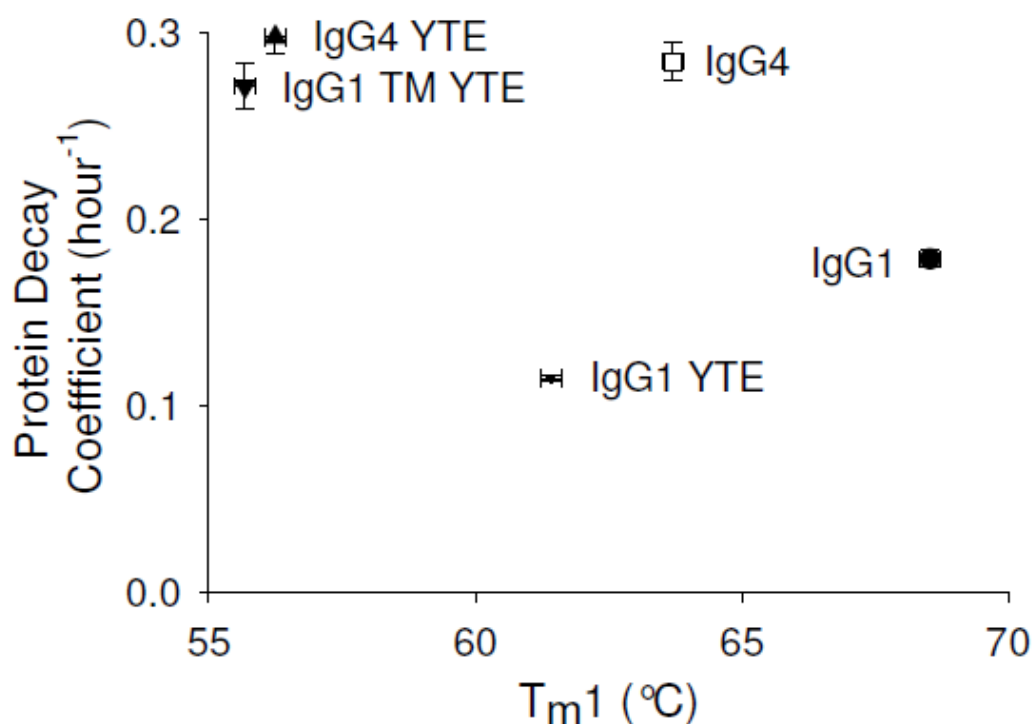
Figure 8-4:   **Comparison of protein decay coefficient with melting temperature 1 for all candidates at a disc rate of 9000 rpm with Y-axis error bars for standard error of PDC fit and X-axis error bars for internal error of DSC.**

The correlation of the thermal stability measured by DSC with conformational stability measured by adsorption to solid surfaces in a high shear environment was assessed. The different antibodies are shown in figure 8-4 in terms of their first melting temperature, T_m1, which represents unfolding of the CH2 region. This comparator is predominantly used in industrial screening of antibody candidates to determine the most stable candidates for accelerated stability studies. Comparison of the two stability indicators showed that there was no correlation between the thermal and the surface adsorption based stability. The IgG4 candidates did show that while they were the least stable in the shear device, they had relatively good thermal stability for this transition. The lack of correlation suggests that different mechanisms of degradation are involved in the two testing methodologies.
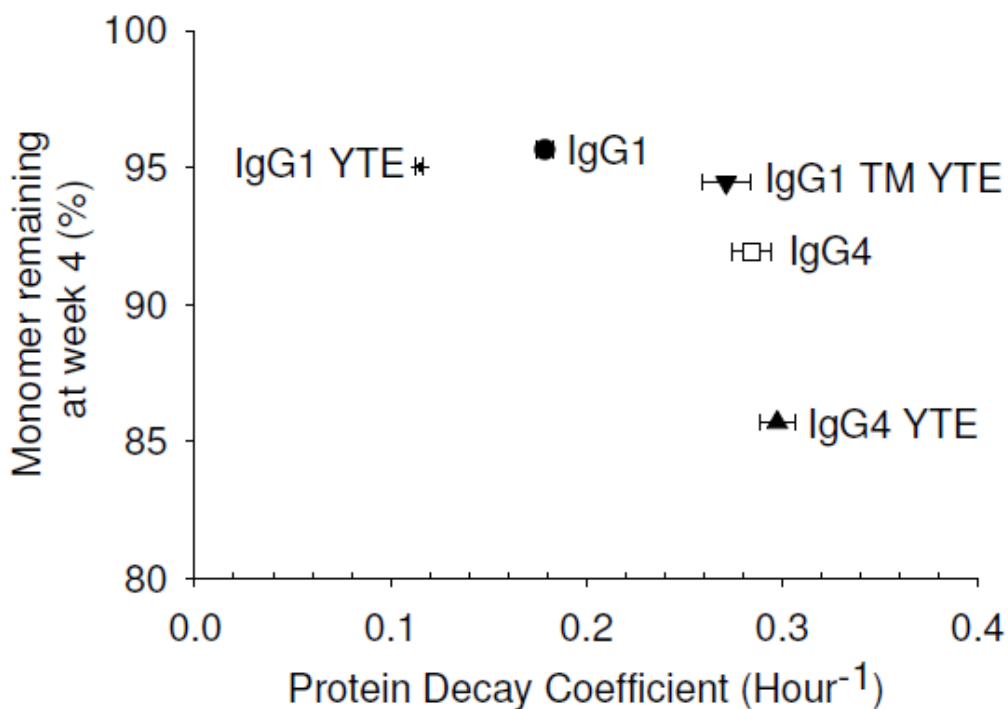
Figure 8-5: Comparison of monomer remaining at week 4 in accelerated stability results, determined by SE-HPLC and the PDC as determined for all candidates at a disc rate of 9000 rpm with X- Axis error bars for standard error of PDC fit.

Comparison of PDC using 1 mg/ml protein with monomer percentage determined from accelerated stability studies at 40 °C using 10 mg/ml protein, shown in figure 8-5, revealed little trend between the two stability indices. The concentrations of antibody solution were kept at the standard operating conditions of each method. The IgG4 accelerated stability data supported the Tm2 results from the DSC analysis, highlighting the inability of the T_m1 values to differentiate between IgG1 and IgG4. IgG1 YTE was shown to be significantly more stable to damage via interfacial effects than IgG1 WT, yet slightly less thermally stable. This would indicate that the two methods are not directly comparable. Finally the monomer remaining at week 4 from accelerated stability study was compared to the T_m1 from DSC. As with the other comparisons, there was little correlation with the different methods, this can be explained by DSC's inability to differentiate IgG1 and IgG4's stabilities.
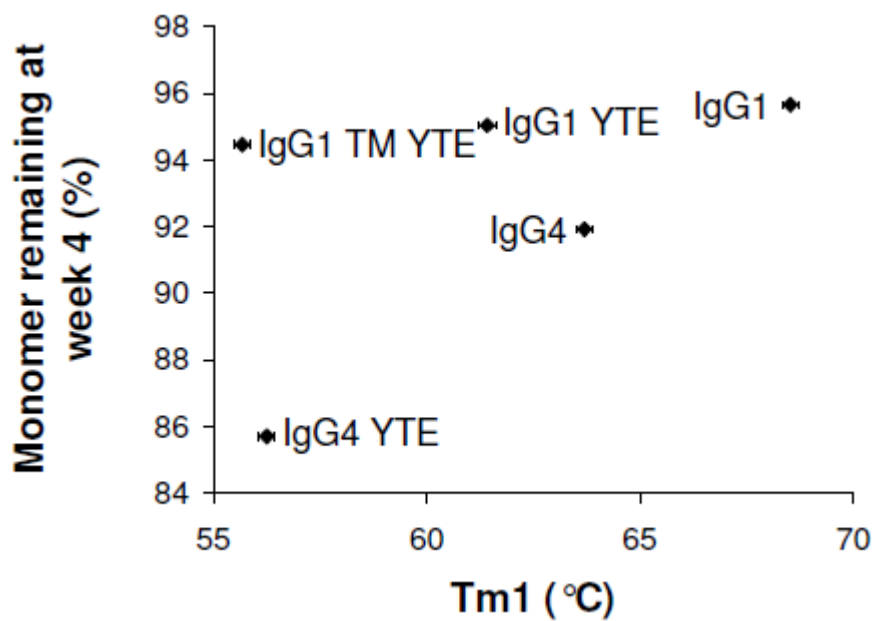
Figure 8-6: Comparison of monomer remaining at week 4 in accelerated stability results, determined by SE-HPLC and melting temperature 1 for all candidates with X-axis error bars for internal error of DSC.

8.6   Making molecular models of the candidates

Molecular models were produced for each of the antibodies according to the method described in the materials and methods section. Each model was tested for spatial aggregation propensity (SAP) and the regions with high propensities were identified.
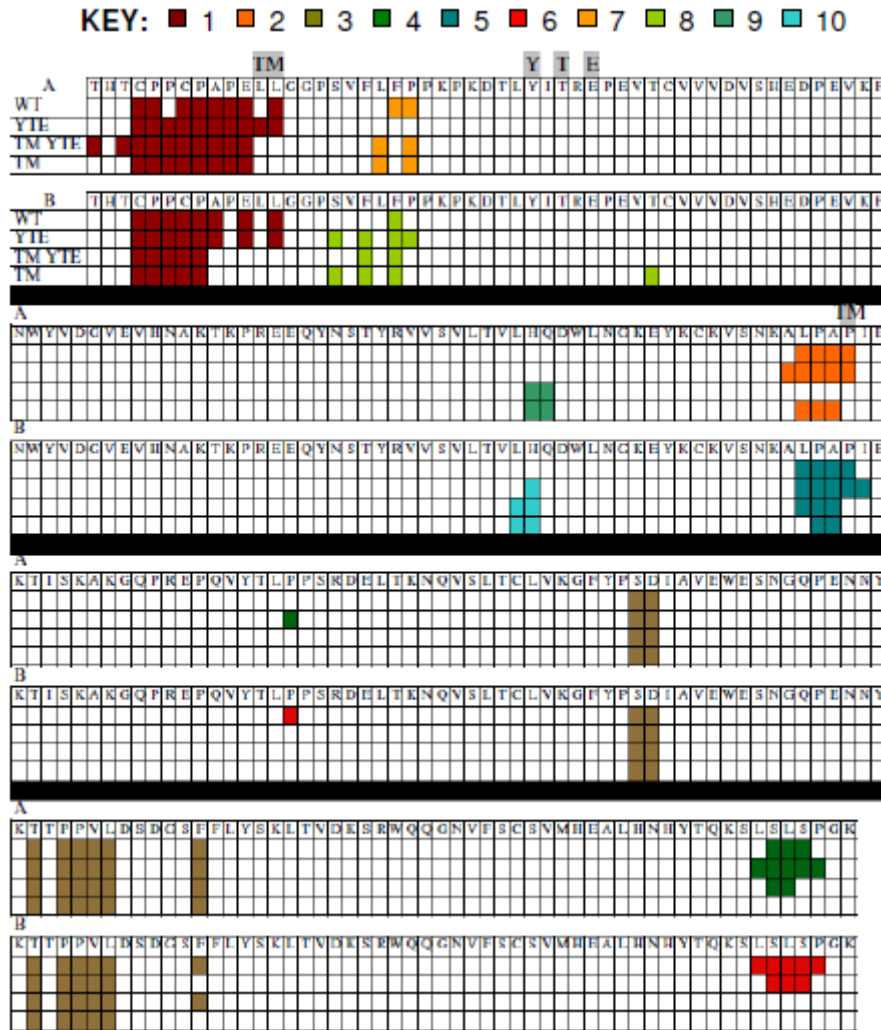
Figure 8-7: Sites of high aggregation propensity on IgG1 candidates as determined by SAP analysis.

Figure 8-7 shows the different regions on both chains of the Fc highlighted against a map of the IgG1 YTE amino acid sequence. It is shown clearly that the SAP is high in only six different regions down the amino acid sequence of each chain. Some regions seem to have a similar SAP score across the antibodies such as region 3, but others seem to be modulated by the modifications, like at hot-spots 4 and 6 which occur at the same point in the sequence on opposite chains.

8.7 The effect of the modifications on the secondary structure and charge of the candidates

FTIR of the antibody and molecular modeling of Fc were used to determine why the modifications were affecting the stability of the antibodies. Table 8-2 shows the percentages of various motifs in the secondary structures of the candidates, intimating a difference in the tertiary structure that is evident in the models. The higher levels of more complex motifs in the IgG4 candidates would require more energy to unfold and would help explain the inability of DSC analysis to differentiate them from the typically more temperature stable IgG1's.

Table 8-2: FTIR and hinge SAP results for IgG1 and IgG4 antibodies (Medi/UCL003-008).

	Helix (%)	Sheet (%)	Bend (%)	Turn (%)	Coil (%)	Total (%)	Hinge SAP
IgG1 WT	12.0	38.1	9.9	13.7	23.9	97.6	10.4
IgG1 YTE	11.7	37.7	10.6	13.5	24.1	97.7	12.7
IgG1 TM YTE	15.9	34.1	9.8	13.2	24.0	96.9	7.9
IgG4 WT	7.1	39.0	10.5	13.6	25.6	95.9	-
IgG4 YTE	13.1	36.1	9.3	13.4	24.4	96.2	-

Molecular models of the IgG1 Fc with two internal fucosylated glycans were analyzed for their SAP and electrostatic surface charge displayed in figure 8-7. There are known docking postures of the Fab onto the hinge and the superior surface of the Fc. The CH1-1 loop of the Fab is more intrinsically disordered than even vhCDR3 (Sela Culang et al., 2012) and is oriented towards the central hinge in the full-length mAb crystal structure (Saphire, 2012), though it does not have electron density in the model 1HZH (PDB). This, together with high sequence variability in this loop, would imply that it has no conserved interactions with the hinge region. The minor hinge, however, has greater sequence conservation and is shown in a stably docked posture in the full-length antibody crystal structure (Saphire, 2012), orientated with the minor-hinge of the light chain forming an interface with the location of the first two mutants of the "TM".

There is no significant difference shown in the electrostatic results and the overall surface charges of the proteins remain the same, showing that the difference in stability is not from electrostatic interactions, a key component of colloidal stability. The SAP models do however show a very noticeable difference in the hydrophobicity of the hinge region of the Fc with the rest of the molecule not showing any significant differences. The an increase in the hinge SAP scores shown in figure 8-8 correlates with a reduction in the PDC, suggesting this is the area of the molecule responsible for the change in stability documented in this instance. It is postulated that having a more hydrophilic upper hinge would reduce the range of motion of the Fab in respect to the Fc, giving a more rigid antibody structure that is less able to fold in on itself to conserve hydrophobic sections on the Fc. In the case of the TM this allows the enhanced binding to the Neonatal Fc Receptor, but also seems to allow easier degradation through adsorption at solid/liquid interfaces. It is suggested that the mobility of the hinge region is very important, not only in exposing effector functions of the Fc (Dall'Acqua et al., 2006a), but in keeping the antibody stable in solution.
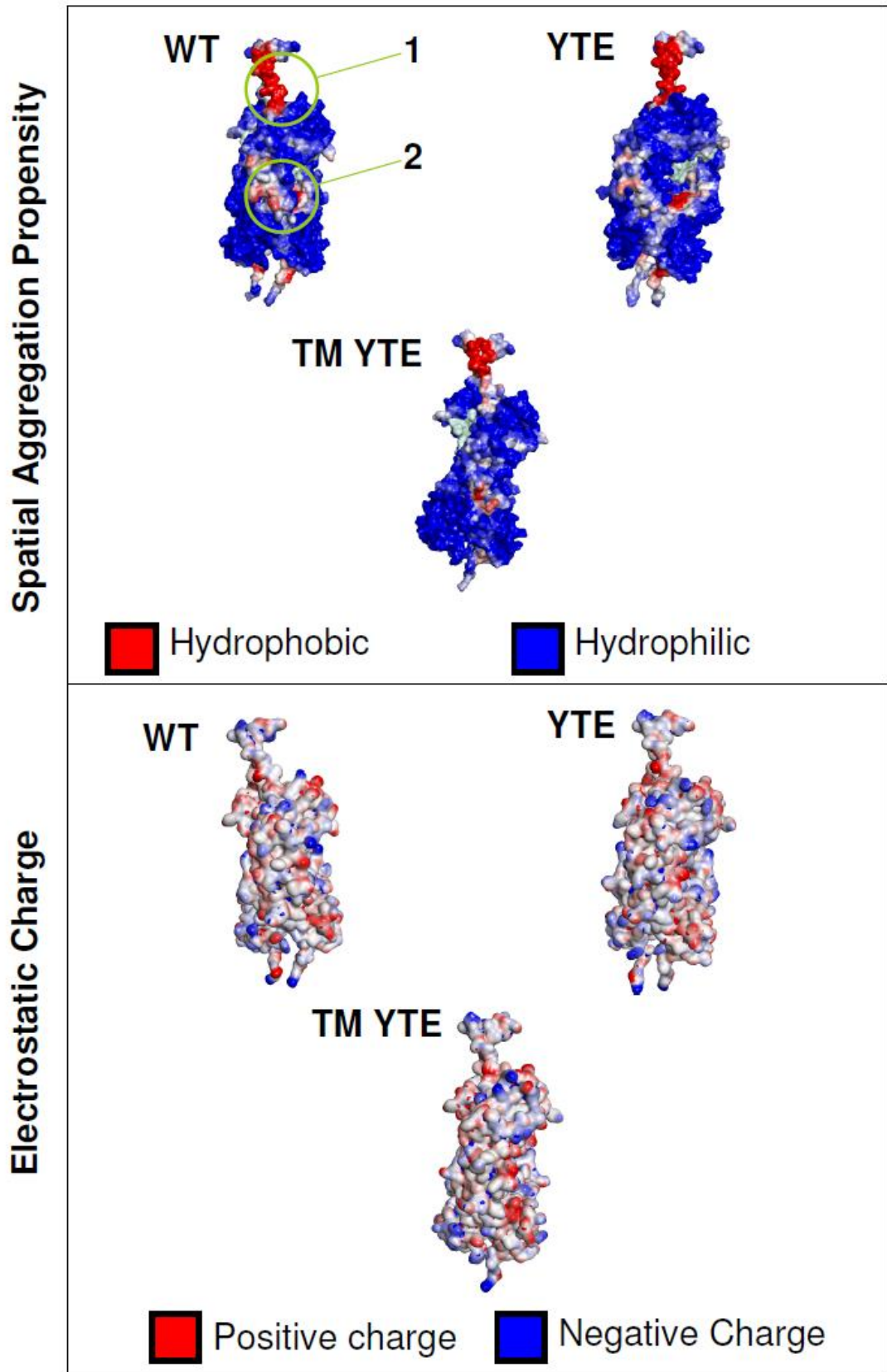
Figure 8-8: Comparison of Spatial aggregation propensity and surface charge of IgG1 WT Fc with the YTE and TM YTE modified IgG1 Fc's with site 1 as the site of the Tm modification and site 2 as the site of the YTE modification.

8.7.1 Mechanism of aggregation seen in the shear device
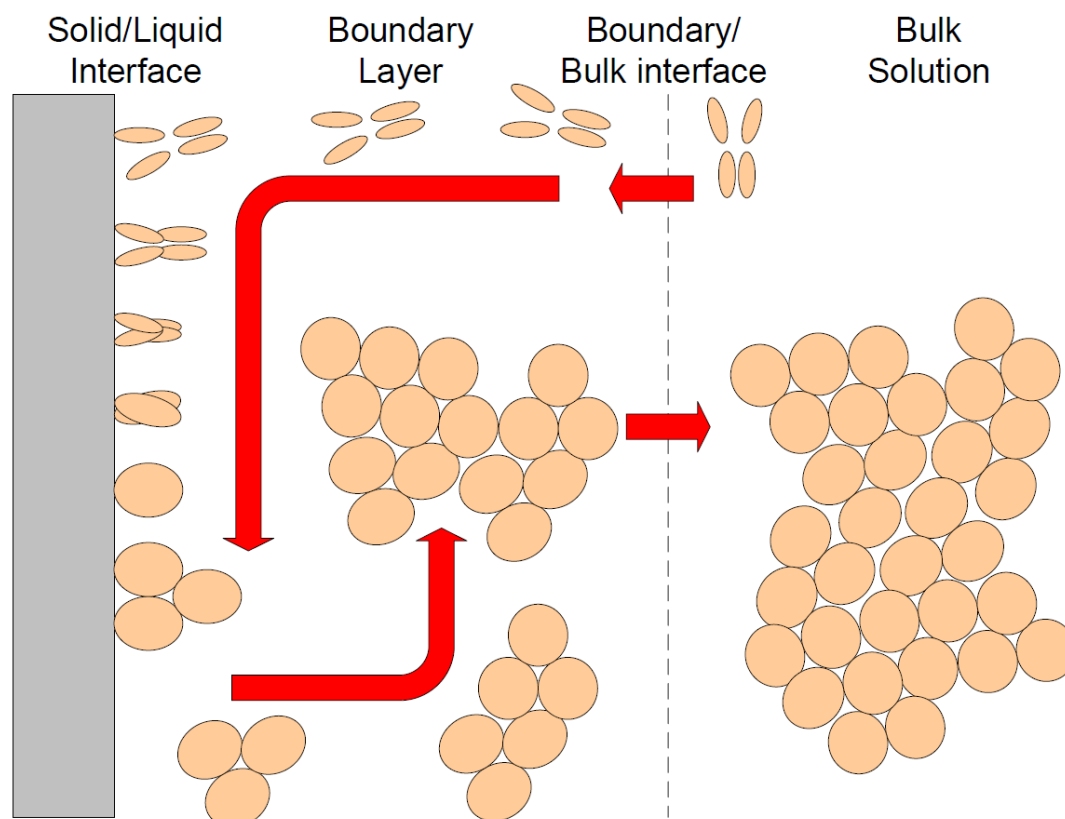
Figure 8-9: Diagram of mechanisms of aggregate formation in the shear device.

The shear device does not appear to have any low molecular weight aggregates present in samples taken from the device, even if they are placed in the SE-HPLC minutes after being taken. This suggests either very short lived intermediaries, or intermediary species which form and aggregate together within the boundary layer before being released into the bulk solution where they react further. Figure 8-9 gives a proposed diagrammatic mechanism for this growth to the point where the aggregate moves out to bulk solution. There would appear to be a concentration dependence on the movement of the antibodies into the boundary layer as reported elsewhere (Stenberg and Nygren, 1988, Shojaaee et al., 2012). Materials then adhere to the surface (Bee et al., 2010) where the material changes to a non-native state. This state exposes aggregation hot spots which quickly react with other molecules to start the aggregation process (Roberts, 2007). There are spatial limitation on the level of adsorption to the solid/liquid interface which can be altered

by changing the disc rotational speed to effect the shear expedited removal of material from the interface which will then make its way out of the boundary layer and back into the bulk solution (Doran, 1995, Shojaaee et al., 2012), possibly aggregating further before returning to the bulk solution.

8.8   Conclusion: Which methods to use and how do modifications affect stability?

The systematic use of known monoclonal antibody variants of IgG1 and IgG4 subtypes reveals the complexity of protein stability in solution. The three testing methods used, DSC, accelerated stability at 40°C and stability to solid-liquid interfaces all provided different rankings of stability, inferring differing mechanisms of damage predominant in each. The shear device provides an orthogonal approach that can be used as part of an overall screening process for protein stability. This provides the basis to characterize the critical routes of degradation encountered during therapeutic protein processing and storage. The shear device gives relative stability for routes involving shear and solid-liquid interfaces, which are present in many different steps of protein purification and in transport and storage of drug product.

The mechanism of degradation in the device is proposed and involves the transfer of antibodies into the boundary layer and adsorption to the surface (Shojaaee et al., 2012). Degradation occurs on the surface and exposed hydrophobic aggregation hot spots initiate aggregation. Aggregates then continue to grow on the surface until shear causes their disassociation, at which point, they continue to aggregate in the boundary layer until they pass back into the bulk solution.

The correlation of the molecular modeling results with the shear device results not only helps to explain the reason behind the change in stabilities, but underlines the benefits of using *in silico* methods for the evaluation of drug candidates in the future (Zurdo, 2013).

A broader knowledge of antibody characteristics earlier in the drug lifecycle would allow candidates to be selected for stability through the primary recovery and downstream processing stages of production and will allow better analysis of long

term storage stability. Increased stability is however not an indicator for increased

product efficacy, another factor that should be considered.

9 Final conclusions and future work

9.1 *Review of project objectives*

9.1.1 Complete characterisation of the custom UCL disc interfacial shear device

The work that has been described has provided significant further characterisation of the disc interfacial shear device. Prior work from the group described a disc shear device and the effect of the shear regime within the chamber and the effect of time and disc speed on the level of monomer loss, to give results for the stabilities of multiple proteins (Biddlecombe et al., 2007, Biddlecombe et al., 2009). The device employed in the previous studies built up evidence for using shear devices to emulate downstream operating conditions which was different from previous work using similar devices to determine the effect of shear on large biological materials such as cells.

The latest shear device further refines the ability of the method to be applied to downstream processing operations. It is designed to give the best level of control over air-liquid interfaces by excluding everything but sample from the chamber. It has very precise control over the rotational speed of the disc and an optimised cooling system.

The temperature of cooling water required at a set cooling water recirculation rate for different disc speeds was determined to remove the effect of temperature on the degradation rate.

The wavelength of light to be used in the SE-HPLC analysis of sheared samples was defined as 280nm.

The optimum disc speed was further defined to 9000rpm as an optimisation between the level of monomer loss produced and the reliability of the reading.

Finally, extensive testing was performed on the concentration of monomer to be used in the machine. Higher concentrations did give more differentiation of antibody stabilities, but this may have been resultant of the lower reliability of the result at higher concentrations. It was decided to optimise reliability and in doing so reduce protein mass required, by using a low concentration. 1mg/ml was the optimal concentration decided upon.

9.1.2 Develop a higher throughput method of gaining comparable results to the disc shear device

Strong foundations were set for developing a higher throughput method of obtaining comparable results to the disc shear device. The ability of the capillaries to enable parallel processing with a similar mechanism of protein aggregation to the disc device opens the door to the possibility of producing simpler and further refined devices. The use of 96 well plates would allow for 96 samples to be queued up. It is possible to use parallel capillary devices to process 8 wells simultaneously every 2 hours before CIP, with the samples ready to be placed directly onto a HPLC for SE-HPLC analysis. The work also helped to highlight important stages in the mechanism of aggregation in the capillaries that had been witnessed in other circumstances, both from entry into the boundary layer (Shojaaee et al., 2012) and adsorption to the steel surface (Bee et al., 2010).

The simplicity of the method could allow automation either on an established robotic platform such as a Tecan, or on a custom produced platform that could be designed and assembled in the future. A fully developed technique of this kind, with a 15 minute clean in place protocol included, would be able to process 96 different samples within 27 hours. Multiple plates could be loaded onto a system before the weekend to allow 192 or 288 samples to be processed in one batch using a total of 57.6mg of protein per plate. Using the current method, a maximum of 3 runs can be completed in a working day so it would take 32 days, or six and a half weeks and

672mg of protein to get the same number of results as one 96 well plate. This is an order of magnitude reduction in time and material requirements.

9.1.3 Finding an appropriate way to analyse aggregates formed through processing

Aggregates produced in the course of the project were analysed using a wide range of techniques not all of which were described in the results section of this study. The problem with analysing the aggregate profiles developed was the large range of sizes of aggregates produced (Joubert et al., 2011). The range effectively precludes the use of a single method to determine the size of aggregates produced (Philo, 2006). The second major issue is that the cost, time and expertise needed to use the majority of the techniques is quite intensive. The project recommends a portfolio of three techniques that cover the range from 1nm to 100μm. Two well characterised techniques in the SE-HPLC and microflow imaging can be teamed with the emerging nanoparticle tracking analysis technique with the use of the Nanosight which was shown to be very powerful at imaging particle size with excellent resolution in the range between the two other techniques (Filipe et al., 2009). The Nanosight was shown to be able to accurately track the particle size distribution in the linking range of 50nm to 2μm between the SE-HPLC and microflow imaging techniques. The results showed the ability of the device to pick out the trends in growth and reduction in different size ranges of aggregates as more antibody passed into ever larger aggregate species during operation of the disc shear device.

9.1.4 Determine the effect of reversible self-association on the bioprocess of a target molecule

The work described takes a detailed look at the reversible self association (RSA) of an RSA exhibiting IgG1 (Medi/UCL009). RSA is a phenomenon that is becoming

noticed more frequently in drug production (Bethea et al., 2012, Chaudhri, 2012) The reversible association of antibodies could effect their purification (Liu et al., 2005) and could lead to further aggregation. By first determining the factors which affect the antibody's tendency to exhibit the phenomenon and subsequently moving through the various steps in purification of the molecule, the effect of RSA on bioprocessing was characterised. During exposure to interfacial shear in the disc device, further aggregation in conditions promoting RSA was not observed which does not support the idea that RSA promotes aggregation. It was determined that RSA does not prevent nor considerably effect the operation of most of the steps in antibody purification. The main consideration taken from the results is that filtration steps should not be performed in conditions that encourage RSA. In particular, the antibodies should be put into formulation conditions prior to final viral filtration and should not have RSA present as this will have a largely detrimental effect on the operation of the step. As injection of any aggregated species into a patient is advised against (Joubert et al., 2012), this should not greatly effect the operation of antibody bioprocessing, but will add another parameter to test for during formulation studies performed on the antibody candidates.

The RSA in this case was determined to be a product of a large hydrophobic patch on the c-terminus of the Fc, reaching around to the anterior face of the Fc determined by the SAP algorithm (Kayser et al., 2011, Chennamsetty et al., 2010). This region would normally be exposed to the solution, and it is postulated that it would have a tendency to bind reversibly with one other similar unit on the mirrored patch on its c-terminus.

9.1.5 Comparison of interfacial shear disc device with thermal methods as tools for determining antibody stability and the use of molecular modelling to explain the difference

The relationship between the thermal methods for determining antibody stability and use of the disc shear device were explored in depth as no current methods are fully representative of antibody stability upon storage. Using differential scanning calorimetry showed that while it was possible to observe the thermal unfolding of the domains, none of the melting temperature transitions were found to correlate with accelerated stability results, highlighted by the inability of DSC to distinguish between the IgG1 and IgG4 subtypes. The accelerated thermal stability is a well known method for predicting the comparative shelf life of an antibody product (Joubert et al., 2011) but there is growing consensus in industry that the method is far from the golden standard. The disc device results were shown not to correlate with the accelerated stability results or the DSC, indicating a fundamental difference in the mechanism of aggregation that is determined through each of the approaches. Further investigation into the three dimensional antibody structures of the molecules showed that the difference in stability determined by the shear device correlated to the hydrophobicity of the hinge region of the Fc. This inferred the disc device was giving a stability measurement based on the exposed surface of the molecule's three dimensional structure. It is determining the proteins ability to conserve this structure and the regions that may be involved in adsorption and desorption from surfaces they come into contact with during bioprocessing (Sela Culang et al., 2012, Saphire, 2012). It was concluded firstly that the molecular modelling techniques are a powerful technique in helping to understand antibody stability in preparation for lab scale experiments. Secondly, it was concluded that the disc shear device provides an orthogonal approach that can be used as part of an overall screening process for ranking protein stability. There are many different degradation pathways in a proteins lifecycle and it is important to inhibit the most

predominant routes. The shear device gives relative stability for routes involving shear and solid-liquid interfaces which are present in many different steps of protein purification and in transport and storage of drug product.

9.2   Final comments

The project has looked at a wide variety of process related stability issues and highlighted methods that can be used to implement a robust characterisation system for antibody stability and measurement of aggregate impurities. Included in this system is the recommendation that classical thermal stability testing should be augmented with results from the complementary interfacial shear methods. This will give an orthogonal measure of protein stability based on the solid-liquid interactions that are prevalent in manufacturing shipping and storage of biological products. By proving concept and starting to develop a higher throughput method for delivering comparable results to the disc shear device, the project naturally leads into a programme of extra work in further developing the method to take the measurement in an industrially acceptable format.

Substantial work was also performed in creating homology models for subsequent analysis of antibody stability, a field that is quickly developing and can be used to help screen ever larger numbers of drug candidates as computing power becomes cheaper. As the available processing power increases, these methods will come to the fore in early stability analysis of potential drug molecules. It is therefore important to establish correlations to experimental methods and the different mechanisms of aggregation.

9.3   Future Work

9.3.1 Short term work (0-3 months)

These proposals are designed to be possible during the course of an MEng or MSc project by one candidate with supervision from a doctoral level student.

Membrane blockage

With respect to the RSA experiments, it would be beneficial to determine the cause for membrane blockage with Medi/UCL009 (IgG1) during viral clearance filter operation. If there a surface chemistry interaction with the membrane (Ahmad and Hairul, 2008) this problem could be solved by using a different material or coating, but if it is mechanical blockage of the pores, the conditions going into the filter will need to be altered. This could be tested by recreating the blockage of a filter by running it through with Medi/UCL009 in RSA forming conditions until the flowrate fell. The membrane could then be removed from the filter housing and confocal microscopy could be used to look at a cross section of filter membrane to determine the cause of blockage (M. Shotton, 1989). If the antibody has permeated to different distances through the membrane based on pore sizes, this would point to a mechanical blockage, whereas a coating of protein on the membrane surface would point to a surface chemistry interaction.

Computational fluid dynamics of capillaries

With respect to the higher throughput interfacial shear device, computational fluid dynamics analysis should be performed to analyse fluid flow at different flow rates in the coiled capillaries, determining the exact flow patterns involved. The effect of altering the tightness of the coil should be examined to determine if that is a way to increase the shear the antibody is exposed to. It is important to understand and maximise the shear in the system to give the greatest level of monomer removal

from the capillary surface, which in turn gives a greater level of monomer loss. This will allow greater differentiation of different antibodies and can be achieved using an appropriate package such as COMSOL to design the 3D capillaries and apply the appropriate analysis.

Un-attributed capillary monomer loss

With respect to the higher throughput interfacial shear device, it was observed that there was a base level monomer loss of 2% that was additional to the rate of monomer loss from operation. The capillary device should be investigated to determine whether this is due to protein bound to the capillary surface that is not expelled with the rest of the sample to be tested. This is important as it would cause a source of error in monomer loss readings for devices with different dimensions or made with different materials or surface roughness. If the loss is caused by surface adsorption, it was calculated that there was a protein density of $17.1 g/m^{-2}$ at the surface. By using capillaries of different diameters it would be possible to have different size to volume ratios, with different areas of surface area exposed to the sample. By performing experiments using these different sizes for different lengths of operating time, it would be possible to calculate the base level of monomer loss again and use this percentage to determine the protein density at the surface. If this is equal to the $17.1 g/m^{-2}$ then it would be concluded that the loss is due to protein bound to the capillary surface.

9.3.2 Medium term work (3 months -1 year)

These proposals are designed to be sufficient for testing as a significant part of a doctoral project or in the course of post-doctoral work.

Nanoparticle tracking analysis

With regards to the nanoparticle tracking analysis using the Nanosight, it was concluded that the Nanosight technique was very powerful at determining the particle size distribution within the 50nm to 2μm range for antibody aggregates. It was capable of providing these results in a timely manner once the parameters of operation were set. Determining the conditions for operation of the device however took a long time for different samples and set-up of the device was time consuming at the beginning of any set of results. To this end the Nanosight technique should be further developed and defined to give a more robust, standard framework for its use. This includes work for the physical loading of sample and focussing of the microscope as well as developing the settings that should be used to firstly capture the samples and then to subsequently process them.

During operation of the device it was found that larger particles forming during operation of the technique were an issue. Further work should go into developing multiple new methods with their own defined settings that are able to isolate and focus on different size ranges of particles within highly disperse samples. This would mitigate the effects of the larger aggregates and avoid sampling them as part of the results.

The mechanism of protein adsorption to stainless steel

With regards to protein adsorption to the stainless steel of the interfacial shear devices, it would be beneficial to get more information on the mechanism of protein degradation. This could be achieved by using a microscopy technique such as confocal microscopy (M. Shotton, 1989) to look at the density of the antibody adsorbed to the metal surface after it was exposed to shear and an antibody solution. A high density would suggest that the aggregation was occurring at the solid/liquid interface, whereas a low concentration would indicate degradation on the solid/liquid interface followed by aggregation in the boundary layer.

It would be ideal if a more detailed analysis such as electron tomography (Lučić et al., 2005) could also be performed on antibody adsorbed to the metal surface in similar process conditions to look into the conformation of the antibodies as they undergo different stages of unfolding in the shear device. This would provide a lot of information on the mechanism of protein degradation at the solid/liquid interface.

9.3.3 Long term work (more than 1 year)

These proposals are designed to be appropriate for either the main focus of a doctoral project or as part of an ongoing portfolio of work within a university department.

Development of a capillary interfacial shear device

With regards to development of the capillary interfacial device, work would need to go into the next generation of the device. Although the syringe pump system gave reliable and reproducible results, there was still a level of uncertainty in the results and the operator needed to be very careful at every stage not to alter the calibration of the device or introduce any unwanted variables. The flowrate achievable in the device is not sufficient to give large levels of monomer loss within two hours of operation, so using a different pumping method would add to the reliability of the results and give more differentiation between samples to be analysed. Finally, the device is not suitable for automation, which would allow for a very high throughput operation. These factors would make the capillary device highly effective in determining relative stability of a whole range of proteins in many different buffers at a very low cost. This would be very valuable to industry where they could look at a more comprehensive view of the antibody stability earlier in the drug production cycle for a very low cost. This would save companies significant amounts of time and money on the process development of candidates and help reduce the cost of therapies at a time when buyers are putting pressure on them to do so.

The development of the next generation of device can be done by either modifying an existing robotic device or platform such as a Tecan, which is able to use 96 well plates to use capillaries, or by creating a bespoke automated liquid handling platform to achieve the same thing. The use of 96 well plates is important as it is a standard lab consumable that the device can be designed around and allows the tests to be easily queued up. An additional concern is that if the samples are queued for a significant amount of time, they will be exposed to ambient temperatures, which over the operating time of the device may affect the stability of the samples. To negate this factor, the sample storage chamber should be temperature controlled.

Development of modelling techniques

Development of modelling techniques is already at the forefront of research into protein characterisation. Models can be created for analysing static antibody structures relatively easily, but as the technique develops, it is important to be able to produce models that also take into account both the variability of glycosylation patterns and the dynamic nature of a proteins interaction with its environment. This will allow modelling techniques to give predictions of stability based on the entire sample. Currently, it is difficult to create models of entire antibodies (Chennamsetty et al., 2010) so forcefields need to be developed that allow design of an entire antibody model, and that can then map and take into account glycosylation. These models need to have heterogeneous glycosylation patterns that would be representative of real samples.

The next step is allowing dynamic action in the antibody in the model. This will permit the model to take into account the specific exposure of different portions of the molecule as they move, exposing and conserving different parts to solution. The final dynamic interaction that needs to be modelled is the interaction with the solution and with ions present. While there are currently ways of producing models

that take the solution conditions into account, preparing models for this kind of dynamic analysis is incredibly time consuming (Gu et al., 2012) and can take up to 2 months to get to the point where they can be run. Programs should be developed to allow the assembly of complex models to be completed quicker by standardising the addition of excipients and water molecules and to take into account the effect of changes in pH and salt concentration. As computing power continues to increase, it will be more and more important to develop new tools to push the capability of this field of research and make it easier to set up analyses.

Development of an understanding of the effect of excipients

The ultimate goal of this project and of many research departments is to produce more stable antibody therapeutics. This can be done in two ways; either by designing the stability into the protein structure, or by stabilising the protein during processing and storage with the use of excipients. The solution to this problem is ultimately going to be a mixture of the two approaches. This project looked into the effect of modifications to the protein primary structure on the stability of the resulting three dimensional molecules, but more work needs to go into characterising the effect of stabilising agents. To begin with, this work can be done by using tests like DSC and high throughput interfacial shear devices to screen the effects of changing concentrations of different excipients on the various stability parameters. This screening could also introduce controlled amounts of contaminant such as stainless steel particulates or glass shavings to the samples to build up information of how these all interact with each other. I believe this data should ultimately be used to draw up a model for interaction of antibodies with solution excipients that can form the basis of a forcefield for molecular modelling.

10 Validation chapter (EngD requirement)

10.1 Introduction

The project aims to find ways to reduce the level of antibody aggregation found in typical biopharmaceutical processes by either preventing the formation of aggregates or removing their precursors from solution.

The reason to focus on this issue is the benefits to industry of a better understanding of the causes of aggregation. It will not only allow for faster screening of potential drug molecules for stability, but increase the stability of the final product. The first experiments performed confirmed the results seen in a previous report using a shear device, but then the range of antibodies, concentrations and excipients were all increased and the Nanosight analytical technique was used to elucidate further information.

Use of the Nanosight will allow the visualisation of particles between 50nm and 2 micron in diameter which would help to create a taxonomy of aggregate species within this range.

The long term objective from this project is to produce a high throughput capillary shear device capable of evaluation of antibody stability with different surface materials and to validate the accuracy of such a system.

With the expanding production of bio-therapeutics, removal of protein aggregates, either by stopping their formation or by physical or chemical removal is of ever great importance in the bioprocess industry. Since 2007, antibodies have been the highest selling category of biologics, with a market value of $21.9 billion which is estimated to rise to over $70 billion in 2015 (Visiongain, 2008). In a recent review of pharmaceutically relevant monoclonal antibodies and Fc fusion proteins, around half of them were found to possess aggregation issues following protein-A purification (Shukla et al., 2007a).

A more important factor is the loss of bioactivity of the formulation (Sluzky et al., 1991, Pease et al., 2008) which will effect the dose required by a patient.

Of greatest importance is the possibility of the aggregate eliciting an immunological response in patients (Chennamsetty et al., 2009b). This could involve neutralisation of antibodies, cross reactive neutralisation of endogenous protein counterparts, or anaphylaxis and this is the reason for the strict guidelines on their removal.

10.2 Regulatory burden

Regulations currently dictate that the level of aggregates above a certain size has to be kept below specific thresholds. Being able to more fully understand the problem will not only allow for faster screening of potential drug molecules for stability, decreasing the time to market and increasing drug selling time under patent, but could allow for smaller doses that could be kept longer if aggregation can be stopped throughout drug storage.

The regulatory issues faced by my sponsor company, MedImmune, are vast in scope. As a company they are involved in the development of numerous drugs at various stages in their lifecycle, from pre-clinical to stage 3 clinical trials. There is a huge emphasis within the company on acquiring the largest design space information for each step of a process, which in turn allows the determination of a suitable control space, outside of which the product could still be viable.

10.3 Quality by design

The quality by design begins with prior organisational knowledge. This is one of the great advantages of MedImmune and its large portfolio of ongoing projects. The quality attributes and process parameters that need to be controlled and the rough values that these should be in can all be extracted from prior knowledge, process and product understanding.

Getting this prior knowledge, in the form of a platform process into an optimal system, for example, requires process development and characterisation which involves small scale studies involving process models and Design of Experiment (DoE) studies on a whole range of parameters before scaling up to validate these results. Worst case studies are performed to view the compounded effect of being at the lower, or upper, end of the design space. From these experiments the more critical and key factors can be determined and the optimal operating ranges for each factor can be set. Quality Control (QC) and good quality assurance (QA) is still required to validate the results seen in the initial screenings.

The Critical Quality Attributes (CQA) of the drug are needed to be able to determine the suitability of a candidate molecule and process, so these are identified and ranked before anything else. Prior knowledge and experience is helpful in choosing the CQA.

10.4 Validation at MedImmune

The purification process validation is performed to demonstrate that the process does what it is supposed to. It must demonstrate that the process as set out will remove DNA, host cell proteins, media components and so on to a pre-defined, acceptable level. Furthermore it needs to show that this removal is robust, so that the level of purification is not affected by process variations and loss of efficiency of certain components from reuse. Most importantly, the validation should show that the product integrity and activity is maintained.

Within each project, the design does not stop with the initial validation. Continuous process monitoring and improvement are undertaken to extend the process characterisation and increase the knowledge space of the company. Obviously, there is full life cycle management of the processes and process performance

verification is undertaken with each batch and fed back to continually improve the process.

There is a very big emphasis within the company on the quality control of the reagents used both in process and in research. Every batch of buffer is recorded and labelled, with the lot number, date opened and weight of the reagents used, the pH and the conductivity of the buffer all recorded.

It is also very important to validate the equipment and techniques used to gain any results or purification. Equipment is validated upon installation in the labs or process facility, but routine validation is required from time to time. In terms of chromatography, packed column heights are measured, dynamic binding capacities are checked, Height of Equivalent Theoretical Plates (HETP) and asymmetries tested and the number of reuses is tracked to view the degradation of the matrix beads. There is constant testing of analytical tests, with standards being run at the beginning of assays to check the technique is working. With some methods that run for a long time, such as Size Exclusion HPLC (SE-HPLC), standards are run after a set number of assays to check there is no change in the validity of the results.

There is a lot of work that goes into the validation of the formulation used to store the drug for long periods of time. Degradation studies are a common technique used to determine the stability of a drug in a given solution. Studies used at MedImmune include pH, salt concentration, excipient and temperature accelerated studies which help validate shelf life of the product.

10.5 *Validation implications of the thesis*

My research into aggregation and the stability of monoclonal antibodies would have a few regulatory validation issues. The research itself has two possible methods of reducing the level of aggregation plus methods to determine the ability of these reducing methods to do what they say they can. The first of these reducing methods

is to find excipients to interact with the antibodies to reduce their ability to aggregate. The second possible method is to determine if a sub-population is prone to aggregation and then to remove this population early on in the process to stop them aggregating later on.

The techniques used to determine the propensity of the antibodies to aggregate do so by accelerating the process by increasing the level of the solid-liquid interaction and the level of the shear the antibodies are exposed to. The current method achieves this by using a rotary disc inside a chamber to process 8ml of sample. Future work involves a method that achieves similar levels of both these forces using pumping through a capillary for 1ml samples.

Validation issues with the excipients involve their effect on the solution they are added to. If added during a process step, the effect of adding too little or too much will have to be determined in terms of the effect on the antibody and on the impurity clearance of the step. It would also be needed to show that the excipient has no effect on the solutions behaviour on future processing steps before it is removed and that it is indeed removed before final formulation if it is needed to be. If the excipient is added for long term storage stability then validation needs to be done on the levels acceptable and the effective levels.

For the aggregate removal solution, validation would centre upon how robust the clearance is. It would have to be shown that the same level of aggregate can be removed each time, and the effect of having more or less aggregate to begin with would have to be assessed on its effect on the aggregation removal step. More importantly, the effect of having differing levels of aggregate on subsequent optimised steps would have to be looked into. Stability studies would have to be performed to prove that the antibody is later less prone to aggregation, and again would need to involve excipient, pH, salt concentration and temperature accelerated studies.

The effect of any of the modifications to the process may be to change the folding properties or the activity of the antibody, so it needs to be shown that this is not the case by the use of various analytical techniques such as SDS page, SE-HPLC, or a bioactivity assay.

Validation of the equipment will involve the development of a stable standard that can be used to determine that the equipment is still running according to specification. Plenty of suitable standards can be purchased readily from suppliers. The standard should be run once every set number of tests to ensure that the equipment is still running to specification, as with many other assays.

10.6 Conclusion

To summarise, the regulatory validation issues of my work are very much the standard issues already faced by my sponsor company and the industry as a whole. Validation requires thorough documentation and traceability of work through GMP and GLP, in addition to a good QA department to ensure everything is kept to a high standard.

11 References

AALBERSE, R. C. & SCHUURMAN, J. 2002. IgG4 breaking the rules. *Immunology,* 105**,** 9-19.

AALBERSE, R. C., VAN DER GAAG, R. & VAN LEEUWEN, J. 1983. Serologic aspects of IgG4 antibodies. I. Prolonged immunization results in an IgG4-restricted response. 130**,** 722-726.

AGRAWAL, N. J., KUMAR, S., WANG, X., HELK, B., SINGH, S. K. & TROUT, B. L. 2011. Aggregation in protein-based biotherapeutics: computational studies and tools to identify aggregation-prone regions. *J Pharm Sci,* 100**,** 5081-95.

AHMAD, A. L. & HAIRUL, N. A. H. 2008. The effect of protein–membrane interactions on filtration behavior in forced-flow electrophoresis of protein solutions. *Separation and Purification Technology,* 61**,** 384-390.

AHRER, K., BUCHACHER, A., IBERER, G., JOSIC, D. & JUNGBAUER, A. 2003. Analysis of aggregates of human immunoglobulin G using size-exclusion chromatography, static and dynamic light scattering. *Journal of Chromatography A,* 1009**,** 89-96.

ANDYA, J. D., HSU, C. C. & SHIRE, S. J. 2003. Mechanisms of aggregate formation and carbohydrate excipient stabilization of lyophilized humanized monoclonal antibody formulations. *AAPS PharmSci,* 5**,** E10.

ARAKAWA, T., PHILO, J. S., TSUMOTO, K., YUMIOKA, R. & EJIMA, D. 2004. Elution of antibodies from a Protein-A column by aqueous arginine solutions. *Protein Expr Purif,* 36**,** 244-8.

AROSIO, P., JAQUET, B., WU, H. & MORBIDELLI, M. 2012. On the role of salt type and concentration on the stability behavior of a monoclonal antibody solution. *Biophys Chem,* 168-169**,** 19-27.

ASHTON, L., DUSTING, J., IMOMOH, E., BALABANI, S. & BLANCH, E. W. 2009. Shear-Induced Unfolding of Lysozyme Monitored In Situ. *Biophysical Journal,* 96**,** 4231-4236.

AZIZ, Z., BEHLKE, J., BERNARDI, G., BOURDILLON, L., BUTLER, P. J. G., CARELS, N., CLAY, O., COLFEN, H., CORREIA, J. J., DAUGHERTY, M.

A., DE LA TORRE, J. G., DEMELER, B., DOUADY, C. J., DURCHSCHLAG, H., FLEMING, K. G., FRIED, M. G., FURTADO, P. B., GILBERT, H. E., GILBERT, R. J. C., HARDING, S. E., HOLLADAY, L. A., KREBS, A., LAIDLAW, I., LEE, Y. C., LEWIS, M. S., ORTEGA, A., PERKINS, S. J., REILY, M. M., RISTAU, O., ROWE, A. J., SANCHEZ, H. E. P., SCHUCK, P., SHERWOOD, P. J., SONTAG, C. A., STAFFORD, W. F., STEINMETZ, M., SUN, Z., TATE, C. G., WANDREY, C., WILLS, P. R., WINZOR, D. J. W., ZIPPER, P. & COLE, J. 2005. *Analytical Ultracentrifugation: Techniques and Methods*, RSC Publishing.

BACHER, G., SZYMANSKI, W. W., KAUFMAN, S. L., ZOLLNER, P., BLAAS, D. & ALLMAIER, G. 2001. Charge-reduced nano electrospray ionization combined with differential mobility analysis of peptides, proteins, glycoproteins, noncovalent protein complexes and viruses. *J Mass Spectrom,* 36**,** 1038-52.

BAM, N. B., CLELAND, J. L. & RANDOLPH, T. W. 1996. Molten globule intermediate of recombinant human growth hormone: stabilization with surfactants. *Biotechnol Prog,* 12**,** 801-9.

BEE, J. S., DAVIS, M., FREUND, E., CARPENTER, J. F. & RANDOLPH, T. W. 2010. Aggregation of a monoclonal antibody induced by adsorption to stainless steel. *Biotechnology and Bioengineering,* 105**,** 121-129.

BEE, J. S., STEVENSON, J. L., MEHTA, B., SVITEL, J., POLLASTRINI, J., PLATZ, R., FREUND, E., CARPENTER, J. F. & RANDOLPH, T. W. 2009. Response of a concentrated monoclonal antibody formulation to high shear. *Biotechnology and Bioengineering,* 103**,** 936-943.

BEKARD, I. B. & DUNSTAN, D. E. 2009. Shear-Induced Deformation of Bovine Insulin in Couette Flow. *The Journal of Physical Chemistry B,* 113**,** 8453-8457.

BENGALI, A. N. & TESSIER, P. M. 2009. Biospecific protein immobilization for rapid analysis of weak protein interactions using self-interaction nanoparticle spectroscopy. *Biotechnol Bioeng,* 104**,** 240-50.

BETHEA, D., WU, S.-J., LUO, J., HYUN, L., LACY, E. R., TEPLYAKOV, A., JACOBS, S. A., O'NEIL, K. T., GILLILAND, G. L. & FENG, Y. 2012. Mechanisms of self-association of a human monoclonal antibody CNTO607. *Protein Engineering Design and Selection,* 25**,** 531-538.

BHAK, G., CHOE, Y.-J. & PAIK, S. 2009. Mechanism of amyloidogenesis: nucleation-dependent fibrillation versus double-concerted fibrillation. *BMB Reports,* 42**,** 541.

BIDDLECOMBE, J. G., CRAIG, A. V., ZHANG, H., UDDIN, S., MULOT, S., FISH, B. C. & BRACEWELL, D. G. 2007. Determining Antibody Stability: Creation of Solid-Liquid Interfacial Effects within a High Shear Environment. *Biotechnology Progress,* 23**,** 1218-1222.

BIDDLECOMBE, J. G., SMITH, G., UDDIN, S., MULOT, S., SPENCER, D., GEE, C., FISH, B. C. & BRACEWELL, D. G. 2009. Factors influencing antibody stability at solid–liquid interfaces in a high shear environment. *Biotechnology Progress,* 25**,** 1499-1507.

BÓDALO, A., GÓMEZ, J. L., GÓMEZ, E., MÁXIMO, M. F. & MONTIEL, M. C. 2004. Study of l-aminoacylase deactivation in an ultrafiltration membrane reactor. *Enzyme and Microbial Technology,* 35**,** 261-266.

BRUGGEMAN, J. 2010. Mass Spectroscopy lecture.

BRUMMITT, R. K., NESTA, D. P., CHANG, L., CHASE, S. F., LAUE, T. M. & ROBERTS, C. J. 2011. Nonnative aggregation of an IgG1 antibody in acidic conditions: Part 1. Unfolding, colloidal interactions, and formation of high-molecular-weight aggregates. *Journal of Pharmaceutical Sciences,* 100**,** 2087-2103.

CARPENTER, J. F., RANDOLPH, T. W., JISKOOT, W., CROMMELIN, D. J. A., MIDDAUGH, C. R., WINTER, G., FAN, Y.-X., KIRSHNER, S., VERTHELYI, D., KOZLOWSKI, S., CLOUSE, K. A., SWANN, P. G., ROSENBERG, A. & CHERNEY, B. 2009. Overlooking subvisible particles in therapeutic protein products: Gaps that may compromise product quality. *Journal of Pharmaceutical Sciences,* 98**,** 1201-1205.

CASSOU, C. A. & WILLIAMS, E. R. 2014. Anions in electrothermal supercharging of proteins with electrospray ionization follow a reverse Hofmeister series. *Anal Chem,* 86**,** 1640-7.

CHAO, Z. & PAOLO, C. 2012. Salt effects on water/hydrophobic liquid interfaces: a molecular dynamics study. *Journal of Physics: Condensed Matter,* 24**,** 124109.

CHAUDHRI, A. V., G;SHIRE, S; PATAPOFF, T; ZARRAGA, D 2012. Self-Association of therapeutic Monoclonal Antibodies: A Coarse-Grained

Perspective on the Role of Electrostatics and More. BITC Summer Symposium.

CHEN, M. C., LORD, R. C. & MENDELSOHN, R. 1974. Laser-excited Raman spectroscopy of biomolecules. V. Conformational changes associated with the chemical denaturation of lysozyme. *Journal of the American Chemical Society,* 96**,** 3038-3042.

CHENNAMSETTY, N., HELK, B., VOYNOV, V., KAYSER, V. & TROUT, B. L. 2009a. Aggregation-Prone Motifs in Human Immunoglobulin G. *Journal of Molecular Biology,* 391**,** 404-413.

CHENNAMSETTY, N., VOYNOV, V., KAYSER, V., HELK, B. & TROUT, B. L. 2009b. Design of therapeutic proteins with enhanced stability. *Proceedings of the National Academy of Sciences*.

CHENNAMSETTY, N., VOYNOV, V., KAYSER, V., HELK, B. & TROUT, B. L. 2010. Prediction of Aggregation Prone Regions of Therapeutic Proteins. *The Journal of Physical Chemistry B,* 114**,** 6614-6624.

CHI, E. Y., KRISHNAN, S., RANDOLPH, T. W. & CARPENTER, J. F. 2003. Physical stability of proteins in aqueous solution: mechanism and driving forces in nonnative protein aggregation. *Pharm Res,* 20**,** 1325-36.

CHI, E. Y., WEICKMANN, J., CARPENTER, J. F., MANNING, M. C. & RANDOLPH, T. W. 2005. Heterogeneous nucleation-controlled particulate formation of recombinant human platelet-activating factor acetylhydrolase in pharmaceutical formulation. *J Pharm Sci,* 94**,** 256-74.

CHU, B. 1991. Laser light scattering: Basic principles and practice.

COLCHER, D., MILENIC, D., ROSELLI, M., RAUBITSCHEK, A., YARRANTON, G., KING, D., ADAIR, J., WHITTLE, N., BODMER, M. & SCHLOM, J. 1989. Characterization and biodistribution of recombinant and recombinant/chimeric constructs of monoclonal antibody B72.3. *Cancer Res,* 49**,** 1738-45.

COMBET, C., JAMBON, M., DELÉAGE, G. & GEOURJON, C. 2002. Geno3D: automatic comparative molecular modelling of protein. *Bioinformatics,* 18**,** 213-214.

CROMWELL, M. E., HILARIO, E. & JACOBSON, F. 2006. Protein aggregation and bioprocessing. *AAPS J,* 8**,** E572-9.

DALL'ACQUA, W. F., COOK, K. E., DAMSCHRODER, M. M., WOODS, R. M. & WU, H. 2006a. Modulation of the effector functions of a human IgG1 through engineering of its hinge region. *J Immunol,* 177**,** 1129-38.

DALL'ACQUA, W. F., KIENER, P. A. & WU, H. 2006b. Properties of Human IgG1s Engineered for Enhanced Binding to the Neonatal Fc Receptor (FcRn).

DANDLIKER, W. B., ALONSO, R., DE SAUSSURE, V. A., KIERSZENBAUM, F., LEVISON, S. A. & SCHAPIRO, H. C. 1967. The Effect of Chaotropic Ions on the Dissociation of Antigen-Antibody Complexes*. *Biochemistry,* 6**,** 1460-1467.

DANGL, J. L., WENSEL, T. G., MORRISON, S. L., STRYER, L., HERZENBERG, L. A. & OI, V. T. 1988. Segmental flexibility and complement fixation of genetically engineered chimeric human, rabbit and mouse antibodies. *EMBO J,* 7**,** 1989-94.

DE FORESTA, B., LEGROS, N., PLUSQUELLEC, D., LE MAIRE, M. & CHAMPEIL, P. 1996. Brominated detergents as tools to study protein-detergent interactions. *Eur J Biochem,* 241**,** 343-54.

DEE, K. C., PULEO, D. A. & BIZIOS, R. 2003. Protein-Surface Interactions. *An Introduction To Tissue-Biomaterial Interactions.* John Wiley & Sons, Inc.

DONG, A., PRESTRELSKI, S. J., ALLISON, S. D. & CARPENTER, J. F. 1995. Infrared spectroscopic studies of lyophilization- and temperature-induced protein aggregation. *J Pharm Sci,* 84**,** 415-24.

DORAN, P. M. 1995. 7 - Fluid Flow and Mixing. *Bioprocess Engineering Principles.* London: Academic Press.

DUNN, M. J. 1993. *Gel electrophoreses: Proteins,* Oxford, Bios scientific publishers in association with the Biochemical Society.

FASMAN, G. D. 1996. *Circular Dichrosm and the Conformational Analysis of Biomolecules,* New York, Plenum press

FERRONE, F. 1999. Analysis of protein aggregation kinetics. *Methods Enzymol,* 309**,** 256-74.

FESINMEYER, R., HOGAN, S., SALUJA, A., BRYCH, S., KRAS, E., NARHI, L., BREMS, D. & GOKARN, Y. 2009. Effect of Ions on Agitation- and

Temperature-Induced Aggregation Reactions of Antibodies. *Pharmaceutical Research,* 26**,** 903-913.

FILIPE, V., HAWE, A. & JISKOOT, W. 2009. Critical Evaluation of Nanoparticle Tracking Analysis (NTA) by NanoSight for the Measurement of Nanoparticles and Protein Aggregates. *Pharmaceutical Research,* 27**,** 796-810.

GAZA-BULSECO, G., HICKMAN, K., SINICROPI-YAO, S., HURKMANS, K., CHUMSAE, C. & LIU, H. 2009. Effect of the conserved oligosaccharides of recombinant monoclonal antibodies on the separation by protein A and protein G chromatography. *J Chromatogr A,* 1216**,** 2382-7.

GEKKO, K. & TIMASHEFF, S. N. 1981. Mechanism of protein stabilization by glycerol: preferential hydration in glycerol-water mixtures. *Biochemistry,* 20**,** 4667-4676.

GILL, P., MOGHADAM, T. T. & RANJBAR, B. 2010. Differential scanning calorimetry techniques: applications in biology and nanoscience. *J Biomol Tech,* 21**,** 167-93.

GU, J., BAI, F., LI, H. & WANG, X. 2012. A Generic Force Field for Protein Coarse-Grained Molecular Dynamics Simulation. *International Journal of Molecular Sciences,* 13**,** 14451-14469.

HAMMES, G. G. 2005. Mass Spectrometry. *Spectroscopy for the Biological Sciences.* John Wiley & Sons, Inc.

HAWE, A., KASPER, J. C., FRIESS, W. & JISKOOT, W. 2009. Structural properties of monoclonal antibody aggregates induced by freeze–thawing and thermal stress. *European Journal of Pharmaceutical Sciences,* 38**,** 79-87.

HAWE, A., SUTTER, M. & JISKOOT, W. 2008. Extrinsic Fluorescent Dyes as Tools for Protein Characterization. *Pharmaceutical Research,* 25**,** 1487-1499.

HEADS, J. T., ADAMS, R., D'HOOGHE, L. E., PAGE, M. J., HUMPHREYS, D. P., POPPLEWELL, A. G., LAWSON, A. D. & HENRY, A. J. 2012. Relative stabilities of IgG1 and IgG4 Fab domains: influence of the light-heavy interchain disulfide bond architecture. *Protein Sci,* 21**,** 1315-22.

HOLM, N. K., JESPERSEN, S. K., THOMASSEN, L. V., WOLFF, T. Y., SEHGAL, P., THOMSEN, L. A., CHRISTIANSEN, G., ANDERSEN, C. B., KNUDSEN, A. D. & OTZEN, D. E. 2007. Aggregation and fibrillation of

bovine serum albumin. *Biochimica et Biophysica Acta (BBA) - Proteins and Proteomics,* 1774**,** 1128-1138.

HUANG, C. T., SHARMA, D., OMA, P. & KRISHNAMURTHY, R. 2009. Quantitation of protein particles in parenteral solutions using micro-flow imaging. *J Pharm Sci,* 98**,** 3058-71.

ISHIKAWA, T., ITO, T., ENDO, R., NAKAGAWA, K., SAWA, E. & WAKAMATSU, K. 2010. Influence of pH on heat-induced aggregation and degradation of therapeutic monoclonal antibodies. *Biol Pharm Bull,* 33**,** 1413-7.

JAHN, T. R. & RADFORD, S. E. 2005. The Yin and Yang of protein folding. *FEBS J,* 272**,** 5962-70.

JANEWAY, C. A. 2001. Immunobiology. *Garland Publishing*.

JASPE, J. & HAGEN, S. J. 2006. Do Protein Molecules Unfold in a Simple Shear Flow? *Biophysical journal,* 91**,** 3415-3424.

JIMENEZ, M., RIVAS, G. N. & MINTON, A. P. 2007. Quantitative Characterization of Weak Self-Association in Concentrated Solutions of Immunoglobulin G via the Measurement of Sedimentation Equilibrium and Osmotic Pressure *Biochemistry,* 46**,** 8373-8378.

JONES LATOYA, S., BAM NARENDRA, B. & RANDOLPH THEODORE, W. 1997. Surfactant-Stabilized Protein Formulations: A Review of Protein-Surfactant Interactions and Novel Analytical Methodologies. *Therapeutic Protein and Peptide Formulation and Delivery.* American Chemical Society.

JOUBERT, M. K., HOKOM, M., EAKIN, C., ZHOU, L., DESHPANDE, M., BAKER, M. P., GOLETZ, T. J., KERWIN, B. A., CHIRMULE, N., NARHI, L. O. & JAWA, V. 2012. Highly aggregated antibody therapeutics can enhance the in vitro innate and late-stage T-cell immune responses. *J Biol Chem,* 287**,** 25266-79.

JOUBERT, M. K., LUO, Q., NASHED-SAMUEL, Y., WYPYCH, J. & NARHI, L. O. 2011. Classification and characterization of therapeutic antibody aggregates. *J Biol Chem,* 286**,** 25118-33.

KAMEOKA, D., MASUZAKI, E., UEDA, T. & IMOTO, T. 2007. Effect of Buffer Species on the Unfolding and the Aggregation of Humanized IgG.

KANAI, S., LIU, J., PATAPOFF, T. W. & SHIRE, S. J. 2008. Reversible self-association of a concentrated monoclonal antibody solution mediated by Fab–Fab interaction that impacts solution viscosity. *Journal of Pharmaceutical Sciences,* 97**,** 4219-4227.

KAYSER, V., CHENNAMSETTY, N., VOYNOV, V., FORRER, K., HELK, B. & TROUT, B. L. 2011. Glycosylation influences on the aggregation propensity of therapeutic monoclonal antibodies. *Biotechnol J,* 6**,** 38-44.

KHURANA, R., COLEMAN, C., IONESCU-ZANETTI, C., CARTER, S. A., KRISHNA, V., GROVER, R. K., ROY, R. & SINGH, S. 2005. Mechanism of thioflavin T binding to amyloid fibrils. *J Struct Biol,* 151**,** 229-38.

KIESE, S., PAPPPENBERGER, A., FRIESS, W. & MAHLER, H.-C. 2008. Shaken, not stirred: Mechanical stress testing of an IgG1 antibody. *Journal of Pharmaceutical Sciences,* 97**,** 4347-4366.

KILAR, F., SIMON, I., LAKATOS, S., VONDERVISZT, F., MEDGYESI, G. A. & ZAVODSZKY, P. 1985. Conformation of human IgG subclasses in solution. Small-angle X-ray scattering and hydrodynamic studies. *Eur J Biochem,* 147**,** 17-25.

KIM, Y.-S., RANDOLPH, T. W., STEVENS, F. J. & CARPENTER, J. F. 2002. Kinetics and Energetics of Assembly, Nucleation, and Growth of Aggregates and Fibrils for an Amyloidogenic Protein.

KING, D. J., ADAIR, J. R., ANGAL, S., LOW, D. C., PROUDFOOT, K. A., LLOYD, J. C., BODMER, M. W. & YARRANTON, G. T. 1992. Expression, purification and characterization of a mouse-human chimeric antibody and chimeric Fab' fragment. *Biochem J,* 281 (Pt 2)**,** 317-23.

KUELTZO, L. A., WANG, W., RANDOLPH, T. W. & CARPENTER, J. F. 2008. Effects of solution conditions, processing parameters, and container materials on aggregation of a monoclonal antibody during freeze-thawing. *J Pharm Sci,* 97**,** 1801-12.

LEDNEV, I. K., SHASHILOV, V. & XU, M. 2009. Ultraviolet Raman spectroscopy is uniquely suitable for studying amyloid diseases. *Current Science,* 97**,** 180.

LEHR, H.-A., BRUNNER, J., RANGOONWALA, R. & JAMES KIRKPATRICK, C. 2002. Particulate Matter Contamination of Intravenous Antibiotics Aggravates Loss of Functional Capillary Density in Postischemic Striated Muscle. 165**,** 514-520.

LIU, J., ANDYA, J. & SHIRE, S. 2006. A critical review of analytical ultracentrifugation and field flow fractionation methods for measuring protein aggregation. *The AAPS Journal,* 8**,** E580-E589.

LIU, J., NGUYEN, M. D. H., ANDYA, J. D. & SHIRE, S. J. 2005. Reversible self-association increases the viscosity of a concentrated monoclonal antibody in aqueous solution. *Journal of Pharmaceutical Sciences,* 94**,** 1928-1940.

LU, Y., HARDING, S. E., MICHAELSEN, T. E., LONGMAN, E., DAVIS, K. G., ORTEGA, Á., GROSSMANN, J. G., SANDLIE, I. & GARCÍA DE LA TORRE, J. 2007. Solution Conformation of Wild-Type and Mutant IgG3 and IgG4 Immunoglobulins Using Crystallohydrodynamics: Possible Implications for Complement Activation. *Biophysical Journal,* 93**,** 3733-3744.

LUČIĆ, V., FÖRSTER, F. & BAUMEISTER, W. 2005. STRUCTURAL STUDIES BY ELECTRON TOMOGRAPHY: From Cells to Molecules. *Annual Review of Biochemistry,* 74**,** 833-865.

LUMRY, R. & EYRING, H. 1954. Conformation Changes of Proteins. *The Journal of Physical Chemistry,* 58**,** 110-120.

M. SHOTTON, D. 1989. Confocal scanning optical microscopy and its applications for biological specimens. *Journal of Cell Science,* 94**,** 175-206.

MAA, Y.-F. & HSU, C. C. 1996. Effect of high shear on proteins. *Biotechnology and Bioengineering,* 51**,** 458-465.

MAHLER, H.-C., MALLER, R., FRIEI, W., DELILLE, A. & MATHEUS, S. 2005. Induction and analysis of aggregates in a liquid IgG1-antibody formulation. *European Journal of Pharmaceutics and Biopharmaceutics,* 59**,** 407-417.

MAHLER, H. C., FRIESS, W., GRAUSCHOPF, U. & KIESE, S. 2009. Protein aggregation: pathways, induction factors and analysis. *J Pharm Sci,* 98**,** 2909-34.

MALE, D., BROSTOFF, J., ROTH, D.B., ROITT, I. 2006. *Immunology*, Mosby publishing.

NANOSIGHT 2009. Applications of nanoparticle tracking analysis in nanopartical research.

NARENDRANATHAN, T. J. & DUNNILL, P. 1982. The effect of shear on globular proteins during ultrafiltration: Studies of alcohol dehydrogenase. *Biotechnology and Bioengineering,* 24**,** 2103-2107.

OGANESYAN, V., DAMSCHRODER, M. M., WOODS, R. M., COOK, K. E., WU, H. & DALL'ACQUA, W. F. 2009. Structural characterization of a human Fc fragment engineered for extended serum half-life. *Molecular Immunology,* 46**,** 1750-1755.

OGANESYAN, V., GAO, C., SHIRINIAN, L., WU, H. & DALL'ACQUA, W. F. 2008. Structural characterization of a human Fc fragment engineered for lack of effector functions. *Acta Crystallographica Section D,* 64**,** 700-704.

PALACIO, L., HO, C.-C. & ZYDNEY, A. L. 2002. Application of a pore-blockage—Cake-filtration model to protein fouling during microfiltration. *Biotechnology and Bioengineering,* 79**,** 260-270.

PE 2008. European directorate for the quality of medicine. Particulate contamination: Subivisible particles.

PEARLSTEIN, R. A., VAZ, R. J., KANG, J., CHEN, X.-L., PREOBRAZHENSKAYA, M., SHCHEKOTIKHIN, A. E., KOROLEV, A. M., LYSENKOVA, L. N., MIROSHNIKOVA, O. V., HENDRIX, J. & RAMPE, D. 2003. Characterization of HERG potassium channel inhibition using CoMSiA 3D QSAR and homology modeling approaches. *Bioorganic & Medicinal Chemistry Letters,* 13**,** 1829-1835.

PEASE, L. F., ELLIOTT, J. T., TSAI, D.-H., ZACHARIAH, M. R. & TARLOV, M. J. 2008. Determination of protein aggregation with differential mobility analysis: Application to IgG antibody. *Biotechnology and Bioengineering,* 101**,** 1214-1222.

PERICO, N., PURTELL, J., DILLON, T. M. & RICCI, M. S. 2009. Conformational implications of an inversed pH-dependent antibody aggregation. *J Pharm Sci,* 98**,** 3031-42.

PETUSHKOV, V. N., GIBSON, B. G. & LEE, J. 1996. Direct measurement of excitation transfer in the protein complex of bacterial luciferase hydroxyflavin and the associated yellow fluorescence proteins from Vibrio fischeri Y1. *Biochemistry,* 35**,** 8413-8.

PHILO, J. 2006. Is any measurement method optimal for all aggregate sizes and types? *The AAPS Journal,* 8**,** E564-E571.

PORTER, M. C. 1972. Concentration Polarization with Membrane Ultrafiltration. *Product R&D,* 11**,** 234-248.

PRIVALOV, P. L. & POTEKHIN, S. A. 1986. Scanning microcalorimetry in studying temperature-induced changes in proteins. *Methods Enzymol,* 131**,** 4-51.

ROBERTS, C. J. 2003. Kinetics of Irreversible Protein Aggregation: Analysis of Extended Lumry−Eyring Models and Implications for Predicting Protein Shelf Life. *The Journal of Physical Chemistry B,* 107**,** 1194-1207.

ROBERTS, C. J. 2007. Non-native protein aggregation kinetics. *Biotechnol Bioeng,* 98**,** 927-38.

ROEFS, S. P. & DE KRUIF, K. G. 1994. A model for the denaturation and aggregation of beta-lactoglobulin. *Eur J Biochem,* 226**,** 883-9.

ROSENBERG, E., HEPBILDIKLER, S., KUHNE, W. & WINTER, G. 2009. Ultrafiltration concentration of monoclonal antibody solutions: Development of an optimized method minimizing aggregation. *Journal of Membrane Science,* 342**,** 50-59.

SALI, A. & BLUNDELL, T. L. 1993. Comparative protein modelling by satisfaction of spatial restraints. *J Mol Biol,* 234**,** 779-815.

SAPHIRE, E. O. 2012. Crystal structure of a neutralizing human IGG against HIV-1: A template for vaccine design. *Science***,** 1155-1158.

SASAHARA, K., YAGI, H., SAKAI, M., NAIKI, H. & GOTO, Y. 2008. Amyloid Nucleation Triggered by Agitation of Î²2-Microglobulin under Acidic and Neutral pH Conditions. *Biochemistry,* 47**,** 2650-2660.

SCHULE, S., FRIESS, W., BECHTOLD-PETERS, K. & GARIDEL, P. 2007. Conformational analysis of protein secondary structure during spray-drying of antibody/mannitol formulations. *Eur J Pharm Biopharm,* 65**,** 1-9.

SCHUURMAN, J., PERDOK, G. J., GORTER, A. D. & AALBERSE, R. C. 2001. The inter-heavy chain disulfide bonds of IgG4 are in equilibrium with intra-chain disulfide bonds. *Mol Immunol,* 38**,** 1-8.

SCHUURMAN, J., VAN REE, R., PERDOK, G. J., VAN DOORN, H. R., TAN, K. Y. & AALBERSE, R. C. 1999. Normal human immunoglobulin G4 is

bispecific: it has two different antigen-combining sites. *Immunology,* 97**,** 693-8.

SELA CULANG, I., ALON, S. & OFRAN, Y. 2012. A Systematic Comparison of Free and Bound Antibodies Reveals Binding-Related Conformational Changes. *The Journal of Immunology,* 189**,** 4890-4899.

SHARMA, D. K., KING, D., MOORE, P., OMA, P. & THOMAS, D. 2007. Flow microscopy for particulate analysis in parenteral and pharmaceutical fluids. *European Journal of Parenteral Sciences and Pharmaceutical Sciences,* 12**,** 97-102.

SHOJAAEE, Z., ROUX, J. N., CHEVOIR, F. & WOLF, D. E. 2012. Shear flow of dense granular materials near smooth walls. I. Shear localization and constitutive laws in the boundary region. *Phys Rev E Stat Nonlin Soft Matter Phys,* 86**,** 011301.

SHUKLA, A. A., GUPTA, P. & HAN, X. 2007a. Protein aggregation kinetics during Protein A chromatography: Case study for an Fc fusion protein. *Journal of Chromatography A,* 1171**,** 22-28.

SHUKLA, A. A., HUBBARD, B., TRESSEL, T., GUHAN, S. & LOW, D. 2007b. Downstream processing of monoclonal antibodies—Application of platform approaches. *Journal of Chromatography B,* 848**,** 28-39.

SLUZKY, V., TAMADA, J. A., KLIBANOV, A. M. & LANGER, R. 1991. Kinetics of Insulin Aggregation in Aqueous Solutions upon Agitation in the Presence of Hydrophobic Surfaces. *Proceedings of the National Academy of Sciences of the United States of America,* 88**,** 9377-9381.

SOME, D., KENRICK, S. 2012. Characterization of Protein-Protein Interactions via Static and Dynamic Light Scattering,. *In:* CAI, D. J. (ed.) *Protein Interactions.* InTech.

STENBERG, M. & NYGREN, H. 1988. Kinetics of antigen-antibody reactions at solid-liquid interfaces. *Journal of Immunological Methods,* 113**,** 3-15.

SZENCZI, A., KARDOS, J., MEDGYESI, G. A. & ZAVODSZKY, P. 2006. The effect of solvent environment on the conformation and stability of human polyclonal IgG in solution. *Biologicals,* 34**,** 5-14.

TESSIER, P. M. & LENHOFF, A. M. 2003. Measurements of protein self-association as a guide to crystallization. *Curr Opin Biotechnol,* 14**,** 512-6.

THUROW, H. & GEISEN, K. 1984. Stabilisation of dissolved proteins against denaturation at hydrophobie interfaces. *Diabetologia,* 27**,** 212-218.

TIMASHEFF, S. N. 1993. The control of protein stability and association by weak interactions with water: how do solvents affect these processes? *Annu Rev Biophys Biomol Struct,* 22**,** 67-97.

TISCHENKO, V. M., ZAV'YALOV, V. P., MEDGYESI, G. A., POTEKHIN, S. A. & PRIVALOV, P. L. 1982. A Thermodynamic Study of Cooperative Structures in Rabbit Immunoglobulin G. *European Journal of Biochemistry,* 126**,** 517-521.

TYAGI, A. K., RANDOLPH, T. W., DONG, A., MALONEY, K. M., HITSCHERICH, C., JR. & CARPENTER, J. F. 2009. IgG particle formation during filling pump operation: a case study of heterogeneous nucleation on stainless steel nanoparticles. *J Pharm Sci,* 98**,** 94-104.

UCL 2010. *Chromatography MBI notes*.

USP 2008. United states Pharmacopoeial Convention USP 2008.

VAN DER ZEE, J. S., VAN SWIETEN, P. & AALBERSE, R. C. 1986. Serologic aspects of IgG4 antibodies. II. IgG4 antibodies form small, nonprecipitating immune complexes due to functional monovalency.

VAN REIS, R. & ZYDNEY, A. 2001. Membrane separations in biotechnology. *Current Opinion in Biotechnology,* 12**,** 208-211.

VENKITESHWARAN, A., HEIDER, P., TEYSSEYRE, L. & BELFORT, G. 2008. Selective precipitation-assisted recovery of immunoglobulins from bovine serum using controlled-fouling crossflow membrane microfiltration. *Biotechnology and Bioengineering,* 101**,** 957-966.

VERMEER, A. W. P. & NORDE, W. 2000. The Thermal Stability of Immunoglobulin: Unfolding and Aggregation of a Multi-Domain Protein. *Biophysical Journal,* 78**,** 394-404.

VISIONGAIN 2008. Therapeutic Monoclonal antibodies report 2008-2023.

WANG, L. & GHOSH, R. 2009. Feasibility Study for the Fractionation of the Major Human Immunoglobulin G Subclasses Using Hydrophobic Interaction Membrane Chromatography. *Analytical Chemistry,* 82**,** 452-455.

WANG, W. 1999. Instability, stabilization, and formulation of liquid protein pharmaceuticals. *Int J Pharm,* 185**,** 129-88.

WATANABE, H., MATSUMARU, H., OOISHI, A., FENG, Y., ODAHARA, T., SUTO, K. & HONDA, S. 2009. Optimizing pH response of affinity between protein G and IgG Fc: how electrostatic modulations affect protein-protein interactions. *J Biol Chem,* 284**,** 12373-83.

WELFLE, K., MISSELWITZ, R., HAUSDORF, G., HÖHNE, W. & WELFLE, H. 1999. Conformation, pH-induced conformational changes, and thermal unfolding of anti-p24 (HIV-1) monoclonal antibody CB4-1 and its Fab and Fc fragments. *Biochimica et Biophysica Acta (BBA) - Protein Structure and Molecular Enzymology,* 1431**,** 120-131.

WEN, J., JIANG, Y., NAHRI, L. 2008. Effect of carbohydrate on thermal stability of antibodies. Formulation & Analytical Resources: Amgen Inc.

ZURDO, J. 2013. Developability assessment as an early de-risking tool for biopharmaceutical development. *Pharmaceutical Bioprocessing,* 1**,** 29-50.

Appendix A: Operation of the USD Surface adsorption shear device

Acknowledgement is made to Olatomirin Kolade for formalising this SOP based on work by the author.

Introduction

Shear forces are experienced to varying degrees by protein therapeutics throughout the manufacturing process and indirectly contribute to aggregates levels observed in the final product. The rotating disk shear device can be used to simulate interfacial shear encountered by protein formulations during manufacture. Solid-liquid interfacial shear is created inside the chamber generating shear strain rates of 3.4 x 10^4 s^{-1} at 9000 rpm[1][2]. The device can therefore be used to monitor the stability of protein therapeutics under defined levels of shear in the presence or absence of an air-liquid interface.

The device (ID sfadsorp.v2.n1 and n2) features a chamber volume of 7.8 - 10 mL, a clear polymethyl methylacrylate (PMMA) lid containing separate ports for sample injection (central port) and recovery (angled port), and incorporates a cooling jacket. The disk rotates around a hollow shaft and is supported by a Teflon prop above the disk and a stainless steel U-ring at its base. Disks of different material types can be used to reflect the range of surfaces encountered by the protein during process operations.

Typically, the effect of interfacial shear is determined by examining reduction in the level of monomeric protein by SEC-HPLC

Materials

10% (w/v) sodium hydroxide
2.5 % (v/v) orthophosphoric acid
Distilled water
Formulation buffer (degassed)
Protein formulation (0.5 – 10 mg/mL)
Sterile disposable syringes (1 mL and 20 mL)

Equipment

Shear device speed controller (sfadsorp.v2.ppk1a and sfadsorp.v2.ppk1b)
Magnetically driven shear device (sfadsorp.v2.n1/n2)
Magnetic disk – 8mm height, 26 mm diameter (surfaces - stainless steel 316L, borosilicate glass, Teflon)
One – way valve for attachment to Luer needle

---

[1] Biddlecombe, JG *et al*., 2007. *Biotechnol. Prog.* 23 (5):1218-1222

[2] Biddlecombe, JG, *et al*., 2009. *Biotechnol. Prog.* 25 (5):1409-1507

Equipment cont'd

Water bath to achieve temperature control at 17°C
Watson-Marlow peristaltic pump 505S or suitable alternative
Silicone/Tefzel tubing (diameter)
GF-250 ZORBAX, TSKgel 3000 SWxl or a suitable SE column
HPLC (or other instrument for monitoring protein species)

Method

Shear device CIP

1. Cleaning-in place is performed before operation of the shear device.

2. Turn on the water bath and check that the temperature set is 16 -17°C. Turn on the pump and check the set speed is 150 rpm. These parameters maintain a chamber operating temperature of 20°C.

3. Turn on the speed controller. If using sfadsorp.v2.ppk1a and sfadsorp.v2.ppk1b, ensure the current is limiting (i.e. set to maximum).

4. Carefully remove the stainless steel U-ring from the hollow shaft (Luer needle). Use pliers if necessary. Hold the top end of the Luer needle[3] and slowly prise the U-ring from the needle shaft. Leave the Teflon spacer in place.

5. Attach the appropriate disk and re-attach the steel ring so that it is flush with the disk but allows it to freely rotate. Hold the top of the Luer needle when performing this action.

6. Carefully seal the chamber with the lid (and attach the one-way Luer valve[4])

7. Fill the chamber with a syringe (approx. 10 mL) through the central port with 10% v/v NaOH until a bubble appears. Start the shear device on a low setting and continuing injecting NaOH until the bubble is removed. Air in the chamber is expelled through the angled port.

8. Run at 9000 ± 300 rpm (for sfadsorp.v2.ppk1a and sfadsorp.v2.ppk1b) for 10 minutes. Reduce the speed to zero[5].

---

[3] The height of the Luer needle is fixed relative to the fitting in the base of the chamber and should not be adjusted. If the Luer needle slips during removal/assembly of the steel U-ring, adjust its position using an Allen key, but do not over-tighten. If operating device on-site return to A. Craig (UCL Biochemical Engineering Workshop) for repositioning.

[4] Check valves are available from www.valueplastics.com. Part no. SCV23050 Female locking luer to male locking luer, cracking pressure ≤ 0.174 psig, flow rate 90 mL/min, clear SAN with silicone diaphragm.

[5] If using the newer speed controller use the stop switch

9. Remove the one-way Luer valve and withdraw the NaOH

10. Replace the one-way Luer valve and fill the chamber with distilled water until the bubble is removed.

11. Run at 9000 rpm for 10 minutes. Reduce the speed to zero.

12. Remove the water and replace with 2.5% (v/v) orthophosphoric acid. Run at 9000 rpm for 10 minutes. Reduce the speed to zero.

13. Remove the acid and replace with buffer. Run at 9000 rpm for 10 minutes. Reduce the speed to zero.

14. Repeat the buffer step for a total of three times.

Shear Device Operation

1. Carefully fill the chamber with sample through the central port using the one-way valve until a bubble appears.

2. Start the device at high speed (9000 rpm or desired speed) whilst filling until the air is expelled from the chamber.

3. Remove 0.1 mL of sample from the angled sample port (t=0 sample).

4. Replace the sample syringe with a 1 mL syringe containing 1 mL of formulation buffer, taking care not to introduce air into the chamber.

5. At designated time points, sample 0.1 mL from the device chamber by careful injection of 0.1 mL of formulation buffer into the chamber. Samples can be stored briefly at 4°C prior to analysis.

6. Changes in the soluble monomer concentration can be monitored by SEC-HPLC[6]. Centrifuge samples at 20°C for 10 minutes at 15, 294 g (12, 000 rpm, rotor FA45-30-11, Eppendorf 5810R benchtop centrifuge) prior to loading.

7. After use, perform CIP on the shear device and rinse with water. Wipe the outside of the device with water and air-dry all components before reassembly of the device.
8. Do not leave chamber in contact with buffer salts when the device is not in operation.

---

[6] Dilution of the chamber contents during sampling should be included in calculations of monomer concentration/peak area.

Safety Precautions

1. Do not run the shear device without liquid in the chamber.

2. Do not run the shear device without the appropriate level of cooling.

3. The shear device should not be operated above 20,000 rpm (n.b. the Teflon spacer should be replaced with a PEEK spacer above speeds of 10,000 rpm).
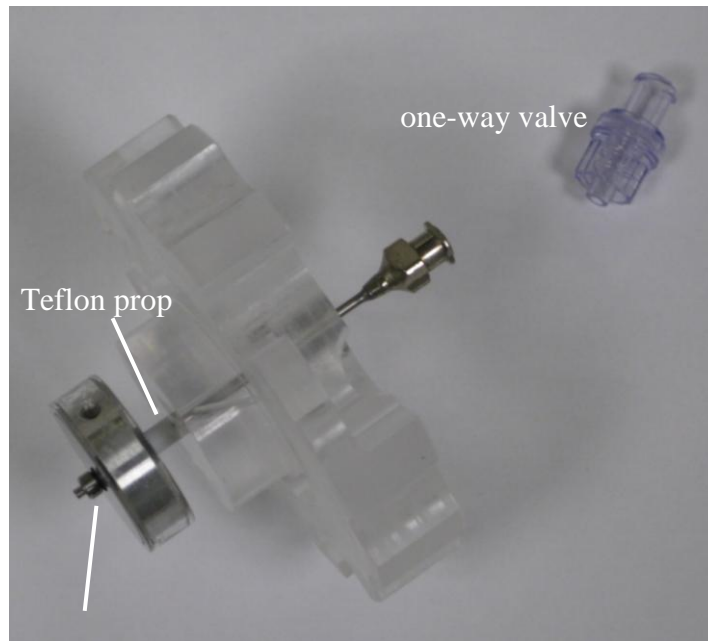
Figure 1. Assembled lid of shear device
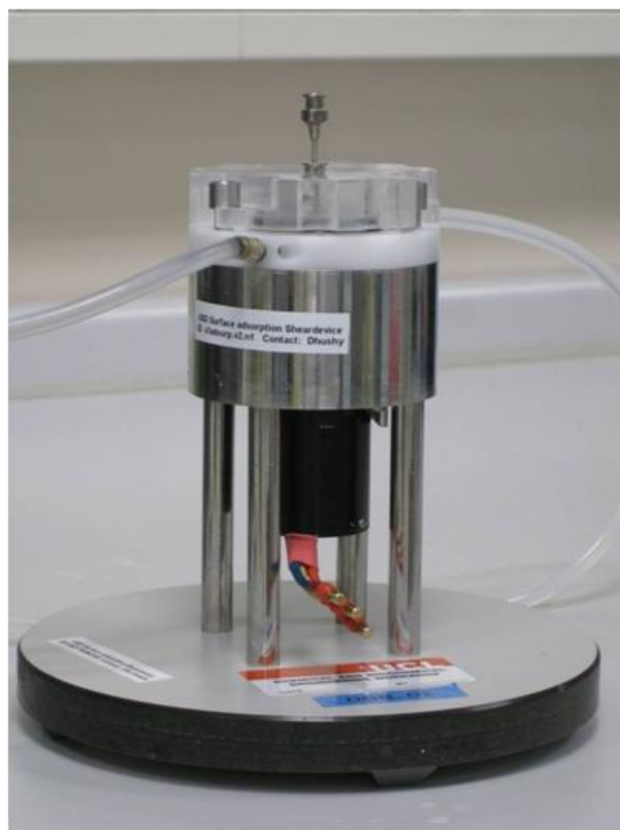
Figure 2. Assembled shear device